

Investigations of chemically and biologically induced transformation reactions of micropollutants during biological wastewater treatment processes

by

Kevin Sean Jewell
born in Frankfurt am Main

Accepted dissertation thesis for the partial fulfilment of the requirements for a
Doctor of Natural Sciences
Fachbereich 3: Mathematik/Naturwissenschaften
Universität Koblenz-Landau

Reviewers:

Prof. Dr. Joachim Scholz
Prof. Dr. Thomas A. Ternes
Prof. Dr. Torsten C. Schmidt, Universität Duisburg-Essen

Examiners:

Prof. Dr. Joachim Scholz
Prof. Dr. Thomas A. Ternes
Prof. Dr. Stefan Wehner

Date of the oral examination: 26th June 2017

Contents

Acknowledgements	vii
Summary	ix
Zusammenfassung	xi
1 General introduction	1
1.1 Micropollutants and wastewater treatment	1
1.2 Removal processes	4
1.2.1 Sorption of micropollutants to sludge	4
1.2.2 Transformation of micropollutants during wastewater treatment	6
1.3 Current progress of research	14
1.4 Project goals	15
1.5 Outline	17
2 Biological transformation of trimethoprim	19
2.1 Introduction	20
2.2 Methods	22
2.2.1 Pilot-scale sequencing batch reactor	22
2.2.2 Chemicals	23
2.2.3 Lab-scale bioreactor incubation experiments	23
2.2.4 Kinetic analysis	24
2.2.5 Analytical methods	24
2.3 Results and discussion	26
2.3.1 Variability of primary removal over time	26
2.3.2 Incubation of trimethoprim in aerobic sludge	27
2.3.3 Identification of transformation products of TMP removal	31
2.3.4 Comparing kinetics and transformation pathways in the laboratory and the SBR	36
2.4 Conclusions	38
3 Nitration of phenolic micropollutants	41
3.1 Introduction	42
3.2 Methods	46
3.2.1 Chemicals	46
3.2.2 Analytical methods	46

3.2.3	Experimental setup for kinetic and mechanistic studies of <i>ortho</i> -Phenylphenol nitration	47
3.2.4	Incubation experiments with activated sludge	47
3.2.5	Effect of freezing samples during storage	48
3.2.6	Environmental sampling at WWTPs	48
3.3	Results and discussion	49
3.3.1	Abiotic nitration of <i>ortho</i> -phenylphenol at varying pH values	49
3.3.2	Impact of <i>N</i> -acetylcysteine and c-PTIO on OPP abiotic nitration and nitrosation	51
3.3.3	Kinetics and mechanism of OPP nitration	54
3.3.4	Uncontrolled nitration of phenolic substances during sample storage	57
3.3.5	Incubation experiments with activated sludge	57
3.3.6	Analysis of wastewater for the presence of nitrophenolic TPs	62
3.4	Conclusions	64
4	Diclofenac in biofilm and sludge processes	67
4.1	Introduction	68
4.2	Methods	71
4.2.1	Chemicals	71
4.2.2	Wastewater treatment plants	71
4.2.3	Aerobic laboratory incubation experiments	72
4.2.4	Monitoring campaign at WWTP Bad Ragaz and WWTP Koblenz	73
4.2.5	Analytical methods	74
4.3	Results and discussion	76
4.3.1	Transformation of diclofenac in lab-scale experiments containing carriers from a WWTP employing an MBBR	76
4.3.2	Incubation experiments with activated sludge from WWTP Koblenz	81
4.3.3	Incubation experiments with carriers from WWTP Klippan	84
4.3.4	Monitoring campaign at WWTP Bad Ragaz	84
4.3.5	Monitoring campaign at WWTP Koblenz	88
4.4	Conclusion	88
5	Conclusion and Outlook	91
5.1	General conclusions	91
5.2	Outlook	94
A	Supplementary data to Chapter 2	97
A.1	LC-tandem MS parameters	97
A.1.1	Chromatography and ESI parameters for analysis of TMP and TPs other than DAPC on API 5500 QTRAP and 5600 QTOF	97
A.1.2	Chromatography and ESI parameters for analysis by HRMS on LTQ-Orbitrap-Velos	98
A.1.3	Chromatography and ESI parameters for analysis of DAPC on API 4000 QTRAP	98
A.2	HR-MS ² spectra and structural characterisation	99
A.3	Pilot-scale SBR and monitoring experiments	103
A.4	Additional figures	104
A.4.1	Abiotic hydrolysis and oxidation of 4-desmethyl-TMP	104

A.5	Synthesis of DAPC	107
A.6	TMP degradation modelling	110
A.6.1	Modeling TMP degradation kinetics in the SBR	110
A.7	Detection of DAPC in wastewater samples	112
B	Supplementary data to Chapter 3	115
B.1	Synthesis of transformation products	115
B.1.1	Synthesis of 2-nitro-6-phenylphenol and 4-nitro-6-phenylphenol	115
B.1.2	Synthesis of 3,3'-dinitro-bisphenol A	116
B.1.3	¹ H NMR shifts for synthesised TPs	116
B.2	Characterisation parameters of WWTPs in Chapter 3	120
B.3	Parameters for LC–Tandem MS in MRM mode	121
B.3.1	Analysis method parameters for environmental analysis of phenols and nitrophenols by standard addition	121
B.3.2	Calculation of recoveries	122
B.4	Additional equations and figures	122
B.5	MS ² Fragmentation of TPs	124
B.5.1	Fragmentation Spectra and annotations	127
C	Supplementary data to Chapter 4	149
C.1	MS ² fragmentation	149
C.1.1	Diclofenac (DCF)	151
C.1.2	4HD	152
C.1.3	5HD	153
C.1.4	DCF-lactam	154
C.1.5	DCF-BA	155
C.1.6	4HDQI	156
C.1.7	5HDQI	157
C.1.8	TP285	159
C.1.9	TP287	160
C.1.10	TP259	161
C.1.11	TP225	162
C.1.12	TP293a	163
C.1.13	TP293b	164
C.1.14	TP391a	165
C.1.15	TP391b	166
C.1.16	TP243	167
C.1.17	TP297	168
C.1.18	TP273	169
C.1.19	TP343a	170
C.1.20	TP343b	171
C.1.21	TP275	172
C.2	Additional figures and tables	173

Acknowledgements

This work was made possible through the financial support of the European Research Council through the EU-project *ATHENE*. I thank also the Bundesanstalt für Gewässerkunde for providing the PhD-position and infrastructure to conduct these studies.

I thank my parents and my sister for their unfaltering, unrelenting and dependably regular encouragement and support. Their patience and faith that this will one day be finished were vital for my state of mind. I also thank Agnessa for believing in the best of me and for being an inspiration for me to follow my work and my hobbies.

Thank you to all my colleagues at the BfG, especially Sandro Castronovo, Kathrin Bröder, and Manoj Schulz, whose assistance in all manner of laboratory problem-solving kept the experiments working. I thank all of the G2 department for their advice and relating their experiences. The hands-on training over the course of many years was priceless. In particular I thank Christian Dietrich, Uwe Kunkel, and Carsten Prasse. My fellow PhD students in the group were also indispensable, always being available to discuss challenges and ideas. I also give my gratitude to everyone who has helped me correct my written (and also spoken) German.

Thank you to my colleagues at EAWAG, Per Falås, who was an invaluable source of experience and was always available for a chat about science and Adriano Joss, for his great insight and advice. His support of the monitoring experiments and pilot reactors was essential and his enthusiasm for the work we were doing helped to overcome the challenges.

I especially thank Arne Wick for his major part in this thesis, he was a source of advice in all aspects of the work. His ideas and perspectives were invaluable. I was very lucky to have him as a mentor.

Lastly my gratitude goes to my supervisor Thomas Ternes. He is well known for his experience and knowledge and desire to pass this on to his students; my experience was no different. I will always aspire to emulate his calmness and methodical nature, his ability to inspire his employees and to push them to do their best work.

Summary

The presence of anthropogenic chemicals in the natural environment may impact both habitats and human use of natural resources. In particular the contamination of aquatic resources by organic compounds used as pharmaceuticals or household chemicals has become evident. The newly identified environmental pollutants, also known as micropollutants, often have i) unknown ecotoxicological impacts, ii) unknown partitioning mechanisms, e.g. sorption to sediments, and iii) limited regulation to control their emission. Furthermore, like any compound, micropollutants can be transformed while in the environmental matrix to unknown transformation products (TPs), which add to the number of unknown chemicals to consider and thus increase the complexity of risk management. Transformation is at the same time a natural mechanism for the removal of anthropogenic compounds, either by complete degradation (mineralisation) or to innocuous TPs. However, how transformation occurs in real-world conditions is still largely unknown. During the transport of micropollutants from household wastewater to surface water, a large amount of transformation can occur during wastewater treatment—specifically during biological nitrifying–denitrifying treatment processes. The thesis considers the systematic optimisation of laboratory investigative techniques, application of sensitive mass-spectrometry-based analysis techniques and the monitoring of full-scale wastewater treatment plants (WWTPs) to elucidate transformation processes of five known micropollutants.

The first of the five compounds investigated was the antibiotic trimethoprim. Incubation experiments were conducted at different analyte spike concentrations and different sludge to wastewater ratios. Using high-resolution mass spectrometry, a total of six TPs were identified from trimethoprim. The types of TPs formed was clearly influenced by the spike concentration. To the best of our knowledge, such impacts have not been previously described in the literature. Beginning from the lower spike concentration, a relatively stable final TP was formed (2,4-diaminopyrimidine-5-carboxylic acid, DAPC), which could account for almost all of the transformed trimethoprim quantity. The results were compared to the process in a reference reactor. Both by the detection of TPs (e.g., DAPC) and by modelling the removal kinetics, it could be concluded that only experimental results at the low spike concentrations mirrored the real reactor. The limits of using elevated spike concentrations in incubation experiments could thus be shown.

Three phenolic micropollutants, the antiseptic *ortho*-phenylphenol (OPP), the plastics additive bisphenol A (BPA) and the psychoactive drug dextrorphan were investigated with regard to the formation of potentially toxic, nitrophenolic TPs. Nitrite is an intermediate in the nitrification–denitrification process occurring in activated sludge and was found to cause nitration of these phenols. To elucidate the processes, incubation experiments were conducted in purified water in the presence of nitrite with OPP as the test substance. The reactive species HNO_2 , N_2O_3 and the radicals $\cdot\text{NO}$ and $\cdot\text{NO}_2$ were likely involved as indicated by scavenger experiments. In conditions found at WWTPs the wastewater is usually at neutral pH, and nitrite, being an

intermediate, usually has a low concentration. By conducting incubation experiments inoculated with sludge from a conventional WWTP, it was found that the three phenolic micropollutants, OPP, BPA and dextrorphan were quickly transformed to biological TPs. Nitrophenolic TPs were only formed after artificial increase of the nitrite concentration or lowering of the pH. However, nitrophenolic-TPs can be formed as sample preparation artefacts through acidification or freezing for preservation, creating optimal conditions for the reaction to take place.

The final micropollutant to be studied was the pain-reliever diclofenac, a micropollutant on the EU-watch list due to ecotoxicological effects on rainbow trout. The transformation was compared in two different treatment systems, one employing a reactor with suspended carriers as a biofilm growth surface, while the other system employed conventional activated sludge. In the biofilm-based system, the pathway was found to produce many TPs each at relatively low concentration, many of which were intermediate TPs that were further degraded to unknown tertiary TPs. In the conventional activated sludge system some of the same reactions took place but all at much slower rates. The main difference between the two systems was due to different reaction rates rather than different transformation pathways. The municipal WWTPs were monitored to verify these results. In the biofilm system, a 10-day monitoring campaign confirmed an 88% removal of diclofenac and the formation of the same TPs as those observed in the laboratory experiments. The proposed environmental quality standard of 0.05 µg/L might thus be met without the need for additional treatment processes such as activated carbon filtration or ozonation.

Zusammenfassung

Die Anwendung von Chemikalien führt in vielen Fällen zu deren Emission in die Umwelt. Besonders organische Substanzen wie zum Beispiel Pharmazeutika, Biozide und Waschmittelinhaltsstoffe wurden in den letzten Jahren vermehrt als Umweltkontaminanten in Oberflächengewässern nachgewiesen. Die organischen Umweltkontaminanten, auch Spurenstoffe genannt, haben oftmals i) unbekannte ökotoxikologische Wirkungen, ii) unbekanntes Verteilungsverhalten, und iii) sind bisher hinsichtlich der Emission kaum reguliert. Wie bei allen Substanzen können Spurenstoffe in der Umweltmatrix und insbesondere auch in der Kläranlage zu sogenannten Transformationsprodukten (TPs) umgewandelt werden. Um den durch Spurenstoffe verursachten Herausforderungen technologisch begegnen zu können, wird ein besseres Verständnis über diese Transformationsprozesse benötigt. Diese Dissertationsarbeit befasst sich deshalb mit der Aufklärung von Transformationsprozessen ausgewählter Spurenstoffe während der biologischen Abwasserreinigung.

Für die Untersuchung des Abbaus von Trimethoprim wurden Inkubationsversuche angewendet und die Auswirkung der steigenden Dotierungskonzentrationen systematisch untersucht. Es wurden insgesamt sechs TPs charakterisiert. Die Dotierungskonzentration hatte sowohl Auswirkungen auf die kinetischen Konstanten, als auch auf die Transformationsreaktionen. Ein solcher Einfluss der experimentellen Bedingungen wurde bisher in der Literatur noch nicht berichtet. Nur bei niedriger Dotierungskonzentration wurde am Ende des Transformationswegs ein stabiles TP gebildet, die 2,4-Diaminopyrimidin-5-carbonsäure (DAPC). Diese Substanz konnte in Laborversuchen den Großteil der abgebauten Menge von Trimethoprim erklären. Durch Untersuchungen an einer Referenzkläranlage konnte festgestellt werden, dass nur die Inkubationsversuche bei niedriger Dotierungskonzentration die realen Prozesse adäquat abbilden konnten. Die Anwendung hoher Dotierungskonzentrationen führte in Laborversuchen zu einer veränderten TP-Bildung.

Drei phenolische Spurenstoffe wurden in Bezug auf ihre Transformation, insbesondere hin zu potenziell toxischen nitrophenolischen TPs, untersucht: das Desinfektionsmittel *ortho*-Phenylphenol (OPP), das Kunststoffadditiv Bisphenol-A (BPA) und das Hustenmittel Dextrophan. Nitrit wurde als ein potenzieller Auslöser für die Nitrierung postuliert. Inkubationsversuche in Reinstwasser wurden mit OPP in Anwesenheit von Nitrit durchgeführt und bestätigten, dass nitro- (und nitroso-) phenolische TPs unter leicht sauren Bedingungen gebildet werden. Da in kommunalen Kläranlagen der pH-Wert in Belebtschlamm zumeist zwischen 7,5 und 8,5 liegt und Nitrit als Zwischenprodukt oft nur in niedriger Konzentration vorhanden ist, wurde die Bildung von signifikanten Konzentrationen nitrophenolischer TPs als unwahrscheinlich eingestuft. Aufgrund der Ergebnisse von Inkubationsversuchen mit inokulierten Belebtschlamm war festzustellen, dass die drei untersuchten Spurenstoffe schnell zu biologischen TPs umgewandelt wurden. Die Studie zeigte wie das Bildungspotenzial von nitrophenolischen TPs gesteigert wird, wenn bestimmte Bedingungen im Belebtschlamm vorliegen: saurer pH und erhöhte Nitritkonzentration. Zudem

wurde auch gezeigt, dass die Bildung von nitrophenolischen TPs durch das Ansäuern oder das Einfrieren von Proben initiiert werden kann.

Die Transformation vom Antiphlogistikum Diclofenac wurde in zwei unterschiedlichen Kläranlagen verglichen. Die erste Kläranlage verwendet Aufwuchskörper für ein verstärktes Biofilmwachstum, während die zweite mit einer konventionellen nitrifizierenden Belebtschlammbehandlung ausgestattet ist. Trotz der unterschiedlichen Behandlungstechniken konnten in beiden Fällen ähnliche Transformationsreaktionen festgestellt werden. Der wesentliche Unterschied bestand in den veränderten Kinetiken: Geschwindigkeitskonstanten (k_{biol}) waren ca. 50 Mal höher in Kontakt mit Aufwuchskörpern als im konventionellen Belebtschlamm. Der Transformationsweg führte zur Bildung einer Vielzahl an gering konzentrierten TPs. Monitoring-Kampagnen an den zwei Kläranlagen wurden zur Bestätigung der Ergebnisse angeschlossen. In der konventionellen Kläranlage wurde keine signifikante Diclofenac Entfernung gemessen. Wohingegen im Aufwuchskörperreaktor eine mittlere Entfernung von 88% gemessen wurde. Damit wäre die vorgeschlagene Umweltqualitätsnorm von 0.05 µg/L möglicherweise auch ohne die Anwendung von weiteren Behandlungsschritten wie z.B. Aktivkohlefiltration oder Ozonung erreichbar.

Chapter 1

General introduction

1.1 Micropollutants in freshwater resources and the challenges for wastewater treatment

Water quality in rivers, lakes and ground water is impacted by anthropogenic chemicals globally. This can lead to the deterioration of ecosystem health and failure of ecosystem services ([Malaj et al., 2014](#); [Daughton and Ternes, 1999](#)). Anthropogenic chemicals can often have unknown ecotoxicological impacts, especially when considering mixture toxicities and long-term exposures ([Kortenkamp, 2007](#); [Henneberg et al., 2014](#)). When polluted river or ground water is used as a fresh water resource e.g., for drinking water production, irrigation or industrial processes, or through recreational uses such as lakes and parks, water pollution can directly impact human health and economies. Unsafe water and sanitation is linked to around 3% of all deaths worldwide ([World Health Organisation, 2002](#)) and future water security is a world-wide challenge.

Recent events have underscored that risks to water quality still exist globally in the 21st century and are not confined to developing countries. To give one recent example, the contamination of the River Möhne in Germany with PFAS (perfluoroalkyl substances) in 2006 led to downstream contamination of the Ruhr and Rhine rivers and even contamination of local drinking water, which partly relies on bank-filtrate. The source of the contamination was debated, but traced partly to local industry and partly to illegal dumping of industrial waste in the catchment of the River Möhne. Concentrations of PFAS in the Möhne of over 4 µg/L and in drinking water up to 0.5 µg/L were reported ([Exner and Färber, 2006](#); [Skutlarek et al., 2006](#)). This led to wide-spread public concern

for the safety of water resources in the area (Kleeschulte et al., 2007).

It is both desirable from an ecological perspective and vital for human health and ecosystem health to improve the quality of polluted water resources by reducing continuous emission of chemicals into these systems. This is an important aspect of sustainability, which has become an important driver for societal change (UN General Assembly, 2015). The public desire to improve and maintain water quality has been anchored into many legislative acts around the world. In Europe, an important body of legislation concerning water quality is the Water Framework Directive (WFD) (European Parliament, 2000). Among other goals, the WFD is there to legislate corrective action if water bodies are not of a good ecological status, imposes limits to the concentrations of priority pollutants in water bodies and enforces the monitoring of suspected harmful pollutants (European Parliament, 2013). Although regulation exists for some well-known pollutants, the production and use of chemicals changes as industries develop. Regulations therefore become outdated while the number of unknown pollutants is constantly growing.

In order to address the emission of anthropogenic chemicals, the characteristics and properties of these chemicals and their sources must be identified. The chemicals can largely be divided into two groups: regulated or legacy contaminants and chemicals of emerging concern (CECs), often referred to as micropollutants. Regulated contaminants are mostly industrial chemicals or pesticides, a number of which have been banned (e.g., Stockholm Convention on Persistent Organic Pollutants). Micropollutants are newly identified, mostly organic compounds and often have limited regulation. Many could pose ecological or human health risks or their impact is unknown. New micropollutants are being continuously identified as progress is made in analytical techniques, more detailed investigations are undertaken and new chemicals are put onto the market.

Micropollutants include a wide range of chemicals including industrial chemicals, household chemicals, human and veterinary medicines, personal care products and other classes. The main source of contamination can in many cases be traced to the emission of municipal wastewater into surface waters (Daughton and Ruhoy, 2009; Metcalfe et al., 2010). Emission into surface waters can in turn lead to contamination of groundwater due to infiltration. The use of groundwater or surface water as a fresh water resource for downstream communities means that these contaminants are returned to consumers either in drinking water or through other uses of fresh water. The interconnections between wastewater and water resources is often referred to as the urban water cycle (McPherson and Schneider, 1974) (Figure 1.1).

The concern surrounding micropollutants is due the high number of compounds, their widespread use and their occurrence in surface water, groundwater and even drinking water (Noguera-Oviedo and Aga, 2016). Pharmaceuticals are designed to have potent biological activity and therefore can have impacts to both humans and ecology even at low concentrations, but this can also be the case for other classes of micropollutants (Henneberg et al., 2014). Micropollutants are chemically very diverse and minimising environmental exposure can often require novel approaches.

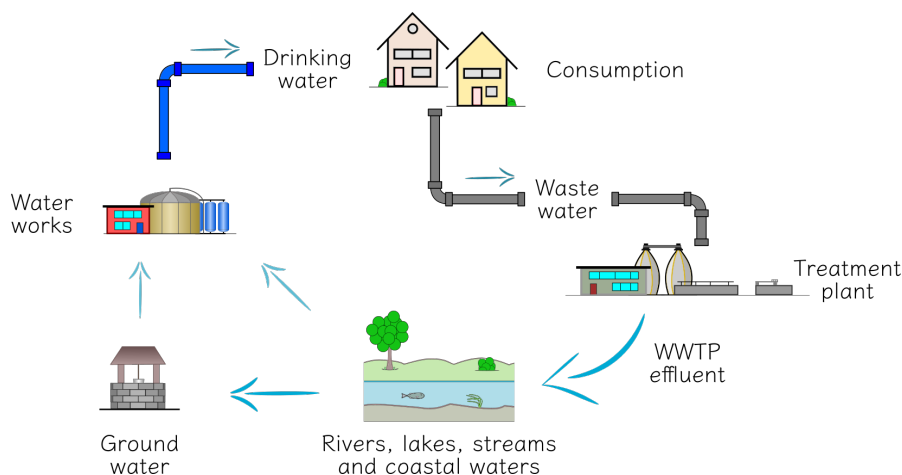


Figure 1.1: A simplified representation of the urban water cycle showing that wastewater can impact downstream water resources including surface water, groundwater and in some cases even drinking water.

There are different approaches suggested to address the issue of micropollutants. Examples include source control, i.e., waste separation, regulating use of certain chemicals, public awareness, or removing them from wastewater at the wastewater treatment stage, the latter otherwise known as *end-of-pipe* solutions (Verlicchi et al., 2012; Ternes and Joss, 2006). Currently, this last point is considered the most effective strategy but a combination of approaches is recommended. In many countries, municipal wastewater is commonly treated in centralised wastewater treatment plants (WWTPs). Already in a few countries political initiatives to regulate the emission of micropollutants at WWTPs are being undertaken. In Germany, this is occurring most prominently in densely populated regions such as Nordrhein-Westfalen (Ministry for Climate Protection, 2014; Hiltenbrand et al., 2015).

The effectiveness of current treatment strategies for the removal of micropollutants by WWTPs is often limited and the need for improved removal is advocated (Joss et al., 2006). Chemical oxidation, e.g., ozone treatment, or activated carbon filtration strategies

have been proposed as viable post-treatment steps to supplement biological treatment and improve micropollutant removal (Hollender et al., 2009). Switzerland has already put policy in place for upgrading WWTPs with such systems (Eggen et al., 2014). However, further understanding of the fate of micropollutants in existing *biological* treatment processes is necessary since i) advanced physicochemical treatment techniques are implemented usually in conjunction with biological processes ii) due to site-specific constraints such as wastewater characteristics, biological treatment may be the only viable alternative and iii) there are concerns about possible side-effects of oxidative treatment (Magdeburg et al., 2014; Alexander et al., 2016).

Improvement in the understanding of the fate and potential removal processes of micropollutants at WWTPs is needed to design effective optimisation of treatment processes. For environmental scientists studying the occurrence of micropollutants in surface or groundwaters, the interactions of micropollutants with WWTP processes may help explain their presence or absence in the environment. In conjunction with knowledge of functions at the microbiological level and process engineering, the complexity of these systems can be elucidated.

1.2 Removal processes of micropollutants during biological wastewater treatment

During wastewater treatment, micropollutants can be impacted by different processes including sorption to sludge (or assimilation into biomass), volatilisation and biological or chemical transformation processes leading ideally to complete degradation (Ternes and Joss, 2006) (Figure 1.2). In this section examples of known processes are discussed together with examples from the current literature.

1.2.1 Sorption of micropollutants to sludge

Sorption to sludge is an important process to consider when investigating the fate of micropollutants during wastewater treatment. Especially for apolar micropollutants or positively charged, ionic micropollutants, sorption can be the major route of elimination. The partitioning of a compound between sludge and liquid phase is described by the partition coefficient K_d (Equation 1.1) (Schwarzenbach et al., 2005).

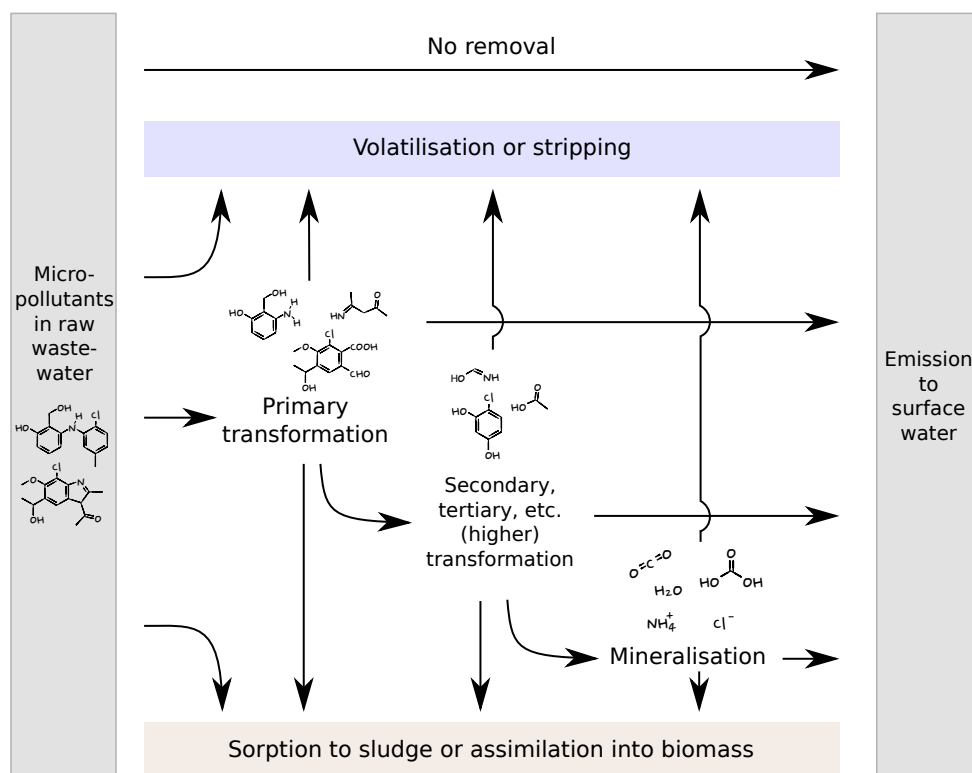


Figure 1.2: Possible fates of micropollutants during biological wastewater treatment. The initial transformation reaction of the precursor micropollutant is the primary transformation. In some cases further transformation reactions occur, i.e., secondary and higher-level, producing small molecules. The transformation in rare cases can continue to mineralisation, i.e., small ions, CO_2 and water.

$$K_d = \frac{C_s}{C_w} \quad (1.1)$$

For polar micropollutants ($K_d < 0.5 \text{ L/g}$) or negatively charged micropollutants such as pharmaceuticals containing carboxylic acid moieties, sorption is often not a significant removal mechanism during wastewater treatment. Sorption equilibrium exists and removal from wastewater is controlled by excess sludge production only (Wick et al., 2011a). The partitioning of uncharged species is often approximated using the octanol-water partition constant K_{ow} . The K_{ow} can be estimated using computational models such as KOWWIN or cLogP, which are empirical calculations based on contributions of single atoms (Machatha and Yalkowsky, 2005; Viswanadhan et al., 1989). However, for charged species or molecules with several polar moieties, the estimation is often inad-

equate and should be treated with caution. Websites such as *chemicalize.org* (Swain, 2012) provide online interfaces to these calculations while the chemical information database *chemspider.com* (Pence and Williams, 2010) also contains experimentally derived values.

1.2.2 Transformation of micropollutants during wastewater treatment

In the ideal case, transformation of micropollutants leads to a break-down of the chemicals to small organic acids, which can be assimilated by microorganisms, or to mineralisation, i.e., conversion to CO_2 and H_2O and other inorganic molecules (Figure 1.2). However, often degradation pathways stop before this stage and micropollutants are merely converted to recalcitrant transformation products (TPs), which include metabolites and products of abiotic (chemical) reactions. TPs can be stable to further degradation and therefore may not represent a true removal of the chemical. Since TPs may have similar properties to their micropollutant precursors or possess different, unknown properties including unknown (eco)toxicological profiles, they can be a potential risk to water quality themselves. On the other hand, the formation of TPs can be part of the natural degradation process and the elucidation of transformation pathways can assist in understanding the fate of micropollutants during wastewater treatment and in the environment.

Biological transformation reactions

Numerous books and reviews have been written on the subject of biological transformation reactions of micropollutants in wastewater treatment processes (Escher and Fenner, 2011; Neilson and Allard, 2007; Lambropoulou and Nollet, 2014; Margot et al., 2015; Wang and Wang, 2016). In this short introduction, recent discoveries related to the transformation of micropollutants are presented in the context of specific functional groups and substance classes, rather than by pharmaceutical classifications.

Transformation reactions of micropollutants can be described as being metabolic or co-metabolic (Fischer and Majewsky, 2014; Alexander, 1981). Through metabolic reactions, micropollutants are metabolised as a nutrient source for the microorganisms and the community will therefore adapt to metabolise these compounds. Direct metabolism of micropollutants as growth substrates leading to enrichment of specialised degrading organisms is often observed at higher micropollutant concentrations or when nutrient sources are low (Ike et al., 2000; Benner et al., 2013). Co-metabolic reactions on the other

hand are reactions of micropollutants which are not directly connected to the metabolism of the compound but occur because other metabolic machinery, e.g., for the degradation of natural organic matter, is also able to act on the micropollutant. It has been suggested that the same enzymes used to metabolise nutrients, e.g., ammonium monooxygenase, could also catalyse transformations of micropollutants (Khunjar et al., 2011; Helbling et al., 2012; Xu et al., 2016). This could be expected to occur if the micropollutants have similar structural features to natural substances typically metabolised by bacteria or the enzymes have a low substrate specificity. Detoxification processes by bacteria are also possible routes of transformation, for example, in the form of conjugation reactions or conversion to more polar TPs for improved transport out of the cell (Singhal and Perez-Garcia, 2016).

A typical biological wastewater treatment process includes both aerobic and anoxic stages for the removal of organic compounds and organically bound nitrogen. The aerobic stage is designed for high elimination of organic matter by heterotrophic organisms and nitrification by ammonium oxidising bacteria, while the anoxic stage (where nitrate is the principal electron acceptor) is designed to allow for heterotrophic denitrification to take place, principally the conversion of nitrate to N_2 . The removal of phosphorous nutrients is carried out by a biological or chemical removal, or a combination, whereby the biological removal is under anaerobic conditions. Therefore, reactions occurring under either aerobic, anoxic or anaerobic conditions might be expected. However, due to the higher biological activity in the aerobic stage, it is expected that most transformations of micropollutants will occur under these conditions (Falås et al., 2016; Reemtsma and Jekel, 1997).

Aromatic moieties The simplest aromatic structure, benzene, can be transformed via the catechol pathway as shown in Figure 1.3. This can proceed via consecutive monooxygenation reactions or by a dioxygenation forming a *cis*-diol followed by rearomatization. Both form catechol as a cleavage substrate (Reineke, 2001). Examples of similar reactions have also been observed to impact micropollutants. Ketoprofen, a non-steroidal anti-inflammatory drug, was transformed during conventional activated sludge treatment. The proposed transformation pathway included a dioxygenation step (Figure 1.3) (Quintana et al., 2005).

The hydroxylation of aromatic moieties is the first step towards formation of a ring-cleavage substrate. Hydroxylation is commonly observed in studies of aromatic micropollutant degradation in activated sludge or in soil environments. Benzotriazols were

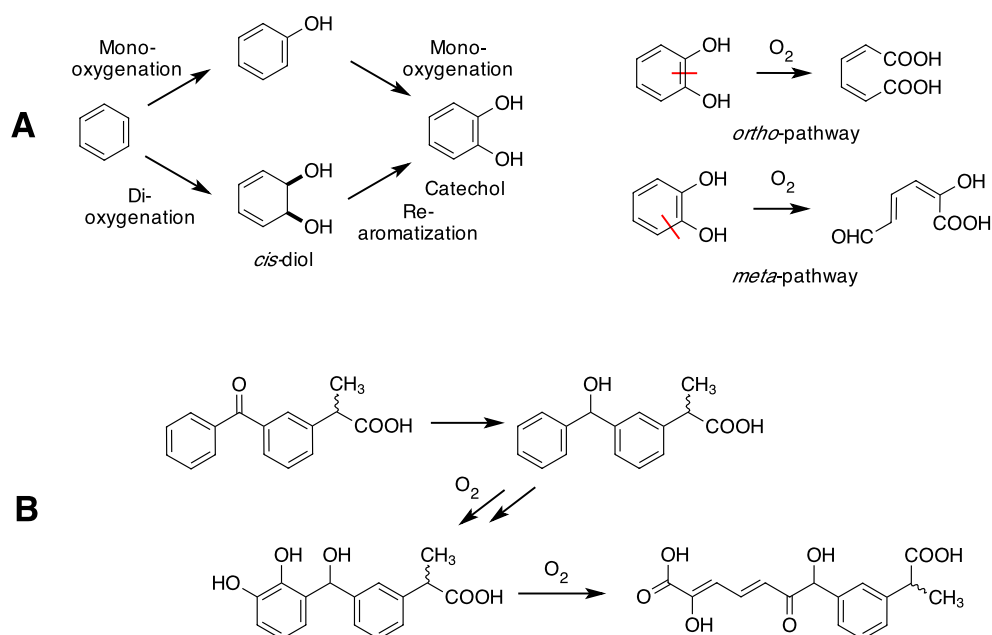


Figure 1.3: A: Reactions of simple aromatic structures by aerobic microorganisms forming the cleavage substrate catechol. Cleavage of catechol by intradiol cleavage (*ortho*-pathway) or extradiol cleavage (*meta*-pathway) (Reineke, 2001). B: Transformation of ketoprofen in contact with activated sludge from a wastewater treatment plant (Quintana et al., 2005)

observed to form various hydroxylated TPs in contact with biofilms in a hybrid moving bed biofilm reactor (Mazioti et al., 2016). In the transformation of triclosan by activated sludge several isomers of mono- and dihydroxy-triclosan TPs were detected (Chen et al., 2015). Further examples include the hydroxylation of the aromatic moieties of irbesartan and ibuprofen in activated sludge (Boix et al., 2016) and the formation of 5-hydroxy-diclofenac during incubation of WWTP effluent (Poirier-Larabie et al., 2016). Heterocyclic aromatics are also known to undergo hydroxylation. For example, the diamino-pteridine moiety of methotrexate was observed to be hydroxylated in activated sludge as a minor transformation reaction of a larger transformation pathway (Kosjek et al., 2015).

Aromatic monooxygenation reactions as described here lead to the formation of phenolic TPs but the subsequent ring-cleavage reactions are not always observed. Phenolic groups are therefore commonly found in transformation pathways either as central intermediate TPs, as final products or as minor TPs alongside the main transformation pathway. Both abiotic and biotic reactions of phenolic moieties were studied in this project due to the important role these types of compounds have (Chapter 3) and the significance of this

transformation process can again be seen in Chapter 4, where hydroxylated aromatics were identified as central, intermediate TPs.

Degradation of aromatic structures under anaerobic conditions via reduction (hydrogenation) is also known to occur (Meckenstock et al., 2004). These types of transformations are not commonly seen with micropollutants in WWTPs but have been studied in other treatment processes such as bank filtration (König et al., 2016).

Aliphatic moieties Degradation of aliphatic carbon chains is typically initiated by activation of the carbon chain by monooxygenation followed by oxidation reactions to produce chain cleavage substrates. The chain is then cleaved in the β -oxidation cycle, first forming a β -keto acid. Cleavage between the α and β carbons leads to loss of acetate in the form of acetyl-CoA (Figure 1.4). Although it is unclear if the same biochemical reactions are involved, similar aliphatic chain shortening reactions have been observed to occur with micropollutants during biological wastewater treatment. An example is the transformation of the antiviral drug penciclovir (Prasse et al., 2011) (Figure 1.4). A similar chain cleavage was observed in metoprolol after O-demethylation and oxidation to metoprolol acid (Rubirola et al., 2014).

Dehydrogenation reactions have also been observed to impact aliphatic carbons, e.g., of bezafibrate, leading to the formation of an alkene (Helbling et al., 2010). Similar reactions with alkyl or aryl hydroxy-groups result in the formation of ketones (Kaiser et al., 2014), quinones or semiquinones (Fischer and Majewsky, 2014; Beel et al., 2013; Gröning et al., 2007). They are commonly observed reactions, are in many cases reversible and may also occur abiotically.

Methoxy groups and ethers Methoxy, or methyl ethers are commonly converted to alcohols or phenols during biological treatment. Examples include the O-demethylation of venlafaxine, which was observed under both aerobic and anaerobic conditions (Gasser et al., 2012), or the O-demethylation of naproxen in soils receiving biosolids (Topp et al., 2008). The cleavage of aromatic ethers such as triclosan (Chen et al., 2015), propranolol (Svan et al., 2016), or mecoprop (Zipper et al., 1999) have also been observed in activated sludge or soil microcosm experiments. One proposed reaction mechanism includes dioxygenation at the α -carbon, producing a hemiacetal which spontaneously cleaves to form alcohol and aldehyde products (White et al., 1996) (Figure 1.5).

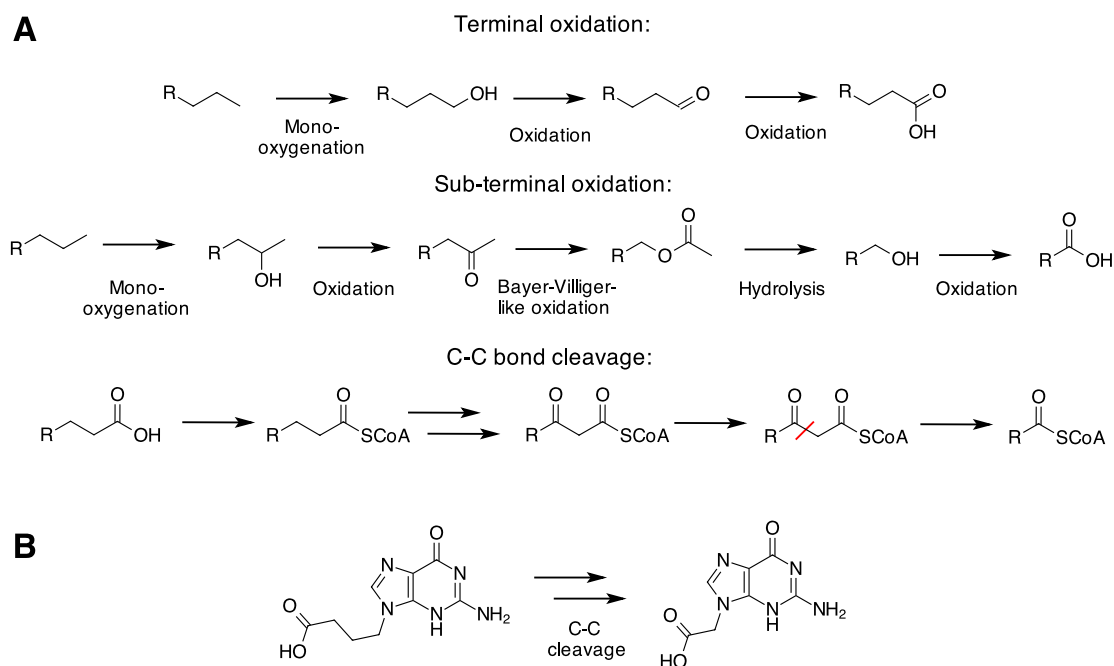


Figure 1.4: A: Typical activation reactions of aliphatic carbon chains forming cleavage substrates (Reineke, 2001). B: Example of the cleavage of the side chain of penciclovir, a reaction which is part of the transformation pathway of penciclovir when in contact with activated sludge (Prasse et al., 2011).

Organohalogenes Degradation of halogenated organic molecules, specifically with Cl-, Br- or I- moieties can entail biological dehalogenation reactions occurring under both aerobic and anaerobic conditions. Many reaction types are known such as dehydrohalogenation, hydrolytic dehalogenation, oxidative dehalogenation and reductive dehalogenation. (Fetzner, 1998). Reductive dehalogenation is of particular interest since in some cases this has been used to initiate the degradation of otherwise recalcitrant, highly halogenated, organic pollutants (Voordeckers et al., 2002; Beeman and Bleckmann, 2002). This type of dehalogenation is more commonly observed in strict anaerobes under anaerobic conditions but has also been postulated to occur under aerobic conditions by different mechanisms (Souchier et al., 2016b). Reductive dechlorination of the micropollutant triclocarban has been observed by the analysis of river sediments, leading to TPs dichlorocarbanilide, monochlorocarbanilide and carbanilide (Miller et al., 2008; Souchier et al., 2016b) (Figure 1.6).

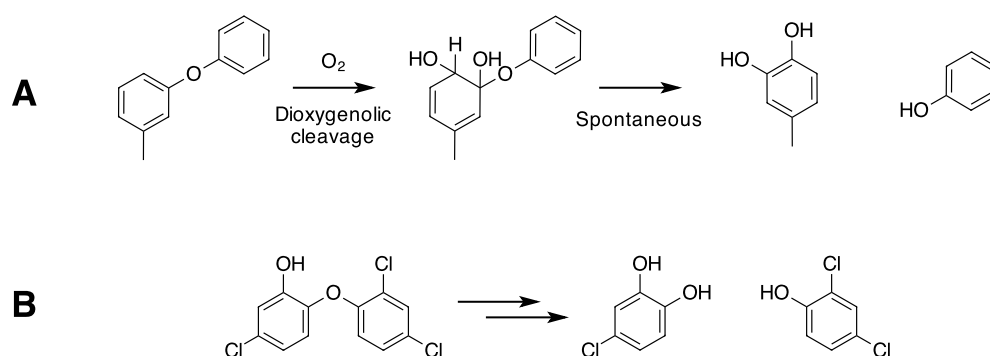


Figure 1.5: A: Proposed bacterial degradation mechanism of 3-methyl-diphenyl ether (Schmidt et al., 1992). B: Observed ether cleavage of triclosan when in contact with activated sludge (Chen et al., 2015).

Amines and amides Micropollutants with methyl amine moieties can be demethylated during biological wastewater treatment leading to the formation of primary or secondary amines. For example, the N-demethylation of methotrexate forming a secondary amine (Kosjek et al., 2015), or similarly the N-demethylation of the dimethylamine moiety of citalopram in activated sludge (Beretsou et al., 2016). These reactions are a type of N-dealkylation that are observed in a large variety of micropollutants, also with larger N-alkyl substituents (Gulde et al., 2016). Other reactions of amines commonly found in biological media include N-oxidation and also conjugation, e.g., acyl conjugation (Gulde et al., 2016). Deamination of the aniline moiety of sulfamethoxazole has been observed in enrichment cultures of ammonium oxidising bacteria (AOB), as well as oxidation to a nitro group (Kassotaki et al., 2016). On the other hand, these reactions have also been observed as chemical transformations under denitrifying conditions (Nödler et al., 2012). Amides are also common structural moieties in micropollutants and hydrolysis reactions have been observed. The cleavage of bezafibrate and valsartan were both observed to occur via amide hydrolysis, producing primary amines and benzoic acid moieties (Helbling et al., 2010).

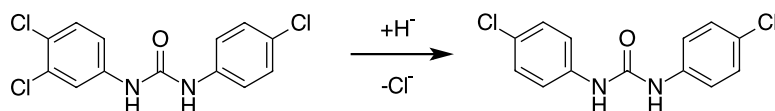


Figure 1.6: One of several postulated reductive dechlorination mechanisms of triclocarban under anaerobic conditions (Souchier et al., 2016b).

Aldehydes, esters, ketones and carboxylic acids Aldehyde moieties, which are also often part of intermediate TPs of micropollutants, e.g., after the cleavage of amines, are in many cases oxidised to carboxylic acids (Gulde et al., 2016). Ester groups in micropollutants are also typically unstable and can hydrolyse as was observed for the methyl ester of the fungicide azoxystrobin (Kern et al., 2009). Many of these reactions can also occur abiotically given the right pH conditions.

Decarboxylation reactions of some carboxylic acid groups can occur abiotically under mild conditions. Biological decarboxylation is well known and as mentioned can be seen in the degradation of aliphatic hydrocarbons. Other forms of decarboxylation have been observed, including oxidative decarboxylation (Kormos et al., 2011). Non-oxidative decarboxylation has also been observed; the decarboxylation of diclofenac observed by Poirier-Larabie et al. (2016) resembles the decarboxylation of 4-hydroxycinnamic acid to 4-hydroxystyrene, which has been observed by strains of facultative anaerobes or lactic acid bacteria (Lindsay and Priest, 1975; van Beek and Priest, 2000).

Conjugation reactions Conjugation reactions of pharmaceuticals (or other chemicals) in the human body is well known (Jakoby and Ziegler, 1990). These reactions have been recently observed in activated sludge, e.g., the sulfate conjugation of triclosan (Chen et al., 2015) as well as N-acylation, N-formylation and N-succinylation of amines (Gulde et al., 2016).

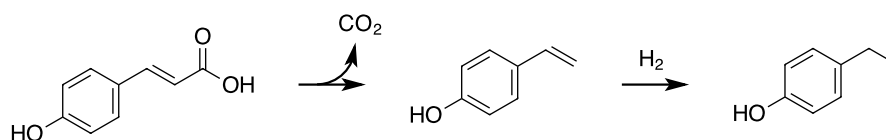


Figure 1.7: Decarboxylation mechanism of 4-hydroxycinnamic acid by lactic acid bacteria (van Beek and Priest, 2000).

Chirality

Micropollutants, like all chemicals, can have chirality. Usually chiral chemicals are sold as racemic mixtures. Some pharmaceuticals may be sold as the pure *R*- or *S*- enantiomer but this is rare (Nguyen et al., 2006). Chiral micropollutants may undergo stereoselective transformation, in the worst case meaning only half of the racemic mixture of stereoisomers is transformed and degraded. Examples are the stereoselective transformation of (*S*)-mecoprop (Zipper et al., 1998) and (*R*)-metoprolol (Souchier et al., 2016a). Chiral

inversion of micropollutants, which can lead to an enantiomeric excess, has also been observed, e.g., for naproxen and ibuprofen (Khan et al., 2014). Finally, the degradation of micropollutants may result in the introduction of further chiral centres forming pairs of diastereomers as postulated by Quintana et al. (2005).

Chemical (abiotic) transformation reactions during biological treatment

Biotic (enzymatically mediated) reactions as mentioned above can involve spontaneous steps, such as the cleavage of hemiacetals formed by oxygenation of ethers. Purely chemically mediated reactions have also been observed to occur during activated sludge treatment. These are reactions which appear to have no connection to the presence of active microorganisms and can impact micropollutants or their biologically formed TPs. For example, Wick et al. (2011b) described the addition of nucleophiles to an α - β -unsaturated ketone in codeinone, similar to a Micheal-addition. The hydrolysis of the antibiotic amoxicillin at neutral pH led to the formation of carboxylic acid moieties, lactam ring formation, and decarboxylation (Hirte et al., 2016). Abiotic reactions can also occur under conditions created due to biological activity, for example, the diazotisation of sulfamethoxazole leading to desamino- and nitro-SMX was observed to occur in the presence of nitrite formed through microbial denitrification (Nödler et al., 2012).

Configuration of biological treatment reactors and the impact on transformation

Many varieties of biological treatment reactor configurations are implemented, examples include conventional activated sludge, granular activated sludge and moving bed biofilm reactors. It is known that reactor configuration can have an impact on micropollutant removal and it has been shown that reactor design can be optimised to improve the degradation of micropollutants (Joss et al., 2006). Reactor configurations promoting the growth of biofilms have shown promising results (Kovalova et al., 2012; Falås et al., 2013), but transformation pathways have not yet been investigated in detail in these systems and how these compare to conventional activated sludge.

1.3 Current progress of research

Current research is dedicated to elucidating transformation pathways of micropollutants during biological wastewater treatment and the knowledge is being collected in databases such as EAWAG-BBD (Kern et al., 2009). The complexity of wastewater treatment processes necessitates detailed investigation of individual compounds and despite the growing body of current literature, for many micropollutants there are still open questions regarding their fate during wastewater treatment. To obtain a detailed and comprehensive picture of micropollutant transformation, more detailed investigations into formation of TPs is needed. Development of research techniques has luckily been accelerated by the recent advances in analytical instrumentation allowing for faster and more sensitive analysis.

The risk of micropollutants in fresh water resources is a public concern and it is the responsibility of public utilities and community leaders to address this issue as quickly as possible. Local and national governments have in some cases taken steps to regulate micropollutant emission to some extent but more comprehensive regulation is needed and also demanded by the public. Detailed understanding of the fate of micropollutants and the associated risks are needed by utilities, regulators and the public to make informed decisions. Removal due to biological or chemical transformation in particular is still a challenge to predict and for many important micropollutants found consistently in WWTP effluents, only an incomplete picture of their fate is available. Transformation reactions can be impacted by the myriad of chemical and biological factors during biological treatment, for example, microbiological community characteristics, process configurations or the structure of biofilms or sludge flocs (Johnson et al., 2015; Khunjar and Love, 2011; Helbling et al., 2012; Göbel et al., 2007; Melvin and Leusch, 2016). However, how these impact specific transformation reactions is not known for most micropollutants and factors influencing removal can not always be generalised across different compounds (Joss et al., 2005). More knowledge of transformation reactions may help explain relationships between diverse groups of micropollutants and their removal. The high complexity may be one cause for the highly variable results of degradation studies, in which a large variance in removal is observed for the same micropollutant, as well as differences in transformation reactions (Göbel et al., 2005; Kovalova et al., 2012; Gröning et al., 2007; Kosjek et al., 2009). Care must also be taken in comparing results from studies which use different experimental procedures. Laboratory testing protocols and experimental techniques used to study micropollutant transformation have been es-

tablished but it is not known if these techniques are applicable for all micropollutants. Further development and standardisation of testing procedures can greatly benefit the interpretation of results across different studies.

1.4 Project goals

The goal of the project was to study the transformation reactions and reaction kinetics of micropollutants during wastewater treatment, considering both chemical and biological reactions in both suspended sludge and biofilm treatment processes. To fill the gaps in the current knowledge of the fate of micropollutants, compounds were chosen for which the understanding of their fate during transformation processes was incomplete. Included in this goal was the task of finding the most appropriate laboratory techniques for the compounds and processes studied. Different test reactor configurations, sampling and analysis strategies were considered and systematically tested. The optimised testing strategies were applied to the investigation of micropollutant transformation with the aims of i) finding possible generalisations in transformation processes which might later aid in the investigation of the fate of similar micropollutants ii) finding possible explanations which underlie the observed removal rates of micropollutants, which are often difficult to interpret with only concentration data of the micropollutant itself and iii) investigating the possible formation of recalcitrant TPs which might pose an environmental risk.

Laboratory batch incubation experiments were implemented with the goal of modelling working treatment processes for the study of micropollutant transformation. A pilot scale, sequencing batch reactor (SBR) system fed with influent wastewater was used as a representative biological treatment reactor. The laboratory incubation experiments were first tested for their applicability in monitoring micropollutant transformation. The model micropollutant used was the antibiotic trimethoprim, which presented an additional challenge for testing due to the possible toxicity of the compound towards microorganisms. Systematic testing of sludge concentrations, dilution types, and spike concentrations in laboratory experiments were carried out to find the appropriate experimental design to mimic the real system. The goal was then to focus on the transformation reactions and kinetics of trimethoprim itself, searching for possible explanations for the high variability of removal of the compound found in different WWTPs.

In the second part of the study, a chemically-mediated transformation of micropollutants

in activated sludge was studied using the model of three phenolic micropollutants. The chemically-mediated reactions were compared to biologically-mediated transformations which occur during wastewater treatment to assess the relevance of each process. Full-scale treatment plants were used to verify lab results. The relevance of the different reaction types and their impact on removal under different conditions was investigated.

Finally, the transformation of the micropollutant diclofenac in WWTPs was investigated. Two different biological process types, moving-bed-biofilm-reactors and conventional activated sludge reactors were compared. A significant difference in the removal of this compound was observed between these two process configurations. The investigation of transformation reactions was carried out with the goal of finding underlying explanations for this variation and to test for the formation of recalcitrant TPs.

1.5 Outline

Biological transformation in contact with activated sludge

Chapter 2 describes investigations into the removal kinetics and transformation reactions of the antibiotic trimethoprim during activated-sludge-based wastewater treatment. The use of laboratory-based incubation experiments to model processes in reactors was systematically tested using different starting conditions. These were compared against monitoring results of a pilot treatment reactor representing a conventional treatment system.

Chemical transformation in contact with activated sludge

Chapter 3 includes the investigations into chemical nitration of phenolic micropollutants (industrial chemicals and one pharmaceutical) which occur in the activated sludge matrix. The reactive species and reaction conditions were investigated in controlled laboratory conditions. The results of these studies were then transferred to laboratory incubation experiments with activated sludge to compare the chemical nitration to biological transformation reactions. Finally, the results were compared to monitoring experiments at two full-scale wastewater treatment plants.

Transformation reactions in contact with biofilms and activated sludge

In Chapter 4, incubation experiments were implemented to investigate transformation reactions in moving bed biofilm reactors and these were compared to those in activated sludge. The investigation focused on the transformation of the anti-inflammatory diclofenac. The transformation pathways in the two systems showed clear differences and the results could be verified by monitoring campaigns at two full-scale wastewater treatment plants which included both reactor types.

Final conclusions

Combined conclusions of the studies and outlook for further research are discussed in Chapter 5.

Chapter 2

New insights into the transformation of trimethoprim during biological wastewater treatment

Kevin S. Jewell, Sandro Castronovo, Arne Wick, Per Falås, Adriano Joss, Thomas A. Ternes. 2016. Water Research 88, pp. 550–557.

Abstract

The antibiotic trimethoprim (TMP), a micropollutant found at $\mu\text{g/L}$ levels in raw wastewater, was investigated with regard to its (bio)transformation during biological wastewater treatment. A pilot-scale, nitrifying/denitrifying sequencing batch reactor (SBR) fed with municipal wastewater was monitored for TMP removal during a 16-month monitoring study. Laboratory-scaled bioreactors spiked with TMP were applied to identify the transformation products (TPs). In total, six TPs could be identified from TMP. However, the TP formation was influenced by the spike concentration. At an initial concentration of $500 \mu\text{g/L}$ TMP, only two TPs were found, whereas at $5 \mu\text{g/L}$ a completely different transformation pathway led to four further TPs. At low concentrations, TMP was demethylated forming 4-desmethyl-TMP, which was then quickly hydroxylated, oxidised and cleaved forming 2,4-diaminopyrimidine-5-carboxylic acid (DAPC) via two intermediate TPs.

DAPC was detected in the SBR effluent in a 3-d composite sample with 61 ng/L, which accounts for 52% of the attenuated TMP. The primary degradation at low spiking levels was best modelled by a pseudo-first order kinetic. Considering the SBR, the model predicted a TMP removal of 88% to 94% for the reactor, consistent with a monitoring campaign exhibiting an average removal of >83%. Both the TP formation profiles and kinetic modelling indicated that only the results from the bioreactor tests at low spike concentrations were representative of the transformation in the SBR.

2.1 Introduction

The consumption of pharmaceuticals has become a common and important part of modern healthcare. However, these anthropogenic compounds are a potential hazard to the aquatic environment (Luo et al., 2014). Predominantly, these compounds are released into the local sewer system either by excretion via urine/faeces or via direct disposal in the toilet. Most wastewater treatment plants (WWTPs) are primarily designed to remove nutrients and easily degradable carbon compounds. It has been shown that they have limited capacities to remove pharmaceuticals (Joss et al., 2006), making them major sources of these micropollutants in rivers and streams (Metcalf et al., 2010; Sengupta et al., 2014). Certain pharmaceuticals, such as antibiotics, are of particular concern since emission may foster the development of resistant pathogens discharged into the aquatic environment (Marti et al., 2014). To mitigate the release of micropollutants, an upgrade of conventional wastewater treatment is currently discussed in many countries, including Germany (Hillenbrand et al., 2015). In Switzerland, 2014 saw a revision of the water protection law, which includes the upgrading of a number of Swiss WWTPs specifically for the elimination of micropollutants (Eggen et al., 2014). In Switzerland, the upgrading approaches are usually based on advanced treatment such as activated carbon filters and ozonation, but there is interest in improving and understanding biological processes, which are already established.

In the current study the antibiotic trimethoprim (TMP) was investigated in detail with regard to its removal via biological wastewater treatment. TMP is an antibiotic usually administered in combination with sulfamethoxazole. These two

antibiotics target two parts of the bacterial tetrahydrofolic acid synthesis pathway, which is an important cofactor, e.g., for DNA synthesis (Brogden et al., 1982). TMP has been detected in WWTP influents at concentrations ranging from (0.14 to 1.3) $\mu\text{g}/\text{L}$ and in effluents from (0.02 to 1.3) $\mu\text{g}/\text{L}$ (Le-Minh et al., 2010). In rivers, concentrations of up to 0.02 $\mu\text{g}/\text{L}$ have been reported in the UK (Roberts and Thomas, 2006) and up to 0.04 $\mu\text{g}/\text{L}$ in Japan (Murata et al., 2011). Reports about the removal of trimethoprim in WWTPs are rather contradictory. In several studies it has been found that TMP is quite resistant to biological wastewater treatment (Göbel et al., 2005; Lindberg et al., 2006), while other studies reported a partial removal of TMP ranging from 40% to 50% (Batt et al., 2006; Radjenović et al., 2009) or even an almost complete removal (Kovalova et al., 2012). However, the reasons for these different results are currently not known. Previous reports about the transformation of TMP also exhibit significant differences. In total, five transformation products (TPs) of TMP have been identified, resulting from hydroxylation reactions and ring opening, but the TPs were not consistent between the different studies (Brenner et al., 2011; Eichhorn et al., 2005; Yi et al., 2012). These TPs have been identified in effluent from an anaerobic reactor treating hospital wastewater, in reactors fed with synthetic wastewater or in lab-scale batch reactors, but have still not been found in municipal WWTPs. Elucidation of TPs is a key aspect of understanding the possible removal mechanisms of micropollutants and to assess whether toxic or refractory products remain after transformation. The current interest in the removal of micropollutants by biological treatment and the growing concern of antibiotic resistant pathogens support the further assessment of the relevance of the reported TPs and the associated transformation pathways of the antibiotic TMP during biological municipal wastewater treatment.

TMP can be transformed in biological wastewater treatment systems. Where removal is observed it is often attributed to removal under aerobic (nitrifying) conditions (Eichhorn et al., 2005; Yi et al., 2012; Batt et al., 2006). However, it is yet unknown if the variability of the TMP removal depends on differences in the investigated treatment processes (Göbel et al., 2007) or if there is temporal variability at fixed treatment conditions over long time scales. Since TMP inhibits the DNA synthesis of certain bacteria, it cannot be ruled out that elevated TMP concentrations often used in lab-scale studies alters the transformation reactions as

well as the transformation kinetics. Thus, a deeper look at the aerobic transformation reactions and kinetics at different TMP concentrations is warranted.

Therefore, the objectives of this study were to i) measure the variability of TMP removal in an activated sludge system treating municipal wastewater over a 16-month monitoring period; ii) measure the kinetics of TMP removal in activated sludge in sludge-seeded laboratory-scale reactors under aerobic conditions spiked at different TMP concentrations; iii) investigate the transformation reactions and removal pathway(s) of TMP in these reactors; and iv) transfer the findings of the laboratory studies to the activated sludge system to assess the relevance to native conditions.

2.2 Methods

2.2.1 Pilot-scale sequencing batch reactor

A 12 L suspended sludge sequencing batch reactor (SBR) situated on the site of a municipal WWTP with 220 000 person equivalents was used for the study. Incoming municipal wastewater with average concentrations of 220 mg/L BOD, 70 mg/L N_{tot} , and 16 mg/L P_{tot} was treated mechanically (screening, grit removal, and sedimentation) at the plant, before being fed to the pilot reactor. The pilot reactor was operated as a conventional nitrification/denitrification process with fixed operational settings: 10 d Solids Retention Time (SRT), 12 h hydraulic retention time (HRT), and a batch duration of 3 h (1 h anoxic conditions followed by 2 h oxic conditions) with a fixed influent volume. On-line sensors connected to a programmable logic controller (Wago 750-881) and a SCADA system (Citect V7.2, Schneider Electric), allowed control of dissolved oxygen concentrations during the oxic phase ((1 to 3) mg/L), and fill levels during all feed and discharge events ((9 to 12) L) as well as continuous monitoring of temperature ((15 to 25) °C) and pH (7.0 to 7.5).

Influent and effluent samples were collected as 3-d composite samples during a 16-month period. Samples were taken after the settling phase by an automated sampler with refrigerated storage containers. After collection, the samples were immediately filtered (0.45 µm, regenerated cellulose) and stored at -20 °C. A

stability test indicated that the compounds of interest were stable during the 3-day collection period. Further details are given in Appendix A. The samples were monitored for TMP and its TP concentrations by direct injection, or in some cases via a Solid Phase Extraction (SPE) enrichment step, as described in Section 2.2.5. Additional measurements of dissolved organic carbon (DOC) and inorganic nitrogen species (NO_3^- -N, NO_2^- -N, and NH_4^+ -N) confirmed a stable removal of DOC averaging 60%, and ammonium removal averaging 95% during the monitoring period. Detailed parameters are given in Appendix A.

2.2.2 Chemicals

Trimethoprim (TMP) was purchased from Sigma Aldrich (Schnelldorf, Germany). Its metabolite 4-desmethyl-TMP the internal standard trimethoprim-d3 was purchased from Toronto Research Chemicals (North York, Canada). Ethyl 2,4-diaminopyrimidine-5-carboxylate was purchased from Activate Scientific (Prien, Germany). All chemicals used for analysis were of $\geq 95\%$ purity.

2.2.3 Lab-scale bioreactor incubation experiments

To study the fate of trimethoprim in contact with nitrifying activated sludge, 400 mL bioreactor experiments were set up in light-protected vessels and inoculated with nitrifying activated sludge from the SBR. Activated sludge was either diluted 1:1 with SBR influent for the low dilution experiments or diluted 20:1 with SBR effluent for the high dilution experiments. Effluent was chosen for the 20:1 dilution, since diluting with influent is not practical due to the large matrix effects of influent leading to analytical difficulties. To test the effect of changing the dilution matrix alone, a third experiment was conducted with 1:1 sludge dilution with WWTP effluent. All incubation experiments were conducted with at least one replicate. Throughout the incubation period, the sludge was stirred and aerated with a regulated mixture of air and CO_2 via a diffuser. CO_2 was added to the gas mixture to compensate for CO_2 loss through purging, which would otherwise have led to pH instability (Wick et al., 2009). The pH was maintained at the same level as in the pilot-scale SBR (6.5–7.5). TMP was spiked to the experiments after at least 1 h equilibration time at concentrations of 5 $\mu\text{g}/\text{L}$ or 500 $\mu\text{g}/\text{L}$. The

lower spike level (5 µg/L) was chosen to ensure that down to 1% of TP formation from the parent was still within a detectable range. Control experiments were left unspiked. Further control experiments without biological activity were run concurrently. For these abiotic controls the sludge was filtered (0.2 µm, polyethersulfone) to remove the microbial biomass. Samples of all lab-scale experiments were taken at regular intervals, were immediately filtered (0.45 µm, regenerated cellulose) and were stored at 4 °C prior to analysis via LC–tandem MS.

2.2.4 Kinetic analysis

The degradation kinetics were modelled according to [Schwarzenbach et al. \(2005\)](#) by either a pseudo-first-order rate law (Equation 2.1) or by a pseudo-zero-order rate law (Equation 2.2):

$$\frac{dC_{\text{TMP}}}{dt} = -k_{\text{biol}}C_{\text{TMP}}X_{\text{SS}} \quad (2.1)$$

$$\frac{dC_{\text{TMP}}}{dt} = -k'_{\text{biol}}X_{\text{SS}} \quad (2.2)$$

where C_{TMP} is the trimethoprim concentration (µg/L), X_{SS} the sludge concentration (g_{SS}/L), k_{biol} is the pseudo-first-order rate constant in L/(g_{SS} · d), and k'_{biol} the zero-order rate constant in µg/(g_{SS} · d). The uncertainty of k_{biol} was determined by analysis of 3 replicate batches, or where only 2 replicates were made, by statistical analysis of the regression.

2.2.5 Analytical methods

TMP and its TPs other than DAPC were analysed by LC–tandem MS via direct injection using an Agilent HPLC system equipped with a ZORBAX Eclipse Plus C18 column (150 mm × 2.1 mm, 3.5 µm, Agilent Technologies) coupled to a QqQ-LIT-MS (API 5500 QTRAP, SCIEX, Darmstadt, Germany) with ESI in positive ionisation mode. As mobile phase, water with 0.1% formic acid buffer and methanol with 0.1% formic acid buffer were used. Quantification of TMP was

performed in MRM mode (Multiple Reaction Monitoring) using trimethoprim-d3 as an internal standard.

High-resolution mass spectra and MSⁿ fragmentation experiments for the identification and characterisation of TPs were obtained by Orbitrap-MS (LTQ Orbitrap Velos) coupled by ESI to an Accela HPLC system (both from Thermo Scientific, Bremen, Germany) running the same chromatographic method as described above.

Analysis of DAPC in effluent wastewater included a sample enrichment step using solid phase extraction. Samples were extracted using ENVI-Carb graphitic carbon cartridges (Sigma Aldrich) at pH 7. The cartridges were conditioned with 6 mL methanol and 8 mL of pristine groundwater (pH 7). Wastewater samples (50 mL, pH 7) were loaded onto the cartridges, which were then dried under a light nitrogen gas flow and eluted with 10 mL methanol. The organic phase was evaporated to 0.5 mL at 35 °C under a gentle nitrogen flow. Water (0.3 mL) was added and the mixture was again evaporated to 0.5 mL. Analysis was carried out by LC–HRMS on a QToF-MS (5600 TripleTOF, Sciex) coupled by ESI in positive ionisation mode to an Agilent HPLC system running the same chromatographic method as described above.

For the quantification of DAPC, a direct injection method was used utilising LC–tandem MS and a standard addition method on the same QqQ-LIT-MS system described. To improve the retention a different chromatographic method was used. The HPLC was equipped with a Hypercarb graphitic carbon column (150 mm × 2.1 mm, 3 µm, Thermo Scientific). The mobile phases for gradient elution were water and acetonitrile. The water was buffered to pH 10 with 0.1% ammonium formate, while 0.1% ammonia was added to acetonitrile.

Detailed instrumental parameters including MRM transitions used in the above methods are provided in Appendix [A.1](#).

2.3 Results and discussion

2.3.1 Variability of primary removal over time

The concentrations of TMP were monitored in the pilot-scale SBR, which was configured as a nitrifying/denitrifying reactor and fed with the primary effluents of a municipal WWTP as described in section 2.1. Both concentrations in SBR influent and effluent were measured in 3-day composite samples. The elevated fluctuations of the TMP influent concentration has been observed previously (Coutu et al., 2013). Variable influent concentrations of pharmaceuticals are a common phenomenon and are linked to temporal/spatial variability in their use as well as changes in water flow of the sewer system (Petrie et al., 2015).

Initially, the removal of TMP was relatively low. During the initial start-up phase, the average TMP removal was 34% (Figure 2.1). This included a period of heavy rainfall in the catchment area of the treatment plant, which caused large variations in the measured TMP removal. These effects can be attributed to dilution of the wastewater and possible biomass loss in the reactor or varying dilution of the SBR influent and effluent samples, which could have led to the very low removals observed. After the start-up phase the removal increased and remained relatively constant with an average of > 83% removal during the operational phase. Although the reactor was able to remove nutrients, nitrogen and other micropollutants during both periods, the high removal efficiency of TMP was first achieved after 7 months of operation.

A TMP removal of > 83% is uncharacteristically high for nitrifying activated sludge reactors with an SRT of 10 d Batt et al. (2006); Radjenović et al. (2009). However, this does not appear to be an intrinsic process and the removal shows development over time. Since the removal of TMP is a biological process, as shown in the next section, this may be attributed to the microbial community in the reactor which developed in the summer of 2013. Incubation experiments conducted with the SBR sludge and TMP were therefore inoculated with sludge after it had achieved this TMP degrading ability.

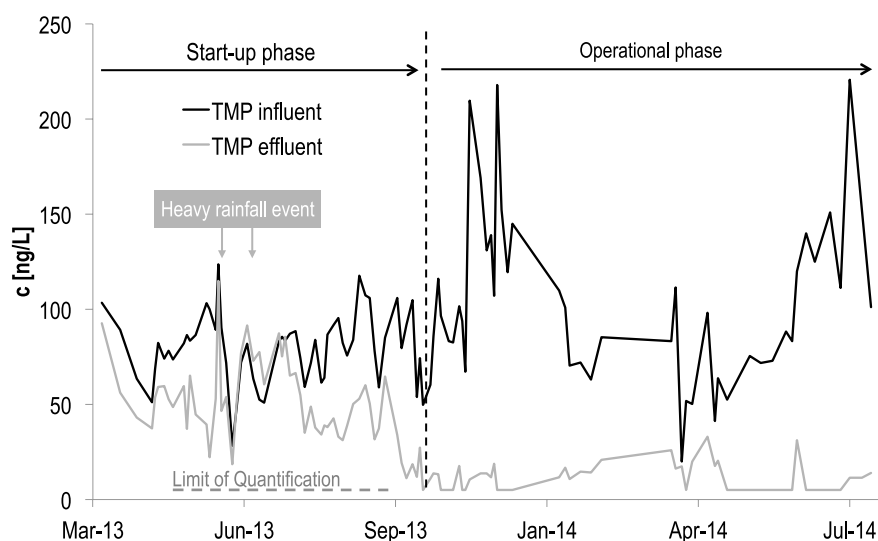


Figure 2.1: Concentrations (ng/L) of TMP in 3-day composite samples of influent and effluent of a pilot-scale SBR over 16 months of the experiment (7-month start-up phase and 9-month operational phase).

2.3.2 Incubation of trimethoprim in aerobic sludge

The degradation of trimethoprim (TMP) was investigated in lab-scale bioreactors inoculated with activated sludge from the SBR. To assess the influence of the TMP concentration and the effects of the wastewater matrix on the TMP removal, incubations were performed at different spike levels (5 $\mu\text{g/L}$ and 500 $\mu\text{g/L}$) and sludge dilutions (1:1 and 1:20) with influent wastewater (primary effluent of the WWTP) or effluent wastewater. To confirm that the removal in these incubations was associated with the biomass, a control reactor with sludge filtrate was also established and exhibited no TMP removal or formation of TPs during 4 days of incubation.

In the first set of experiments, the sludge was diluted 1:1 with influent wastewater and spiked with TMP at two different concentrations (500 $\mu\text{g/L}$ and 5 $\mu\text{g/L}$), (Figure 2.2a and b). Removal of TMP was observed in both of these experiments, but proceeded at different rates (Table 2.1). The primary degradation at 5 $\mu\text{g/L}$ TMP (low spike level) was fast, whereas the primary degradation at 500 $\mu\text{g/L}$ TMP (high spike level) was slower.

When the sludge dilution was increased from 1:1 to 1:20 and the wastewater matrix

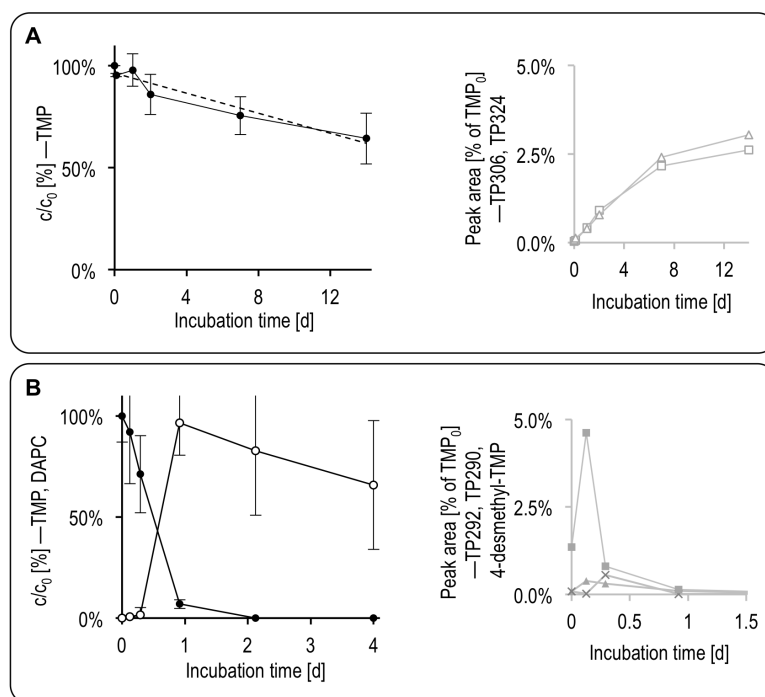


Figure 2.2: Time courses of TMP and TPs in lab-scale reactor experiments with activated sludge diluted with influent wastewater. TMP (●), TP306 (◻), TP324 (△), 4-desmethyl-TMP (■), TP292 (×), TP290 (▲) and DAPC (○). A: $c_0 = 500 \mu\text{g/L}$, influent-sludge ratio = 1:1, 12 d incubation time, $n = 3$. The dotted line represents a zero-order kinetic model. B: $c_0 = 5 \mu\text{g/L}$ influent-sludge ratio = 1:1, 4 d incubation time, $n = 2$.

was changed from influent to effluent, no removal of TMP could be observed in the experiment with high spike level ($500 \mu\text{g/L}$; Figure 2.3a). At the low spike level ($5 \mu\text{g/L}$, Figure 2.3b), a significant dissipation took place. However, this removal was still slower than in the 1:1 dilution experiment (Figure 2.2b).

In the last experiment, $5 \mu\text{g/L}$ TMP was incubated in sludge diluted 1:1 with reactor effluent instead of the reactor influent (Figure 2.3c). The results again show a contrast to the 20:1 dilution with effluent (Figure 2.3b), where the removal is much slower (DT50 of 10 d versus 1 d) (Table 2.1). The kinetics appears to fit more closely to Figure 2.2b, where influent dilution was used (also 1:1), albeit with a longer DT50. Clearly, changing the dilution matrix had an impact on degradation. However, this was not as significant as changing the level of dilution or the spike concentration of TMP.

The data in Figure 2.2 and Figure 2.3 suggest that it would be difficult to fit a

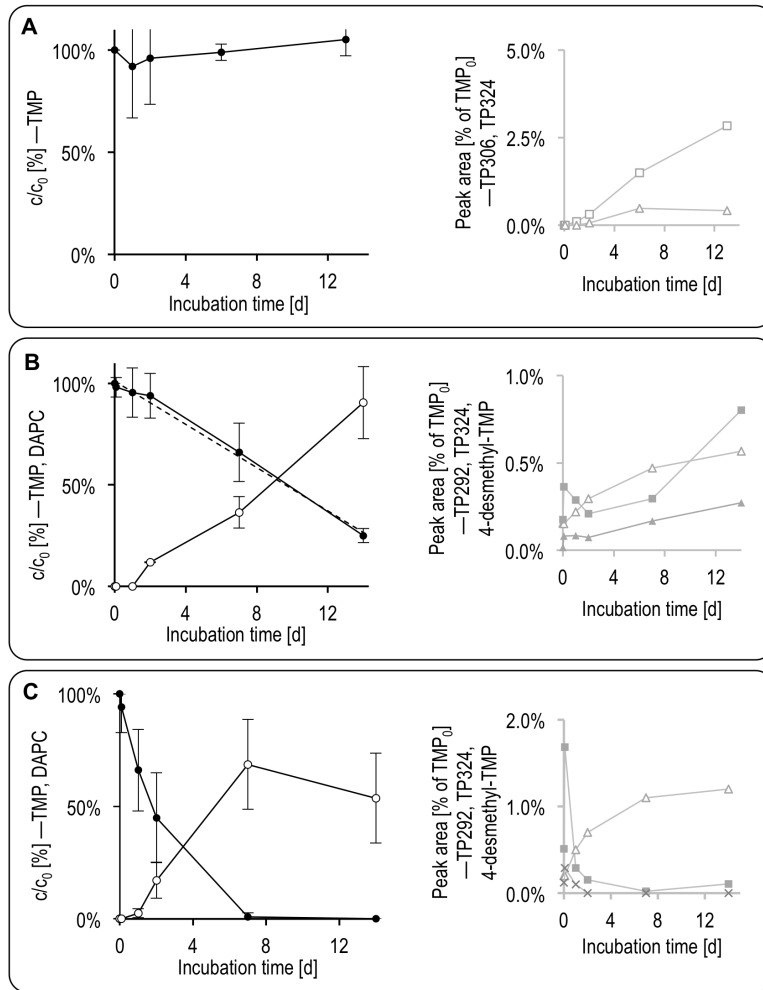


Figure 2.3: Time courses of TMP and TPs in lab-scale reactor experiments with activated sludge diluted with effluent wastewater. TMP (●), TP306 (□), TP324 (△), 4-desmethyl-TMP (■), TP292 (×) and DAPC (○). A: $c_0 = 500 \mu\text{g/L}$, effluent-sludge ratio = 20:1, $n = 2$. B: $c_0 = 5 \mu\text{g/L}$, effluent-sludge ratio = 20:1, $n = 3$. The dotted line represents a zero-order kinetic model. C: $c_0 = 5 \mu\text{g/L}$, effluent-sludge ratio = 1:1, $n = 2$.

pseudo-first-order kinetic model to the degradation shown in Figure 2.2 and Figure 2.3 (high TMP concentration or high sludge dilution). A zero-order model gives a better fit, shown by the dotted lines. The data shown in 2b and 3c suggests more typical degradation kinetics that could fit a pseudo-first order rate law. The rate constants for both kinetic models are given in Table 2.1. However, further studies at higher sampling frequency are needed to confirm the kinetic order. Comparison of pseudo-first order rate constants (k_{biol}), show these to be highest at low spike

Table 2.1: Summary of kinetic results. Rate constants k_{biol} were determined by Equation 2.1 or 2.2 depending on the kinetic order: k_{biol} for pseudo-first-order (1), k'_{biol} for pseudo-zero-order (0). DT50 is time needed for 50% TMP removal, and \pm indicate the uncertainty expressed as 95% confidence intervals.

TMP spike conc. ($\mu\text{g/L}$)	Sludge dilution	Figure	Estimated kinetic order	DT50 (d)	k_{biol} L/(gSS \cdot d)	k'_{biol} $\mu\text{g}/(\text{gSS} \cdot \text{d})$
5	1:1 infl.	2.2b	1	0.2	3.0 ± 0.1	5 ± 3
5	1:20 effl.	2.3b	0	9.6	0.09 ± 0.01	0.23 ± 0.02
5	1:1 effl.	2.3c	1	1.2	0.63 ± 0.02	0.5 ± 0.3
500	1:1 infl.	2.2a	0	> 14	0.03 ± 0.01	9 ± 4
500	1:20 effl. No dilution	2.3a	No removal	–	–	–
1 ^a	No dilution	A.18	1	0.1	4.0 ± 0.5	–

infl.: dilution with WWTP Influent, effl.: dilution with WWTP effluent.

^a Experiment conducted in the SBR running in batch mode (no cycling). The uncertainty was estimated by statistical analysis of the regression.

concentrations and low dilution. The zero-order rate constants (k'_{biol}) are based on absolute concentration changes and are therefore more difficult to compare, but are also generally higher at low sludge dilution.

For a more accurate determination of the kinetics of TMP removal, the SBR itself was spiked with 1 $\mu\text{g/L}$ TMP and run in batch mode (no cycling) for two days. A high sampling frequency (8 samples/d) allowed a clear interpretation of the kinetics showing that a pseudo-first-order model fits very well (Table 2.1 and Figure A.18 in the Appendix).

It can be concluded that increasing the TMP to biomass ratio, either by a higher initial TMP concentration or by a significant sludge dilution, lowers the biological rate constants of TMP. Similar kinetic effects of higher substrate concentration have also been observed in degradation studies of ibuprofen (Collado et al., 2012). More recent studies of TMP degradation have found that rate constants are not impacted as long as the TMP to COD ratio remains below 2×10^{-3} (Su et al., 2015). This level lies approximately between the two extreme cases tested in this study (around 1×10^{-4} and 2×10^{-2}). This supports the result that the removal kinetics can change at higher TMP spike concentration and higher matrix dilutions. To further investigate if this is due to changing kinetics of one primary transformation reaction, as a function of TMP to biomass ratio, or if multiple

transformation reactions are involved, each with different kinetics, the formation of TPs was elucidated.

2.3.3 Identification of transformation products of TMP removal

The TMP incubation experiments with activated sludge were analysed by LC–HRMS to identify transformation products (TPs) and thereby elucidate possible transformation pathways of TMP.

Experiments with high TMP concentration (500 µg/L)

In the experiments with high TMP concentration (Figure 2.2 and Figure 2.3a), in total two TPs were identified during the incubation period: TP306 and TP324. Both could be initially characterised by their chemical formulae and MS² fragmentation spectra (Figure A.2 to A.3 in the Appendix). The two TPs matched well with those reported by Eichhorn et al. (2005) with respect to their exact masses (i.e. their molecular formulae) and their MS² fragmentation spectra. These TPs were present in both high and low sludge-dilution experiments (Figure 2.2 and Figure 2.3a, respectively), although TMP dissipation was only observed at low sludge dilution (Figure 2.2a). Quantification was impossible since reference standards were not available. However, by plotting their peak areas as a percentage of the initial TMP peak area over time, their formation rates were assessed. In the high dilution experiment, although TP formation was observed there was no observable removal of TMP (Figure 2.3a). The low signals of these TPs would suggest they do not represent a significant fraction of TMP removal. TP306 is formed by a hydroxylation, while TP324 is formed by hydroxylations and several subsequent redox reactions (Figure 2.4a).

Experiments with low TMP concentration (5 µg/L)

The TP identification in the experiments with 5 µg/L TMP and with low sludge dilution (1:1) provided a different picture. Surprisingly, four new TPs were found which appeared sequentially as TMP was degraded. The chemical structures of the TPs were elucidated by their MS² fragmentation patterns (Figure A.4 to A.7

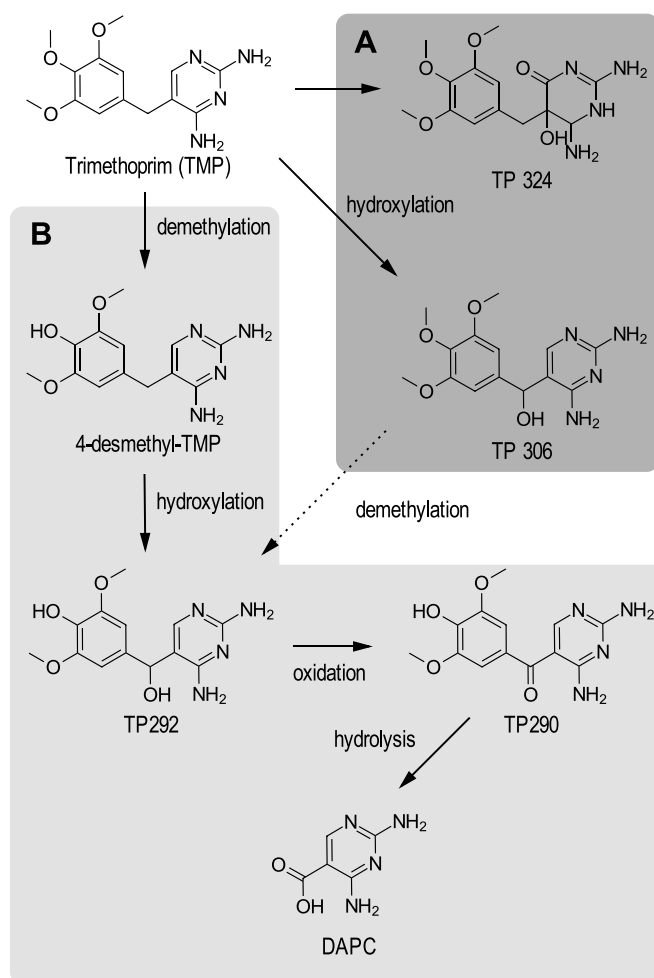


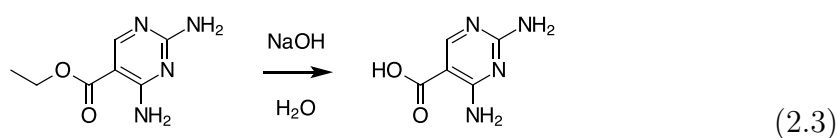
Figure 2.4: Observed TPs of TMP under aerobic conditions in activated sludge. A: Reactions dominating when 500 µg/L TMP were amended. TP306 and TP324 were previously reported by Eichhorn et al. (2005). B: Reactions found to dominate when 5 µg/L TMP were amended to the reactor. The dashed arrow represents a minor pathway.

in the Appendix). The time courses of each TP are shown in Figure 2.2b. The first three TPs were formed and dissipated in quick succession, which is typical of intermediates in consecutive reactions. These also have a low steady-state concentration, which can be seen from their low peak intensities in comparison to TMP. The most prominent of these TPs had an m/z -ratio of 277.13, corresponding to an exchange of $-\text{CH}_3$ by a hydrogen atom resulting from a demethylation of one of the aromatic methoxy moieties present in TMP. By comparing the retention time and fragmentation pattern with an analytical standard, the formation of 4-desmethyl-

TMP was verified (Figure 2.4b). This TP is also a human metabolite of TMP, along with 3-desmethyl-TMP and two N-oxides; in total, around 2.2% of ingested TMP is excreted in the form of 4-desmethyl-TMP (Sigel et al., 1973).

The two other TPs formed at the beginning had the m/z-ratios of 293.12 and 291.11 (TMP has a m/z-ratio of 291.14, which can be easily resolved). Both TPs showed a demethylation of one aromatic methoxy group and the addition of oxygen and differed only by 2H atoms indicating that a redox reaction took place. The position of the oxygen on TP290 could be elucidated by the MS² spectra, showing that an additional oxygen atom was inserted between the phenolic and pyrimidine ring (Figure A.6 in the Appendix). Since the formation of both TPs was closely related and as TP292 was formed before TP290, it can be concluded that TP290 was formed by the oxidation of TP292 (see right graph in Figure 2.2b). All MS² fragments of TP292 showed a loss of water which was not observed in 4-desmethyl-TMP or TP290. This suggests that an aliphatic hydroxyl group is located between the two aromatic rings, which was then oxidised to a ketone forming TP290.

The fourth TP of TMP had a smaller mass with only 155.06 and was more stable in contrast to the other TPs formed. Hence, it accumulated to higher concentration levels in the experiment. Based on the molecular formula and the MS² spectra it was postulated that the pyrimidine ring of TMP was still unaltered, while the di-methoxy-phenolic ring was cleaved and replaced by a carboxylic moiety. Since a reference standard of this TP (2,4-diaminopyrimidine-5-carboxylic acid, DAPC) was not commercially available this TP was synthesised in our laboratory from the ethyl ester derivative by ester hydrolysis (Equation 2.3).



Details of this synthesis are given in Appendix A. The chemical structure of the synthesised DAPC, verified by HRMS and MS², was identical to DAPC formed in the incubation experiments during TMP transformation. The quantification of DAPC showed that it accounted for 90% of the TMP portion degraded in the incubation experiment (Figure 2.2b). Hence, it can be confirmed that the proposed transformation pathway was dominant in this experiment, leading to DAPC via

4-desmethyl-TMP, TP292 and TP290 (Figure 2.4b).

The sequence of the pathway was further verified by directly spiking 4-desmethyl-TMP (500 $\mu\text{g/L}$) separately to a sludge-inoculated reactor. In this experiment, 4-desmethyl-TMP was immediately degraded and TP292, TP290 and DAPC were formed in the same order as was observed when TMP was spiked (Figure A.8a in the Appendix). Although a slow removal of DAPC could be observed (Figure 2.2b), no further TPs could be identified. DAPC was also previously found as a photodegradation product of TMP (Michael et al., 2012).

TP306 was only observed in the experiments with high TMP concentrations (500 $\mu\text{g/L}$), while TP324 was also detected in small amounts when the reactor was amended with low concentrations of 5 $\mu\text{g/L}$ TMP at high dilution or when effluent was used for dilution (Figure 2.3b and c, respectively). It is therefore possible that under these conditions, which are of intermediate TMP to biomass ratio, pathway A (Figure 2.4) plays a minor role. It cannot be totally ruled out that TP306 can be demethylated into TP292 and thus represents a minor transformation pathway (dashed arrow in Figure 2.4). However, this demethylation was not seen in the experiments spiked with 500 $\mu\text{g/L}$ TMP, where TP306 formation was observed. Obviously, the formation of TP306 and TP324 is favoured at higher TMP to biomass ratios, and 4-desmethyl-TMP at lower TMP to biomass ratios, but both reactions, demethylation and hydroxylation, can occur simultaneously as the initial TMP reaction.

Interpretation of the kinetic experiments and observed transformation pathways

Based on the transformation pathways, the different kinetics described in the previous section were caused by more than one initial transformation reaction. At a high initial concentration of TMP (500 $\mu\text{g/L}$), the previously reported hydroxylation reactions (Eichhorn et al., 2005) were dominant (Figure 2.4a), whereas at low initial concentration (5 $\mu\text{g/L}$) a different pathway, beginning with demethylation, was favoured (Figure 2.4b). This example clearly emphasises the importance of the concentration of antibiotics in biodegradation experiments.

Several reasons can be postulated for this observation including toxic or inhib-

ition effect of the antibiotic TMP on bacteria or enzymes that are involved in TMP transformation. Although a general toxic effect on sludge bacteria is rather unlikely, since for sludge bacteria an EC₅₀ of 16 mg/L TMP has been reported (Halling-Sørensen et al., 2000), a toxic/inhibition effect on key species or enzymes carrying out the demethylation of TMP cannot be ruled out.

Another possibility is based on enzyme kinetics with different enzyme saturations of two alternative transformation pathways (Chen et al., 2010; Houston, 2006) or a similar effect caused by differences in membrane transport kinetics. If the enzymes (or transport proteins) of the demethylation pathway quickly reach their saturation at higher TMP concentrations (i.e. the turnover becomes limited by the amount of available free enzyme) the hydroxylation pathway would be favoured, if its enzyme saturation is not reached so quickly. Thus, the hydroxylation rate would increase proportional with the growing concentrations of TMP, meaning these reactions become more dominant. On the other hand at low TMP concentrations the pathway starting with demethylation would be much faster than the hydroxylation pathway and therefore dominates the TMP transformation.

A third possibility is a substrate induced adaption at higher TMP concentrations promoting i) the growth of bacteria involved in the TMP transformation by hydroxylation or ii) the expression of the corresponding enzymes. An induced bacterial growth scenario is considered unlikely, since a lag-phase in TMP removal would be expected to occur in the high spike experiment (Figure 2.2a), which was not observed. However it cannot be excluded that an induced enzyme expression of the existing community might be playing a role. Further investigation could help to elucidate which scenarios are more likely, for example toxicity studies, an examination of enzyme kinetics or gene expression during the incubation experiments. These were however not possible within the scope of this study.

In the experiment where an elevated concentration of 500 µg/L 4-desmethyl-TMP was amended to the bioreactor containing a highly diluted sludge (20:1), a fast removal was observed, comparable to the less diluted sludge with a low TMP spike (Figure 2.2b and A.8a in the Appendix). Thus, regardless of the effect being kinetic or based on toxicity, obviously the O-demethylation reaction is impacted the most by the higher concentration of TMP.

2.3.4 Comparing kinetics and transformation pathways in the laboratory and the SBR

Comparing the trimethoprim degradation kinetics between laboratory- and pilot-scale

In the on-site SBR, where the TMP concentration is low and the sludge concentration is high, it was expected that TMP transformation would occur according to Figure 2.2b (low spiking level, 5 µg/L, low dilution with influent wastewater) or the batch mode-experiment at 1 µg/L (Figure A.18 in the Appendix). To compare this with the observed removal in the pilot reactor, a modelling approach was used. Since studies of the anoxic removal of TMP have found that it has rate constants comparable to, or lower than those under aerobic conditions [Su et al. \(2015\)](#); [Burke et al. \(2014\)](#), two modelling scenarios were applied: one with similar removal under aerobic and anoxic conditions and one with negligible removal under anoxic conditions. Biological degradation in the SBR was modelled at a fixed influent concentration by iterating Equation 2.1 over 20 consecutive batches with a duration of 3 h, a suspended solids concentration of 3.1 g_{SS}/L as measured in the SBR, and the k_{biol} value obtained from the batch-mode experiment (i.e. 4.0 L/(g_{SS} · d), Table 2.1). For the full equations, refer to Appendix A. Based on the biological degradation model, the predicted TMP removal in the SBR is 88% for the scenario with no anoxic removal and 94% for the scenario with comparable aerobic and anoxic removal rate constants. Both removal scenarios are in good agreement with the average TMP removal of > 83% measured in the SBR during the operational period. Thus, the good prediction of the model indicates that the laboratory experiment with the low spiking level of 5 µg/L using only 1:1 diluted sludge with influent wastewater (with an estimated k_{biol} of 3 L/(g_{SS} · d)) would provide the best comparability when modelling the SBR with influent TMP concentrations in the range of 150 ng/L.

Occurrence of aerobic TPs in the on-site SBR

To compare the degradation pathway found in lab-scale experiments with the SBR, the TPs present in the effluent of the SBR were measured. The aerobic/anoxic SBR was fed with municipal wastewater containing (100 to 150) ng/L TMP (Figure

2.1). Using sensitive analytical methods based on detection via LC–tandem MS, the SBR effluent was analysed for the presence of all TPs observed in the lab-scale reactors reported in the previous section. The TP, 4-desmethyl-TMP was detected only in a few 3-day composite samples of SBR effluent with concentrations up to 14 ng/L. However, in most cases this TP was not detected in the SBR effluent above the LOQ of 10 ng/L. The TP is an intermediate in the transformation pathway (Figure 2.4b) with a low steady-state concentration during the laboratory experiments (Figure 2.2b). This might explain its low concentrations and sporadic detection in the SBR effluent despite a consistent removal of TMP during the same period. On the other hand, 4-desmethyl-TMP is also a human metabolite of TMP (Sigel et al., 1973). To confirm that 4-desmethyl-TMP is indeed formed from TMP in the SBR, the reactor was amended with 2.4 µg TMP/reactor (200 ng/L) at the start of every cycle for a period of 12 h (equivalent to the HRT). This led to an elevated concentration of 110 ng/L 4-desmethyl-TMP. This was clear evidence that the initial demethylation of the transformation pathway observed in the lab-scale experiments was also occurring in the on-site SBR.

However, under sterile and aerobic conditions 4-desmethyl-TMP was found to be unstable, since it was oxidised and hydrolysed (for details please refer to Appendix A). These abiotic reactions were found to involve oxidation and the subsequent addition of nucleophiles. Since the wastewater matrix contains a high number of nucleophiles, a large variety of addition products could probably be formed after the oxidation of 4-desmethyl-TMP. Similar additions of nucleophiles during wastewater treatment were postulated for codeinone (α,β -unsaturated ketone) an unstable TP of the opiate analgesic codeine (Wick et al., 2011b).

TP292 and 290 could not be detected in effluent of the SBR, most likely due to their low steady-state concentration, as already observed in the lab-scale experiments. The quantitative analysis of DAPC, the final TP, was challenging due to its high polarity and low molecular mass. Therefore, a pre-concentration step via SPE was added prior to its detection in SBR influent and effluent. DAPC could be identified in the effluent of the on-site SBR in a 3-day composite sample by its MS² fragmentation (Figure A.20 in the Appendix). For quantification the standard addition method was used. In a separate 3-day composite sample of the SBR effluent, taken several months later, 61 ng/L DAPC (TMP < 10 ng/L) was detected (Figure A.21 in the Appendix), while it was not found in the corresponding influent

containing 221 ng/L of TMP. The detected amount of DAPC accounts for 52% of the attenuated TMP. Considering the results obtained so far, it is likely that the remaining dissipation of TMP is caused by i) nucleophilic addition of sludge constituents to 4-desmethyl-TMP leading to an array of addition products, ii) a further transformation of DAPC to unknown TPs.

The detection of 4-desmethyl-TMP and DAPC in the effluent of the SBR supports the hypothesis that the degradation pathway (Figure 2.4b) found in the lab-scale reactors is an important removal pathway of TMP, occurring also in the SBR. Since neither TP306 nor TP324 were detected in the SBR effluent, the pathway (initiated by hydroxylation) detected predominantly at higher spike concentrations, plays obviously no or only a very minor role for the SBR. The variability of TMP removal in the SBR and in municipal WWTPs (Göbel et al., 2005; Batt et al., 2006) is most likely caused by its capability to enable the first demethylation step forming 4-desmethyl-TMP that is rapidly transformed to TP292, TP290 and DAPC.

Previous reports have found hydroxylation (Eichhorn et al., 2005) or hydroxylation followed by catechol ring cleavage (Yi et al., 2012), to be the dominant removal processes of TMP. However, this is the first study to our knowledge to show a different transformation pathway of TMP occurring in a nitrifying/denitrifying activated sludge reactor fed with municipal wastewater. Further monitoring of TMP and the TPs found in this study, especially DAPC, in full-scale WWTP effluent will be part of follow-up studies. This will help better judge the wider environmental occurrence of the transformation pathway in different systems.

2.4 Conclusions

The analysis of transformation reactions in lab-scale bioreactors is a useful tool to assess the transformation of micropollutants in the environment. These findings show that the choice of the initial analyte concentration may not only impact the kinetics of removal but also the dominant reactions themselves can change. This might lead to the transformation pathway stopping at an earlier stage or different TPs becoming more dominant than what is more likely in the natural environment. Although this is shown for one compound, it could have wider implications for biodegradability testing protocols, which often rely on elevated spike concen-

trations to aid the analysis. This might be especially true for compounds with antibacterial properties.

The alternative reactions at different TMP concentrations might be linked to either limited turnover of specific enzymes or processes or to toxic/inhibition or enzyme activation effects of TMP to the sludge bacterial community at higher concentrations. In particular, O-demethylation of TMP was no longer the dominant reaction at high TMP concentrations. A biological analysis of the sludge that is able to carry out O-demethylation or analysis of the enzyme kinetics and how this is changed at higher concentrations was beyond the scope of this investigation. However, this is an important question for further study and may be helpful to understand the successful degradation of TMP and other micropollutants found in wastewater.

Acknowledgements

We are very thankful to Kathrin Bröder (BfG) for analytical assistance and to Carsten Prasse (UC Berkeley) for helpful discussions. We are also very grateful for the financial support from the European Research Council (ERC) through the EU-Project ATHENE (267897) and the German Federal Ministry of Education and Research (BMBF) through the JPI Water project FRAME (02WU1345A).

Chapter 3

Comparisons between abiotic nitration and biotransformation reactions of phenolic micropollutants in activated sludge

Kevin S. Jewell, Arne Wick, Thomas A. Ternes. 2014. Water Research 48, pp. 478–489.

Abstract

The transformation of selected phenolic substances was investigated during biological wastewater treatment. A main emphasis was put on the relevance of abiotic processes leading to toxic nitrophenolic transformation products (TPs). Due to their environmental relevance, the antiseptic *ortho*-phenylphenol (OPP), the plastics additive bisphenol A (BPA) and the psychoactive drug dextropropofol have been studied. Experiments confirmed that nitro- and nitroso-phenolic TPs can be formed under acidic conditions when nitrite is present. HNO_2 , N_2O_3 and radical NO^\bullet and radical NO_2^\bullet are likely involved in the abiotic process. It was found that

the process was promoted by the freezing of water samples, since this can lead to an unexpected pH drop. However, under conditions present at wastewater treatment plants (neutral pH, low nitrite concentrations), the formation of appreciable concentrations is rather unlikely through this process, since HNO_2 concentrations are extremely low and NO^\bullet and NO_2^\bullet radicals will also react with other wastewater constituents. Thus, the transformation of phenolic substances such as OPP and BPA is mainly caused by biotic transformation. In addition to hydroxylation as a common reaction under aerobic conditions, the formation of sulfate conjugates was detected with the original compounds as well as with nitrophenolic TPs. Therefore, even when nitro-phenolic substances are formed it is likely that they are further transformed to sulfate conjugates. In raw wastewater and WWTP effluent nitrated BPA and NO_2 -dextrophan were not detected. Only nitro-OPP was found in the influent of a WWTP with 2.3 ng/L, but it was not identified in the WWTP effluents. The concentrations of dextrophan increased slightly during WWTP passage, possibly due to the cleavage of the glucuronide-conjugate, its human metabolite form, or demethylation of the prodrug dextromethorphan.

3.1 Introduction

An important source of micropollutants in surface waters is municipal or industrial wastewater, which is usually emitted via wastewater treatment plants (WWTPs) into rivers and streams. During wastewater treatment, biological and chemical processes intended for nutrient removal and the removal of easily biodegradable organic compounds may additionally transform refractory micropollutants. As a consequence, transformation products (TPs) of micropollutants are formed and emitted via WWTP effluents into the aquatic environment. Micropollutants containing phenol moieties have received particular attention in this regard, both due to the range of transformation processes which befall many phenols during wastewater treatment (Beel et al., 2013; Chen et al., 2011; Quintana et al., 2005; Skotnicka-Pitak et al., 2008) and their potential for having toxic effects on aquatic organisms, including antibacterial and endocrine disrupting properties (Garg et al., 2001). Understanding of the transformation processes of phenolic micropollutants aids i) their quantification in WWTP effluents and ii) identifying sources of TPs. During biological wastewater treatment, metabolic or co-metabolic reactions

can impact the fate of many phenolic compounds. Biotic degradation reactions of phenolic compounds include ring hydroxylation reactions or oxidation of ring substituents, followed by ring cleavage, for example via the ortho or meta pathway (Reineke, 2001). Additionally, abiotic reactions, e.g., hydroxylation of an α , β -unsaturated ketone (Wick et al., 2011b) or the formation of a nitrobenzene from an aniline moiety in the presence of nitrite (Nödler et al., 2012) are potential transformation routes of micropollutants. Hence, both biotic and abiotic transformation processes could transform these substances in biological wastewater treatment.

An abiotic transformation process of recent interest is the nitration of phenol moieties and the formation of nitrophenolic TPs during biological wastewater treatment (Chiron et al., 2010; Sun et al., 2012). Wick et al. (2011b) reported the formation of nitrophenolic TPs in activated sludge incubation experiments spiked with morphine. Due to their elevated (eco)toxicity, nitrophenols are of environmental concern (Tomei et al., 2003). For instance, the phenolic compound bisphenol A (BPA) exhibited estrogenic effects to goldfish (Toyozumi et al., 2008) and other aquatic organisms (Oehlmann et al., 2006), but after transformation to dinitro-BPA the estrogenic activity decreased while genotoxicity increased (Toyozumi et al., 2008). Recent studies on nitration of phenolic compounds during wastewater treatment have found evidence for different mechanisms but a similar extent of nitration. Acetaminophen for instance, had a reported transformation of 5% to nitro-acetaminophen (Chiron et al., 2010) and BPA of 0.2% to dinitro-BPA (Sun et al., 2012) during wastewater treatment in two different WWTPs. In both studies, concentration of substrate phenols was in the (2 to 6) $\mu\text{g/L}$ range and transformation was reported to occur mostly during biological treatment, in nitrifying reactors or oxidation ditches. Currently, it is unclear which WWTP conditions and agents are favouring the nitration process and which phenolic compounds are more likely to be transformed. Previous reports have attributed two possible agents for the nitration of phenols in WWTPs: nitrite and peroxyxynitrite. Gaulke et al. (2009) proposed that nitrous acid is a reactive species for the nitration of phenols via nitrite. Nitrite is an intermediate for both ammonium oxidation and nitrate reduction and is usually found in low concentrations in nitrifying reactors ((0.5 to 1.0) mg/L NO_2^- -N (Randall and Buth, 1984)). The nitration of phenolic compounds by nitrite is known and has been studied under extreme acidic aqueous

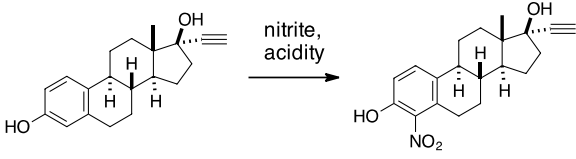
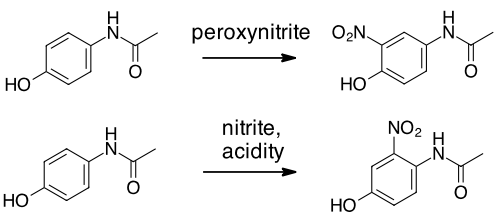
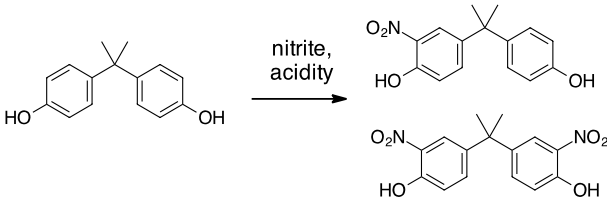
conditions ($\text{pH} < 1$). The reaction mechanism, initially proposed by Al-Obaidi and Moodie (1985) and then further underlined by Beake et al. (1994), involves the formation of nitrogen dioxide radicals from nitrous acid. The formation of nitrogen dioxide and nitric oxide radicals from nitrous acid is known to occur in aqueous solution without the influence of an oxidative agent or photolysis (Vione et al., 2004b; Khalafi and Rafiee, 2010).

At $\text{pH} < 6$ Chiron et al. (2010) reported that the nitration of acetaminophen by nitrite occurs through a different process similar to a Michael Addition (Matsuno et al., 1989) whereby nitrite adds nucleophilically to the β -carbon of the oxidised benzoquinone imine of acetaminophen. A similar process was suggested for catechols (Khalafi and Rafiee, 2010). In activated sludge at neutral pH, Chiron et al. (2010) suggested a phenolic nitration process involving peroxyxynitrite, while a nucleophilic nitration of acetaminophen did not occur. Peroxyxynitrite is a by-product of cell respiration and is known to be formed through the combination of superoxide and nitric oxide (Ferrer-Sueta and Radi, 2009). The nitration mechanism by peroxyxynitrite also involves the initial formation of nitrogen dioxide radicals. It is reported that high AOB (ammonium oxidising bacteria) activity promotes the formation of peroxyxynitrite. Studies of the nitration of estrogens, BPA and nonylphenol in activated sludge proposed that nitrite (Sun et al., 2012) or the protonated form, nitrous acid (Gaulke et al., 2009) is the reactive species (Table 1). Nitrite was measured at (0.08 to 0.34) mg/L NO_2^- -N in an oxidation ditch where BPA nitration was detected (Sun et al., 2012). The evidence for a radical mechanism proposed by Moodie was reported by Vione et al. (2004b) for phenol at $\text{pH} 2$ – 5 , while an alternative reaction mechanism in which nitrosation of phenol is followed by oxidation to nitrophenol (Ridd, 1991) was ruled out. However, it is still an open question as to what extent and by which mechanisms, phenolic compounds entering WWTPs are nitrated and to what extent they are discharged into rivers and streams. Furthermore, it is not clear how the discharge of nitrophenolic compounds can be avoided or minimised.

The objective of the current study was to elucidate the transformation of selected phenolic substances during biological wastewater treatment. The main emphasis was put on the relevance of processes leading to an abiotic nitration in comparison to their enzymatic transformation. Since nitrite is an intermediate in ammonium oxidation, it is possibly responsible for the nitration of phenolic micropollutants.

Due to their environmental relevance, the phenolic antiseptic *ortho*-phenylphenol (OPP), the plastics additive and estrogenic compound BPA and the psychoactive drug dextrorphan were selected. OPP is an anti-fungal agent used for the preservation of citrus fruit. It is degraded in WWTPs (Rudel et al., 1998), however it is unknown to what extent the degradation is due to an abiotic nitration in activated sludge. Kinetic and mechanistic studies were conducted using OPP as the model phenolic micropollutant, comparisons were then made to the phenolic compounds BPA and dextrorphan. BPA is a well-known micropollutant due to its endocrine disrupting activity (Oehlmann et al., 2006). Dextrorphan is a human metabolite of the antitussive prodrug dextromethorphan and has been detected in WWTP effluents (Thurman and Ferrer, 2012), however its potential transformation during wastewater treatment has not been studied so far.

Table 3.1: Reported processes for the nitration of phenolic micropollutants in activated sludge

Precursor compound	Nitration conditions	References
17 α -Ethinyl-estradiol		a, b
Acetaminophen		c
Bisphenol A		d

^aGaulke et al. (2009)^bKhunjar et al. (2011)^cChiron et al. (2010)^dSun et al. (2012)

3.2 Methods

3.2.1 Chemicals

ortho-Phenylphenol (OPP) was purchased from TCI Europe (Eschborn, Germany) and bisphenol A (BPA) from Dr. Ehrenstorfer GmbH (Augsburg, Germany). Dextrorphan tartrate, acetaminophen, carboxy-2-phenyl-4,4,5,5-tetramethyl-imidazolin-1-oxyl-3-oxide (cPTIO), N-acetylcysteine and NaNO₂ were purchased from Sigma Aldrich (Schnelldorf, Germany). LC-MS grade solvents were purchased from LGC Promochem (Wesel, Germany). Purified water was obtained from a Milli-Q water purification system (Millipore, Darmstadt, Germany). The transformation products 4-nitro-6-phenylphenol, 2-nitro-6-phenylphenol and 3,3'-dinitro-bisphenol A were synthesised in the laboratory. Details of the syntheses are given in Appendix B.

3.2.2 Analytical methods

Quantification of phenols and nitrophenols via LC-tandem MS was carried out on an Agilent HPLC system (1200 Series, Agilent Technologies, Waldbronn, Germany) equipped with a Synergi Polar-RP column (150 mm × 3.00 mm, 4 μm; Phenomenex, Aschaffenburg, Germany), coupled to a triple quadrupole tandem-MS (API 4000, Sciex, Langen, Germany) with ESI operated in positive and negative ionisation mode. Mobile phases for gradient elution were A: 0.05% acetic acid in water and B: acetonitrile (gradient for phase A: (0 to 2) min 92%, (5 to 14) min 60%, (15 to 18) min 5%, (19 to 23) min 92%). Quantification via UV-VIS was carried out on a Knauer Smartline HPLC (Knauer, Berlin, Germany) coupled to a UV-Vis detector. Nitrophenols were detected at 300 nm and phenols at 254 nm. High-resolution mass spectrometry for the identification of TPs was carried out on an Agilent HPLC system (as above) coupled to a QToF-MS (TripleToF 5600, Sciex) with ESI operated in positive and negative ionisation mode and by an Accela HPLC coupled with ESI to an LTQ-Orbitrap-MS (LTQ Orbitrap Velos, Thermo Scientific, Bremen, Germany).

3.2.3 Experimental setup for kinetic and mechanistic studies of *ortho*-Phenylphenol nitration

OPP was added in varying concentrations ((0.5 to 1.2) mmol/L) to a NaNO₂ solution ((5 to 15) mmol/L) in buffered, purified water (31 mmol/L sodium acetate, pH 2 to 6). To avoid the photocatalytic formation of radicals, reactions were performed in amber glass flasks. The reaction was monitored by taking 250 µL samples, which were neutralised by diluting to 1 mL with buffered water (pH = 12, 50 mmol/L phosphate). Dinitro-BPA was used as an internal standard in the kinetic and mechanistic studies. Analysis of the samples was carried out by LC–tandem MS for the identification of transformation products and both HPLC–UV and LC–tandem MS for their quantification.

3.2.4 Incubation experiments with activated sludge

To study the transformation characteristics of phenols under conditions found in an activated sludge reactor, 400 mL incubation experiments were set-up in amber glass flasks. Activated sludge was taken from the nitrifying stage of a municipal WWTP with a capacity of 320 000 population equivalents and a daily flow rate of 61 000 m³. The activated sludge stage is operated with a hydraulic retention time of approximately 7 h, a solids retention time of 12 d and achieves a yearly average N-removal of around 81%, measured as total bound N. The sludge was diluted 20:1 with effluent or used undiluted. Throughout the experiment, the solution was stirred and purged with a mixture of air and CO₂ through a diffuser. CO₂ was added to the gas mixture to stabilise the pH, which would otherwise increase due to purging of dissolved CO₂. For a detailed description of the setup see [Wick et al. \(2009\)](#). The pH was maintained between 6.5 and 7.5 by regulating the gas mixture. In some cases, nitrite concentration and pH were adjusted by addition of acetic acid and NaNO₂. After pH equilibration, OPP, BPA and dextrorphan were spiked to the sludge. Samples were filtered (regenerated cellulose, 0.45 µm) and stored at 4 °C. A matrix-matched calibration curve was used for the quantification of OPP and NO₂-OPP. For the calibration and matrix compensation, the sludge was filtered and aliquots were spiked with increasing concentrations of both analytes. This enabled quantification of samples from the incubation experiments by LC–tandem MS. Nitrite, nitrate, ammonia and DOC concentrations were meas-

ured separately on a DR 5000 photometer (Hach-Lange, Düsseldorf, Germany) using test kits from the same supplier.

3.2.5 Effect of freezing samples during storage

To test the effect of freezing samples as a means of storage, incubation experiments were set up with 0.6 mg/L NO_2^- -N and 1 $\mu\text{g/L}$ OPP and BPA in buffered water (50 mmol/L phosphate). Samples were then stored either by refrigeration at 4 °C, acidification to pH 2 with HCl or frozen at -20 °C. The samples were then analysed for nitrophenols by LC-tandem MS using the same analytical procedure as described for environmental samples (Section 3.2.6).

3.2.6 Environmental sampling at WWTPs

Two German WWTPs implementing denitrification and nitrification processes were sampled for the detection of TPs. Technical parameters of the WWTPs are described in Appendix B. NO_2 -OPP, dinitro-BPA and the phenolic precursors were quantified by the standard addition method. Special care was taken to avoid freezing samples or exposing them to acidity. Mixed samples of influent (flow proportional) were taken at the start of the treatment process (after grit removal) and after primary clarification. Composite samples from 24 h periods of effluent were taken after secondary settling at WWTP 1 and after sand filtration at WWTP 2. During sample collection the samples were stored at 4 °C. On the day of collection both samples and a blank (Milli-Q) were filtered (GF 6, Whatman). The influent was split into 4 aliquots of 150 mL and the effluent and blank into 4 aliquots of 500 mL. These were stored overnight at 4 °C. Three aliquots of influent, effluent and blank were spiked with increasing amounts of the analytes as standards for quantification via the standard addition method. All aliquots were loaded onto SPE cartridges (Oasis HLB 6 cc, Waters, Eschborn, Germany), which were conditioned with groundwater. The SPE cartridges were eluted with acetone and the organic phase was reduced to 100 μL by evaporation under a light nitrogen gas flow. The samples were filled to 500 μL with Milli-Q water and analysed by LC-tandem MS. Details of the analytical method are given in Appendix B.

3.3 Results and discussion

3.3.1 Abiotic nitration of *ortho*-phenylphenol at varying pH values

To study the abiotic nitration and to exclude biological transformation processes, incubation experiments without the addition of activated sludge were conducted in buffered solution containing nitrite and *ortho*-phenylphenol (OPP). The initial rates of reaction decreased rapidly when increasing the pH from 2.0 to 4.5. In Figure 3.1a the initial rates of OPP elimination and of nitro-phenylphenol (NO₂-OPP) formation are plotted against the pH. Above pH 5 the formation of NO₂-OPP was not detectable by HPLC–UV. The dotted curves show the results of fitting the experimental data to the equilibrium concentration of nitrous acid (Equations 3.1, 3.2 and 3.3). The quotient in Equation 3.3, where [NO₂[−]]₀ is the initial nitrite concentration, is the nitrous acid concentration at equilibrium (for derivation Appendix B Equations B.2 to B.6). This approach has been reported previously by Vione et al. (2004b). The pH-trend for OPP nitration closely mirrors the acid-base equilibrium of nitrous acid, pointing to this as a reactive species.



$$K_a = \frac{[\text{H}^+][\text{NO}_2^-]}{[\text{HNO}_2]} \quad (3.2)$$

$$\text{Initial rate} = k \cdot \frac{[\text{H}^+][\text{NO}_2^-]_0}{K_a + [\text{H}^+]} \quad (3.3)$$

Three products were identified via LC–HRMS, the *ortho*- and *para*-isomer of nitro-2-phenylphenol (NO₂-OPP), and one isomer of nitroso-2-phenylphenol (NO-OPP). For the latter, the location of -NO substitution is unknown, but is assumed to occur at the *para*-position since in similar experiments with BPA and dextrorphan, where the *para*-position is blocked, nitrosation was not detected. Both isomers of NO₂-OPP had similar rates of formation (see Appendix B Figure B.6). Further discussion of NO₂-OPP formation is based on *para*-NO₂-OPP, however *ortho*-NO₂-OPP appears to be formed analogously.

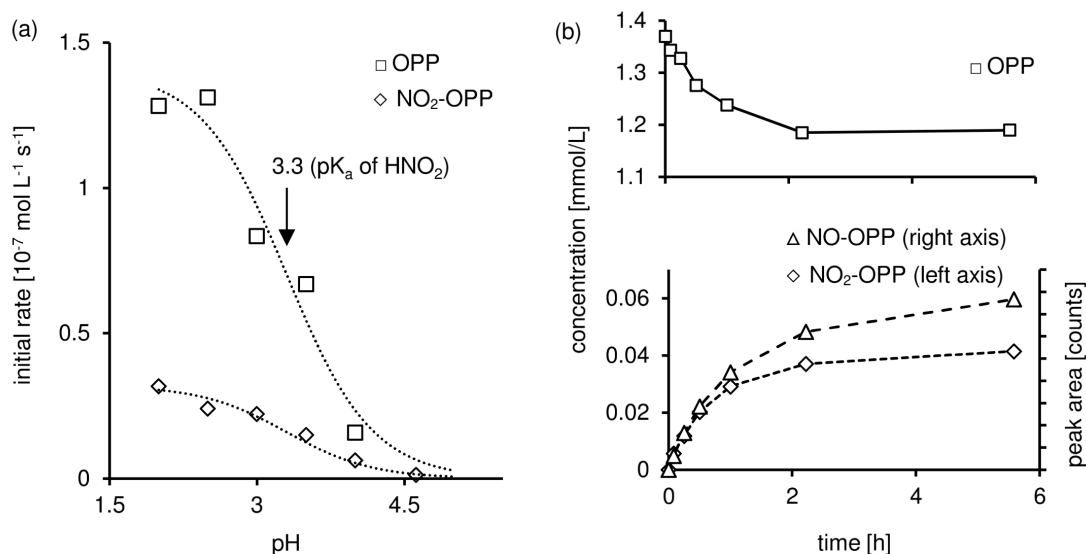
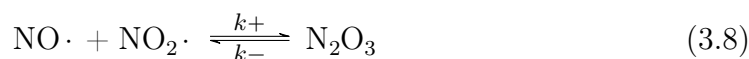
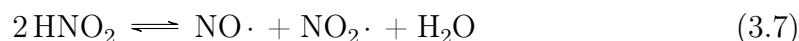
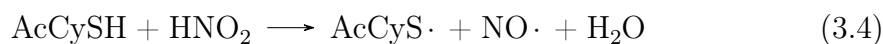


Figure 3.1: A: pH trend of the initial rate of abiotic OPP elimination and $\text{NO}_2\text{-OPP}$ formation (absolute values). Conditions: $[\text{OPP}]_0 = 1 \text{ mmol/L}$, $[\text{NaNO}_2]_0 = 5 \text{ mmol/L}$. Dotted lines are curves of the acid–base equilibrium of HNO_2 , fitted to the experimental data. B: Formation of $\text{NO}_2\text{-OPP}$ and NO-OPP , characteristic of two parallel reactions. Conditions: $\text{pH } 3.5$, $[\text{NaNO}_2]_0 = 5 \text{ mmol/L}$.

The results confirm a strong pH trend and that the rate of abiotic nitration at higher pH (> 5) is expected to be extremely low. Furthermore, the results do not support a mechanism in which the nitration occurs via nitrosation by nitrosonium ion followed by an oxidation of the nitrosophenol to the nitrophenol as described by Ridd (1991), since under conditions in which both products are formed (Figure 3.1b), the rate of $\text{NO}_2\text{-OPP}$ formation did not increase with increasing NO-OPP concentration (i.e. an initial rate of zero for $\text{NO}_2\text{-OPP}$ was not observed). NO-OPP concentrations were also stable for $> 10 \text{ h}$ after reaching equilibrium (data not shown). This implies that $\text{NO}_2\text{-OPP}$ is, at least to a large degree, a direct product from OPP. To confirm this, experiments were carried out using the antioxidant *N*-acetylcysteine, which reacts with HNO_2 and N_2O_3 , and using the nitrogen radical scavenger carboxy-PTIO.

3.3.2 Impact of *N*-acetylcysteine and c-PTIO on OPP abiotic nitration and nitrosation

In the presence of the antioxidant *N*-acetylcysteine (AcCySH), NO₂-OPP was not formed, whereas no change was observed in the formation of NO-OPP (Figure 3.2). By LC–Orbitrap-MS, using high-resolution mass spectra, both AcCySNO and AcCySSCyAc dimer were identified in the aqueous nitrite solution, confirming that both N₂O₃ and HNO₂ react with AcCySH (Equations 3.4, 3.5 and 3.6), analogously to cysteine (CySH), which forms CySNO and the dimer CySSCy (Grossi and Montevicchi, 2002). HNO₂ oxidises AcCySH to AcCyS· radicals, which combine to form the dimer AcCyS-SCyAc. N₂O₃ is present due to the dissociation of HNO₂ in aqueous solution, (Equations 3.7 and 3.8) (Park and Lee, 1988) but reacts with thiols. Thus, excess AcCySH effectively eliminates HNO₂ and N₂O₃.



Therefore, it can be suggested that HNO₂ and/or N₂O₃ are the predominant agents for the formation of NO₂-OPP. Since the NO-OPP formation was not affected by AcCySH addition, different processes must be involved. It can be assumed that AcCySNO leads to the formation of NO-OPP since *S*-nitrosothiols are known to act as nitrosating agents of phenolic compounds (Noble and Williams, 2002). NO-OPP formed via AcCySNO appeared stable with respect to oxidation to NO₂-OPP in the presence of O₂, again suggesting that a consecutive mechanism

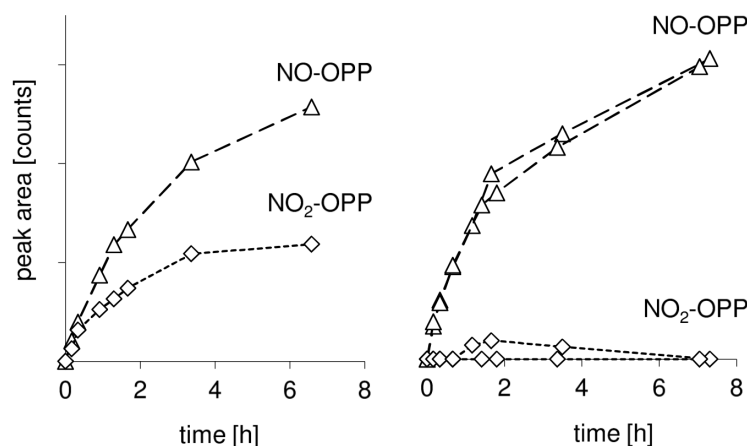


Figure 3.2: The effect of the antioxidant AcCySH on the nitration and nitrosation of OPP; Conditions: pH 4, $[\text{OPP}]_0 = 1 \text{ mmol/L}$, $[\text{NaNO}_2]_0 = 5 \text{ mmol/L}$. Left: No addition of AcCySH. Right: Addition of $1 \mu\text{mol/L}$ AcCySH (duplicate experiment).

$\text{OPP} \rightarrow \text{NO-OPP} \rightarrow \text{NO}_2\text{-OPP}$ does not take place. Furthermore, the product AcCyS-OPP could also be observed by LC-Orbitrap-MS using high resolution MS and the MS^2 fragmentation spectrum (see Appendix B), which may be resulting from radical coupling of radical $\cdot\text{OPP}$ and AcCyS \cdot , suggesting the involvement of $\cdot\text{OPP}$ radicals in the reaction.

N_2O_3 is known not only to nitrosate thiols (Equation 3.6) but also to nitrosate phenolic substances (Noble and Williams, 2002). N_2O_3 is in equilibrium with the dissociated form ($\cdot\text{NO}$ and $\cdot\text{NO}_2$, Equation 3.8), but the equilibrium favours N_2O_3 with $k_+ = 1.1 \times 10^9 \text{ M}^{-1}\text{s}^{-1}$ versus $k_- = 8.1 \times 10^4 \text{ s}^{-1}$ (Goldstein et al., 2003). Due to the equilibrium, the impact of AcCySH is likely to be similar on both forms. It is reported that the formation of nitrosophenol is likely caused by N_2O_3 rather than $\cdot\text{NO}$ reacting with phenol (Noble and Williams, 2002), however the formation of NO-OPP through the radical coupling of $\cdot\text{NO}$ and $\cdot\text{OPP}$ radicals cannot be excluded. A radical mechanism including radical $\cdot\text{NO}_2$ might also be responsible for the formation of $\text{NO}_2\text{-OPP}$.

To test the involvement of $\cdot\text{NO}_2$ and $\cdot\text{NO}$, the nitration reactions were repeated with the addition of carboxy-2-phenyl-4,4,5,5-tetramethyl-imidazolin-1-oxyl-3-oxide (cPTIO), which is a known radical scavenger for both $\cdot\text{NO}$ and $\cdot\text{NO}_2$ (Equations 3.9, 3.10 and 3.11; (Goldstein et al., 2003)). In the presence of cPTIO the equilib-

rium concentrations of NO-OPP and NO₂-OPP are significantly reduced by 78% and 65%, respectively, and the initial rate of NO-OPP formation is much lower than that for NO₂-OPP formation (Figure 3.3). The concentration of cPTIO was not high enough to cause a complete inhibition of the reaction but in a further experiment at lower OPP concentrations, a complete inhibition of NO-OPP was observed (see Appendix B Figure B.7). Since cPTIO scavenges specifically ·NO and ·NO₂ radicals, this confirms that at pH 4 both ·NO and ·NO₂ are involved in the reactions leading to NO-OPP and NO₂-OPP. N₂O₃ is known to react as a nitrosating species, however the involvement of the dissociated form of N₂O₃ (·NO and ·NO₂ radicals) could not be excluded considering the impact of cPTIO.

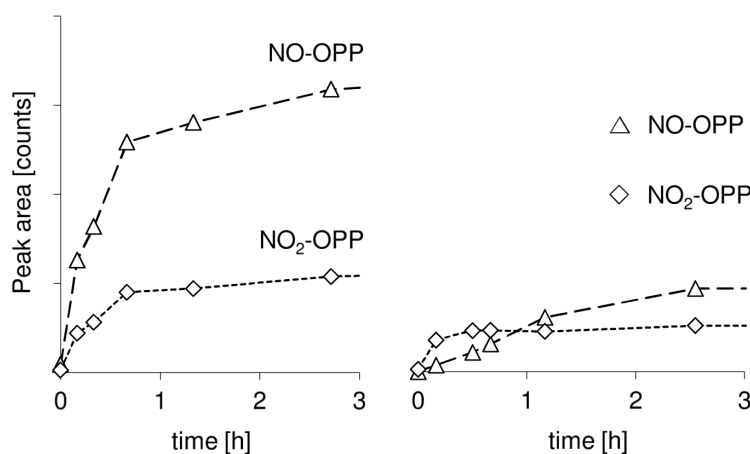
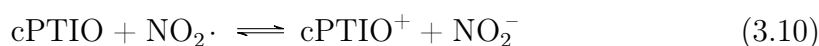


Figure 3.3: The formation of NO₂-OPP and NO-OPP from two experiments, Left: without cPTIO, Right: with 100 μmol/L cPTIO. Peak areas are relative to an internal standard. Conditions: pH 4, [OPP]₀ = 1 mmol/L, [NaNO₂]₀ = 5 mmol/L.

In summary, NO₂-OPP formation was impacted when either HNO₂, N₂O₃ or pos-

sibly $\cdot\text{OPP}$ radicals were scavenged by AcCySH, and the involvement of $\cdot\text{NO}_2$ or $\cdot\text{NO}$ radicals was shown by the cPTIO experiment, therefore $\text{NO}_2\text{-OPP}$ should be formed by a radical reaction. Since it is not formed via oxidation of NO-OPP , these experiments support a two-step mechanism in which $\text{NO}_2\text{-OPP}$ is being formed by oxidation of OPP by HNO_2 , followed by reaction of $\cdot\text{OPP}$ with $\cdot\text{NO}_2$ radical to form the nitrophenol, shown by Equations 3.1, 3.7 and 3.8 and Figure 3.4, as described by Beake et al. (1994) for the nitration of *para*-methoxyphenol by HNO_2 . $\cdot\text{NO}_2$ radicals, although being present at a low concentration, would be constantly replenished due to the equilibrium in Equation 3.8.

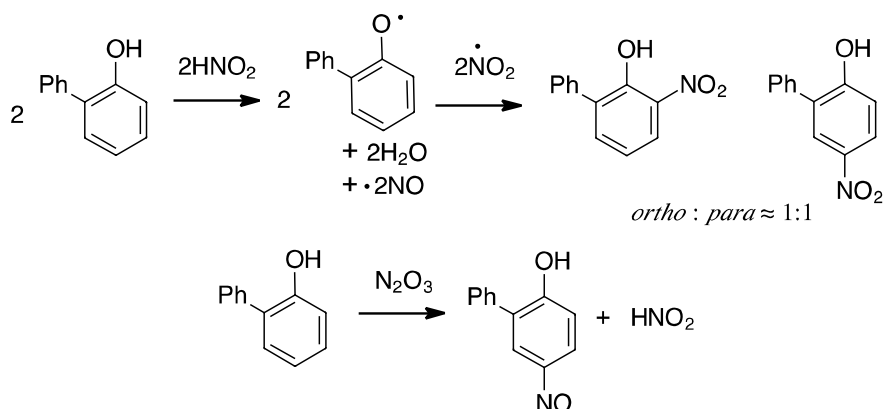


Figure 3.4: Postulated mechanism for the nitration and nitrosation of OPP.

3.3.3 Kinetics and mechanism of OPP nitration

At conditions typical for a German WWTP, (WWTP 1, see Section 3.3.6) i.e. neutral pH and nitrite concentrations below 1 mg/L NO_2^- -N in the biological wastewater treatment stage, the nitration of phenolic compounds should be extremely low following the abiotic mechanism suggested above. Only when technical problems at WWTPs lead to a drop of pH or an accumulation of nitrite (Randall and Buth, 1984) might an appreciable formation of NO-OPP or $\text{NO}_2\text{-OPP}$ occur. In order to predict the potential of $\text{NO}_2\text{-OPP}$ formation, a model was developed based on kinetic studies at different pH and nitrite concentrations.

The reaction order determined by the method of initial slopes (Atkins and de Paula, 2002) indicated that at pH 4 the rates of *para*- and *ortho*- $\text{NO}_2\text{-OPP}$ formation were first order with respect to HNO_2 and half order with respect to OPP (Fig-

ure 3.5. The fractional order of 1/2 with respect to OPP is an indication that a dissociation is taking place (Houston, 2006), e.g., formation of $\cdot\text{OPP}$ radicals by HNO_2 . This would also account for the first order dependence on HNO_2 . In a separate experiment, the rate of HNO_2 elimination was found to be second order in HNO_2 (Figure 3.6a). Assuming that the reaction of OPP with nitrous acid ($\text{HNO}_2 + \text{PhPhOH} \rightarrow \text{PhPhO}\cdot + \text{NO}\cdot + \text{H}_2\text{O}$) is the rate-limiting step, the following rate laws can be described based on NO_2 -OPP formation and HNO_2 elimination (Equations 3.12 and 3.13).

$$\frac{d[\text{NO}_2\text{-OPP}]}{dt} = k_1[\text{HNO}_2][\text{OPP}]^{1/2} \quad (3.12)$$

$$-\frac{1}{2} \frac{d[\text{HNO}_2]}{dt} = k_2[\text{HNO}_2]^2 \quad (3.13)$$

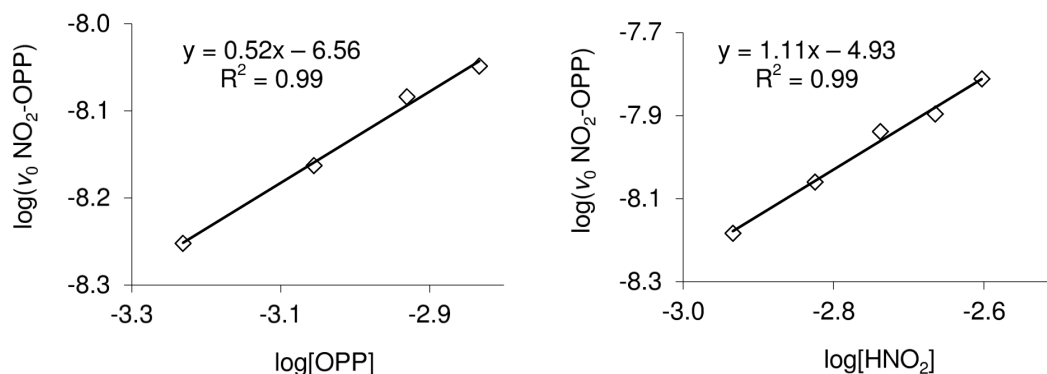


Figure 3.5: Correlation of the initial rate of NO_2 -OPP formation with changing initial concentrations of reactive species (from the method of initial slopes). Left: Rate of NO_2 -OPP formation with respect to OPP concentration. Conditions: pH 4, 22 °C, $[\text{NaNO}_2]_0 = 9 \text{ mmol/L}$, $[\text{OPP}]_0 = (0.6 \text{ to } 1.5) \text{ mmol/L}$. Right: Rate of NO_2 -OPP formation with respect to HNO_2 concentration. Conditions: pH 4, 22 °C, $[\text{NaNO}_2]_0 = (0.8 \text{ to } 2.5) \text{ mmol/L}$, $[\text{OPP}]_0 = 1 \text{ mmol/L}$.

The rate constant k_2 is the slope of the reciprocal nitrous acid concentration over time (Figure 3.6a). Integration of Equation 3.13 and solving for $[\text{HNO}_2]$ gives Equation 3.14.

$$[\text{HNO}_2] = \left(2k_2t + \frac{1}{[\text{HNO}_2]_0} \right)^{-1} \quad (3.14)$$

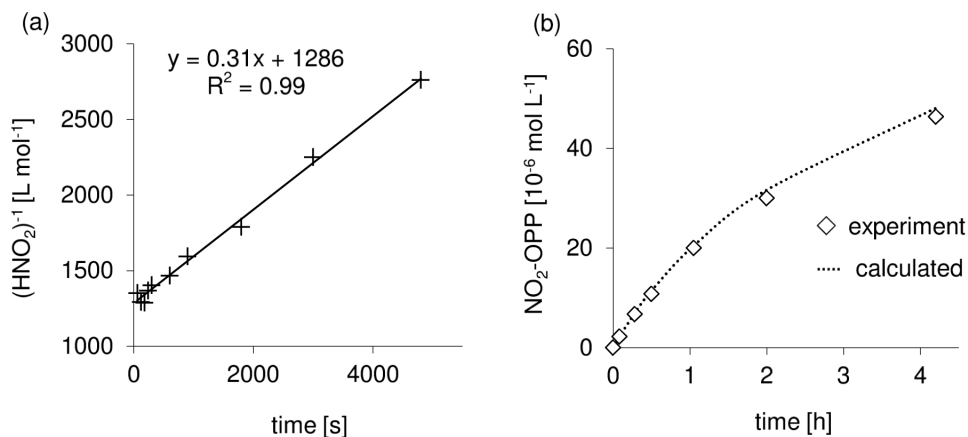


Figure 3.6: A: Plot of reciprocal nitrous acid concentration as a function of time. The second order rate constant $2k_2$ is the slope, $0.31 \text{ L/s} \cdot \text{mol}$. B: Estimated $\text{NO}_2\text{-OPP}$ concentration using Equation 3.15 (dotted line) versus experimental results. Conditions: pH 4, $[\text{OPP}]_0 = 1 \text{ mmol/L}$, $[\text{NaNO}_2]_0 = 5 \text{ mmol/L}$.

If the OPP concentration is high compared to HNO_2 and/or conversion to $\text{NO}_2\text{-OPP}$ remains low, then $[\text{OPP}]$ can be approximated by $[\text{OPP}]_0$. Substituting Equation 3.14 into Equation 3.12 and integrating gives Equation 3.15.

$$[\text{NO}_2\text{-OPP}] = \frac{k_1 \sqrt{[\text{OPP}]_0}}{2k_2} \ln(2k_2 t [\text{HNO}_2]_0 + 1) \quad (3.15)$$

The rate constant k_1 ($2.5 \times 10^{-4} \text{ L}^{0.5} \text{ mol}^{-0.5} \text{ s}^{-1}$) was found by fitting the calculated concentration to the experimental results of Figure 3.5. Equation 3.15 was tested by carrying out an experiment at a longer duration and was found to accurately model the experimentally determined concentrations of $\text{NO}_2\text{-OPP}$ (Figure 3.6b).

The developed model enables the calculation of the $\text{NO}_2\text{-OPP}$ concentrations formed in the incubation experiments by the reaction of OPP with $\text{HNO}_2/\cdot\text{NO}_2$ radicals. As other wastewater constituents (e.g. further phenolic compounds) are probably also reacting with $\text{HNO}_2/\cdot\text{NO}_2$ this model allows prediction of the upper limit of formation (maximum concentration). For instance, at pH 7, a maximum concentration of $\text{NO}_2\text{-OPP}$ of 1 ng/L is predicted after 6 h for $1 \mu\text{g/L}$ OPP and 1 mg/L $\text{NO}_2^- \text{-N}$. However, if the nitrite concentration is increased to 20 mg/L $\text{NO}_2^- \text{-N}$ and the pH reduced to 6.5, a maximum of 80 ng/L $\text{NO}_2\text{-OPP}$ is

predicted to be formed under this idealised case where only OPP is reacting with HNO_2 . During certain treatment processes, such as the Sharon–Anammox for nitrification of digester effluents, nitrite concentration reaches 600 mg/L NO_2^- -N (van Dongen et al., 2001). In another example, ammonium oxidation in urine wastewater has been observed at pH 4 and it is reported that at this acidic pH, nitrite oxidation is a chemical process resulting from the same decomposition reaction of nitrous acid that leads to the formation of $\cdot\text{NO}_2$ radicals (Udert et al., 2005). Under such extreme conditions (low pH, elevated nitrite concentration), higher concentrations of nitrophenolic transformation products are expected.

3.3.4 Uncontrolled nitration of phenolic substances during sample storage

Freezing of neutral (pH 7) water samples containing nitrite (0.6 mg/L) and phenolic compounds (1 $\mu\text{g/L}$ BPA and OPP) led to formation of NO_2 -OPP, NO_2 -BPA and dinitro-BPA (Figure 3.7). The extent of nitration was similar to an acidified sample, where a significant formation of NO_2 -OPP (> 100 ng/L) can be estimated from Equation 3.15. Storage at 4 °C did not cause the artificial formation of nitrophenolic compounds (Figure 3.7). An explanation could be found in publications reporting a shift to lower pH values when freezing buffered solutions (Sundaramurthi et al., 2010; Goyal and Hafez, 1995). Thus, freezing is an inappropriate storage method for samples to be analysed for phenolic compounds if nitrite is present. Sample storage should occur at 4 °C instead.

3.3.5 Incubation experiments with activated sludge

In activated sludge from a municipal WWTP, the formation of nitrophenolic compounds cannot reach the maximum concentration estimated by the kinetic studies, since it i) contains microorganisms enabling an additional biotic transformation of the phenolic compounds and ii) it contains several components that are also able to react with HNO_2 or $\cdot\text{NO}_2$. Dissipation of phenolic compounds and the formation of nitrophenolic substances were monitored in incubation experiments with diluted nitrifying activated sludge under varying conditions (pH and nitrite). In addition to OPP, bisphenol A and dextrorphan were spiked to investigate whether the OPP results can be transferred to further phenolic substances.

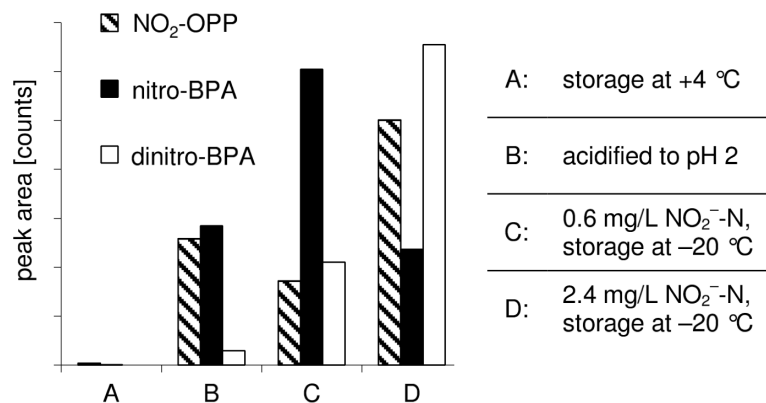


Figure 3.7: Nitrophenol formation resulting from sample storage or preparation: Incubation experiments in pH 7 buffered water were spiked with 1 $\mu\text{g/L}$ BPA and OPP, and varying nitrite concentrations: A–C: 0.6, D: 2.4 mg/L NO₂⁻-N.

In incubation experiments without alteration of the pH and without artificial addition of nitrite or ammonium, the concentrations of BPA and OPP decreased rapidly, while dextrorphan was found to be more recalcitrant as its concentration remained mainly constant (Figure 3.8a). No evidence of nitrophenol formation from any of these three phenolic substances was found. The elimination of BPA and OPP under these conditions is attributed predominantly to biotic transformation processes, as shown below.

To rule out the possibility that other processes associated with ammonium oxidation (e.g. build-up of peroxyxynitrite) were causing a significant nitration, as found by Chiron et al. (2010), the experiment was repeated with an increased ammonium concentration of 240 mg/L NH₄⁺-N. During 4 days, in which the system was continually purged with air, it caused nitrate concentrations to increase from 9 mg/L to 76 mg/L NO₃⁻-N while the ammonium concentration decreased to 210 mg/L NH₄⁺-N. The formation of nitrophenolic compounds was not detected in this experiment.

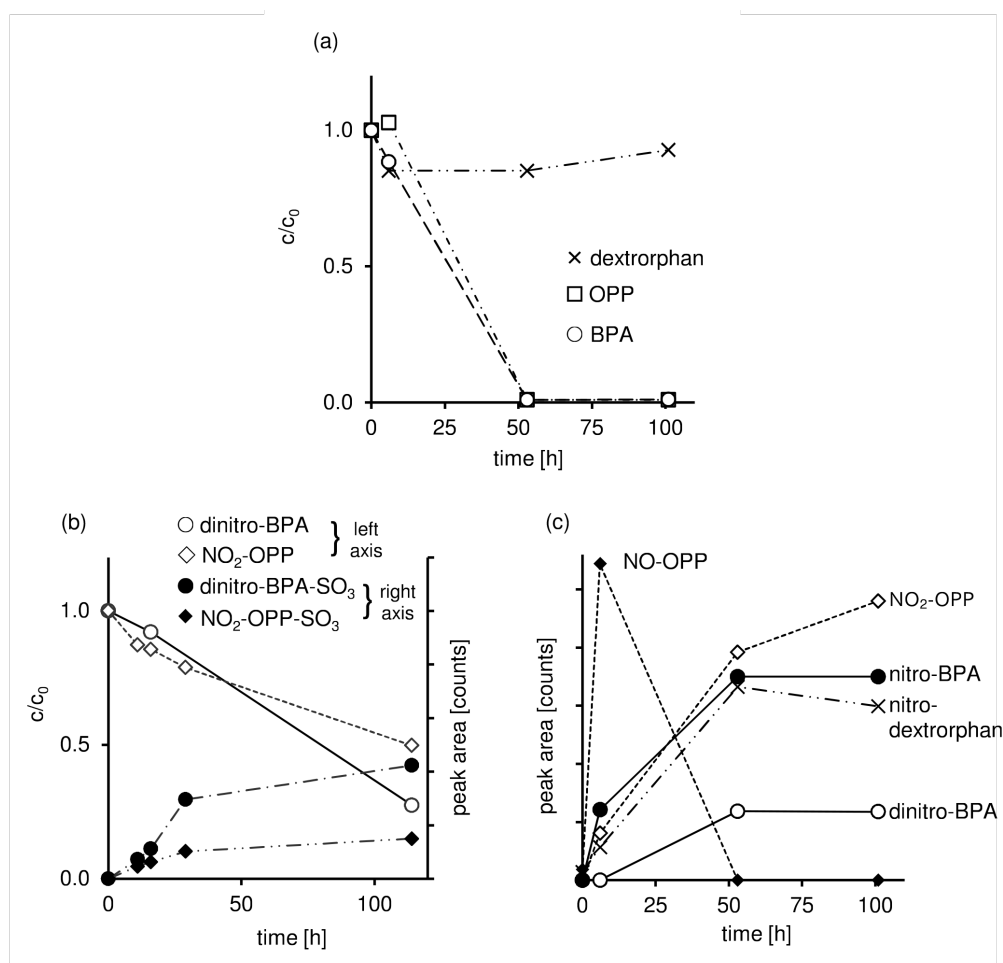


Figure 3.8: (a) Concentration of phenolic parent compounds in an incubation experiment: $c_0 = 200 \mu\text{g/L}$. Conditions: activated sludge (0.2 g/L sludge), pH 7.2 to 7.5. (b) Stability of nitrophenols to biodegradation. Conditions: activated sludge (0.2 g/L sludge), pH 7.2 to 7.5, dinitro-BPA and NO₂-OPP, $c_0 = 200 \mu\text{g/L}$. (c) Formation of nitrophenols in activated sludge. Conditions: activated sludge (0.2 g/L sludge), pH 3.3, 4.2 mg/L NO₂⁻-N.

TPs formed under neutral pH conditions

Via their MS² fragmentation patterns using LC-QToF-MS, several TPs could be identified (Figure 3.9), giving insights into the relevant transformation or degradation pathways of these compounds in nitrifying activated sludge.

The TP hydroxy-OPP was formed in the incubation experiments containing activated sludge described above and was itself eliminated, suggesting the degradation of OPP proceeds via this catechol intermediate in activated sludge. This OPP-TP

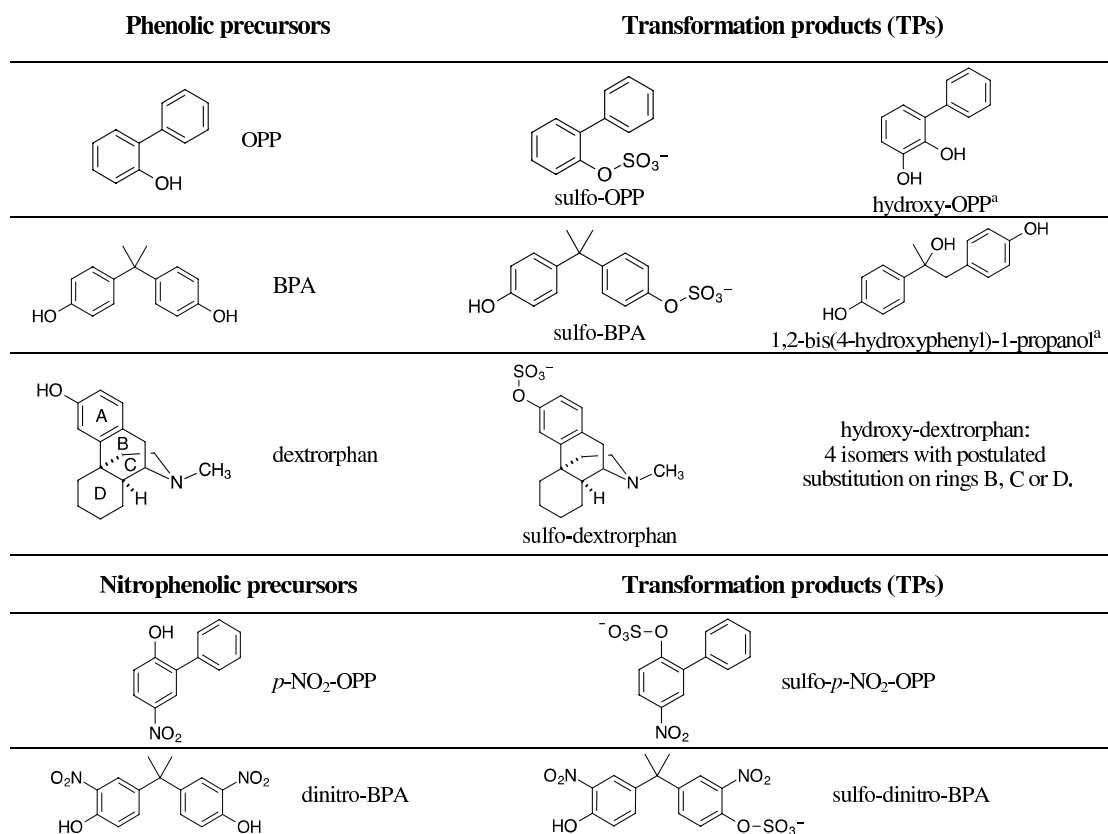


Figure 3.9: Biotic transformation products observed from BPA, OPP and dextrorphan. ^aTPs identified in enrichment culture studies (Kohler et al., 1988; Ike et al., 2000).

was previously reported to be formed by a soil bacterium and is the substrate for an oxidative meta cleavage leading to degradation of OPP (Kohler et al., 1988). In the case of BPA, the presence of hydroxy-BPA (1,2-bis(4-hydroxyphenyl)-1-propanol) was identified by LC-QToF-MS as an intermediate species. Fragmentation spectra of this TP suggest a structure that is formed via rearrangement of the quaternary carbon centre of BPA (see Appendix B). Ike et al. (2000) detected this TP in sludge enrichment cultures degrading BPA (concentrations of 100 mg/L), but it was further degraded to benzoic acid derivatives. Detection of the TPs of OPP and BPA in samples of the incubation experiments of the current study confirms the relevance of these degradation pathways in mixed cultures from municipal WWTPs at substrate concentrations of 200 µg/L. Although the concentration of dextrorphan remained relatively constant ($\approx 10\%$ elimination), several hydroxylated dextrorphan-TPs were identified in small concentrations. In total

four isomers of hydroxy-dextrorphan TPs were identified with similar MS² spectra, possibly due to the formation of diastereomeric pairs from the chiral precursor. Due to the low proportion of dextrorphan conversion, an isolation of TPs for structure confirmation was impossible. In addition, sulfate conjugation products of all three phenols were detected. Sulfo-OPP was quickly eliminated, while the others persisted in the incubation experiment. Sulfate conjugation is discussed below in more detail. The characterisation of TPs by MS² is described in Appendix B.

Incubation experiments were also conducted with the nitrophenolic TPs of OPP and BPA, to test their stability towards (bio)degradation in activated sludge. NO₂-OPP and dinitro-BPA were transformed in the experiments during the 6-day period to approximately 50% and 80%, respectively (Figure 3.8b). For both nitrophenols the phenolic hydroxyl group was conjugated with sulfate (-SO₃, Figure 3.9). Further TPs were not observed.

The sulfate conjugation seems to be a very common microbial process occurring in activated sludge from biological wastewater treatment with a wide substrate spectrum. Sulfate conjugation (sulfurylation) is a widely occurring biological process in cells. It has various functions including detoxification of xenobiotic substances (Malojčić and Glockshuber, 2010). Sulfurylation of estrogens has previously been observed by mixed bacterial cultures from activated sludge (Khunjar et al., 2011). Further studies have reported these sulfate conjugates can also be de-conjugated in sludge with resulting release of estrogens (Kumar et al., 2012), an indication of the reversibility of this type of transformation.

Formation of nitrophenols in activated sludge

In an activated sludge medium, a rapid formation of nitrophenols from the three precursor phenols was observed under acidic conditions (pH 3.3 to 3.5). Figure 3.8c shows the formation of nitrophenols measured over time. The formation of NO-OPP was also observed. However it was no longer detected in samples after 6 h, no TPs of NO-OPP could be detected. After 50 h of incubation, nitrite was no longer present and the formation of nitrophenols had slowed down or stopped.

In incubation experiments with activated sludge the formation of NO₂-OPP was quantified at varying pH (3.3 to 7.0). Using the initial nitrite and OPP con-

centration and pH, the predicted maximal formation of NO₂-OPP was calculated with Equation 3.15. Only around 10% of the predicted maximum concentrations were detected in the incubation with activated sludge (Table 3.2), since HNO₂ and ·NO₂ are probably reacting with other sludge constituents (DOC of the sludge ≈ 10 mg/L). Therefore, it can be concluded that the nitration process with HNO₂ can be neglected in contact with activated sludge. Other processes leading to nitro-phenolic TPs could not be observed, neither with elevated ammonium nor with elevated nitrite concentrations. Thus, the formation of significant levels of nitrophenolic TPs from BPA, OPP and dextrorphan can be ruled out in incubation experiments with activated sludge at the conditions expected at the WWTPs in this study. It seems very unlikely that nitrophenolic substances are formed in biological wastewater treatment.

Table 3.2: Quantification of NO₂-OPP formed in incubation experiments with activated sludge.

Incubation experiment ^a	pH	[HNO ₂] ₀	[OPP] ₀ ^b	[NO ₂ -OPP] after 5 h	NO ₂ -OPP detected compared to modeling ^c
1	3.3	1.50×10^{-4}	6.8×10^{-7}	3.7×10^{-8}	8%
2	3.6	7.03×10^{-5}	9.72×10^{-7}	2.0×10^{-8}	9%
3	3.9	4.50×10^{-5}	8.22×10^{-7}	8.9×10^{-9}	9%
4	4.2	2.35×10^{-5}	8.58×10^{-7}	3.2×10^{-9}	6%
5	7	1.54×10^{-9}	7.69×10^{-7}	n.d.	–

^a Conditions: activated sludge (experiment 1: 0.2 g/L sludge, experiments 2–5: 4 g/L sludge), nitrite addition: experiments 1–4: 3 mg/L NO₂-N, experiment 5: no nitrite addition, c₀ = 0.6 mg/L NO₂-N.

^b [OPP]₀ < [HNO₂]₀, however due to low conversion, OPP concentration can be treated as constant.

^c Theoretical formation according to Equation 3.15.

n.d.: not detected.

3.3.6 Analysis of wastewater for the presence of nitrophenolic TPs

The concentrations of three nitrophenolic substances, NO₂-OPP, dinitro-BPA, and NO₂-dextrorphan, and their precursors (OPP, BPA, dextrorphan) were analysed in wastewater samples from two German WWTPs. Flow-proportional composite samples were taken from the influent and the final effluent over a 24 h period.

Concentrations of OPP and BPA decreased from the low µg/L range before the activated sludge reactor to the low ng/L range in the WWTP effluent in both

sites studied (Table 3.3). The removal of these compounds is mainly caused by biodegradation as sorption to sludge is negligible (Zhao et al., 2008; Zheng et al., 2011). Several TPs detected in incubation experiments, hydroxylated-OPP, sulfo-OPP and sulfo-BPA (Figure 3.9) were also identified by LC–tandem MS in raw wastewater and WWTP effluents, suggesting that transformation processes identified in incubation experiments may also be occurring during drainage and wastewater treatment. For TP identification, quadrupole-tandem MS in MRM mode was used with characteristic MS² fragments for each TP (See Supplementary Data for MS² spectra). However, it was impossible to quantify these TPs due to the lack of authentic standards. Nitrophenolic TPs of OPP, dextrophan and BPA were not detected in WWTP effluents as shown in Table 3.3. Only NO₂-OPP was detected in raw wastewater with 2.3 ng/L at WWTP 1 and was not found in the WWTP effluent. It can be assumed that NO₂-OPP originated from sources other than biological wastewater treatment. For instance, if favourable conditions in the sewer system were present, e.g., a local acidification, this could lead to a nitration of OPP. Alternatively, UV radiation can also promote OPP nitration (Suzuki et al., 1990). This could occur during surface run-off before entering the sewer system. The slight increase of the dextrophan concentrations, e.g., from (5 to 15) ng/L in WWTP 2, might be caused by the hydrolysis of *O*-glucuronide conjugates as suggested by Thurman and Ferrer (2012), who detected dextrophan in WWTP effluent and a US river. *O*-Demethylation of dextromethorphan, the prodrug of dextrophan, during treatment would also lead to dextrophan formation.

These results underline the prediction that NO₂-OPP and dinitro-BPA are not formed in appreciable concentrations during biological wastewater treatment. According to a prediction of NO₂-OPP concentrations using Equation 3.15 for the conditions found in WWTP 1, taking into consideration the influence of the sludge matrix, not more than 0.1 ng/L NO₂-OPP would be expected. Thus, these concentrations would be far below the quantification limits of the method (see Section 3.2 and Appendix B for details). It might be possible that the formation of dinitro-BPA ((1.9 to 3.7) ng/L) reported by Sun et al. (2012) and of nitro-acetaminophen ((180 to 320) ng/L) reported by Chiron et al. (2010) might be caused by different treatment processes, such as the formation of peroxyxynitrite. However, in our study no indication for the peroxyxynitrite mechanism was found. Nitro-acetaminophen was included in the analytical method described above and acetaminophen was

Table 3.3: Concentrations of parent phenols and nitrophenols detected in two German WWTPs [ng/L].^{ab}

	WWTP 1 influent	WWTP 1 effluent	WWTP 2 influent	WWTP 2 effluent
OPP	1660	12	1590	30
NO ₂ -OPP	2.3	< LOQ (2)	< LOQ (2)	< LOQ (2)
BPA	6000 ^d	100	1170	19
Dinitro-BPA	< LOQ (2)	< LOQ (1)	< LOQ (2)	< LOQ (2)
Dextrorphan	4	39	5	15
NO ₂ -dextrorphan ^c	n.d.	n.d.	n.d.	n.d.

^a Samples before and after the primary clarifier gave similar concentrations so only the latter is given.

^b LOQs are given in brackets.

^c Due to a lack of an authentic standard no LOQ could be determined. n.d.: not detected.

^d Concentration out of range for standard addition, estimated by matrix-matched calibration curve.

also spiked into a neutral incubation experiment (Table 3.2, experiment 5). Neither in incubation experiments, nor in raw wastewater or WWTP effluents was nitroacetaminophen found despite acetaminophen being permanently present in the raw wastewater.

3.4 Conclusions

The transformation processes of three model phenolic micropollutants, bisphenol A (BPA), *ortho*-phenylphenol (OPP) and dextrorphan, during wastewater treatment has been studied with emphasis on the role of abiotic nitration. It was found that the reaction leading to nitro-phenols is most likely due to the formation of radicals from nitrous acid.

Kinetic studies under idealised conditions revealed that a significant nitrophenolic TP formation can only be expected in cases of nitrite build-up and/or pH reduction.

- Incubation experiments with activated sludge indicated that a significant formation of nitrophenols could be ruled out under typical conditions at the WWTPs included in this study, i.e. neutral pH and low nitrite concentration.

- Since nitrophenols are immediately formed under acidic conditions as well as during freezing or thawing of aqueous samples containing nitrite, such conditions have been avoided to prevent an artificial formation of nitrophenolic TPs during sample preparation.
- In incubation experiments under neutral conditions, the transformation of OPP, BPA and dextrorphan was observed via biotic pathways including hydroxylation and sulfurylation.
- In accordance with the laboratory experiments, the formation of nitrophenolic TPs was not observed in WWTPs. Previous findings reporting the contrary may be the result of processes specific to those sites studied.

Acknowledgments

We thank Christian Lütke Eversloh (BfG) and Davide Vione (U. Torino) for helpful discussions and Manfred Wagner at the MPIP in Mainz for NMR analysis of the nitrophenolic TPs. Financial support from the European Research Council (ERC) through the EU-Project *ATHENE* is gratefully acknowledged.

Chapter 4

Transformation of diclofenac in hybrid biofilm–activated sludge processes

Kevin S. Jewell, Per Falås, Arne Wick, Adriano Joss, Thomas A. Ternes. 2016. Water Research 105, pp. 559–567.

Abstract

The biotransformation of diclofenac during wastewater treatment was investigated. Attached growth biomass from a carrier-filled compartment of a hybrid-MBBR at the wastewater treatment plant (WWTP) in Bad Ragaz, Switzerland was used to test the biotransformation. Laboratory-scale incubation experiments were performed with diclofenac and carriers and high-resolution LC–QToF-MS was implemented to monitor the biotransformation. Up to 20 diclofenac transformation products (TPs) were detected. Tentative structures were proposed for 16 of the TPs after characterisation by MS² fragmentation and/or inferring the structure from the transformation pathway and the molecular formula given by the high resolution ionic mass. The remaining four TPs were unambiguously identified via analytical reference standards. The postulated reactions forming the TPs were: hydroxylation, decarboxylation, oxidation, amide formation, ring-opening

and reductive dechlorination. Incubation experiments of individual TPs, those which were available as reference standards, provided a deeper look into the transformation pathways. It was found that the transformation consists of four main pathways but no pathway accounted for a clear majority of the transformation. A 10-day monitoring campaign of the full-scale plant confirmed an 88% removal of diclofenac (from approximately 1.6 $\mu\text{g/L}$ in WWTP influent) and the formation of TPs as found in the laboratory was observed. One of the TPs, *N*-(2,6-dichlorophenyl)-2-indolinone was detected at concentrations of around 0.25 $\mu\text{g/L}$ in WWTP effluent, accounting for 16% of the influent diclofenac concentration. The biotransformation of carriers was compared to a second WWTP not utilising carriers. It was found that in contact with activated sludge, similar hydroxylation and decarboxylation reactions occurred but at much slower rates, whereas some reactions, e.g., reductive dechlorination, were not detected at all. Finally, incubation experiments were performed with attached growth biomass from a third WWTP with a similar process configuration to Bad Ragaz WWTP. A similarly effective removal of diclofenac was found with a similar presence of TPs.

4.1 Introduction

The non-steroidal anti-inflammatory diclofenac (DCF) belongs to the group of chemicals of emerging concern (CECs) and has an elevated environmental relevance. In addition to the well-known toxic effects of DCF to vultures (Oaks et al., 2004), renal and hepatic toxicity has also been recorded in certain fish species at concentrations in the low $\mu\text{g/L}$ range (Fent et al., 2006; Triebskorn et al., 2004). As a consequence of its environmental significance, DCF has been included in the *Watch List*, which contains the candidates for a revised list of priority substances for the European Water Framework Directive (WFD, European Parliament and Council of the European Union (2013)). The well-documented ecotoxicological effects of DCF have resulted in the proposal of a relatively low environmental quality standard (EQS) of 0.1 $\mu\text{g/L}$ as an annual average for inland surface waters (The European Commission, 2012).

It is well known that DCF is mainly discharged into the aquatic environment via WWTPs (Luo et al., 2014). A review by Verlicchi et al. (2012), of mainly

European wastewater studies, reported a median concentration in raw wastewater of 0.7 µg/L with a maximum concentration of 11 µg/L. Conventional activated sludge treatment is usually rather ineffective for the removal of DCF with a median removal range of 20% to 30% (Zhang et al., 2008). As a consequence, an exceedance of the EQS in surface waters is likely if the proportion of treated wastewater is higher than 10%. This has already been observed in European surface waters (Patrolecco et al., 2015; Nödler et al., 2010). Therefore, going forward, an overall improvement of municipal wastewater treatment would be crucial to fulfil the requirements of the revised WFD. It is noted that this applies not only to DCF but a whole range of CECs, both known and unknown, which are emitted into receiving waters due to inadequate removal.

Although a low median removal for DCF is reported, there are cases where biological treatment is able to remove this CEC. The WWTP in Bad Ragaz, Switzerland, has previously been shown to be effective at removing DCF and other, typically poorly biodegradable CECs, including trimethoprim. In addition to a conventional nitrifying/denitrifying suspended sludge treatment stage, the WWTP is equipped with a third biological compartment filled with carrier-attached biofilms (hybrid-moving bed biofilm reactor, MBBR). The carriers are small plastic disks with a mesh structure to provide a high surface area to support biofilm growth. In the previous study, the removal of DCF was attributed to biological degradation by contact with the carrier biomass, while sorption was negligible (Falås et al., 2013). MBBRs have been studied with respect to the degradation of various CECs (Hapeshi et al., 2013; Escolà Casas et al., 2015) and an improved DCF removal of MBBRs over suspended sludge was also observed in laboratory-scale reactors (Zupanc et al., 2013). However, the transformation pathway of DCF and the transformation products (TPs) which may be formed are still unknown.

One main focus of current research in the area of CECs is the elucidation of TPs during biological wastewater treatment, since this provides useful clues to elucidate i) transformation processes (Quintana et al., 2005) and ii) potential formation of stable TPs, which might pose ecotoxicological effects even after a complete removal of the parent CEC (Escher and Fenner, 2011). Several studies have previously investigated the transformation of DCF in municipal WWTPs (Vieno and Sillanpää, 2014). Hitherto identified TPs include nitro- and nitroso-derivatives of DCF (Pérez and Barceló, 2008), an indolinone derivative resulting from in-

tramolecular ring closure (DCF-lactam) (Kosjek et al., 2009) and the hydroxylated derivative of DCF-lactam (Bouju et al., 2016). Studies with soil/sediment systems have found 4'-hydroxy-DCF (4HD), 5-hydroxy-DCF (5HD) and a 5HD derivative, 5HD-quinone imine (5HDQI) (Gröning et al., 2007). Another study dealing with the fate of DCF in soil identified the formation of 5HD and several isomers of dichlorobenzoic acid (Dodgen et al., 2014). The principal human metabolites of DCF are 4HD and 5HD (Stierlin et al., 1979). HDQIs are also known metabolites (Poon et al., 2001) as well as the acyl glucuronide conjugate of DCF (Seitz and Boelsterli, 1998). A study of mouse metabolism found numerous metabolites of DCF including hydroxylated DCF, the aforementioned lactam, a benzoic acid derivative resulting from decarboxylation and subsequent oxidation (DCF-BA) also referred to as DCF-carboxylic acid, as well as several different conjugates of these metabolites (Sarda et al., 2012).

The transformation pathways in biological wastewater treatment reported thus far stop mostly at the level of primary TPs (direct TPs of DCF) and do not include secondary or tertiary TPs, although the biodegradability of some primary TPs is already known (Lee et al., 2012). The slow and incomplete transformation of DCF poses a challenge to identify TPs, since long incubation periods are needed and the TP concentrations are rather low. Due to major differences in the reported DCF transformation pathways (Gröning et al., 2007; Kosjek et al., 2009), the question arises whether parts of the transformation pathway are specific to the system studied or can be generalised across all types of microbial degradation.

In this study, we investigated the biotransformation of DCF in two hybrid-MBBR systems in Bad Ragaz, Switzerland and Klippan, Sweden. Specifically, the study looked at whether special primary degradation reactions were responsible for the high degradability of DCF and if these treatment processes were capable of degrading primary TPs as well as DCF. The aims were to i) identify TPs and transformation pathways ii) measure the formation of any formed TPs in full-scale WWTPs and iii) compare the hybrid-MBBRs to conventional activated sludge systems without carriers. To model the full-scale WWTPs, laboratory-scale bioreactors were inoculated with biomass from the hybrid-MBBRs and activated sludge-based WWTPs. High-resolution mass spectrometry was employed to identify TPs and monitor transformation kinetics.

4.2 Methods

4.2.1 Chemicals

Diclofenac (DCF) was purchased from Sigma Aldrich and diclofenac- d_4 (CAS: 153466-65-0) was purchased from Dr. Ehrenstorfer (Teddington, UK). DCF transformation products (TPs) 4HD (4'-hydroxy-DCF, CAS: 64118-84-9), 5HD (5-hydroxy-DCF, CAS: 69002-84-2), DCF-lactam (*N*-(2,6-dichlorophenyl)-2-indolinone, CAS: 15362-40-0) and DCF-BA (DCF-Benzoic Acid, CAS: 13625-57-5) were purchased from TRC (Toronto, Canada). All chemical standards were >95% purity grade. Acetonitrile (LC-MS grade) was received from Merck (Darmstadt, Germany) and water was prepared with a Milli-Q system (Merck Millipore).

4.2.2 Wastewater treatment plants

The municipal WWTP in Bad Ragaz (WWTP-BR) has 25 500 PE (person equivalents) connected and an average influent load of 3200 m³/d. The WWTP is equipped with a biological activated sludge treatment stage, which is separated into a series of three compartments by low walls, i.e., cascades. The first compartment is a denitrifying compartment and the second is aerobic (2 mg/L O₂). In both compartments the biomass is suspended in sludge flocs. The third compartment is the nitrifying stage with a higher aeration rate (3 mg/L O₂). It contains carriers (Biofilm Chip M, AnoxKaldnes, 35% filling ratio, ≈ 420 m²/m³) for biofilm growth (hybrid-moving bed biofilm reactor, MBBR). The carriers are retained in the third compartment by a screen. A recirculation of roughly 0.7 parts (ratio to influent) takes place from the 3rd to the 1st compartment.

In addition to the Bad Ragaz WWTP, two further WWTPs were studied. Both WWTPs were sampled to provide inoculant for batch experiments. One is located in Klippan, Sweden (WWTP-KL), with 13 000 PE connected and has a similar configuration to WWTP-BR (hybrid-MBBR). In one of its treatment lines, two denitrifying compartments are followed by an aerobic compartment with 2 mg/L O₂. All three are activated sludge compartments without carriers. These are followed by a fourth compartment (nitrifying) with 3 mg/L O₂ containing carriers (Biofilm Chip M, 40% filling ratio, ≈ 480 m²/m³) for biofilm growth. The third

WWTP is located in Koblenz, Germany (WWTP-KO), with 220 000 PE connected and an average load of 61 000 m³/d. This plant has denitrifying, followed by nitrifying (1.5 mg/L O₂, 4 g/L) suspended sludge compartments but does not make use of carriers in any stage of the treatment.

4.2.3 Aerobic laboratory incubation experiments

Incubation experiments in batch mode up to two weeks in duration were conducted in bench-top vessels using either biofilms on carriers from WWTP-BR or WWTP-KL or, for comparison, activated sludge from WWTP-KO as inoculant. In these experiments 400 mL of WWTP effluent (from WWTP-KO) was inoculated with carriers from WWTP-BR to a concentration of 35 carriers/L ($\approx 300 \text{ m}^2/\text{m}^3$, 2.2 g/L total biomass). Carriers were sampled from WWTP-BR on 2nd March, 18th May and 9th July 2015. The experiments were started a day after sampling due to transport time. After inoculation of the reactors the system was equilibrated for at least 3 h, after which DCF was spiked to concentrations of 5 $\mu\text{g}/\text{L}$ or 200 $\mu\text{g}/\text{L}$ and DCF-TPs were spiked to individual reactors to concentrations of 200 $\mu\text{g}/\text{L}$. The experiments with low DCF spike concentrations were conducted in triplicate. The other experiments were run at least as duplicates. During the incubation period, the vessels were constantly stirred and purged with air (flow rate: 50 mL/min). To maintain a constant pH, either by CO₂ added to the purge air mixture ($\approx 1:1000$) or NaOH solution (1 mol/L) was added drop-wise. Water samples of 2 mL were taken at defined intervals (for 200 $\mu\text{g}/\text{L}$ spike: at the start, after 2 h and 1 d and then approximately every 2 d; for 5 $\mu\text{g}/\text{L}$ spike: approximately every 3 h for the first day and then every 3 d). After sampling, the water samples were immediately filtered (0.45 μm regenerated cellulose, Whatman) and then frozen at -25°C . In a previous study, sorption of DCF to this filter material was investigated and was observed to be low, $\approx 8\%$ (Hebig et al., 2014). Sorption of DCF ($\text{p}K_a = 4.15$ (Sangster, 1997)) to sludge or biomass was estimated based on distribution coefficients for activated sludge, $K_d \approx 0.03 \text{ L/g}$ (Stevens-Garmon et al., 2011; Fernandez-Fontaina et al., 2014) and was likely to be small, $\leq 6\%$ (Schwarzenbach et al., 2005).

Experiments with activated sludge from WWTP-KO were conducted in parallel under exactly the same conditions as those with carriers from WWTP-BR. Sludge was taken from the nitrifying reactor of WWTP-KO and diluted by a factor of

two with effluent from WWTP-KO (final sludge concentration 1.6 g/L). Incubation experiments in batch mode with carriers from WWTP-KL were conducted in 6 L vessels using 62.5 carriers/L ($\approx 525 \text{ m}^2/\text{m}^3$) and WWTP effluent as the liquid phase (4.75 g/L total biomass). These were also aerated to maintain oxic conditions. DCF was spiked to 1 $\mu\text{g}/\text{L}$. Samples were taken at defined intervals (every 2 h) during an incubation time of 24 h. The water samples from all experiments were analysed without further sample preparation (i.e., direct injection) by LC-QToF-MS as described in Section 4.2.5.

Determination of carrier-attached biomass and suspended sludge concentration

To determine the amount of carrier biomass, 5 replicates each of 5 carriers were dried overnight at 105 °C then weighed. The carriers were then soaked in 2 mol/L HCl overnight, cleaned with sonication, stirring and scrubbing, twice with 2 mol/L HCl, twice with detergent and three times with Milli-Q water over the course of several days (including overnight soaking periods). Finally, the cleaned carriers were again dried overnight and weighed again. To determine the suspended sludge concentration, WWTP sludge (25 mL) was filtered onto dried and pre-weighed glass fiber filters (GF6, Whatman) followed by overnight drying at 105 °C and finally weighed (5 replicates).

4.2.4 Monitoring campaign at WWTP Bad Ragaz and WWTP Koblenz

Flow-proportional composite samples of WWTP influent and effluent during 10 consecutive 24 h periods as well as grab samples of each reactor compartment were taken in July 2015 from WWTP-BR. During collection the samples were refrigerated at 4 °C in automated sample collectors. After collection was complete the composite samples were filtered (0.45 μm regenerated cellulose, Whatman) and stored at -25 °C. PP and PE plastics used in sampling and storage have been reported to not significantly sorb DCF (Hebig et al., 2014). As was the case for the batch experiments, sorption of DCF to reactor biomass was calculated to be low (15% based on carrier biomass and suspended sludge concentrations of 4.7 g/L and 1.2 g/L (Falås et al., 2013)) and not significant for removal (see section

4.2.5). Most DCF-TPs contain similar structural moieties and have lower chromatographic retention times than DCF indicating they should have similar or lower sorbed fractions. TPs such as DCF-lactam, which do not have a carboxylic acid moiety show slightly higher sorption, this was tested in a batch experiment with sterilised sludge. Water samples were analysed for the presence of DCF and DCF-TPs without further preparation by LC-QToF-MS as described in Section 4.2.5. During the sampling period there were no major rain events. The average hydraulic load was $(2800 \pm 300) \text{ m}^3/\text{d}$ with a hydraulic retention time (HRT) of 16 h for the whole system. The sludge age was 5 d, the average water temperature $21 \text{ }^\circ\text{C}$ and the ammonium removal was $> 99\%$. For WWTP-KO, time-proportional composite samples of WWTP influent and effluent were taken on 2 consecutive 3 d (72 h) periods in December 2015. These were prepared and analysed analogously to the monitoring campaign at WWTP-BR.

4.2.5 Analytical methods

Analysis was conducted with a high-resolution LC-QToF-MS system (HPLC: Agilent 1260 series, MS: Sciex 5600 TripleTOF). The HPLC consisted of a degasser, a binary pump to provide the gradient mobile phase flow, a second pump to provide an isocratic flow to the MS while the divert valve was in use, an autosampler with a refrigerated vial tray and a column oven. The HPLC was equipped with a Zorbax Eclipse Plus C18 column ($150 \text{ mm} \times 2.1 \text{ mm}$, $3.5 \mu\text{m}$, Agilent Technologies). The chromatographic method used a gradient elution with water and acetonitrile both with 0.1% formic acid buffer. The HPLC was coupled to the MS via electrospray ionisation (DuoSpray Source, Sciex). Data was acquired in both positive and negative ionisation modes, separate injections were used for each mode. The instrument was automatically recalibrated every 2.5 h using an automated calibrant delivery system (CDS) which injected a calibration solution into the MS via the APCI probe of the DuoSpray source. A divert valve was used to divert the first 1.5 minutes and the last 7 minutes of each chromatographic run to the waste. MS scans in each scan cycle included one full scan of (100 to 1200) u and eight data-dependant MS^2 scans, which were product ion scans of the most intense peaks from the full scan (mass range of 30 u to mass of the precursor ion). An exclusion list was used to avoid acquiring MS^2 scans of background signals and a precursor mass list was used to ensure that MS^2 scans of known TPs were acquired. Further details

of the chromatography and acquisition method can be found in [Schlüsener et al. \(2015\)](#) and [Nürenberg et al. \(2015\)](#). For analysis of the high-resolution MS data, PeakView and MasterView software were used for the identification and structural characterisation of TPs and MultiQuant software was used to obtain peak areas (all provided by Sciex). Data was analysed and presented using R ([R Core Team, 2015](#)) and the *ggplot2* package ([Wickham, 2009](#)). For compounds with available standards, MultiQuant was used for quantification. These were DCF and the TPs 4HD, DCF-lactam and DCF-BA. The concentration of the TP 5HD was estimated based on the calibration of 4HD. DCF- d_4 was used as an internal standard (2 µg/L) and the linear calibration ranged from (5 to 5000) ng/L. Recoveries and LOQs for the method are provided in Table 4.1. The degradation of DCF removal during the incubation experiments was modelled by pseudo-first-order kinetics according to [Schwarzenbach et al. \(2005\)](#) (Equation 4.1).

$$\frac{dC_{\text{DCF}}}{dt} = -k_{\text{biol}}C_{\text{DCF}}X_{\text{SS}} \quad (4.1)$$

Where k_{biol} is the first-order rate constant in L/(g d) (g biomass or suspended sludge), C_{DCF} is the DCF concentration in µg/L and X_{SS} is the carrier-attached biomass concentration or suspended sludge concentration in g/L. A simplified model of a completely stirred tank reactor was used to estimate residual fraction of DCF ($S_{\text{out}}/S_{\text{WW}}$) in a full-scale reactor assuming negligible removal due to sorption (Equation 4.2), ([Joss et al., 2006](#)), where θ_h is the hydraulic retention time (HRT) of the reactor. The removal of DCF due to excess sludge production was previously modelled by [Falås et al. \(2013\)](#) for WWTP-BR and found to be not significant.

$$\frac{S_{\text{out}}}{S_{\text{WW}}} = \frac{1}{1 + k_{\text{biol}}X_{\text{SS}}\theta_h} \quad (4.2)$$

Table 4.1: Recoveries and LOQs for the analysis method for DCF and TPs in wastewater samples

	DCF	4HD	DCF-lactam	DCF-BA
Recovery influent	107% ± 4%	73% ± 3%	114% ± 6%	114% ± 2%
Recovery effluent	115% ± 4%	93% ± 5%	125% ± 5%	117% ± 4%
LOQ (ng/L)	10	5	10	20

4.3 Results and discussion

4.3.1 Transformation of diclofenac in lab-scale experiments containing carriers from a WWTP employing an MBBR

Elevated diclofenac concentrations (200 µg/L) to elucidate transformation products

To study the influence of an MBBR on the removal of diclofenac (DCF), laboratory-scale incubation experiments were conducted with carriers taken from WWTP-BR and WWTP-KL (see Section 4.3.3 for WWTP-KL experiments). In initial experiments with WWTP-BR carriers, 200 µg/L DCF was spiked to the bioreactors and the formation of TPs was studied over a period of 12 d by analysing the aqueous phase with LC-QToF-MS. Within the first 24 h of incubation the DCF concentration was reduced by > 99%. However, the elimination of DCF was concurrent with the appearance of a large number of TPs. In total, more than 20 different TPs were observed (Figure 4.1). The identification of each TP was based on the high resolution ion mass and isotopic pattern, which was used to calculate a plausible molecular formula, and the MS² fragmentation spectrum providing structural fragments of the TP. Details of the TP identification, including the MS² spectrum and structural elucidation are provided in the Supplementary Data. Confidence levels (1–4) for the structures, based on the categorisation proposed by Schymanski et al. (2014) are given in Figure 4.1 with level 1 indicating a confirmed structure. For confidence levels 2–4 an alternative characterisation method is needed to confirm their identity. However, accumulated concentrations were not high enough for the isolation of TPs.

The TPs DCF-lactam, 4HD (4'-hydroxy-DCF), 5HD (5-hydroxy-DCF) and DCF-BA (DCF-benzoic acid) were identified as primary TPs. Fortunately, they were available as analytical reference standards and hence they were also individually incubated in separate bioreactor experiments. It was found that in the lab-scale systems with carriers from WWTP-BR, the biodegradation of these four primary TPs led to the formation of all other TPs observed in the experiments where DCF was spiked. Each primary TP was transformed into several secondary TPs (Table C.23 in the Appendix) in the supplementary data) which in turn were frequently further converted. The overall outcome of these experiments was a complex web of

transformation pathways, which can be predominantly explained by six reactions: a hydroxylation of the aromatic rings A and B, an intramolecular amidation/deamidation, a sulfate conjugation of phenolic hydroxyl groups, a reductive dechlorination of the aromatic ring A, an oxidative ring-opening of ring B and oxidations by dehydrogenation of phenolic moieties. TP structures, their time courses during the experiment and their position in the overall transformation pathway are shown in Figure 4.1, along with a categorisation of the reactions leading to the individual TPs. It must be noted that except for TP343, TP243 and TP287, all TPs are intermediates since they are further degraded. The subsequent TPs are unknown since no further TPs could be detected. The concentrations of TP343 and TP243 reached a plateau after a few days, while those of TP287 increased constantly until day 12. However, it was estimated from the peak areas that these did not account for a significant proportion of the transformed DCF.

The four primary TPs were formed within the first 24 h in the carrier-based, lab-scale experiment, but were quickly converted to secondary TPs. Hence, the sum of the primary TPs did not close the mass balance of DCF transformation (Figure C.23 in the Appendix). DCF-lactam reached the highest concentration of the four primary TPs and had the highest peak area of all TPs (9 µg/L, 4.5% of the spiked DCF). This TP is formed by intramolecular amidation of the carboxylic acid with the primary amine. The primary TP DCF-BA is formed by a formal decarboxylation and an oxidation of the aliphatic CH₂ moiety to a carboxylic acid group. In these experiments the concentration reached 0.5 µg/L which accounts for 0.25% of the spiked DCF. The ring hydroxylation of DCF led to 4HD and 5HD, known as both bacterial and mammalian TPs of DCF (Gröning et al., 2007; Sarda et al., 2012; Stülten et al., 2008). Both are formed and dissipated within the first 2 d of incubation and many secondary TPs are formed from these compounds.

4HD Six DCF-TPs formed via 4HD and are shown on the left side of Figure 4.1. TP293b is formed via intramolecular amidation while TP297 is formed via decarboxylation and oxidation. A sulfate conjugation of the phenolic hydroxyl group of 4HD led to the formation of TP391b. The molecular formulas and isotopic patterns of TPs 259 and 225 show that these were formed through dechlorination reactions. A lactam structure is postulated to account for the fragmentation pattern and loss of oxygen while to account for the additional hydrogen, a reductive

dechlorination reaction is proposed (further details are in the Appendix Section C.1.10). A dechlorination did not occur via any other primary TP, suggesting the hydroxy group on ring A is necessary for dechlorination. This may be explained by electron-donor effects or the ability to bind into an enzyme active site. Finally, TP275 could be explained by a formal oxidation by dehydrogenation of 4HD, due to the similar fragmentation spectrum. All the secondary TPs of 4HD appeared during the first day of incubation but were quickly dissipated, indicating that these were all intermediates of a larger transformation pathway leading to small molecules. However, no further TPs could be found, most likely because i) their concentrations were below the limits of detection of the instrument and ii) small, highly polar TPs were formed that are not detectable with the analytical method used or degradation proceeded to a mineralisation.

5HD Nine TPs were formed via 5HD and are shown on the right side of Figure 4.1. TP293a is formed via intramolecular amidation. A sulfate conjugation of the phenolic hydroxyl group of 5HD formed TP391a. An oxidation of 5HD by dehydrogenation was responsible for the formation of 5HDQI (hydroxy diclofenac quinone imine). 5HD was already converted into 5HDQI in ultra-pure water by an abiotic reaction (Gröning et al., 2007), and this was also observed to occur in standards of 5HD prepared for this study. However, the conversion is quite slow compared to the biological conversion. A sterile control with autoclaved carriers did not show conversion of 5HD within a 6 d incubation period (data not shown), indicating that the biological reaction dominates in this environment. Via 5HD, six further TPs were observed whose MS² spectra indicated an oxidative opening of the non-chlorinated ring, B. This was postulated due to the large number of oxygen atoms on the right side of the molecule and consecutive CO₂, CO, and CH₂ neutral losses while ring A was left unchanged. Due to the ring opening there were several potential chemical structures based on the MS² spectra. For TP285, a plausible structure was found, while for the others the fragmentation was more ambiguous so the data could provide only the sum formula of the cleaved ring B.

DCF-lactam The reactions of DCF-lactam are associated with an opening of the lactam ring and a subsequent reaction such as oxidation (two electron transfer) to

4HDQI or decarboxylation to DCF-BA. In addition, a hydroxylation of the chlorinated ring A led to the formation of TP293b. The 4HDQI TP was not observed as a direct TP of 4HD, but rather only via DCF-lactam. This might be due to the fast dissipation kinetics of 4HD in this environment, allowing little oxidation to take place, while DCF-lactam is more stable, allowing the formation of 4HDQI over a different route, e.g., by combined mono-oxygenation and deamination.

DCF-BA This TP is transformed by hydroxylation into TP297 (which is also formed by decarboxylation of 4HD) as well as to two further TPs (TP285 and TP287) where the non-chlorinated ring B is oxidatively opened. Both of these TPs are also formed by the ring opening of 5HD as was discussed previously.

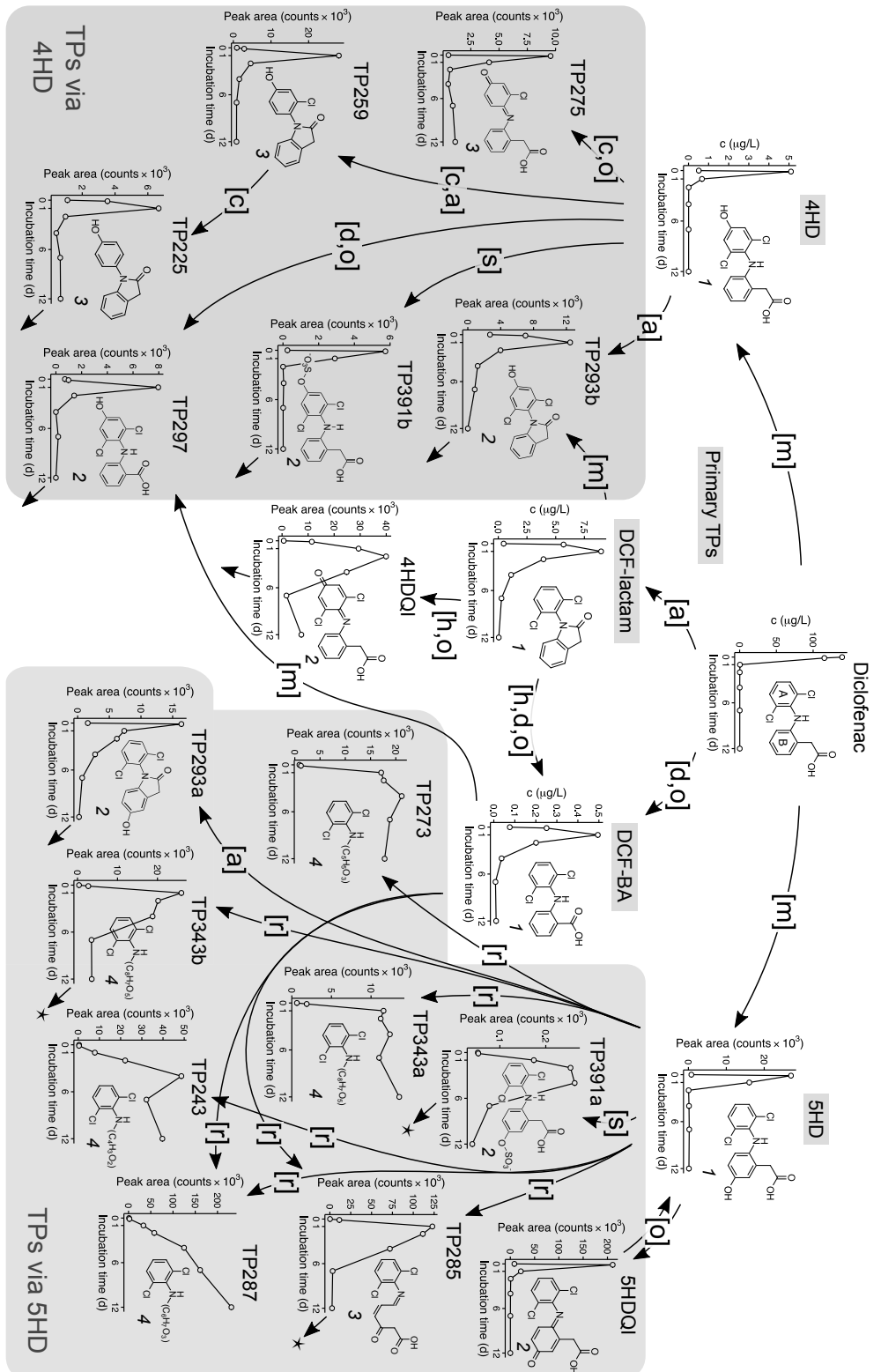


Figure 4.1: Formation of TPs from DCF during the incubation with carriers showing time courses and structures. Arrows indicate pathways elucidated by separate incubations of DCF and primary TPs. Abbreviations for postulated reaction types: [m] mono-oxygenation, [o] oxidation (dehydrogenation), [a] amidation, [d] decarboxylation, [s] sulfate conjugation, [r] ring-opening reactions and [c] reductive dechlorination, [h] amide hydrolysis. Numbers at the bottom right of each structure indicate the confidence level. 1: Confirmed structure based on reference standard. 2: Proposed structure based on MS² characterisation and evidenced by plausible transformation reactions. 3: Tentative structure similar to level 2 confidence, but alternative structures cannot be totally ruled out. 4: Plausible chemical structure could not be derived from the MS² spectrum. The molecular formula and only one structural moiety (ring A) could be confirmed. Transformation to unknown TPs in indicated by *.

Environmental diclofenac concentrations (5 µg/L)

Lab-scale experiments at DCF concentrations of 5 µg/L with carriers from WWTP-BR exhibited similar results as obtained by spiking 200 µg/L: The DCF concentration was reduced by > 99% within the first 24 h with a similarly high degradation rate constant (Table 4.2). In total, 11 TPs were detected from DCF (Figure C.22 in the Appendix), all of which were already seen at the 200 µg/L spike level as the most intense peaks at that level. Thus, the reduced number of detected TPs is most likely caused by the detection limits of the LC-QToF-MS measurements. It can be concluded that the results obtained with 200 µg/L DCF spike can be transferred to lower concentrations with respect to both the kinetics of DCF removal and the transformation pathways. The kinetics of TP formation and removal were in some cases different, both TP285 and 4HDQI show more persistence in these experiments suggesting these might be present in WWTP effluent.

4.3.2 Incubation experiments with activated sludge from WWTP Koblenz

Incubation experiments were conducted with suspended sludge from WWTP-KO, which does not use carriers anywhere on the treatment train. The removal rate of DCF in contact with this biomass was significantly slower in comparison to the incubation with carriers from WWTP-BR (Figure 4.2 and Table 4.2). These experiments were conducted in parallel and in duplicate using the same reactor set-up and similar biomass concentrations. A long incubation time was chosen to be able to see a significant removal of DCF in the suspended sludge reactors. Even after 12 d only 50% of DCF was dissipated, while in experiments with carriers from WWTP-BR DCF was completely removed after 24 h.

In contact with suspended sludge, the same primary TPs (4HD, 5HD, DCF-lactam and DCF-BA) and a few secondary TPs (4- and 5HDQI and TP293) were observed as were found in the carrier-inoculated experiments. The formation rates of primary TPs were much slower, as could be expected due to the slower DCF removal rate. However, also the rates of dissipation of the primary TPs were slower compared with the incubation with carriers (Figure 4.2). Reactions occurring in both systems are hydroxylation of the aromatic rings, the intramolecular

amidation, decarboxylation and oxidation reactions. Several TPs, such as TP259 (the result of dechlorination) and TP285 (the result of oxidative ring opening) are unique to the carrier-inoculated system. The TP with mass 259, might require anaerobic zones to be formed, which are more likely to occur in the dense biofilm growth on carriers than in the suspended sludge flocs. Reductive dehalogenation reactions are more commonly observed in the absence of aerobic conditions (Zhang and Bennett, 2005; de Beer et al., 1997). No TPs were found to be unique to degradation in contact with suspended sludge. A full list of the TPs formed in suspended sludge can be taken from Figure 4.2.

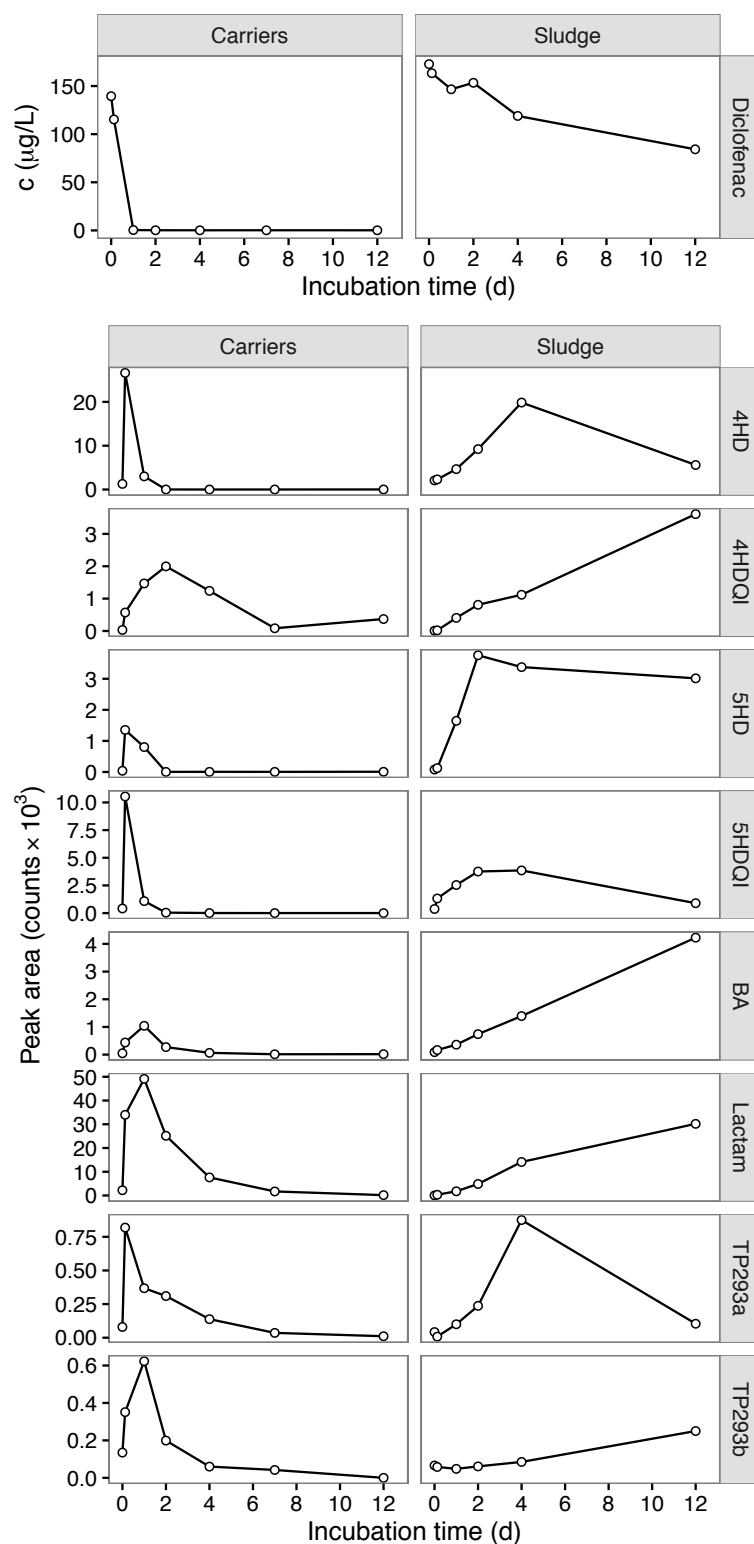


Figure 4.2: Formation and dissipation of DCF-TPs in incubations with carriers from WWTP-BR (left) versus suspended sludge from WWTP-KO (right).

4.3.3 Incubation experiments with carriers from WWTP Klippan

To investigate the transferability of the results from WWTP-BR to other MBBR systems, the removal of DCF was investigated in WWTP-KL, which has a similar set-up to WWTP-BR and employs a compartmentalised reactor with activated sludge and carrier-filled compartments. Lab-scale incubation experiments were conducted in lab-scale bioreactors inoculated with carriers from WWTP-KL. DCF was spiked to 1 $\mu\text{g/L}$ to the bioreactors. A fast dissipation of DCF was observed, with a reaction rate constant of about 1.4 L/(g d), which was similar to that found in the lab-scale experiments with carriers from WWTP-BR (Table 4.2), while typical literature rate constants for DCF in activated sludge are (0.01 to 0.5) L/(g d) (Tran et al., 2009; Urase and Kikuta, 2005). The primary TPs DCF-lactam and DCF-BA were identified as well as TP285, which were observed in lab-scale experiments of WWTP-BR and detected in the effluent of WWTP-BR (for identification, see Table C.24 in the Appendix). Signals for the other TPs were either too weak for proper identification, or they were not observed at all. In summary, a fast degradation of DCF might be linked to hybrid-MBBR biomass, and certain TPs might be markers for these processes, e.g., the formation of TP285. The signal intensity of TP285 is nevertheless very low and is unlikely to account for the majority of DCF removal.

Table 4.2: Pseudo-first-order rate constants of DCF in different biomass types

Source of biomass	Concentration of DCF ($\mu\text{g/L}$)	k_{biol} (L/(g d))
WWTP-BR	5	1.4 ± 0.1
WWTP-BR	200	$\geq 1.5^a$
WWTP-KL	1	1.4
WWTP-KO	200	0.03 ± 0.01

^aEstimate, not enough data points for a precise determination.

4.3.4 Monitoring campaign at WWTP Bad Ragaz

To verify the transferability of the lab-scale results to full-scale, WWTP-BR was monitored over a dry-weather period during the summer of 2015. From ten consecutive days, 24 h-composite samples of WWTP influent and effluent were analysed

by LC-QToF-MS. The results for compounds for which reference standards were available are shown in Figure 4.3. The DCF concentration was reduced from a median of 1.6 $\mu\text{g/L}$ in WWTP influent to 0.2 $\mu\text{g/L}$ in WWTP effluent. This corresponds to an average removal of 88% during the 10-day monitoring period.

The formation of TPs was also observed in the full-scale plant. An average concentration of 0.25 $\mu\text{g/L}$ DCF-lactam was detected in the effluent of the WWTP, accounting for about 16% of the influent DCF concentration. DCF-lactam was the most predominant TP in both WWTP effluent and in lab scale experiments where DCF-lactam reached 13% of spiked DCF (Figure C.22). The TP 4HD was present at relatively high concentrations in WWTP influent but was removed in the biological treatment as was the case in the lab-scale experiments. The TP 5HD was also found in the influent, albeit at lower concentrations and was no longer detected in the effluent. Both TPs 4HD and 5HD are human metabolites of DCF explaining their detection in WWTP influent. No evidence for the formation of these TPs during the treatment process could be obtained due to i) the high influent concentrations and ii) the fast transformation of these TPs. The TP DCF-BA was observed at low concentrations of (23 ± 8) ng/L in WWTP effluent, whereas in the influent it was below the LOQ of 20 ng/L . Thus, a minor fraction of DCF-BA might be formed. The presence of several secondary TPs could be confirmed based on their exact mass, retention time and fragmentation spectrum, which matched very well with the results of the lab-scale experiments. These were TP293b, TP259 and TP285 (for identification see Table 4.3). In all samples the signal intensities were relatively low, comparable with the peak areas of DCF-BA, which was present with about 20 ng/L . In the results of the lab-scale experiments, TPs 259 and 285 had very high signal intensities compared to all other secondary (or tertiary) TPs (Figure 4.1), which hints at their relative importance in the transformation pathway. Since standards of these TPs could not be obtained, peak areas in the WWTP influent and effluent were compared to estimate if a formation took place (Figure 4.3). Both TP259 and TP285 were only detected in WWTP effluent, indicating that a formation is possible, whereas TP293b was detected in both WWTP influent and effluent at similar intensities. Making such comparisons between different matrixes without standards should be treated as an initial estimate and the results should be taken with caution. In summary, out of 11 TPs detected in the lab, 7 TPs were detected at the WWTP, the exceptions being the

two HDQIs, TP293a and TP287.

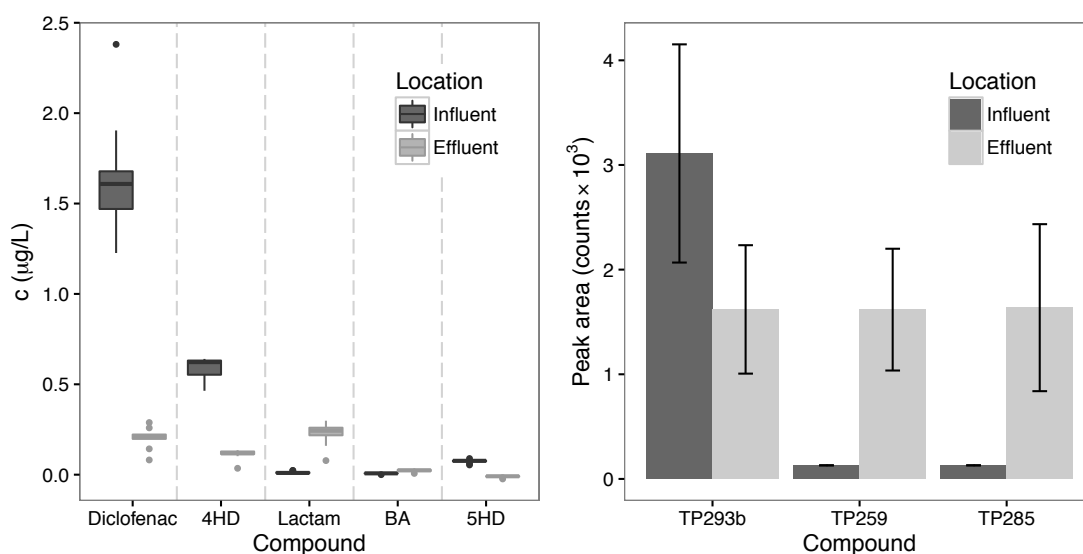


Figure 4.3: Left: Analysis of samples from WWTP-BR (hybrid-MBBR) for DCF and DCF-TPs for which standards were available. Right: Comparison of concentrations of DCF-TPs in influent and effluent based on peak areas (no available standards).

It can be concluded from the results that i) the laboratory incubation experiments were able to accurately represent the treatment process with respect to DCF ii) DCF and its TPs were substantially removed by the WWTP, and low concentrations of some DCF-TPs were detected in the effluent iii) although a wide array of TPs were found using incubation experiments, the majority of these were not detected in the WWTP, since their concentrations were probably below the limits of detection.

The influent and effluent samples of the WWTP provide only a picture of the full treatment process, which includes reactor compartments with activated sludge (no carriers) and a carrier-filled MBBR. To test if the TP formation was occurring primarily in the carrier-filled compartment, grab samples were taken from each reactor compartment. By comparing the different compartments, it was found that TPs 259, 285 and DCF-lactam showed the most intense signals in the carrier-filled compartment (Figure 4.4). DCF itself had a much lower concentration in this compartment compared with the aerobic and denitrification compartments. The high concentration decrease of DCF between the influent and the denitrification stage is at least partly caused by dilution, since a recirculation of approximately 0.7 parts

took place in the reactor. The expected concentration of DCF in the denitrifying stage resulting from dilution alone would be approximately $1 \mu\text{g/L}$, which is close to the detected concentration of $0.8 \mu\text{g/L}$. The increased concentrations of TPs in the denitrifying stage can also be explained by the recirculation. The results as a whole support the conclusion found by Falås et al. (2013), that the carrier-filled stage is mainly responsible for the DCF removal. Here this can be seen from the point of view of the TPs that are formed.

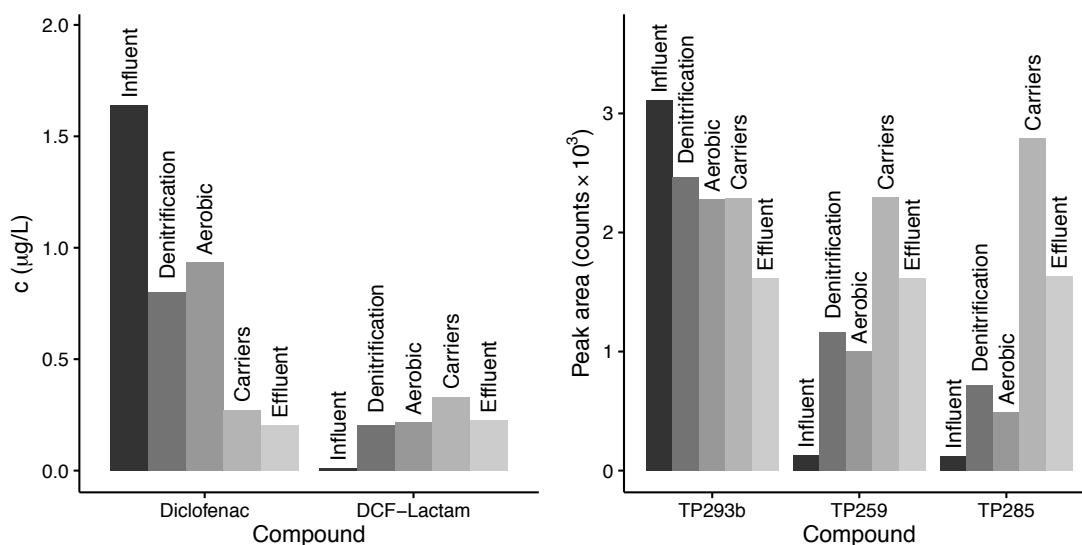


Figure 4.4: Concentrations of DCF and DCF-lactam and peak areas of TP293b, TP259 and TP285 in different compartments of the biological reactor of WWTP-BR (hydrid-MBBR).

Table 4.3: Identification of TP285 and TP259 in WWTP-BR effluent samples by comparison to lab-scale experiments

	TP285		TP259	
	Lab-scale	WWTP	Lab-scale	WWTP
Retention time (min)	8.6	8.7	10.1	10.2
$[M + H]^+$ mass (u)	286.0035	286.0029	260.0465	260.0454
isotope peak ratio (^{37}Cl)	67%	64%	37%	29%
Fragment ions from the MS ² spectrum (u)	177.0330	177.0319	168.0800	168.0803
	242.0118	242.0138	196.0758	196.0753
			197.0840	197.0775

4.3.5 Monitoring campaign at WWTP Koblenz

To compare the relatively good removal of DCF observed at WWTP-BR with a conventional WWTP not employing an MBBR, a monitoring campaign of WWTP-KO was carried out. In composite samples of WWTP influent and WWTP effluent no significant removal of DCF was detected ($< 20\%$), while influent concentrations were approximately $3.5 \mu\text{g/L}$. This agrees with the slower removal of DCF observed in lab-scale incubation experiments with activated sludge not using carriers (Section 4.3.2 and Table 4.2). Using Equation 4.2 to model the full scale reactor, a 3% (negligible) removal would be expected based on the k_{biol} found (4 g/L sludge concentration and 6 h HRT). Examining the measured data, although no detectable removal of DCF took place, low signals for several DCF-TPs and human metabolites were observed. These included 4HD, 5HD and TP293b, which were detected in both WWTP influent and effluent, as was the case at WWTP-BR. DCF-lactam was detected in the effluent of WWTP-KO, but not in WWTP influent, indicating a small formation took place. As was the case with the lab-scale experiments, TP285 and TP259 were not detected in the effluent of WWTP-KO, which is consistent with these being unique to the degradation of DCF in contact with the carrier biomass.

4.4 Conclusion

DCF can be removed effectively in a cascaded hybrid moving bed biofilm reactor (hybrid-MBBR) achieving nitrification and denitrification. The degradation primarily occurred in the last compartment containing the carrier-attached biomass. In this study, a fast dissipation was observed but many TPs were formed. Due to the highly branched nature of the transformation pathway, these are mostly present at very low concentrations in the WWTP effluent. The sum of all quantifiable TPs did not explain the degraded quantity of DCF, since these were further degraded. Estimating from the peak intensities of the remaining TPs, these made up a small fraction ($< 5\%$) of the transformed DCF. Hence, although ecotoxicological studies of the complex TP mixtures formed from DCF are missing, it is likely that biological degradation of DCF results in significantly lowering its ecotoxicological impact.

After long incubation times, it was evident that the main reactions leading to DCF removal had the potential to also occur in contact with conventional activated sludge (i.e., suspended sludge with no biofilm carriers). However, based on the much slower reaction rates the transformations were not observed to occur to a significant degree in the full-scale activated sludge process. It can be concluded that the observed transformation of DCF in hybrid-MBBR systems is linked to different reaction kinetics of two very similar transformation pathways rather than one system able to perform special reactions which the other system cannot. Some reactions forming secondary TPs were unique to the carrier systems, but these did not appear to be the main drivers for the removal of DCF. The underlying microbiological causes of the faster kinetics are still an open question.

It could also be observed that not one but all the different reaction types leading to DCF degradation were significantly faster in the hybrid-MBBR compared with conventional sludge. Therefore, it is likely that other reaction types are faster under these conditions as well, and that in combination this might lead to an improved removal of other CECs. This was indeed observed by [Falås et al. \(2013\)](#) for CECs such as mefenamic acid, bezafibrate and valsartan.

Acknowledgements

The authors thank Bernd Lindner and Peter Zai from ARA Bad Ragaz for their support and technical assistance during the sampling campaign. Funding: This work was supported by the European Research Council [Project *ATHENE*, grant number 267897] and the German Federal Ministry of Education and Research [JPI-Water joint call project *FRAME*, grant number 02WU1345A].

Chapter 5

Conclusion and Outlook

5.1 General conclusions

The goal of achieving a more detailed understanding of biological transformation processes of micropollutants has been achieved through the elucidation of transformation reactions of five micropollutants representing different classes of pharmaceuticals, i.e., antibiotics, NSAIDs and psychoactive drugs; and industrial chemicals. The transformation was studied considering both chemical and biological transformation reactions and different biological reactor configurations including sequencing batch reactors, flow-through reactors and moving bed biofilm reactors.

Investigation of the antibiotic trimethoprim showed that, depending on the concentration of the micropollutant spiked to the experiment, different kinetic results were obtained, which was due to different pathways being dominant in the transformation of the micropollutant at different concentrations. It could be shown that in a pilot-scale wastewater treatment plant (WWTP) used as a reference reactor, the transformation pathway observed at a lower spike concentration was dominant. This transformation pathway was previously not known, although other pathways had been reported. Until now, the concentration of the TPs found in WWTP-effluent has been quite low (ng/L-range), such that an ecotoxicological impact is considered unlikely. The results also highlight the importance of experimental design for elucidating the transformation of micropollutants and how changing

parameters such as sludge concentration and starting concentrations can influence the results.

The transformation of phenols to nitro-phenolic TPs was identified as occurring by a radical reaction through the presence of nitrous acid which decomposes to $\cdot\text{NO}_2$ and $\cdot\text{NO}$ radicals. The reaction is therefore biologically mediated and distinguished from other biological transformation reactions in that it is not enzymatically catalysed. The formation of nitrous acid occurs at acidic pH and in the presence of nitrite, which is an intermediate in the nitrification and denitrification process. Therefore, only in special conditions of nitrite build-up or acidification could a significant formation of nitro-phenolic TPs be expected. This outcome has important consequences for interpreting micropollutant results from processes with high nitrite concentrations. In general, considerations should be made regarding sample preparation, where sample freezing or acidification may result in artificial formation of nitrophenolic-TPs. It was found that during freezing a significant pH reduction of the concentrated liquid phase can occur. During laboratory experiments and monitoring of full-scale WWTPs, it was observed that the phenolic micropollutants studied are more typically transformed by biological processes and the chemical transformation to nitro-phenolic TPs is at most a minor pathway. Reported findings of investigations of other phenolic micropollutants impacted by this type of transformation have found that reactivity can be substance-dependant (Brezina et al., 2015) and may for some micropollutants be the result of different reactive nitrogen species.

The comparison of two biological process types (conventional activated sludge and a hybrid-moving bed biofilm reactor, MBBR) regarding the transformation of diclofenac found similar transformation reactions in both processes but significantly different transformation kinetics. The rates of all the transformation reactions were slower in the activated sludge process, although both had similar biomass concentrations and similar nitrifying activity. In the MBBR process, a large number of TPs were formed, each at relatively low concentration at the low ng/L level. This is a positive finding for the biofilm process indicating that i) the transformation of diclofenac is likely to have low environmental impact due to the almost complete transformation of the precursor and the low concentration of individual TPs and ii) the large number of relatively fast transformation reactions occurring in the biofilm may positively impact the removal of other

micropollutants.

Through systematic testing of experimental procedures, experience has been gained to allow for better design of laboratory incubation experiments in the future. Due to the high variability in the properties of micropollutants, designing more tailored incubation experiments is necessary. While previously applied experimental procedures may be appropriate for the micropollutants studied in those experiments, new micropollutants might pose different challenges. Particularly challenging compounds have properties such as toxicity to degrading microorganisms, as seen in the study of trimethoprim, or susceptibility to acidity as seen with the study of phenols, both of which require special precautions during testing.

The knowledge of transformation pathways of micropollutants can make analysis results, such as concentration changes of the compound in the environment, more meaningful and allow better interpretation of monitoring results. Analysis of TPs together with the precursor micropollutants can i) give better indication of process performance than measuring precursors alone, especially if TPs have similar toxicological properties to their precursors and ii) be used to ask deeper questions into the underlying biological activity of the treatment process. The transformation reactions of trimethoprim, BPA, *o*-phenylphenol, dextrorphan and diclofenac can be assessed in WWTP processes based on analysis of the identified TPs. As mentioned in sections 2.1 and 4.1, high variability in the removal of compounds such as diclofenac and trimethoprim is found in different WWTPs. Understanding of the underlying transformation processes could assist in finding more consistent performance in the removal of these micropollutants. For example, if transformation to a primary TP (for which the ecotoxicological impact is unknown) with a similar structure to diclofenac is occurring, a persisting ecotoxicological risk can not be ruled out. However, if many transformation reactions occur leading to the formation of an array of secondary and tertiary TPs, this is an indication that the ecotoxicological impact has been reduced (Escher and Fenner, 2011).

The investigation of the transformation pathways of five micropollutants reported in this work revealed that some reactions were not unique to one compound, this indicates that these reactions may be generic and can impact different micropollutants. This can add confidence when interpreting data from transformation tests of other micropollutants when similar reactions are observed. In addition, it may

be useful for the prediction of transformation reactions. To make the data more easily accessible and to combine information from other studies these can be added to databases such as EAWAG-BBD (Kern et al., 2009). Repeatedly occurring reactions include the sulfate conjugation, which was observed to occur to phenolic micropollutants and phenolic TPs in chapters 3 and 4. Hydroxylation was observed as a transformation reaction of all five micropollutants investigated and in the case of trimethoprim and diclofenac, hydroxylation reactions were followed by dehydrogenation reactions leading to formation of a ketone in trimethoprim-TP 290 and semi-quinones in the diclofenac-TPs 4HDQI and 5HDQI.

The recent increased availability of high-resolution analysis techniques and versatile data evaluation software is a powerful tool to gain new insight and a detailed perspective on the fate of micropollutants during wastewater treatment. High-resolution and highly sensitive MS instrumentation, coupled with the ability to perform fragmentation experiments *on-the-fly*, i.e., without prior knowledge of the TP's mass, allowed for a detailed analysis of transformation pathways. The high sensitivity permitted the detection of more TPs, including intermediate TPs with low steady-state concentrations; giving clues to elucidate the transformation steps to important final TPs. An iterative approach was applied, which included laboratory incubation experiments, high-resolution MS experiments, identification of TPs and repeating the incubation experiments for TPs or related compounds. The approach was most effective to study the diclofenac transformation pathway in biofilm processes, where primary, secondary and higher levels of TP formation took place in an interconnected transformation pathway.

5.2 Outlook

The results represent an evolution in our understanding of transformation reactions of micropollutants and how to overcome experimental challenges associated with their investigation. Adding further micropollutant case studies and specific process conditions to this knowledge base, beyond those studied here can improve the prediction of the formation of TPs from other micropollutants and is vital to identify potentially toxicologically relevant TPs, which need to be regulated together with their precursors.

The underlying reasons for the different transformation pathways of trimethoprim at different initial spike concentrations in incubation experiments remains unknown. Several possible explanations were postulated (Section 2.3.3) but these could not be tested within the scope of this work. Similar effects were observed with other micropollutants and a deeper understanding of these effects may give a clearer picture of how differences in micropollutant degradation efficiencies can occur under different conditions.

The further study of promising processes such as hybrid-MBBR or other biofilm-based processes would lead to improved understanding of micropollutant removal. The question of whether the fast reactivity found for some micropollutants applies to micropollutant removal in general is still untested and more importantly, the underlying microbiological community differences leading to this improved removal are not fully understood. Deeper understanding would assist in the more general application of these treatment processes with the goal of decreasing micropollutant emissions into rivers and streams impacted by treated wastewater.

Appendix A

Supplementary data for Chapter 2: Biological transformation of trimethoprim

A.1 LC–tandem MS parameters for analysis of trimethoprim (TMP) and TPs

A.1.1 Chromatography and ESI parameters for analysis of TMP and TPs other than DAPC on API 5500 QTRAP and 5600 QTOF

A Zorbax Eclipse Plus C18 column (150 mm × 2.1 mm, 3.5 μm, Agilent Technologies) was used for separation. Chromatography was conducted with gradient elution (phase A: 0.1% HCOOH in water; phase B: 0.1% HCOOH in methanol). Flow rate: 0.3 mL/min. Gradient for phase A: (0 to 3) min, 100%; 4 min, 80%; (16.5 to 22) min, 0%; (22.1 to 28) min, 100%. Injection volume: 80 μL; Source temperature: 500 °C; ionisation voltage: 5.5 kV; curtain gas: 40 psi; gas 1: 40 psi; gas 2: 45 psi.

A.1.2 Chromatography and ESI parameters for analysis by HRMS on LTQ-Orbitrap-Velos

Chromatography parameters are the same as above. Source temperature: 400 °C; capillary temperature: 350 °C; ionisation voltage: 3 kV; sheath gas: 50; aux gas: 15; sweep gas: 0.

A.1.3 Chromatography and ESI parameters for analysis of DAPC on API 4000 QTRAP

A Hypercarb column (150 mm × 2.1 mm, 3 µm, Thermo Scientific) was used for separation. Chromatography was conducted with gradient elution (phase A: 0.1% NH₃ in water (pH 10); phase B: 0.1% NH₃ in acetonitrile). Flow rate: 0.18 mL/min. Gradient for phase A: (0 to 2) min 98%; (4 to 7) min 2%; (8 to 19) min 98%. Source temperature: 600 °C; ionisation voltage: 5 kV; curtain gas: 20 psi; gas 1: 60 psi; gas 2: 60 psi.

Table A.1: Transitions and method performance for MRM mode analysis.

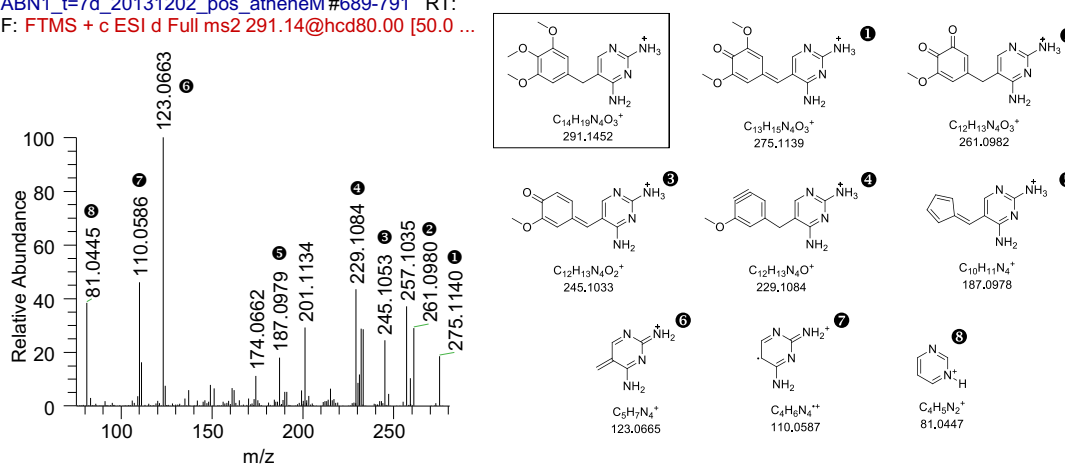
Compound	Transition	Q1	Q3	DP	CE	CXP
TMP (trimethoprim)	A	291	230	86	33	10
	B	291	261	86	35	10
4-desmethyl-TMP	A	277	261	86	38	15
	B	277	123	86	51	10
TP290	A	291	137	80	30	10
	B	291	275	80	30	10
TP292	A	293	243	80	30	10
	B	293	229	80	30	10
DAPC	A	155	137	51	24	10
	B	155	95	51	31	15
	C	155	68	51	35	10
TP306	A	307	243	80	30	10
	B	307	274	80	30	10
TP324	A	325	181	86	50	10
	B	325	137	86	50	10
TMP-d3	A	294	122.9	90	33	10

Table A.2: method performance for MRM mode analysis

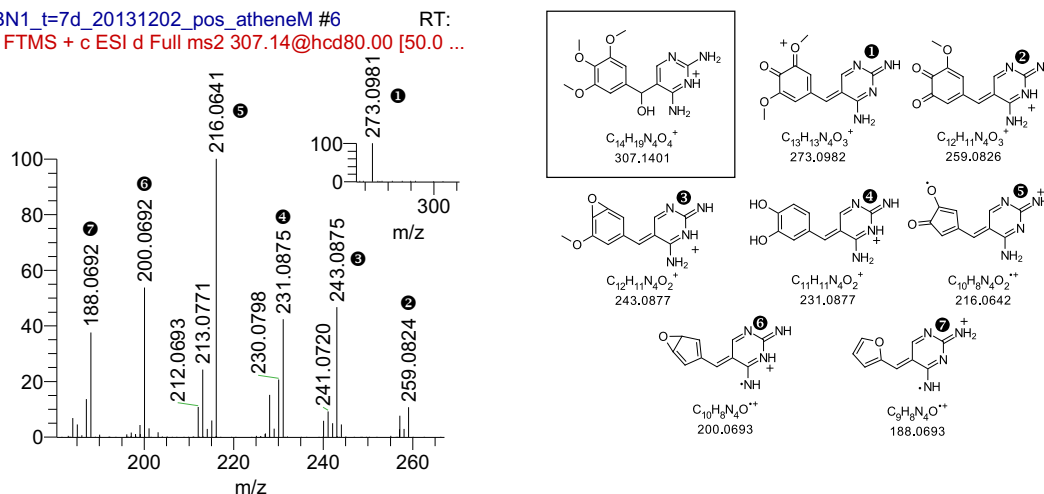
	TMP	4-desmethyl-TMP	DAPC
Estimated LOQ (ng/L)	10	10	40
Relative recovery (%)	95 ± 14 (n=5)	65 ± 20 (n=2)	95 (n=1)

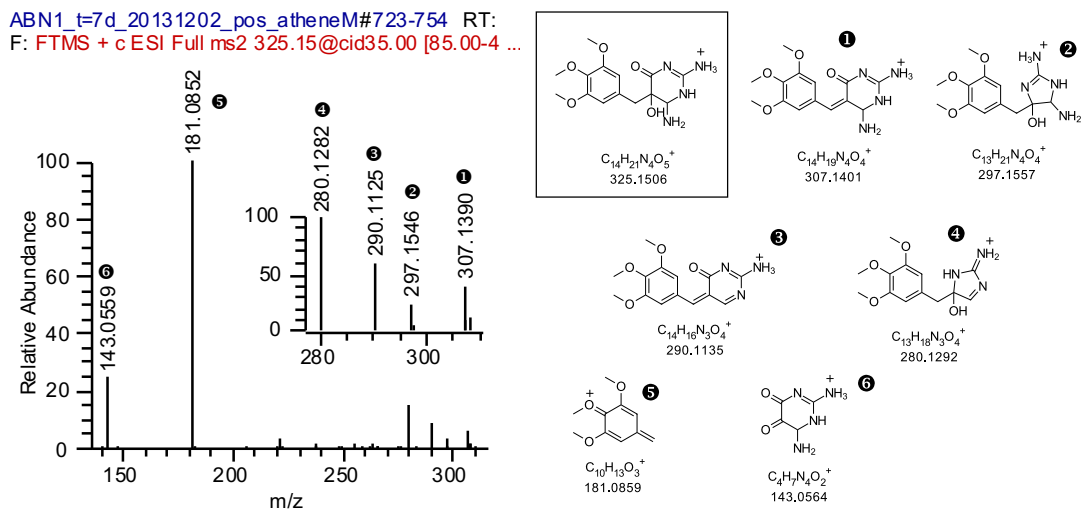
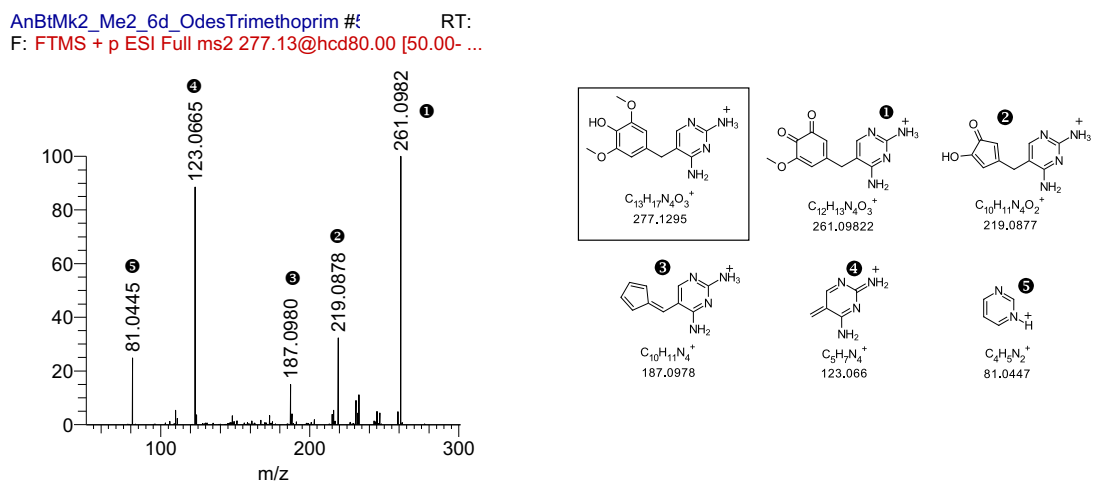
A.2 HR-MS² spectra and structural characterisation of TPs

ABN1_t=7d_20131202_pos_atheneM#689-791 RT:
F: FTMS + c ESI d Full ms2 291.14@hcd80.00 [50.0 ...

Figure A.1: MS² fragmentation of trimethoprim (TMP).

ABN1_t=7d_20131202_pos_atheneM #6 RT:
F: FTMS + c ESI d Full ms2 307.14@hcd80.00 [50.0 ...

Figure A.2: MS² fragmentation of TP306

Figure A.3: MS² fragmentation of Trimethoprim TP324.Figure A.4: MS² fragmentation of 4-desmethyl-TMP.

A2E_5_t=2h_20140206_demeTrim500_ / #629
 F: FTMS + c ESI d Full ms2 293.28@hcd80.00 [100. ...

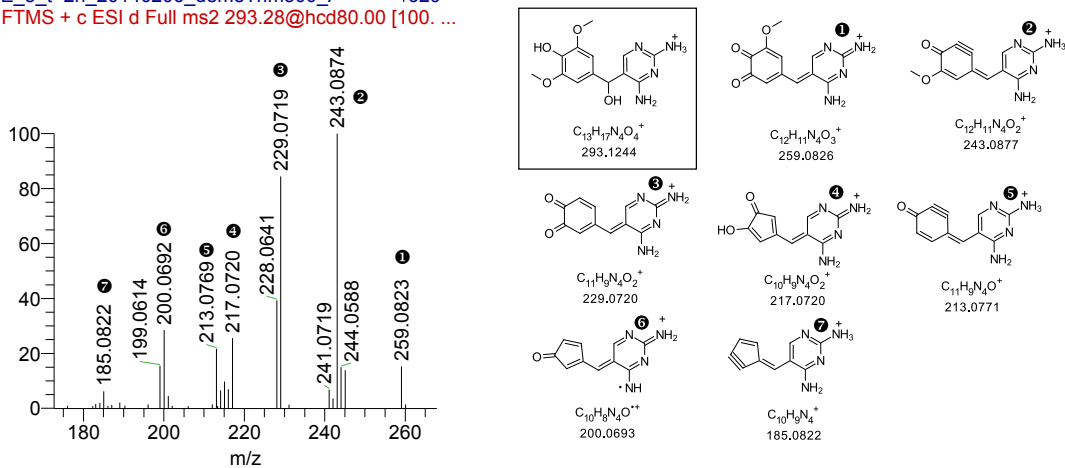


Figure A.5: MS² Fragmentation of TP292.

A2E_5_t=1d_20140206_demeTrim500_ / #824
 F: FTMS + c ESI d Full ms2 291.11@hcd80.00 [100. ...

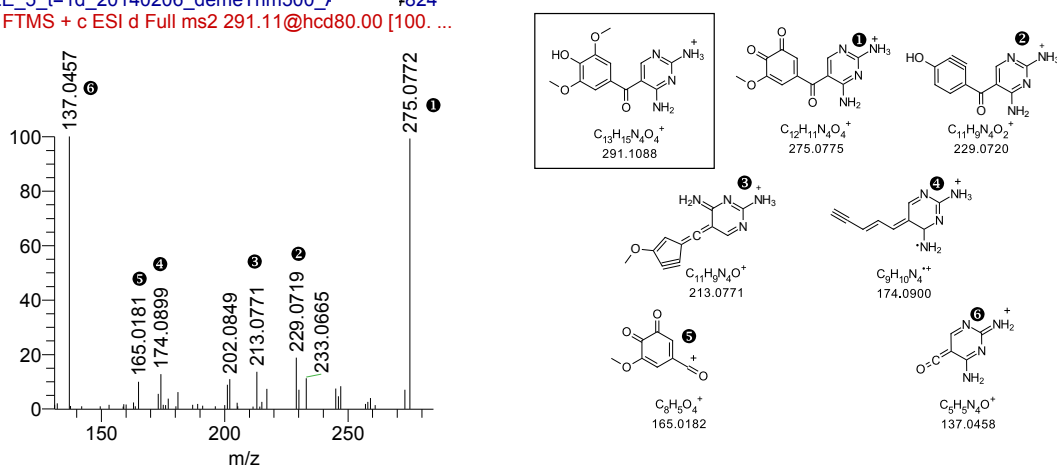


Figure A.6: MS² fragmentation of TP290.

A2E_5_t=2d_20140206_demeTrim500_#
 F: FTMS + c ESI d Full ms2 155.06@hcd80.00 [50.0 ...

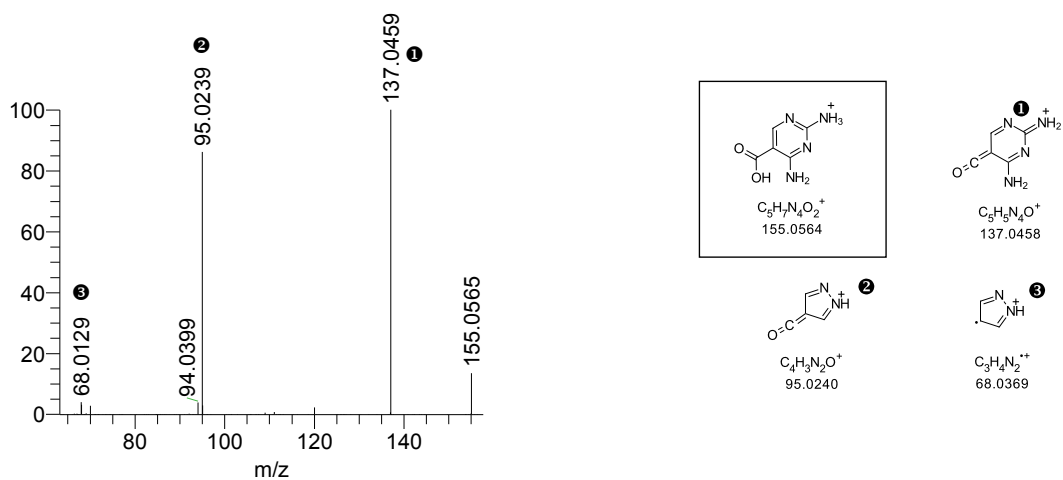


Figure A.7: MS² fragmentation of DAPC (2,4-diaminopyrimidine-5-carboxylic acid).

A.3 Pilot-scale SBR and monitoring experiments

Table A.3: Additional process parameters from the pilot-scale SBR. Average values during the 16-month monitoring period.

	SBR Influent	SBR Effluent
DOC (mg/L)	30.3	11.9
Ammonium (mg/L $\text{NH}_4^+\text{-N}$)	39.4	< 2
Nitrate (mg/L $\text{NO}_3^-\text{-N}$)	0.4	8.4
Nitrite (mg/L $\text{NO}_2^-\text{-N}$)	< 0.02	0.09

Table A.4: Stability test of samples during the 3-day collection period. Storage Temp.: 4 °C

Recovery TMP after 3 days	100%
Recovery 4-desmethyl-TMP after 3 days	94%

A.4 Additional figures from experiments with lab-scale bioreactors

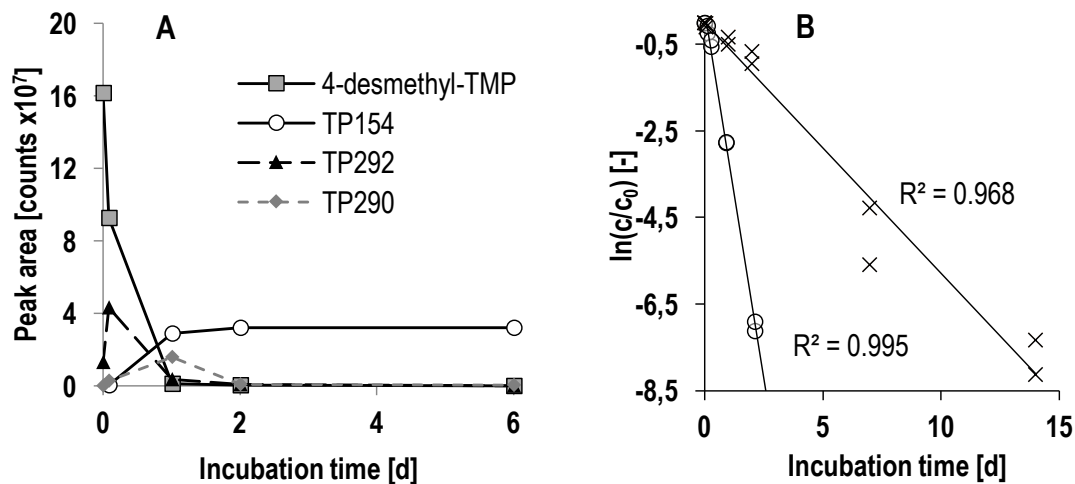


Figure A.8: Incubation of compounds in sludge-inoculated, lab-scale bioreactors. A: Time course of 4-desmethyl-TMP ($c_0 = 500 \mu\text{g/L}$, sludge dilution 20:1 with effluent wastewater) and formation of TP292, TP290 and DAPC. B: Calculation of k_{biol} for TMP according to a pseudo-first-order rate law, $c_0 = 5 \mu\text{g/L}$, sludge dilution 1:1 with either effluent (\times) ($n=2$), or influent (\circ) ($n=2$).

A.4.1 Abiotic hydrolysis and oxidation of 4-desmethyl-TMP

Experiments with 4-desmethyl-TMP have shown that this compound is relatively unstable and will slowly hydrolyse in aqueous solution. Under basic conditions this transformation is much faster. Using high-resolution mass spectrometry the hydrolysis product TP140 could be identified. The hydroxylated 4-desmethyl-TMP (TP292) and the corresponding oxidized ketone TP290 were also detected. A hydrolysis and an oxidation mechanism were postulated based on these TPs (Figure A.9 and A.10).

To test the mechanism in Figure A.10, 4-desmethyl-TMP was added to a basic solution of methanol. A dissipation of the compound was found with a corresponding increase in the formation of TP290 and of a TP with $m/z = 306$, which corresponds to the methoxylated 3-desmethyl-TMP, (TP306b) (Figure A.12).

It follows from the mechanism in Figure A.10, if the nucleophile in the second step

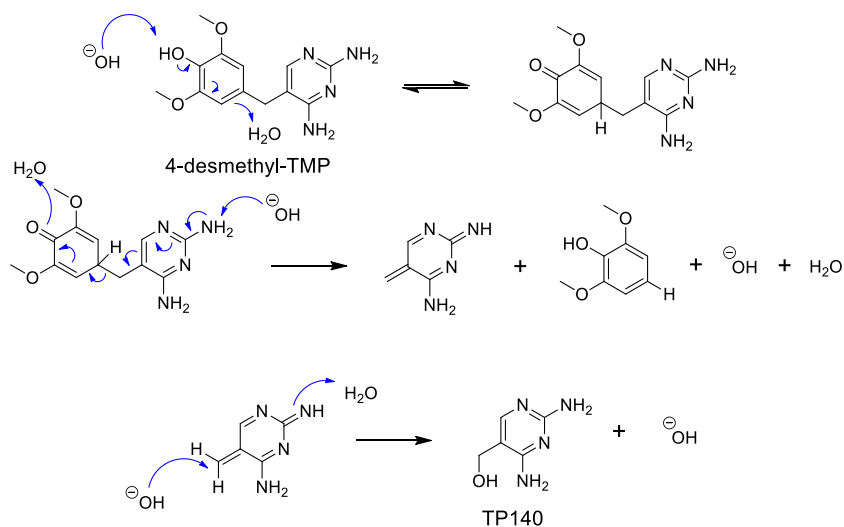


Figure A.9: Postulated hydrolysis mechanism of 4-desmethyl-TMP in basic solution.

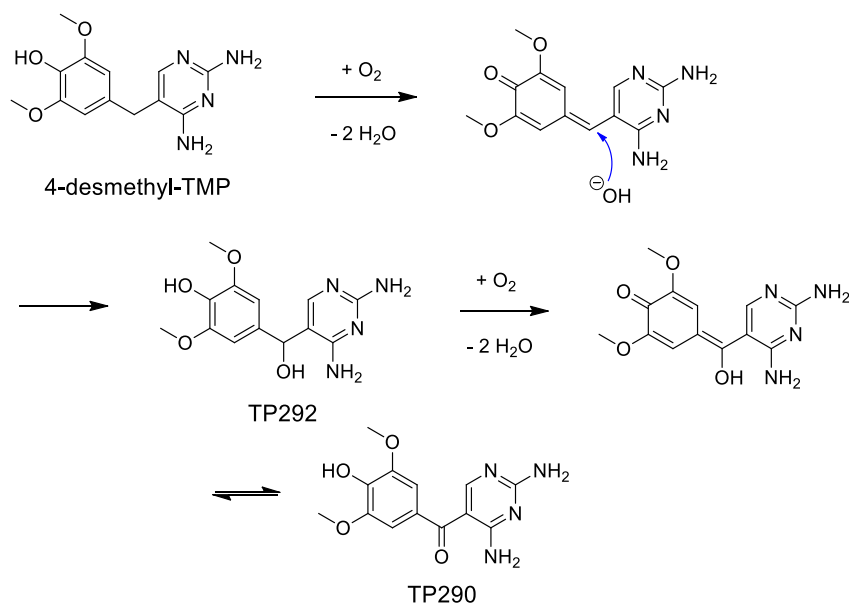


Figure A.10: Postulated oxidation and hydroxylation mechanism of 4-desmethyl-TMP in basic solution.

is changed from -OH to -OMe by changing to a methanol solvent, then 4-desmethyl-TMP is methoxylated rather than hydroxylated. The formation TP306b in the methanol reaction could therefore be the result of nucleophilic attack by -OH and

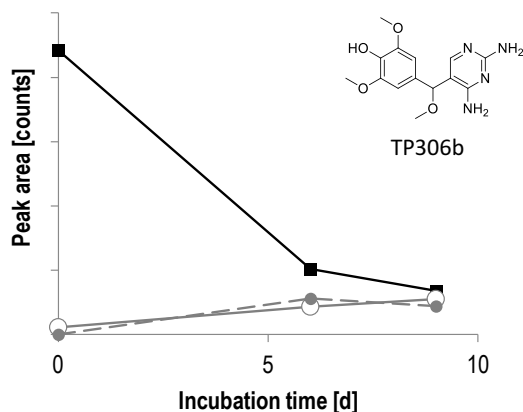


Figure A.11: Time course of 4-desmethyl-TMP (■), TP 306b (methoxy-4-desmethyl-TMP) (●) and TP290 (○) in methanol with 1 mol/L NaOH.

-OMe acting as the leaving group.

Furthermore, it was found that under sterile conditions, in the absence of oxygen, 4-desmethyl-TMP is stable as was observed in lab experiments with sterilised sludge in inert atmosphere (data not shown). In sterilised ultrapure water, when air is purged through the solution, slow dissipation of 4-desmethyl-TMP is observed and compounds TP292 and TP290 are formed (Figure A.12). This indicates that oxygen plays an important role in this abiotic reaction and supports the mechanism proposed in Figure A.10.

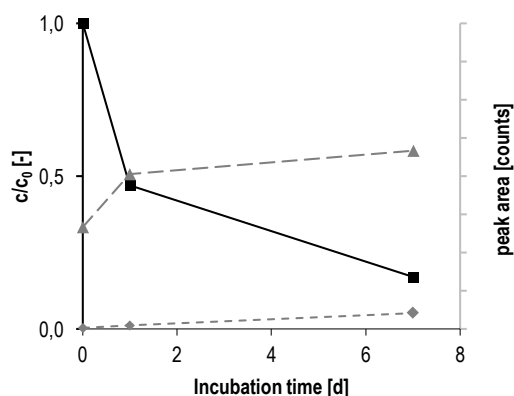
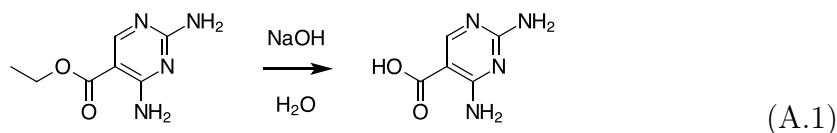


Figure A.12: Time course of 4-desmethyl-TMP (■, left axis) and TP292 (▲) and TP290 (◆) (Peak areas, right axis) in a sterilised, pristine-water medium with air purging.

In a sterilised control experiment of 4-desmethyl-TMP in sterilised sludge with air saturation, conducted in replicate, the compound reacted slowly and 40% dissipation was observed in 7 days in conjunction with a slow formation of TP292 (data not shown). The slow reaction rate indicates that the abiotic oxidation or hydrolysis reactions are unlikely to play a major role in the removal of 4-desmethyl-TMP in activated sludge reactors where the HRT is usually on the order of 6 h.

A.5 Synthesis of 2,4-diaminopyrimidine-5-carboxylic acid (DAPC)



Ethyl 2,4-diaminopyrimidine-5-carboxylate (2.65 mg) was added to a round-bottom flask and dissolved in 40 mL of water kept at 80 °C. NaOH solution (10 mL, 6.4%) was added very slowly, drop-wise, while stirring. After three hours it could be verified by LC–tandem MS that the ester hydrolysis was complete and 2,4-diaminopyrimidine-5-carboxylic acid (DAPC) was formed. Using HPLC–UV–Vis measurements with multiple-wavelength detection, it could be observed that DAPC was the only significant product of the hydrolysis. The purity was estimated by integrating all peaks found at three different wavelengths, DAPC was a minimum of 93% of all peaks (Figure A.13 to A.15). It was therefore assumed that within a 10% error, the reaction could be treated as quantitative. The solution was cooled to room temperature and neutralised with HCl. In a volumetric flask the solution was diluted to 100 mL to give a standard solution of (22 ± 2) mg/L DAPC. Since the ethyl ester starting material and DAPC have similar absorption spectra (Figure A.16), the peak area of the ethyl ester at the start of the hydrolysis was compared to that of DAPC when the reaction was complete. The chromatograms show the DAPC peak area to be 95% of the ethyl ester at 226 nm (λ_{max}) (Figure A.17). This again shows that the hydrolysis can be estimated to be quantitative, with a 10% error. For an initial estimation of the concentration of DAPC in environmental samples in the low ng/L range, this error was considered acceptable. The stability of DAPC was tested over a 4-day period in acidic (pH 2), neutral,

and basic (pH 10) solution. The stability could be verified for all three conditions, the results are shown in Table A.5.

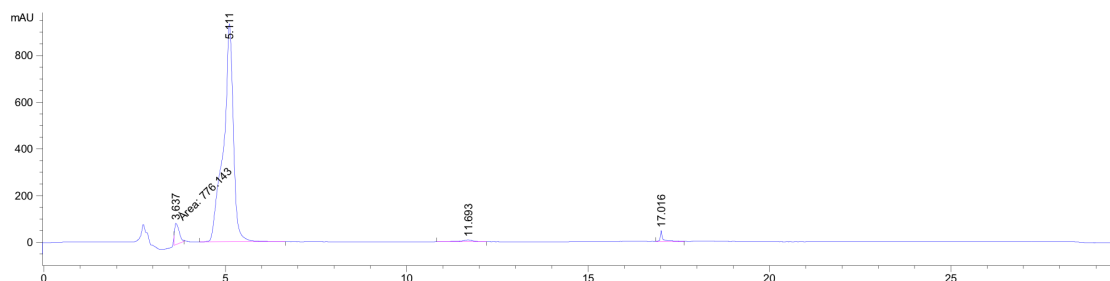


Figure A.13: Chromatogram of DAPC solution at 220 nm showing DAPC (5.1 min) with 93% of the measured peak areas. Peaks at 3.6 min and 11.6 min are unknowns while the peak at 17 min is the residual ethyl 2,4-diaminopyrimidine-5-carboxylate (1.4% of peak area).

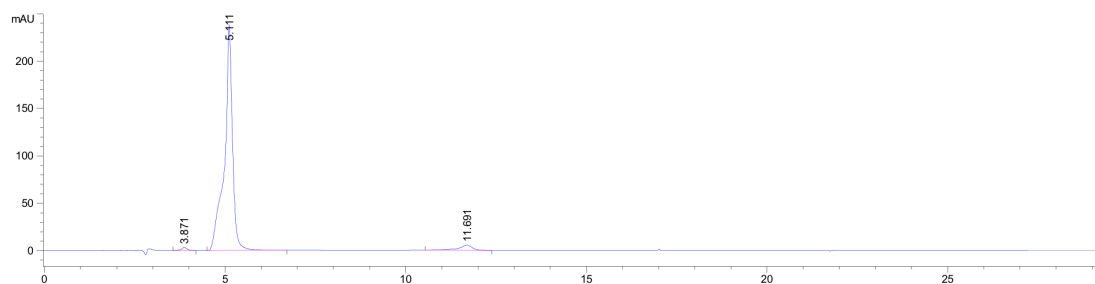


Figure A.14: Chromatogram of the DAPC product at 280 nm. The DAPC peak represents 95% of the total peak area found.

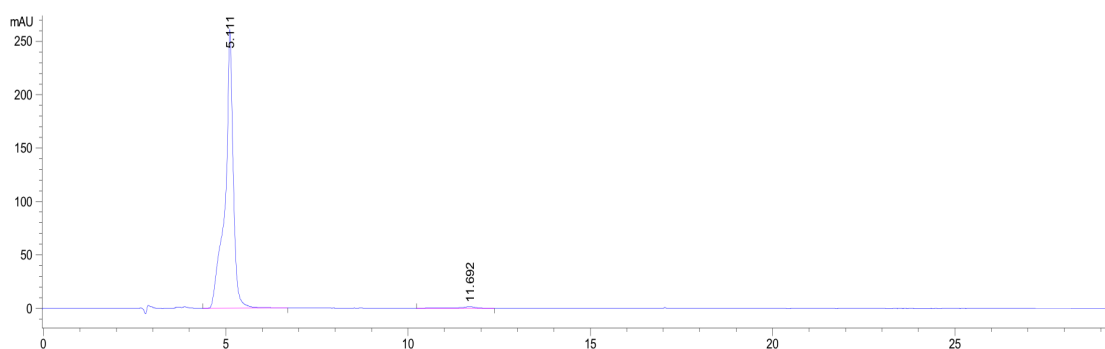


Figure A.15: Chromatogram of the DAPC product at 254 nm. DAPC represents 99% of the total peak area.

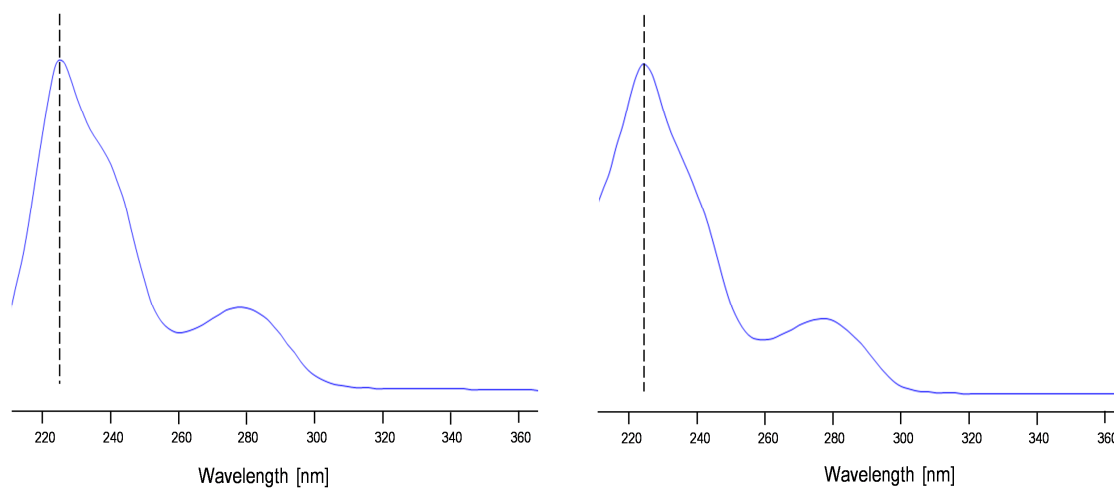


Figure A.16: Left: Spectrum of ethyl 2,4-diaminopyrimidine-5-carboxylate. Right: Spectrum of 2,4-diaminopyrimidine-5-carboxylic acid (DAPC).

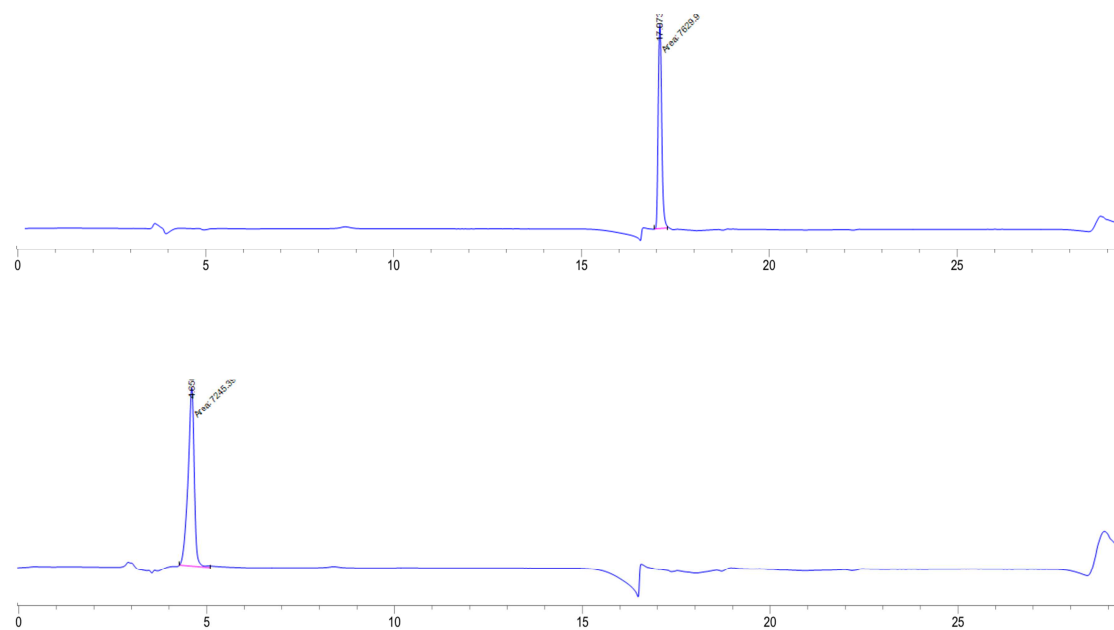


Figure A.17: Above: Chromatogram at 226 nm, of ethyl 2,4-diaminopyrimidine-5-carboxylate before hydrolysis (26 mg/L). Below: Chromatogram at 226 nm after completion of the reaction, 2,4-diaminopyrimidine-5-carboxylic acid (DAPC, 22 mg/L) has a peak area of 95% compared to the starting material.

Table A.5: Stability test for DAPC

Days	Peak area (counts $\times 10^3$)		
	Acidic (pH 2)	Neutral (pH 7)	Basic (pH 10)
1	3.6	3.7	3.7
2	3.6	3.7	3.7
4	3.6	3.7	3.7
10	3.4	3.7	3.7

A.6 Additional information regarding TMP degradation kinetics and modelling

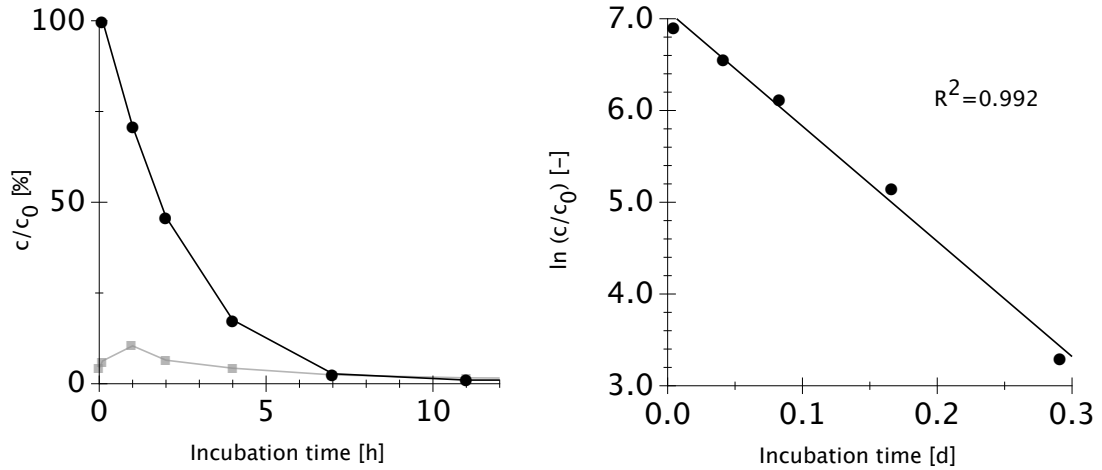


Figure A.18: Experiment run at the SBR in batch mode (no cycling) for the accurate determination of the TMP degradation kinetics and rate constant (k_{biol}). TMP (●) and 4-desmethyl-TMP (■) were monitored during this experiment. Sludge concentration: 3.1 g_{SS}/L.

A.6.1 Modeling TMP degradation kinetics in the SBR

To model the degradation kinetics in the SBR during normal operation, a pseudo-first-order rate law and corresponding rate constant was used (see Table 2.1). The concentration at the end of the first cycle $C_{TMP,t}$ was calculated using Equation A.2.

$$C_{\text{TMP},t} = C_{\text{TMP},0} \cdot e^{-X_{\text{SS}}k_{\text{biol}}t} \quad (\text{A.2})$$

Where $C_{\text{TMP},0}$ is the trimethoprim concentration at the start of the cycle. X_{SS} the sludge concentration (g_{SS}/L), k_{biol} is the pseudo-first-order rate constant in L/(g_{SS} · d) and t is the cycle length (oxic phase 2 h, total 3 h). For each subsequent cycle, the end concentration $C_{\text{TMP},\text{next}}$ was determined by Equation A.3

$$C_{\text{TMP},\text{next}} = \left(C_{\text{TMP},\text{prev}} + \frac{C_{\text{TMP},\text{infl}}}{4} - \frac{C_{\text{TMP},\text{prev}}}{4} \right) e^{-X_{\text{SS}}k_{\text{biol}}t} \quad (\text{A.3})$$

Where *prev* and *infl* refer to TMP concentration in the previous cycle and the concentration in the influent, respectively. In each cycle 1/4 of the reactor volume is removed as effluent and 1/4 is added as influent, this is accounted for by the fraction of $C_{\text{TMP},\text{infl}}$ and $C_{\text{TMP},\text{prev}}$.

A.7 Detection of DAPC in wastewater samples

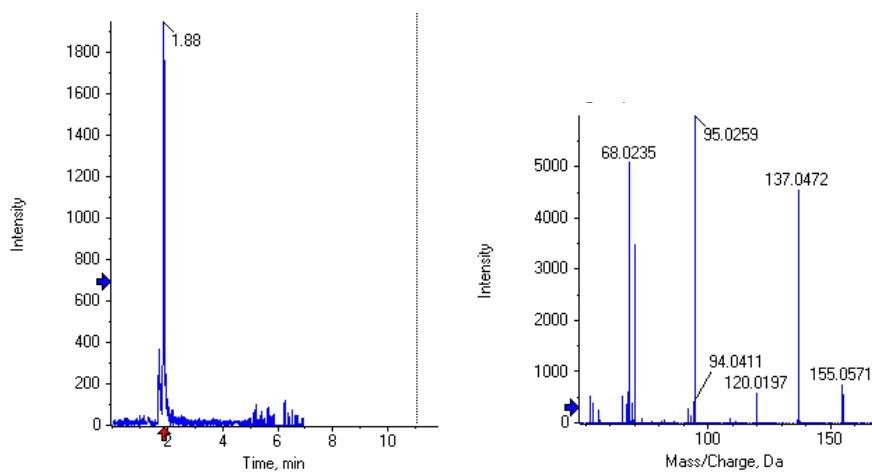


Figure A.19: S17. Chromatogram of DAPC standard (extracted mass $m/z = 155.055$) with MS/MS spectrum.

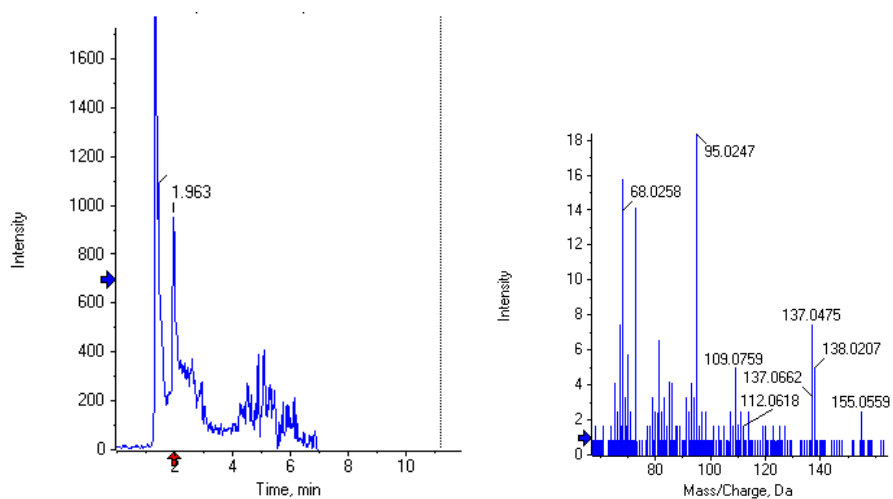


Figure A.20: S18. Chromatogram (extracted mass $m/z = 155.055$) and MS² spectrum showing presence of DAPC in effluent wastewater from the on-site SBR.

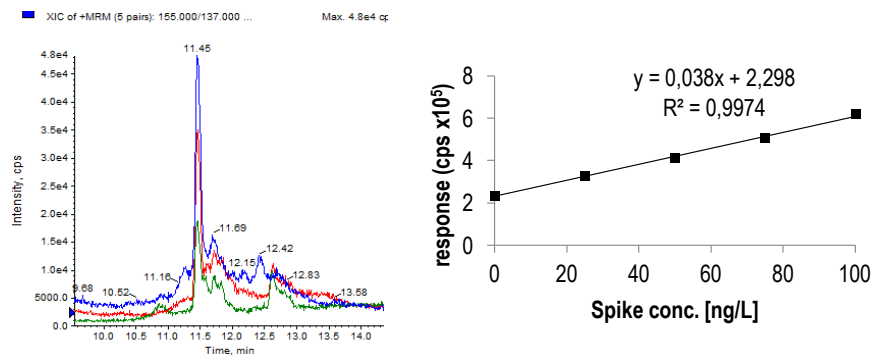


Figure A.21: S19. Left: DAPC detected in composite effluent sample of the SBR. Right: Standard addition of DAPC using a synthesised standard. Estimated concentration: 61 ng/L.

Appendix B

Supplementary data for Chapter 3: Comparisons between abiotic nitration and biotransformation reactions of phenolic micropollutants in activated sludge

B.1 Synthesis of transformation products

B.1.1 Synthesis of 2-nitro-6-phenylphenol and 4-nitro-6-phenylphenol

Nitro-phenylphenol ($\text{NO}_2\text{-OPP}$) was prepared according to [Cheng et al. \(1968\)](#). 2-Phenylphenol (0.5 g, 2.9 mmol) was dissolved in 5 mL glacial acetic acid and cooled in a water bath to 15 °C. Nitric acid (65%, 0.2 mL) in 10 mL acetic acid was added drop-wise while stirring. The dark red solution was quenched with water, turning it yellow. Sodium hydroxide solution was used to neutralise the mixture. The mixture was extracted into DCM (3 repeats of 2 mL) and the combined organic phases were washed with water followed by brine. The organic phase was dried over

anhydrous sodium sulfate and reduced under vacuum. (4-nitro-6-phenylphenol) was isolated from the crude product mixture by column chromatography on silica gel (silica gel 60, pentane-DCM 1:1, $R_f = 0.10$) as a yellow solid in 0.13 g (0.6 mmol) yield. The second NO₂-OPP isomer (2-nitro-6-phenylphenol) was also isolated as a yellow oil ($R_f = 0.46$). Exact [M-H]⁻ ion mass (m/z), calc.: 214.0504, experiment: 214.0510. Estimated purity by HPLC-UV-VIS was 98% with no contamination from the starting material. ¹H NMR 4-nitro-6-phenylphenol (600 MHz, acetone-*d*₆) δ ppm: 9.88 (1H b s -OH); 8.20 (1H d ⁴*J*=2.81 H₁1); 8.14 (1H d d ³*J*=8.89 ⁴*J*=2.87 H9); 7.65 (2H d ³*J*=7.72 H 1,5); 7.48 (2H t ³*J*=7.70 H2,4); 7.40 (1H t ³*J*=7.22 H3); 7.19 (1H d ³*J*=8.91 H8). ¹H NMR 2-nitro-6-phenylphenol (600 MHz, acetone-*d*₆) δ ppm: 10.96 (1H s- OH); 8.17 (1H d d H9 ³*J*=8.54 ⁴*J*=1.58); 7.76 (1H d d ³*J*=7.59 ⁴*J*=1.58); 7.60 (2H d ³*J*=7.73 H1,5); 7.47 (2H t ³*J*=7.60 H2,4); 7.41 (1H t ³*J*=7.43 H3), 7.19 (1H t ³*J*=7.99 H10).

B.1.2 Synthesis of 3,3'-dinitro-bisphenol A

3,3'-Dinitro-bisphenol A (dinitro-BPA) was prepared according to [Babu et al. \(2011\)](#). 5.1 g (22.3 mmol) BPA was dissolved in 50 mL acetone and cooled to 0 °C. Nitric acid (65%, 4.2 mL) was added drop-wise while stirring. After completion of the reaction, the dark red mixture was quenched with cold water yielding a yellow precipitate. The crude product was filtered and washed with cold acetone/water (3:1) and re-crystallised in ethanol yielding yellow needles (62% yield). Negative ion mass (m/z): calc.: 317.0779, experiment: 317.0776. Estimated 99% purity by LC-UV-Vis. ¹H NMR (600 MHz, acetone-*d*₆) δ ppm: 10.37 (2H b s -OH); 8.06 (2H d ⁴*J*=2.41 H8); 7.55 (2H d d ³*J*=8.77 ⁴*J*=42.40); 7.13 (2H d ³*J*=8.71); 1.76 (6H s).

B.1.3 ¹H NMR shifts for synthesised TPs

See next page.

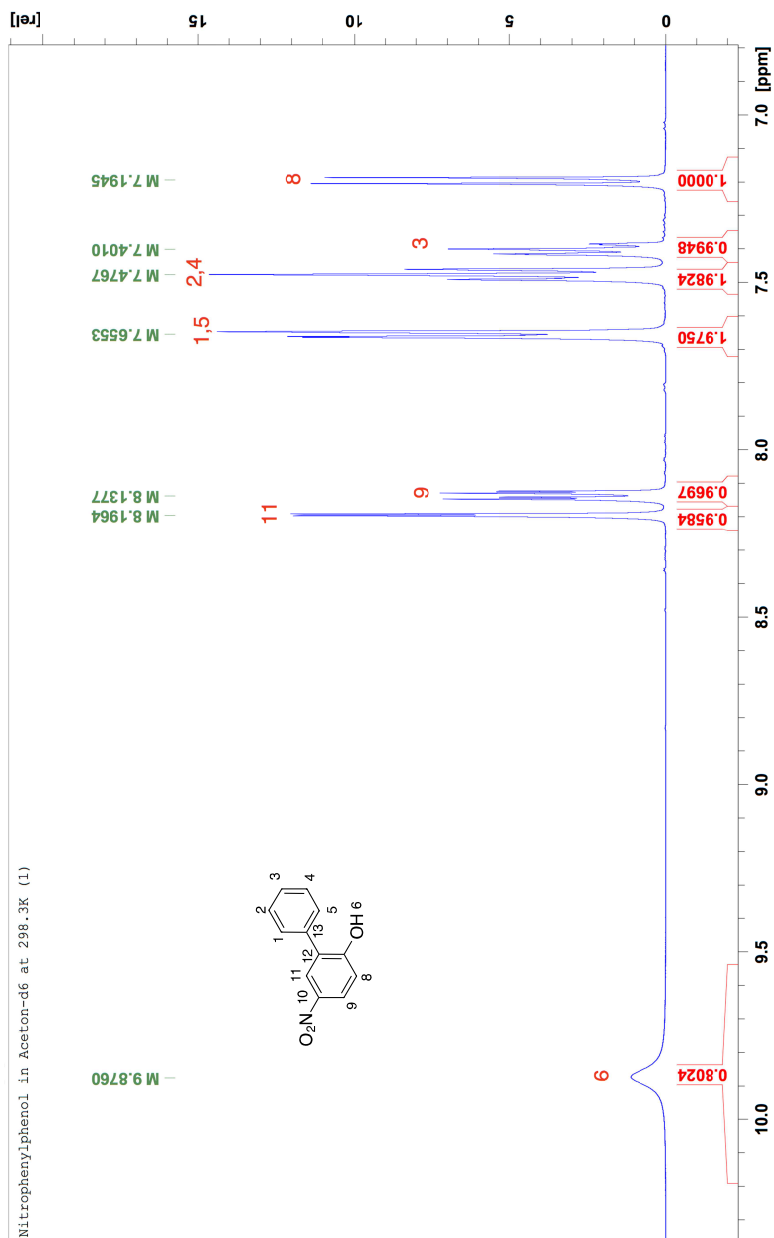
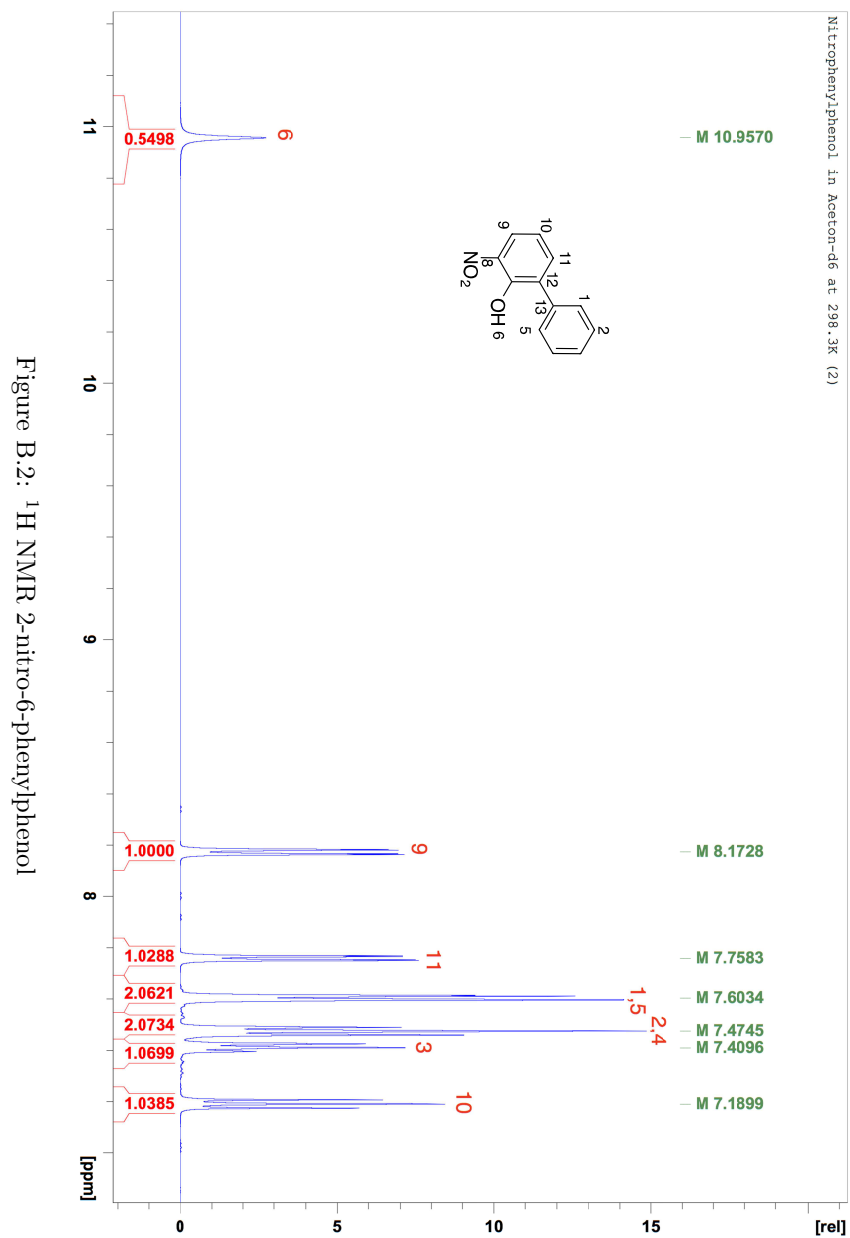
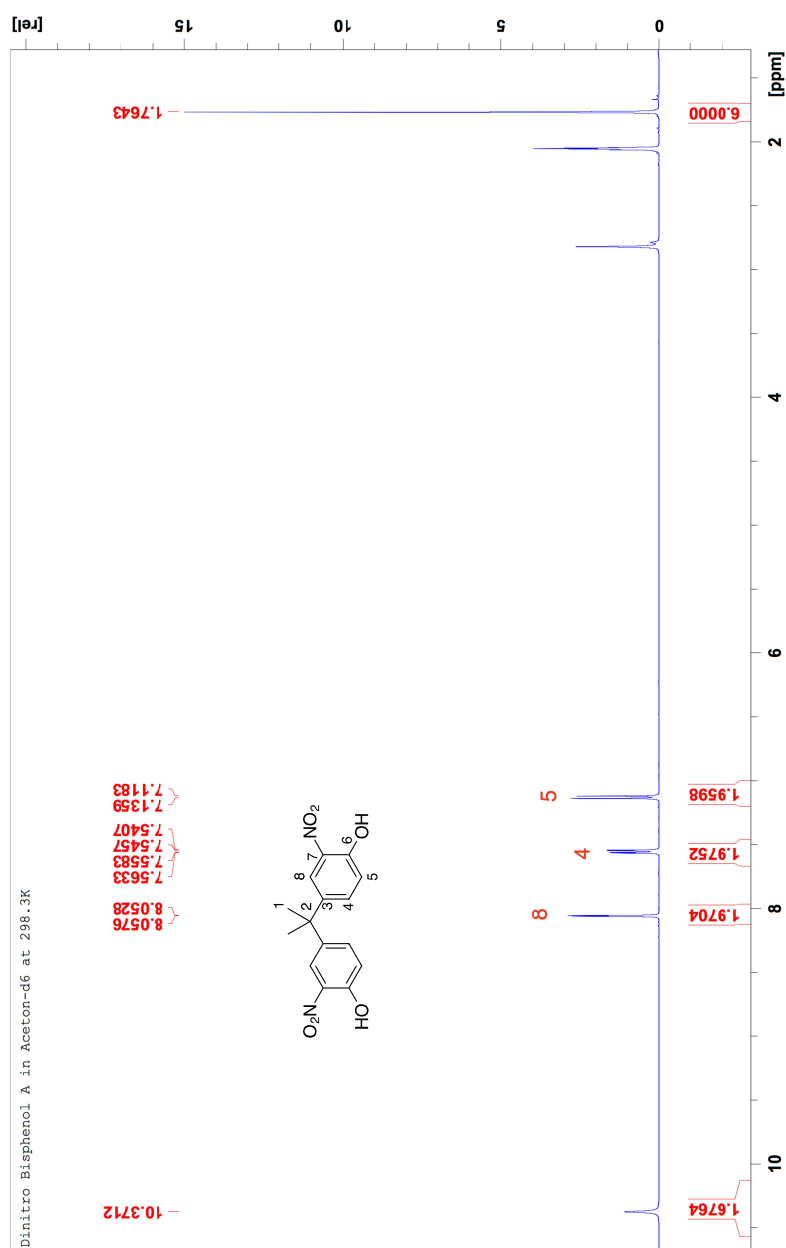


Figure B.1: ¹H NMR 4-nitro-6-phenylphenol



Figure B.3: ^1H NMR 3,3'-dinitro-bisphenol A

B.2 Characterisation parameters of WWTPs in Chapter 3

Table B.1: Process parameters for the WWTPs studied

	WWTP 1	WWTP 2
wastewater type	domestic/urban	domestic/urban
population equivalents	320 000	285 000
SRT	12 d	16 d
HRT	11 h	60 h
average inflow	61 000 m ³ /d	35 500 m ³ /d

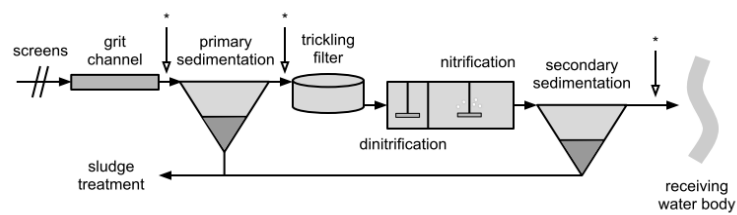


Figure B.4: Flow scheme for WWTP 1. *: Sampling locations

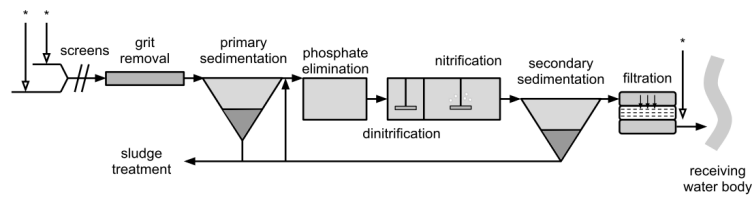


Figure B.5: Flow scheme for WWTP 2. *: Sampling locations

B.3 Parameters for LC-Tandem MS in MRM mode

Table B.2: Transitions used for MRM mode analysis

Compound	Pol.	m/z	Transitions		DP	CE a/b	DP a/b
			a/b				
OPP	neg	169.1	141.1/115		-60	-34/-42	-10/-10
BPA	neg	227.1	133/93		-105	-35/-60	-9/-7
Dextrorphan	pos	258.2	157.2/201.1		106	49/33	14/4
Acetaminophen	pos	152.1	110/43		70	22/50	12/12
<i>p</i> -Nitro-OPP	neg	214	168/184		-60	-34/-25	-10/-10
<i>o</i> -Nitro-OPP	neg	214	184/156		-60	-35/-35	-10/-10
Nitroso-OPP	neg	198.1	168/167		-63	-28/-38	-10/-10
Nitro-BPA	neg	272.1	240/257		-80	-34/-34	-10/-10
Dinitro-BPA	neg	317.1	285/212		-85	-36/-66	-7/-9
Nitro-dextrorphan	pos	303.17	198.1/256.2		110	42/41	15/15
Nitro-dextrorphan	pos	303.17	198.1/244.1		110	42/36	15/15
2-Nitro-acetaminophen	neg	195.04	150/165.2		-65	-22/-18	-9/-11

B.3.1 Analysis method parameters for environmental analysis of phenols and nitrophenols by standard addition

Table B.3: Chromatography figures of merit

	LOQ WWTP influent (ng/L)	LOQ WWTP effluent (ng/L)	Recovery influent	Recovery effluent
OPP	27	10	91%	114%
NO ₂ -OPP	2	2	100%	90%
BPA	20	5	96%	97%
dinitro-BPA	2	2	106%	114%
dextrorphan	2	1	107%	109%

^a LOQs are given from the estimated peak area at 10·S/N.

^b Analytical standards for nitro-dextrorphan and nitro-acetaminophen were not available however an SPE extraction efficiency of 89% for nitro-dextrorphan and 83% for nitro-acetaminophen was estimated by comparing extracted with non-extracted samples.

B.3.2 Calculation of recoveries

$$\text{Recovery} = \frac{(\text{conc. in spiked sample}) - (\text{conc. in orig. sample})}{\text{conc. of spike}} \cdot 100\% \quad (\text{B.1})$$

B.4 Additional equations and figures from mechanism studies

Equations B.2 to B.6 describe the derivation of Equation B.7:

$$K_a = \frac{[\text{H}^+][\text{NO}_2^-]}{[\text{HNO}_2]} \quad (\text{B.2})$$

At equilibrium, NO_2^- is partially protonated ($\text{p}K_a = 3.26$). Assuming no subsequent protonation of HNO_2 occurs ($\text{p}K_a = -6.5$ is reported for the protonation of HNO_2 , (Vione et al., 2004a)):

$$K_a = \frac{([\text{H}^+]_0 - x)([\text{NO}_2^-]_0 - x)}{x} \quad (\text{B.3})$$

Where $x = [\text{HNO}_2]$. Since the solution is buffered, the approximation is made that $[\text{H}^+]$ remains constant:

$$K_a = \frac{[\text{H}^+]([\text{NO}_2^-]_0 - x)}{x} \quad (\text{B.4})$$

After rearrangement:

$$K_a = \frac{[\text{H}^+][\text{NO}_2^-]_0}{x} - \frac{[\text{H}^+]x}{x} \quad (\text{B.5})$$

Substituting $[\text{HNO}_2]$ and rearranging:

$$[\text{HNO}_2] = \frac{[\text{H}^+][\text{NO}_2^-]_0}{K_a + [\text{H}^+]} \quad (\text{B.6})$$

This gives Equation 3.3 in Chapter 3:

$$\text{Initial rate} = k \cdot \frac{[\text{H}^+][\text{NO}_2^-]_0}{K_a + [\text{H}^+]} \quad (\text{B.7})$$

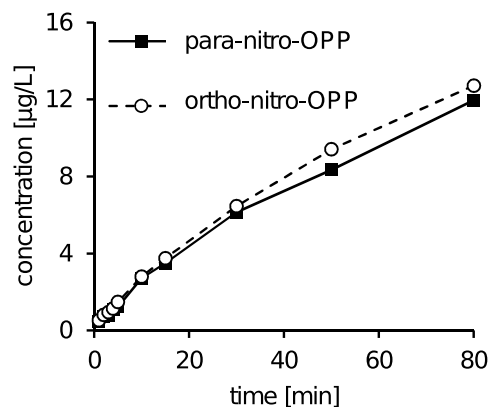


Figure B.6: Formation of two isomers of $\text{NO}_2\text{-OPP}$ in aqueous nitrite. Conditions: pH 4, $[\text{NaNO}_2]_0 = 15 \text{ mmol/L}$, $[\text{OPP}]_0 = 1.2 \text{ mmol/L}$.

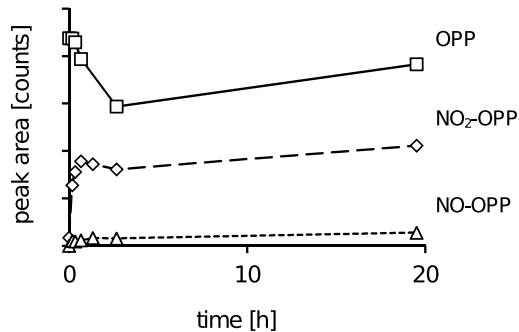


Figure B.7: Reaction of OPP with HNO_2 in the presence of $c\text{-PTIO}$. Conditions: pH 4, $[\text{OPP}]_0 = 0.1 \text{ mmol/L}$, $[\text{NaNO}_2]_0 = 5 \text{ mmol/L}$.

B.5 MS² Fragmentation and structural characterisation of TPs

All compounds were detected with (-)ESI unless otherwise stated.

Table B.4: MS² spectral masses of 2-phenylphenol (OPP) and TPs

Compound	m/z (u)	Proposed formula
OPP	93.0345	C ₆ H ₅ O
	115.0549	C ₉ H ₇
	141.0706	C ₁₁ H ₉
	169.0659	C ₁₂ H ₉ O
hydroxy-OPP	117.0333	C ₈ H ₅ O
	141.0705	C ₁₁ H ₉
	156.0575	
	157.0654	C ₁₁ H ₉ O
	183.0443	C ₁₂ H ₇ O ₂
	184.0517	
sulfo-OPP	141.0697	C ₁₁ H ₉
	169.0653	C ₁₂ H ₉ O
	249.0233	C ₁₂ H ₉ O ₄ S
<i>p</i> -NO ₂ -OPP	168.0577	C ₁₂ H ₈ O
	184.0529	C ₁₂ H ₈ O ₂
	214.0511	C ₁₂ H ₈ NO ₃
<i>o</i> -NO ₂ -OPP	156.0583	C ₁₁ H ₈ O
	184.0534	C ₁₂ H ₈ NO ₂
	214.0518	C ₁₂ H ₈ NO ₃
sulfo- <i>p</i> -NO ₂ -OPP	184.0533	C ₁₂ H ₈ O ₂
	214.0511	C ₁₂ H ₈ NO ₃
	No [M-H] ⁻	C ₁₂ H ₈ NO ₆ S

Table B.5: MS² spectral masses of bisphenol A (BPA) and TPs

Compound	m/z (u)	Proposed formula
BPA	133.0653	C ₉ H ₉ O
	211.0756	C ₁₄ H ₁₁ O ₂
	212.0837	
	227.1078	C ₁₅ H ₁₅ O ₂
hydroxy-BPA	93.0348	C ₆ H ₅ O
	211.0771	C ₁₄ H ₁₁ O ₂
	225.0886	C ₁₅ H ₁₃ O ₂
	243.1020	C ₁₅ H ₁₅ O ₃
sulfo-BPA	79.9573	SO ₃
	133.0629	C ₉ H ₉ O
	212.0835	
	227.1065	C ₁₅ H ₁₅ O ₂
	307.0633	C ₁₅ H ₁₅ O ₅ S
nitro-BPA	227.0714	C ₁₄ H ₁₁ O ₃
	240.0666	C ₁₄ H ₁₀ NO ₃
	255.0901	C ₁₅ H ₁₃ NO ₃
	257.0693	C ₁₄ H ₁₁ NO ₄
	272.0927	C ₁₅ H ₁₄ NO ₄
dinitro-BPA	227.0600	C ₁₃ H ₉ NO ₃
	255.0552	C ₁₄ H ₉ NO ₄
	285.0527	C ₁₄ H ₉ N ₂ O ₅
	286.0555	C ₁₄ H ₁₀ N ₂ O ₅
	317.0785	C ₁₅ H ₁₃ N ₂ O ₆
sulfo-dinitro-BPA	285.0531	C ₁₄ H ₉ N ₂ O ₅
	317.0792	C ₁₅ H ₁₃ N ₂ O ₆
	397.0361	C ₁₅ H ₁₃ N ₂ O ₉ S

Table B.6: MS² spectral masses of dextrorphan and TPs

Compound	m/z (u)	Proposed formula
dextrorphan (DXO) (+ESI)	133.0652	C ₉ H ₉ O
	145.0651	C ₁₀ H ₉ O
	157.0649	C ₁₁ H ₉ O
	159.0805	C ₁₁ H ₁₁ O
	199.1120	C ₁₄ H ₁₅ O
	201.1277	C ₁₄ H ₁₇ O
	258.1858	C ₁₇ H ₂₄ NO
hydroxy-DXO-1 (+ESI)	145.0653	C ₁₀ H ₉ O
	157.0651	C ₁₁ H ₉ O
	173.0598	C ₁₁ H ₉ O ₂
	199.1116	C ₁₄ H ₁₅ O
	215.1063	C ₁₄ H ₁₅ O ₂
	274.1801	C ₁₇ H ₂₄ NO ₂
hydroxy-DXO-2 (+ESI)	157.0640	C ₁₁ H ₉ O
	199.1124	C ₁₄ H ₁₅ O
	217.1202	C ₁₄ H ₁₇ O ₂
	256.1687	C ₁₇ H ₂₂ NO
	274.1806	C ₁₇ H ₂₄ NO ₂
hydroxy-DXO-3 & -4 (+ESI)	133.0651	C ₉ H ₉ O
	145.0624	C ₁₀ H ₉ O
	157.0641	C ₁₁ H ₉ O
	199.1107	C ₁₄ H ₁₅ O
	201.1257	C ₁₄ H ₁₇ O
	256.1680	C ₁₇ H ₂₂ NO
	274.1790	C ₁₇ H ₂₄ NO ₂
sulfo-DXO	79.9569	SO ₃
	256.1698	C ₁₇ H ₂₂ NO
	336.1272	C ₁₇ H ₂₂ NO ₄ S
nitro-DXO-1 (+ESI)	170.0726	C ₁₂ H ₁₀ O
	198.1030	C ₁₄ H ₁₄ O
	303.1700	C ₁₇ H ₂₃ N ₂ O ₃
nitro-DXO-2 (+ESI)	167.0836	C ₈ H ₁₁ N ₂ O ₂
	170.0726	C ₁₂ H ₁₀ O
	190.0492	C ₁₀ H ₈ NO ₃
	198.1020	C ₁₄ H ₁₄ O
	244.0975	C ₁₄ H ₁₄ NO ₃
	303.1700	C ₁₇ H ₂₃ N ₂ O ₃

B.5.1 Fragmentation Spectra and annotations

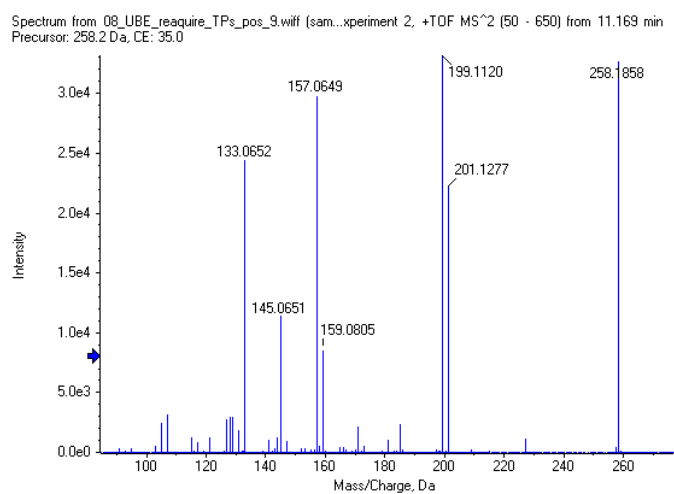


Figure B.8: Fragmentation spectrum of dextrorphan

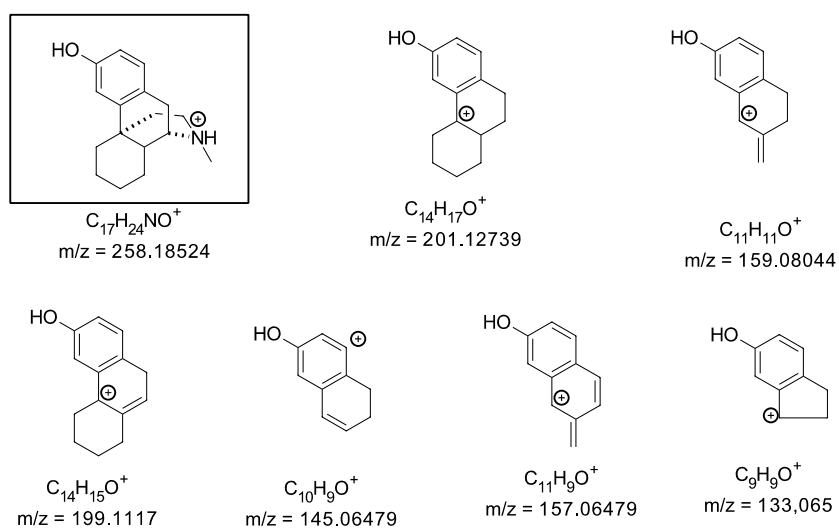


Figure B.9: Proposed fragment structures of dextrorphan

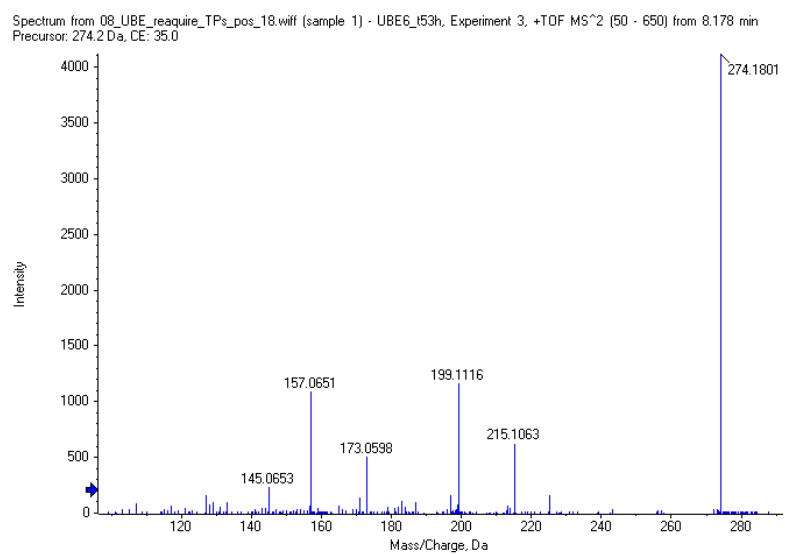


Figure B.10: Fragmentation spectrum of hydroxy-DXO-1

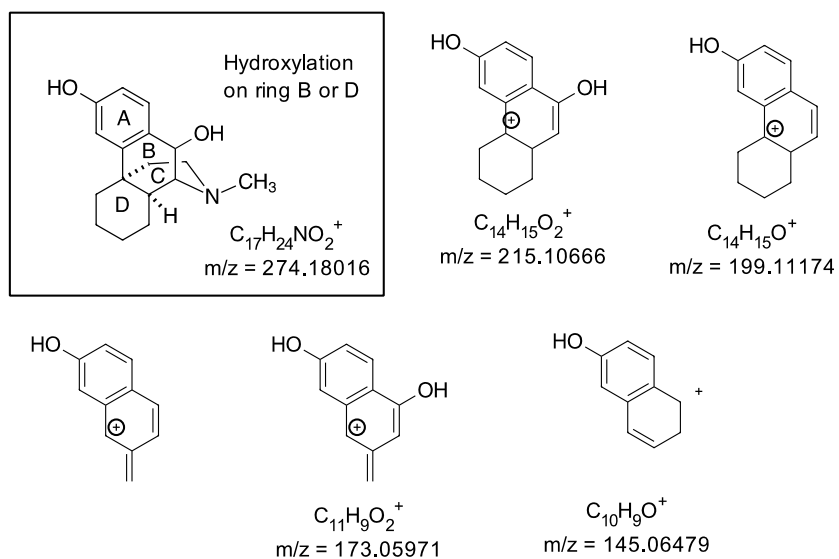


Figure B.11: Proposed fragment structures of hydroxy-DXO-1

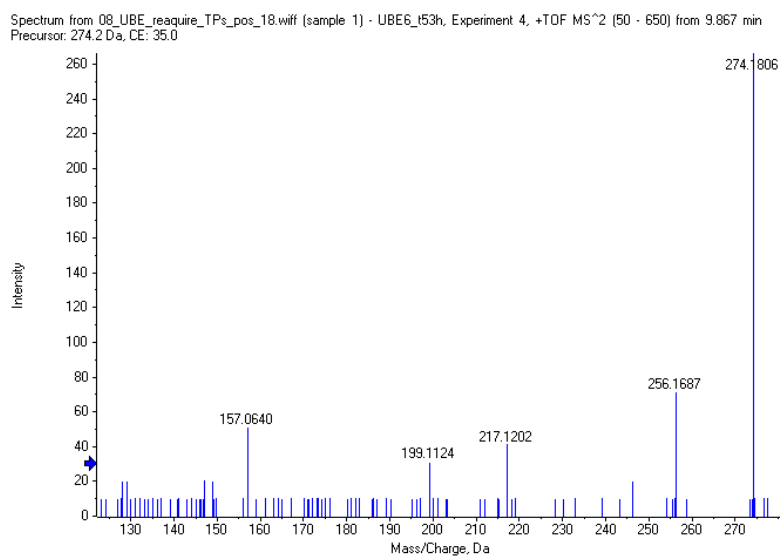


Figure B.12: Fragmentation spectrum of hydroxy-DXO-2

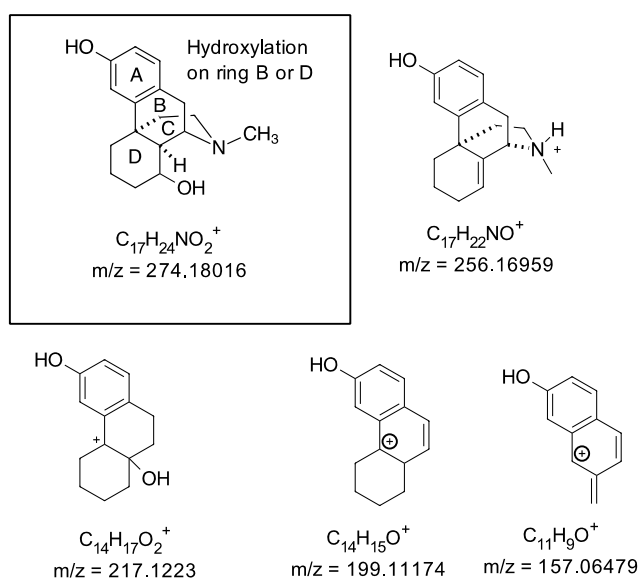


Figure B.13: Proposed fragment structures of hydroxy-DXO-2

Spectrum from 08_UBE_reaquire_TPs_pos_18.wif (sample 1) - UBE6_t53h, Experiment 4, +TOF MS² (50 - 650) from 12.423 min
Precursor: 274.2 Da, CE: 35.0

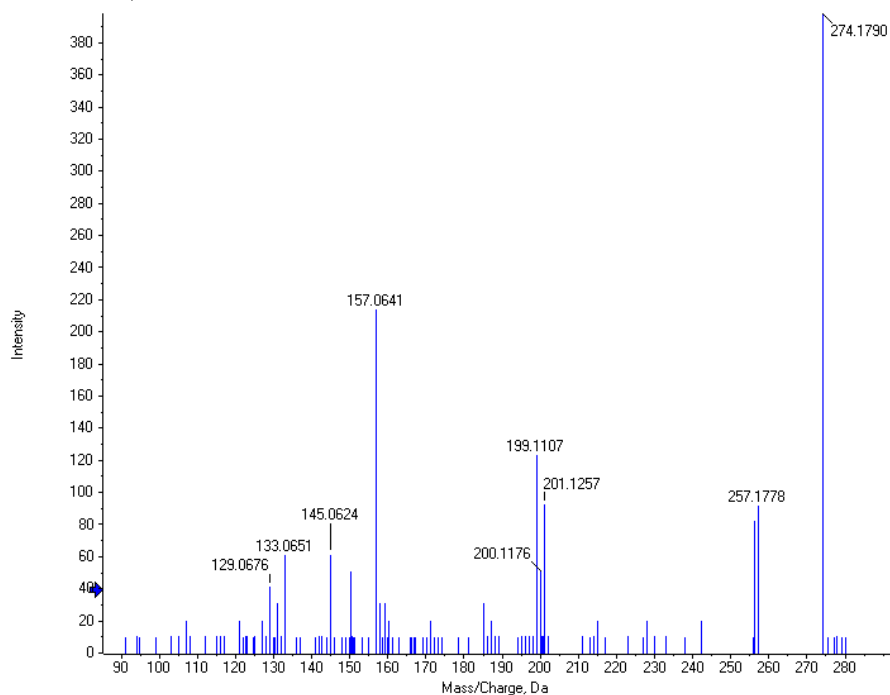


Figure B.14: Fragmentation spectrum of hydroxy-DXO-3 and -4

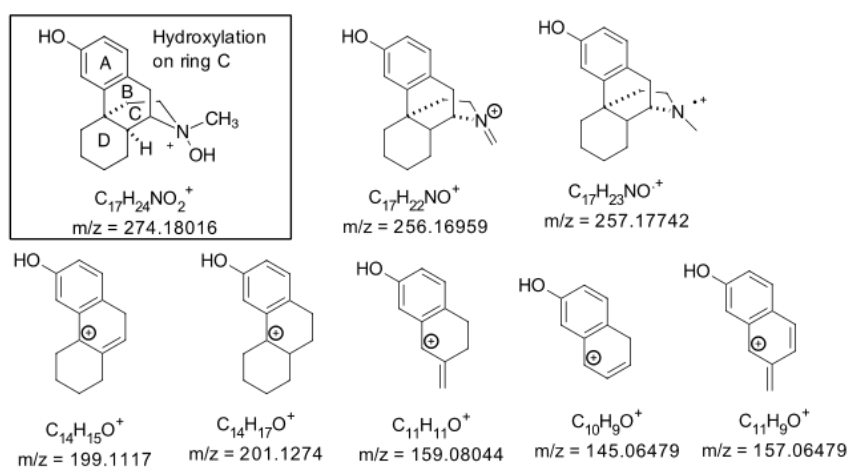


Figure B.15: Proposed fragment structures of hydroxy-DXO-3 and -4

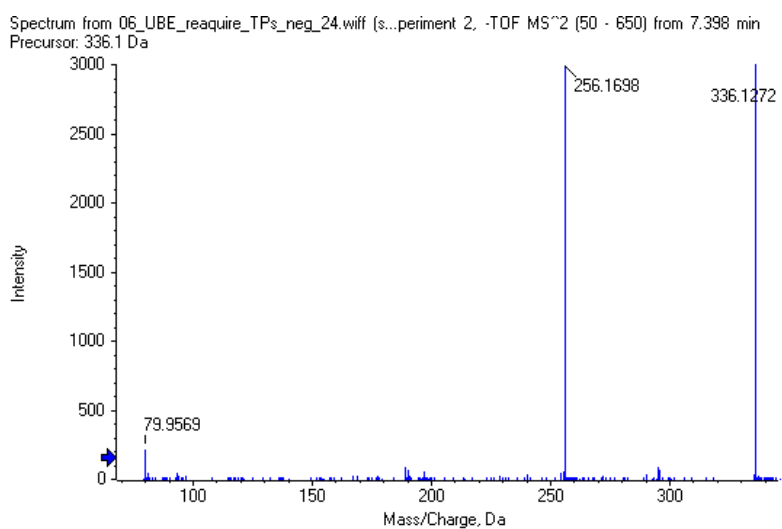


Figure B.16: Fragmentation spectrum of dex-SO3

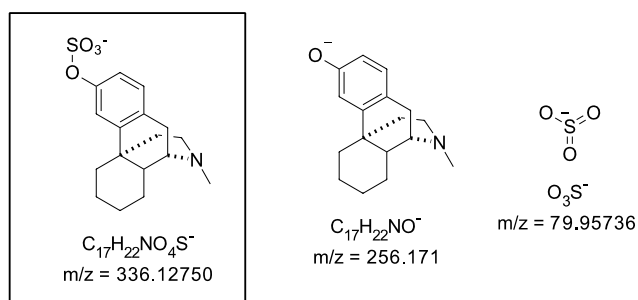


Figure B.17: Proposed fragment structures of dex-SO3

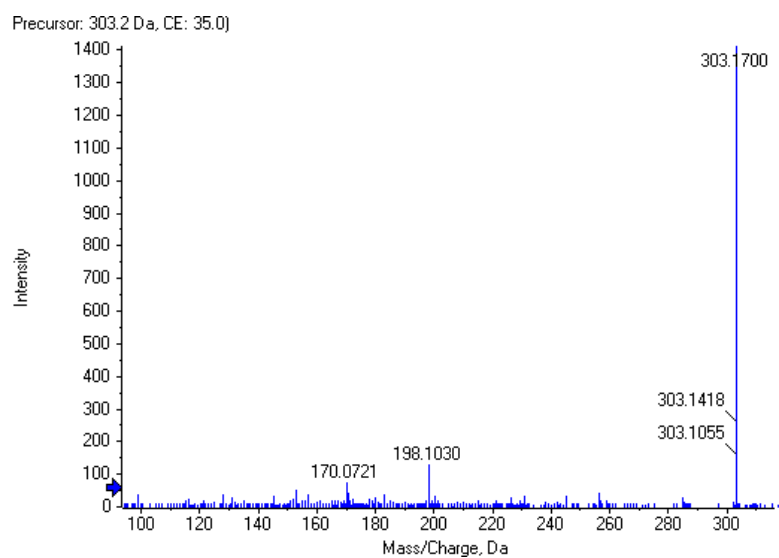


Figure B.18: Fragmentation spectrum of nitro-DXO-1

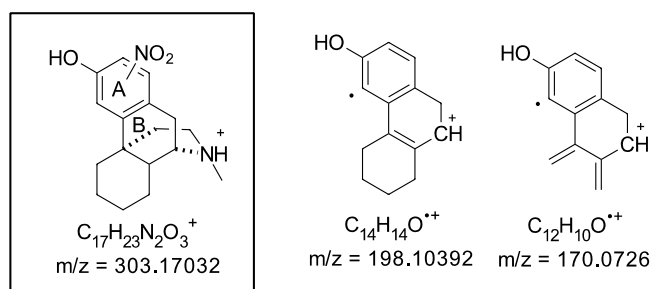


Figure B.19: Proposed fragment structures of nitro-DXO-1. Note: Unknown substitution position for nitro group, postulated on ring A or B.

Spectrum from 08_UBE_require_TPs_pos_11.wiff (sa...periment 2, +TOF MS² (50 - 650) from 17.358 min
 Precursor: 303.2 Da, CE: 35.0, added to (Spectrum f...Experiment 2, +TOF MS² (50 - 650) from 17.418 min
 Precursor: 303.2 Da, CE: 35.0)

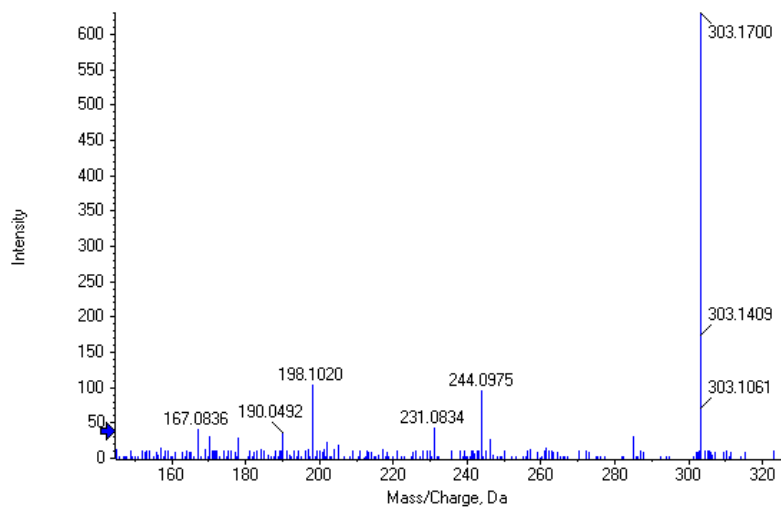


Figure B.20: Fragmentation spectrum of nitro-DXO-2

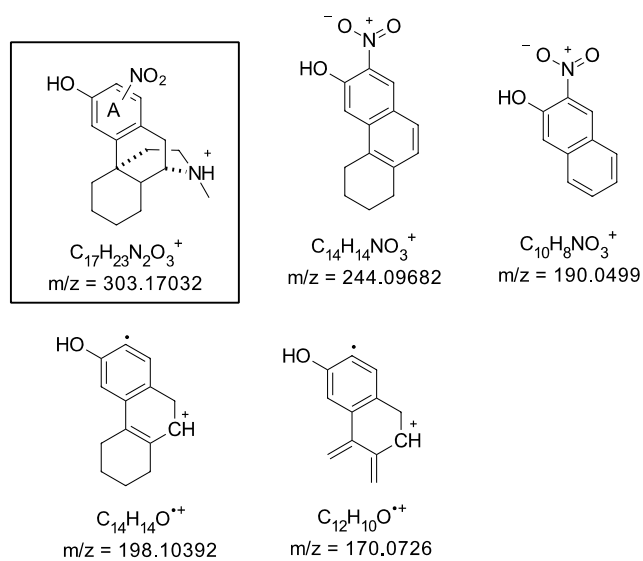


Figure B.21: Proposed fragment structures of nitro-DXO-2. Note: Unknown substitution position for nitro group, postulated on ring A.

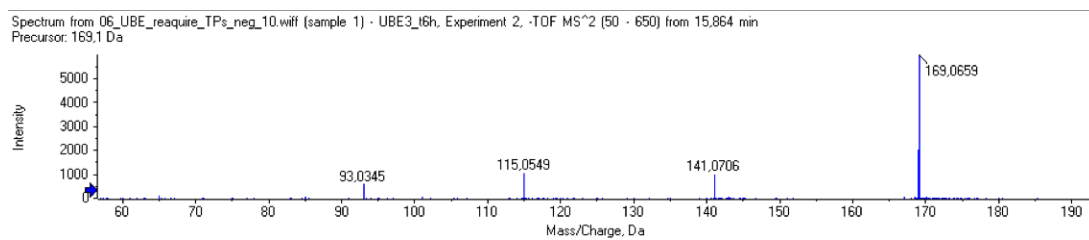


Figure B.22: Fragmentation spectrum of OPP

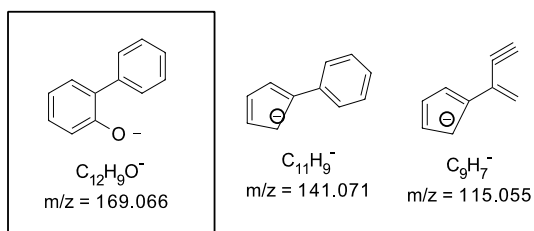


Figure B.23: Proposed fragment structures of OPP.

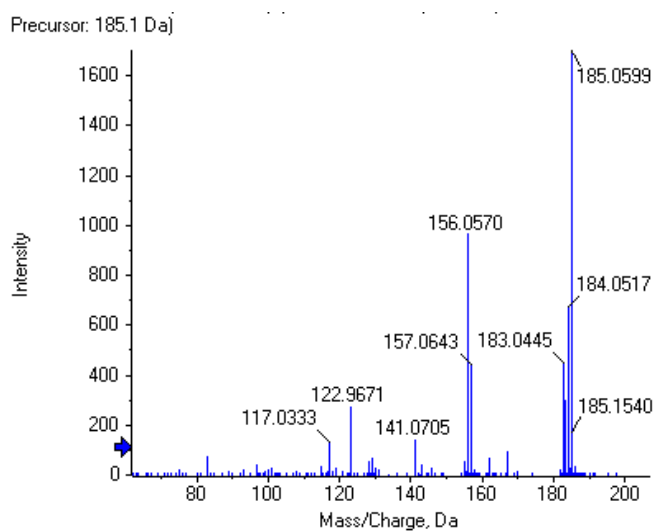


Figure B.24: Fragmentation spectrum of hydroxy-OPP. Note: 122.9665 is an artifact.

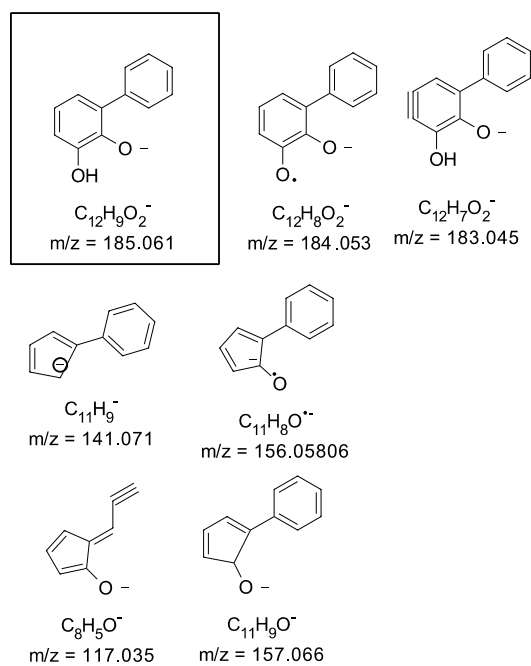


Figure B.25: Proposed fragment structures of hydroxy-OPP.

Spectrum from 06_UBE_reaquire_TPs_neg_10...t 2, -TOF MS² (50 - 650) from 2.708 min
Precursor: 249.0 Da

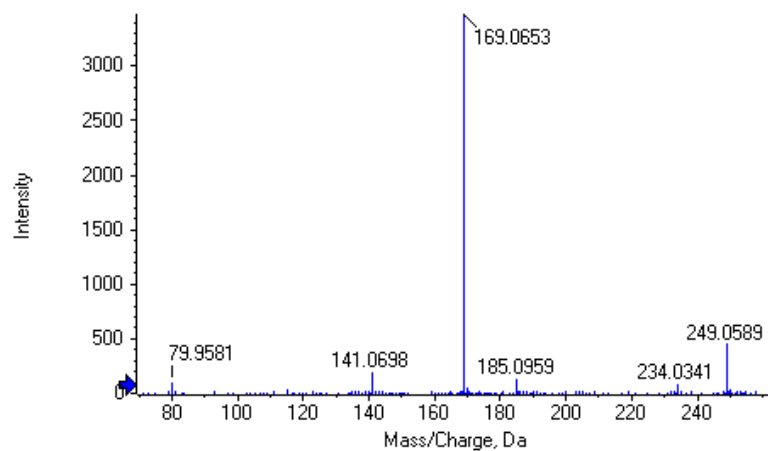


Figure B.26: Fragmentation spectrum of OPP-SO₃.

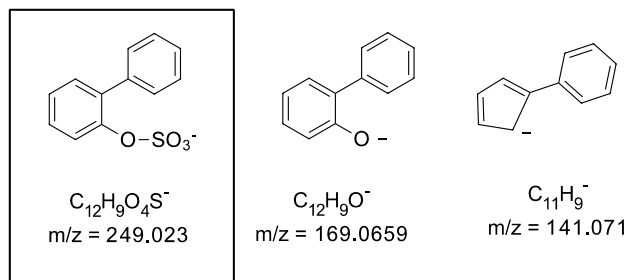
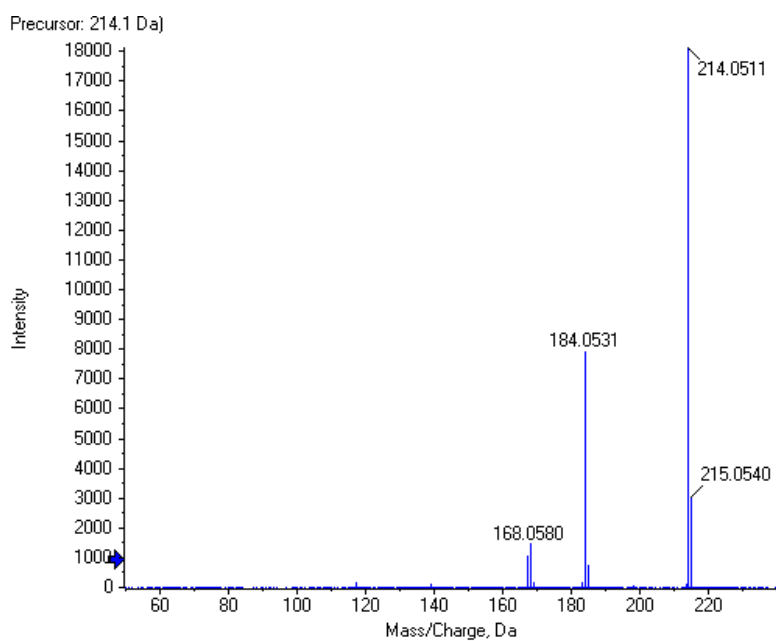
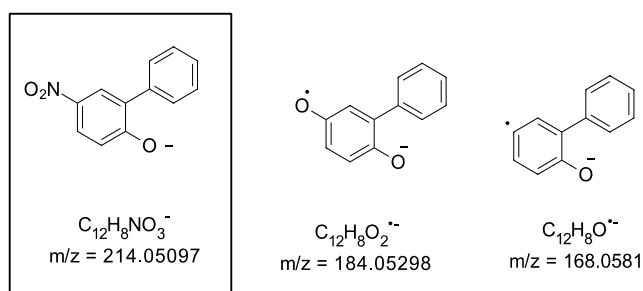
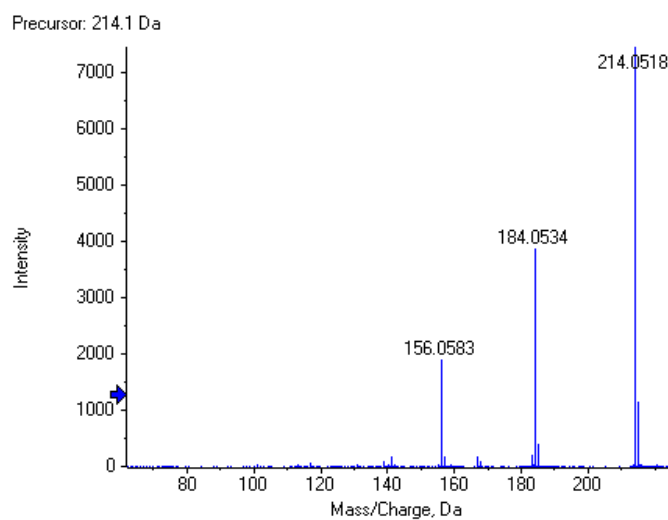
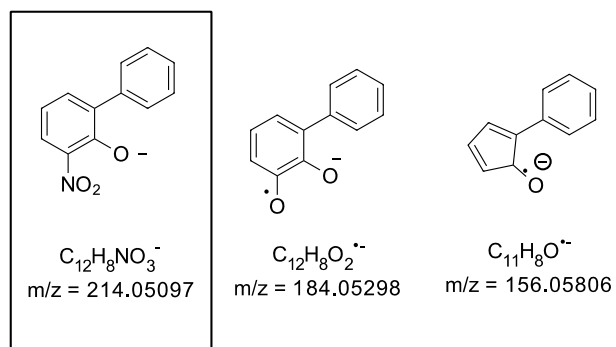
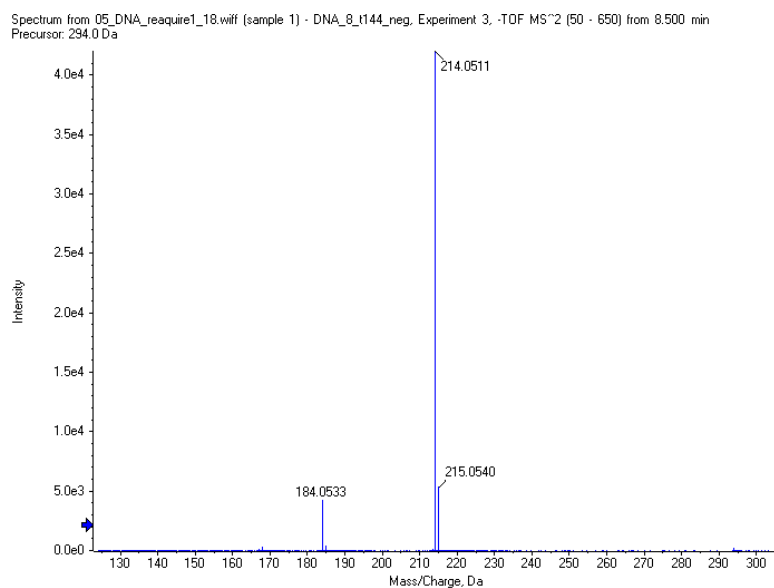
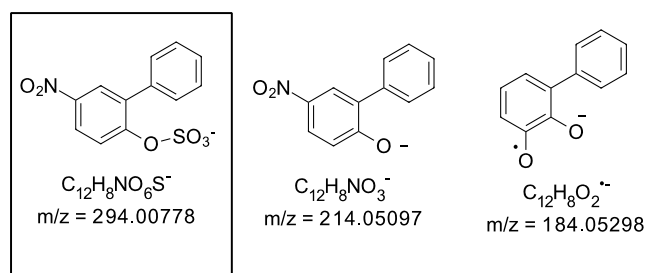


Figure B.27: Proposed fragment structures of OPP-SO₃.

Figure B.28: Fragmentation spectrum of *p*-NO₂-OPP.Figure B.29: Proposed fragment structures of *p*-NO₂-OPP.

Figure B.30: Fragmentation spectrum of *o*-NO₂-OPP.Figure B.31: Proposed fragment structures of *o*-NO₂-OPP.

Figure B.32: Fragmentation spectrum of sulfo-*p*-NO₂-OPP.Figure B.33: Proposed fragment structures of sulfo-*p*-NO₂-OPP.

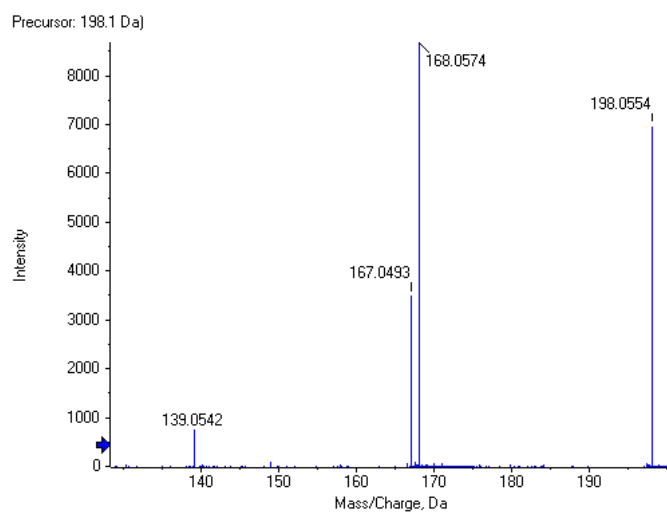


Figure B.34: Fragmentation spectrum of NO-OPP.

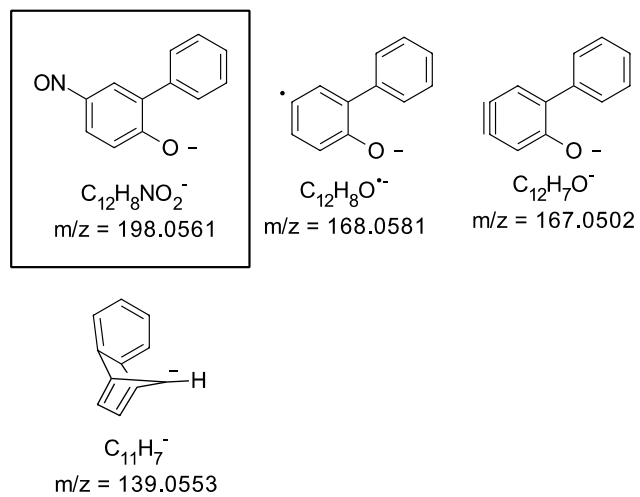


Figure B.35: Proposed fragment structures of NO-OPP.

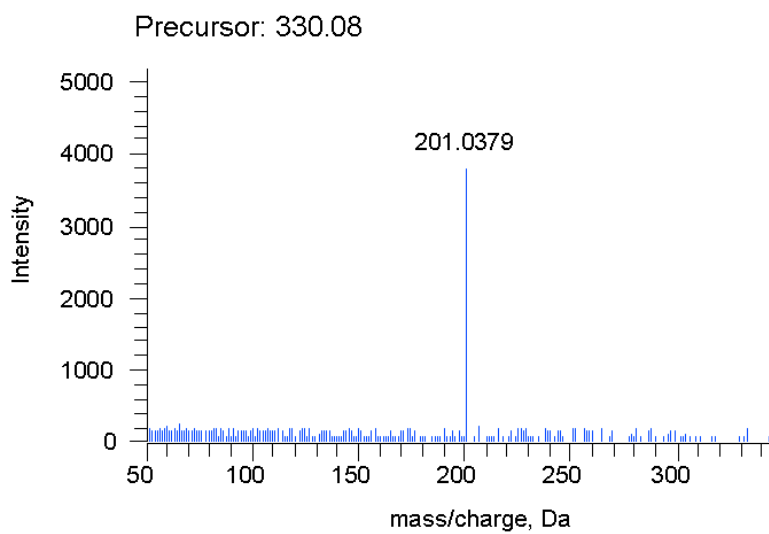


Figure B.36: Fragmentation spectrum of AcCyS-OPP.

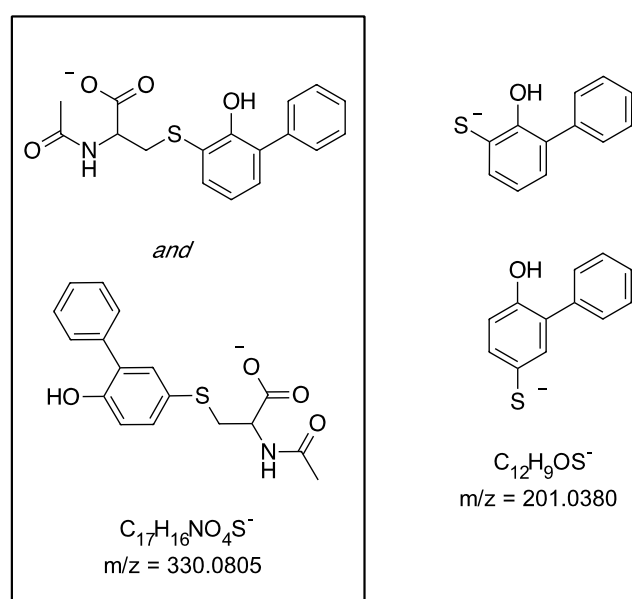


Figure B.37: Proposed fragment structures of AcCyS-OPP.

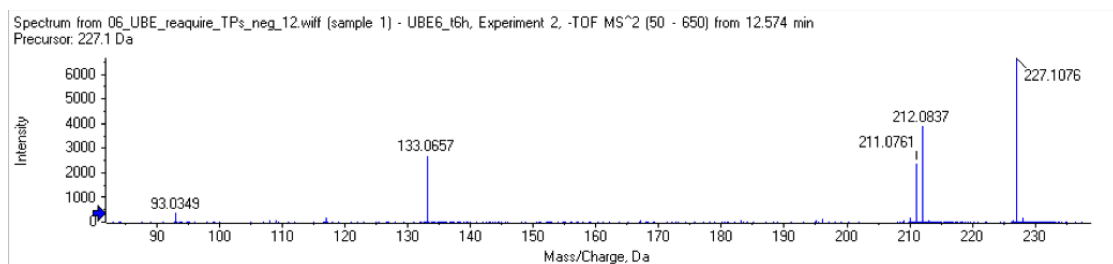


Figure B.38: Fragmentation spectrum of BPA.

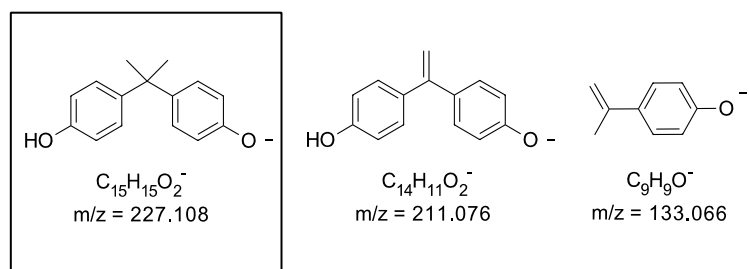


Figure B.39: Proposed fragment structures of BPA.

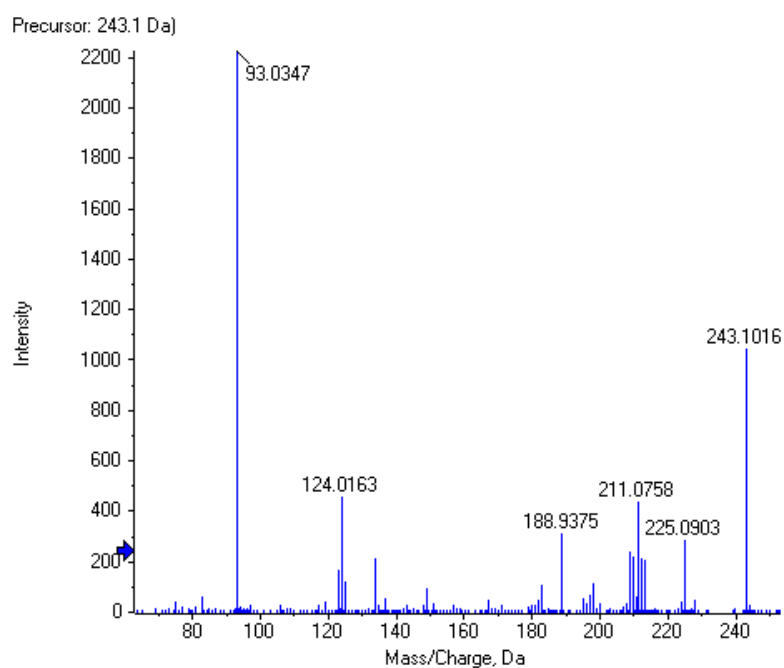


Figure B.40: Fragmentation spectrum of hydroxy-BPA-1. Note: 188.9375 is an artefact signal.

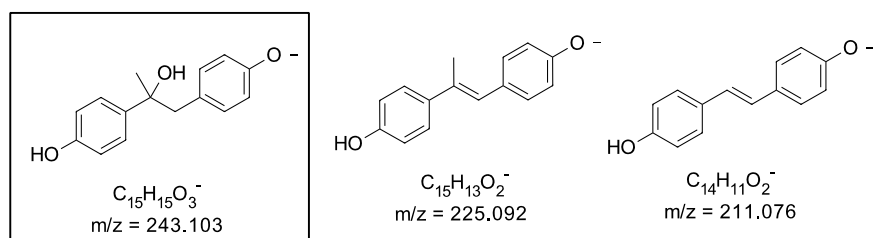
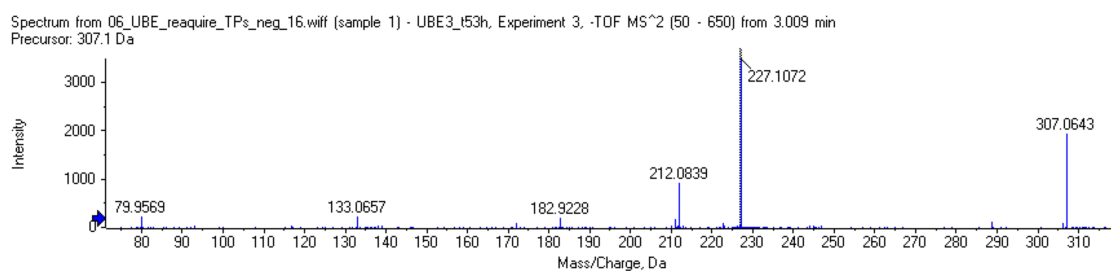
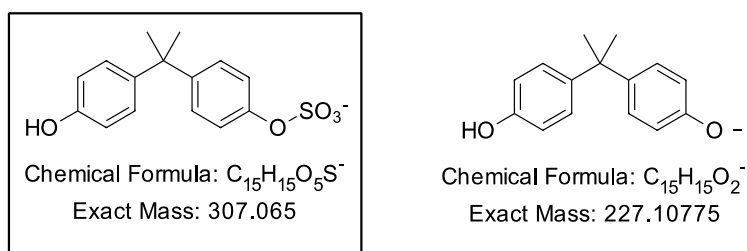
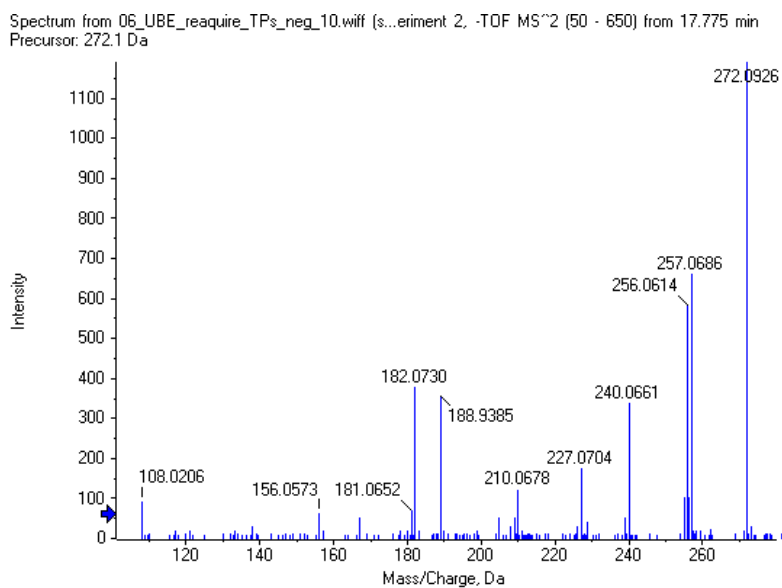
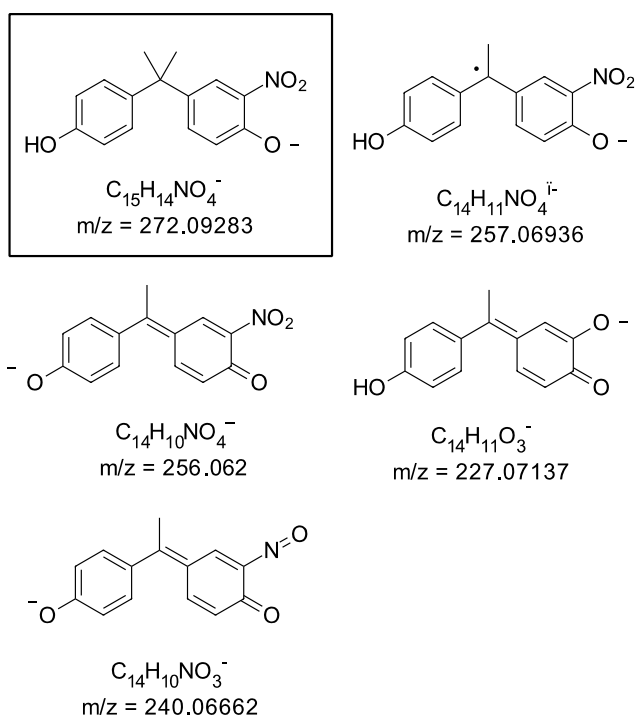


Figure B.41: Proposed fragment structures of hydroxy-BPA-1. No plausible structure could be suggested for fragment with mass 124.0163.

Figure B.42: Fragmentation spectrum of BPA-SO₃.Figure B.43: Proposed fragment structures of BPA-SO₃.

Figure B.44: Fragmentation spectrum of NO₂-BPA.Figure B.45: Proposed fragment structures of NO₂-BPA.

Spectrum from 05_DNA_reaquire1_9.wiff (sample 1) - DNA_E_t11_neg, Experiment 2, -TOF MS² (50 - 650) from 18.464 min
Precursor: 317.1 Da

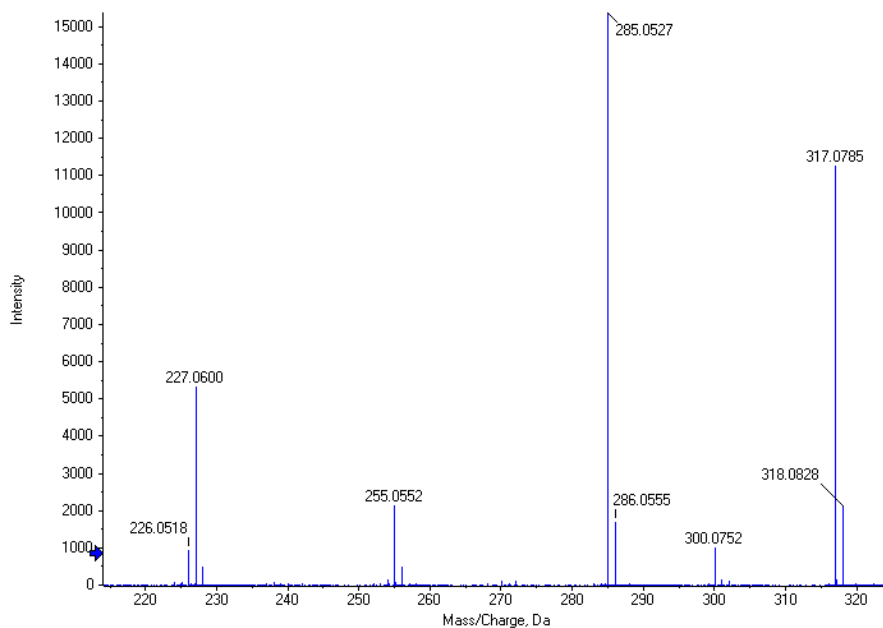


Figure B.46: Fragmentation spectrum of dinitro-BPA.

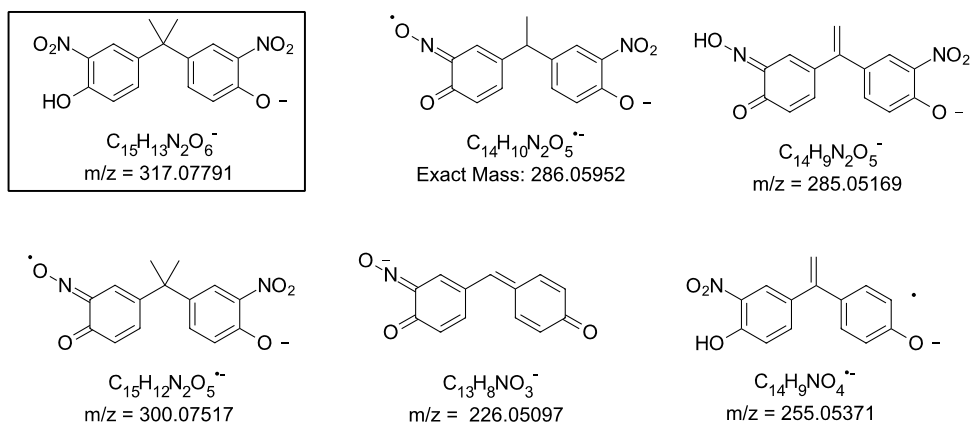


Figure B.47: Proposed fragment structures of dinitro-BPA.

Spectrum from 05_DNA_require1_12.wiff (sample 1) - DNA_6_t144_neg, Experiment 2, -TOF MS² (50 - 650) from 9.027 min
Precursor: 397.0 Da

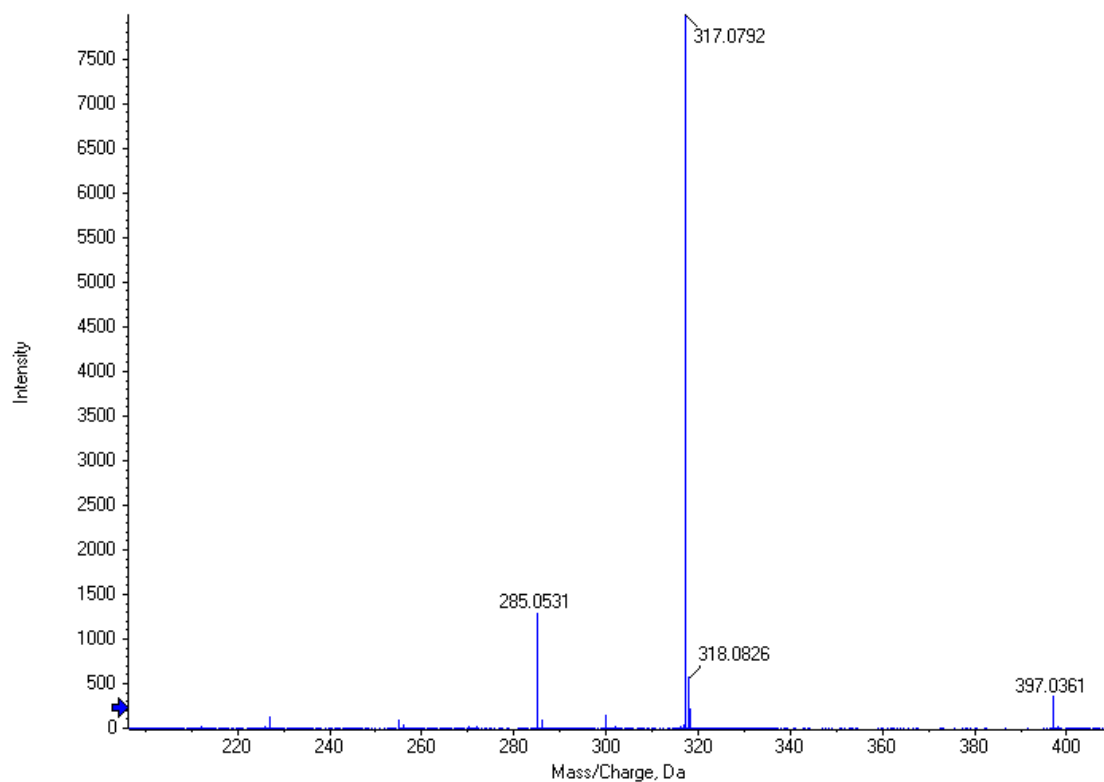


Figure B.48: Fragmentation spectrum of sulfo-dinitro-BPA.

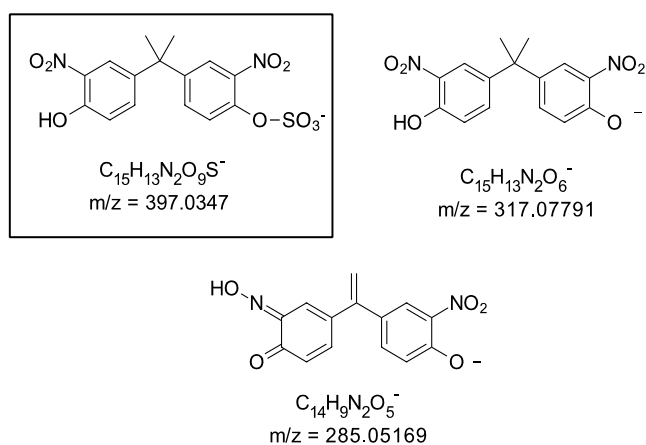


Figure B.49: Proposed fragment structures of sulfo-dinitro-BPA.

Appendix C

Supplementary data for Chapter 4: Transformation of diclofenac in hybrid biofilm–activated sludge processes

C.1 Compound details, MS² fragmentation and elucidation of TP structures

Different levels of confidence are given for the structures based on the categorisation proposed by [Schymanski et al. \(2014\)](#). For 4HD, 5HD, DCF-lactam and DCF-BA, the identity could be confirmed with authentic reference standards. For the other TPs, the structure was postulated based on the exact mass, isotope pattern, retention time, MS² fragmentation spectrum, the similarities or differences of the MS² spectrum to that of DCF and other TPs and based on the primary TPs from which they were formed. Software tools that were used to aid structural identification include PeakView and MasterView (Sciex), ChemDoodle (iChemLabs) and ChemCalc.org ([Patiny and Borel, 2013](#)).

Table C.1: TPs identified in lab-scale experiments with the recorded experimental m/z ($[M+H]^+$ or $[M-H]^-$) and retention time.

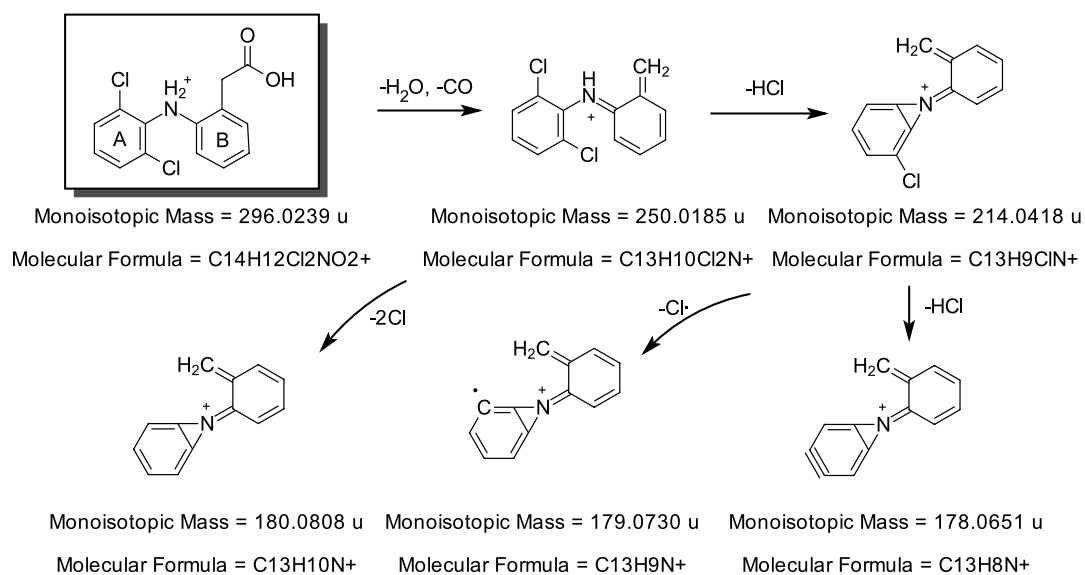
Name	Formula	Monoisotopic mass (u)	Retention time (min)	Confidence level	Polarity	mass/charge (exp.) (u)
DCF	$C_{14}H_{11}Cl_2NO_2$	295.0167	12.74		pos	
5HD	$C_{14}H_{11}Cl_2NO_3$	311.0116	10.16	1	pos	312.0184
5HDQI	$C_{14}H_9Cl_2NO_3$	308.9959	10.52	2	pos	310.0035
DCF-d4	$C_{14}H_7D_4Cl_2NO_2$	299.0418	12.71		pos	
4HD	$C_{14}H_{11}Cl_2NO_3$	311.0116	10.60	1	pos	312.0191
4HDQI	$C_{14}H_9Cl_2NO_3$	308.9959	10.90	2	pos	310.0031
DCF-lactam	$C_{14}H_9NOCl_2$	277.0061	12.52	1	pos	278.0132
DCF-BA	$C_{13}H_9Cl_2NO_2$	281.0010	13.05	1	pos	282.0083
TP285	$C_{12}H_9Cl_2NO_3$	284.9959	8.59	3	pos	286.0031
TP287	$C_{12}H_{11}Cl_2NO_3$	287.0116	7.02	4	pos	288.0191
TP259	$C_{14}H_{10}NO_2Cl$	259.0400	10.10	3	pos	260.0467
TP225	$C_{14}H_{11}NO_2$	225.0790	9.06	3	pos	226.0856
TP293a	$C_{14}H_9Cl_2NO_2$	293.0010	10.64	2	pos	294.0082
TP293b	$C_{14}H_9Cl_2NO_2$	293.0010	11.14	2	pos	294.0088
TP391a	$C_{14}H_{11}Cl_2NO_6S$	390.9683	8.34	2	neg	389.9605
TP391b	$C_{14}H_{11}Cl_2NO_6S$	390.9683	9.61	2	neg	389.9592
TP297	$C_{13}H_9Cl_2NO_3$	296.9960	11.08	2	pos	298.0032
TP273	$C_{11}H_9Cl_2NO_3$	272.9959	7.14	4	pos	274.0030
TP243	$C_{10}H_7Cl_2NO_2$	242.9854	9.34	4	pos	243.9922
TP343a	$C_{14}H_{11}Cl_2NO_5$	343.0014	7.25	4	pos	344.0088
TP343b	$C_{14}H_{11}Cl_2NO_5$	343.0014	7.65	4	pos	344.0086
TP275	$C_{14}H_{10}ClNO_3$	275.0349	9.87	3	pos	276.0422

C.1.1 Diclofenac (DCF)

DCF fragmentation is included for the purposes of comparison. The fragmentation spectrum and corresponding postulated fragment ions are shown in Table C.2 and Figure C.1.

Table C.2: Fragmentation spectrum of DCF

Mass/Charge	Intensity
178.0640	2%
179.0720	2%
180.0801	2%
214.0425	100%
250.0180	5%

Figure C.1: Characterisation of MS² fragment ions of DCF

C.1.2 4HD

This TP of DCF was available as a reference standard (level 1 confidence). The relatively simple fragmentation pattern with $-\text{CO}$ and $-\text{Cl}$ losses is characteristic of secondary TPs formed from 4HD, e.g., TP259 and TP225.

Table C.3: Fragmentation spectrum of 4HD

Mass/Charge	Intensity
195.0651	4%
230.0367	100%
266.0137	5%

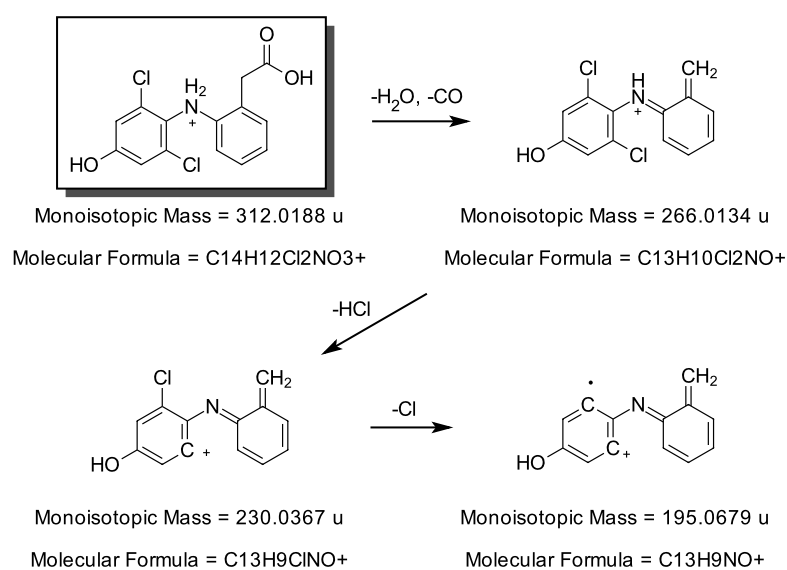


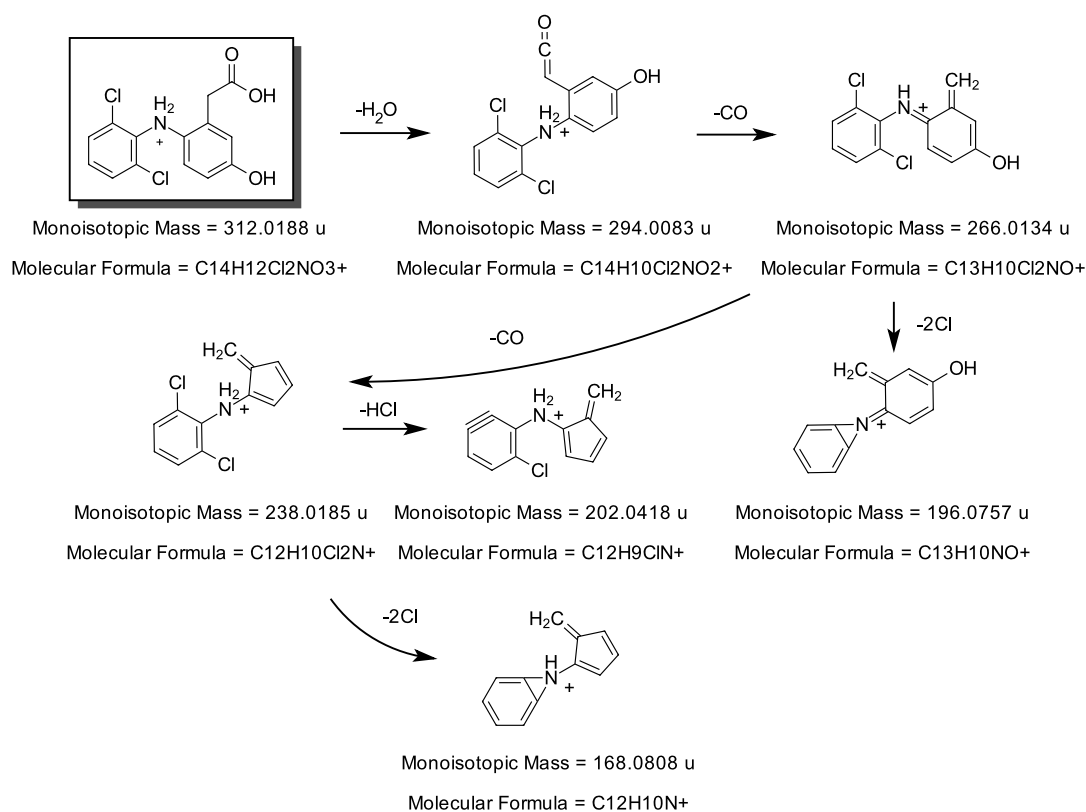
Figure C.2: Characterisation of MS^2 fragment ions of 4HD

C.1.3 5HD

This TP, for which a reference standard was used (level 1 confidence) shows characteristic multiple -CO and -Cl losses similar to DCF and most other TPs. 5HD was found to be an intermediate of nine other TPs in the DCF transformation pathway many of which share a similar fragmentation pattern to 5HD.

Table C.4: Fragmentation spectrum of 5HD

Mass/Charge	Intensity
168.0791	65%
196.0719	50%
202.0395	85%
238.0223	50%
266.0194	35%
294.0077	100%

Figure C.3: Characterisation of MS² fragment ions of 5HD

C.1.4 DCF-lactam

A reference standard of this TP was available (level 1 confidence). The lactam TP shows typical CO and Cl losses as well a characteristic fragment at mass 171.9715, which it shares with other TPs such as TP285 and TP287.

Table C.5: Fragmentation spectrum of DCF-Lactam

Mass/Charge	Intensity
171.9698	26%
180.0800	26%
208.0751	34%
214.0406	100%
215.0448	16%
243.0429	13%
250.0193	5%
278.0133	45%

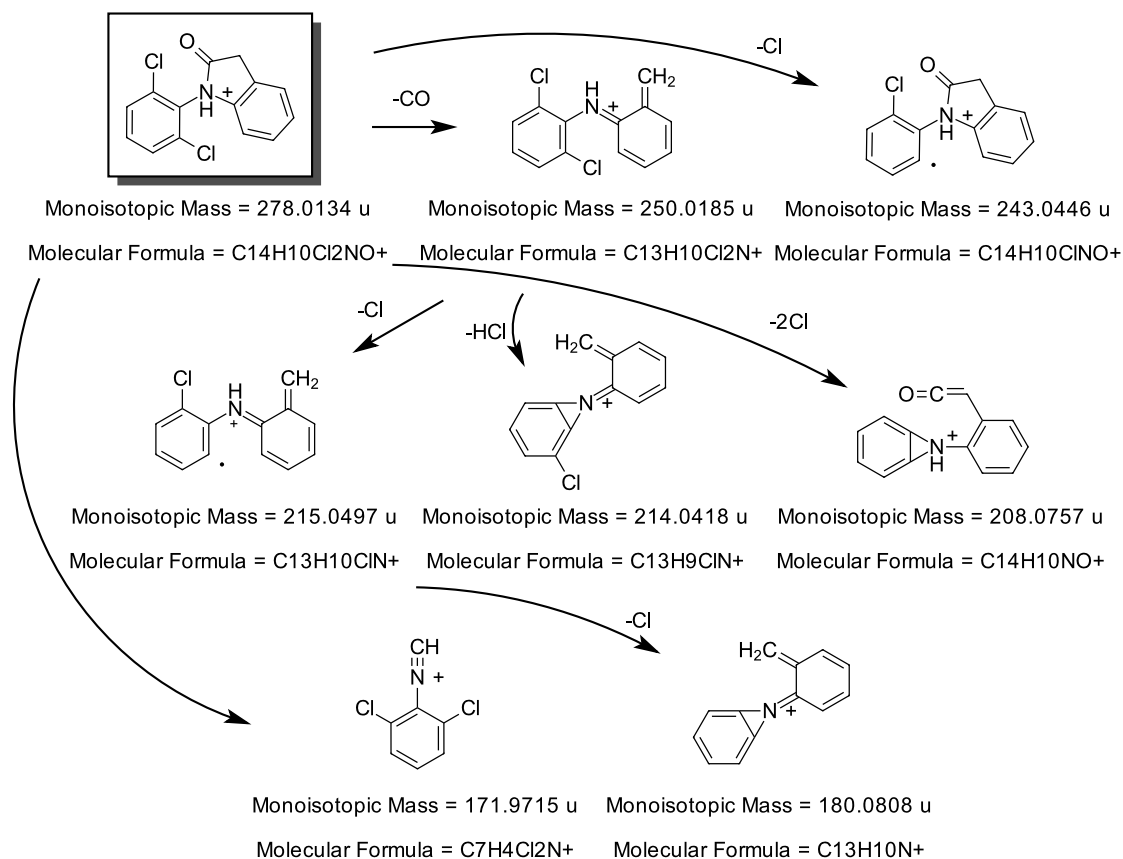


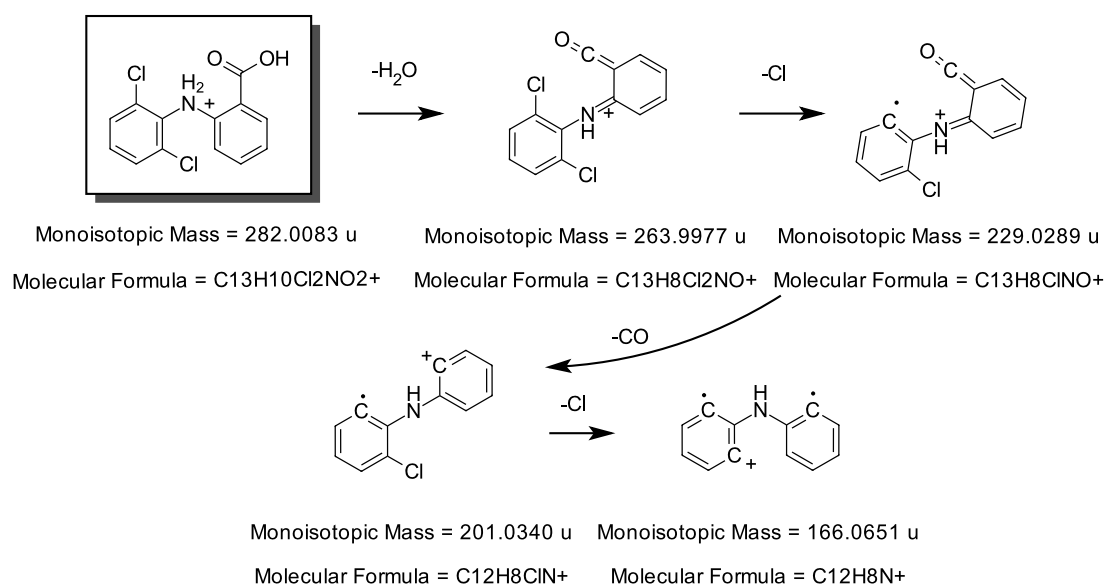
Figure C.4: Characterisation of MS² fragment ions of DCF-Lactam

C.1.5 DCF-BA

A reference standard of this compound was available (level 1 confidence). The fragmentation pattern is typical of DCF TPs, showing loss of -CO and multiple -Cl losses.

Table C.6: Fragmentation spectrum of DCF-BA

Mass/Charge	Intensity
166.0655	11%
201.0339	16%
229.0292	100%
263.9979	16%

Figure C.5: Characterisation of MS² fragment ions of DCF-BA

C.1.6 4HDQI

4HDQI is a known human metabolite of DCF (Poon et al., 2001) and is reported to form by oxidation of 4HD. In this study, 4HDQI was identified by its very similar fragmentation pattern to 4HD and similar retention time (level 2 confidence). However, in incubation experiments of 4HD, 4HDQI was not formed whereas it was formed in incubations of DCF-lactam (and incubations of DCF itself). This might be due to the fast dissipation kinetics of 4HD, which

is quickly transformed to other TPs, allowing little oxidation to take place, while DCF-lactam is more stable, allowing the formation of 4HDQI over a different route (e.g., by combined mono-oxygenation and de-amidation).

Table C.7: Fragmentation spectrum of 4HDQI

Mass/Charge	Intensity
263.9944	54%
229.0288	100%

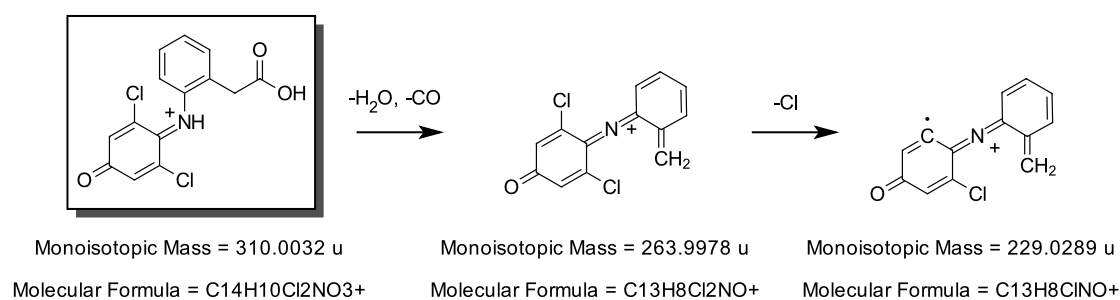


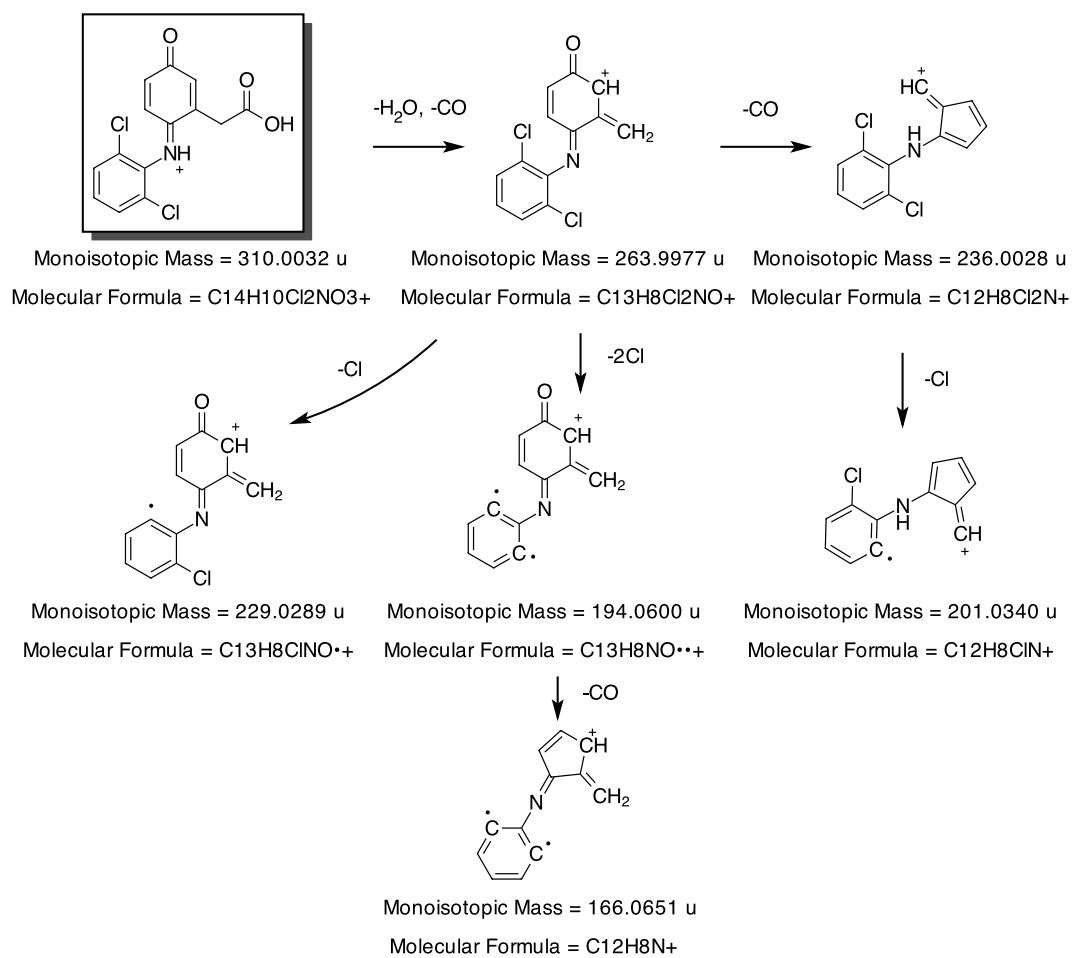
Figure C.6: Characterisation of MS² fragment ions of 4HDQI

C.1.7 5HDQI

This TP was previously identified in soil/sediment systems (Gröning et al., 2007) and was identified in this study by the similar fragmentation pattern and retention time to 5HD (level 2 confidence).

Table C.8: Fragmentation spectrum of 5HDQI

Mass/Charge	Intensity
166.0652	100%
194.0583	38%
201.0334	88%
229.0286	35%
236.0008	23%
263.9964	23%
291.9919	81%

Figure C.7: Characterisation of MS² fragment ions of 5HDQI

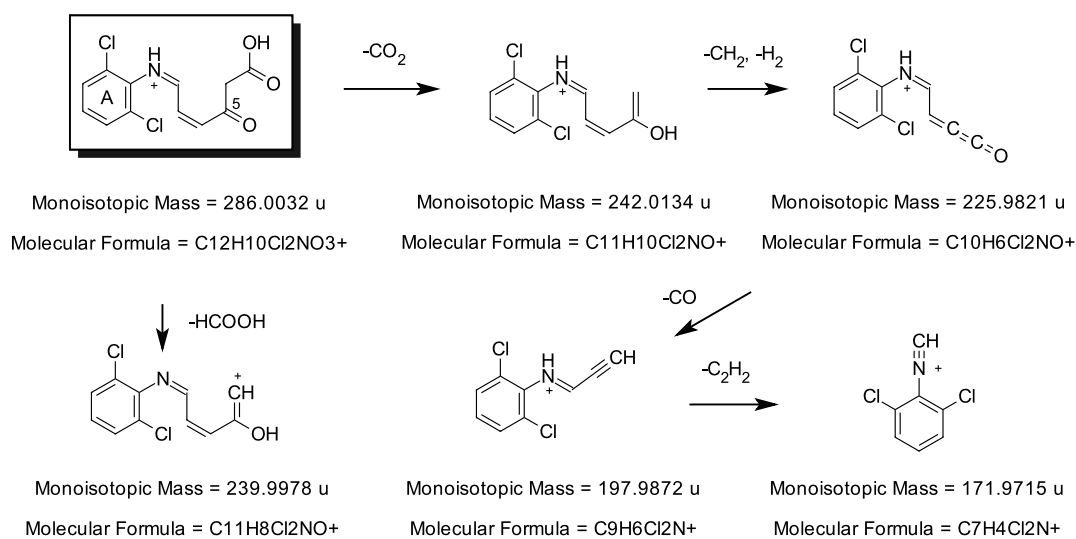
C.1.8 TP285

The characterisation of TP285 was based firstly on the presence of fragment 171.9715, which indicated that ring A was not hydroxylated. TP285 was formed from DCF via 5HD so one oxygen should be located on position 5. The remaining 2 oxygens were considered to be part of a carboxylic acid group which would explain the loss of -CO₂. It was postulated that TP285 was formed as a result of ring-opening of ring B since consecutive -CH₂, -CO and -C₂H₂ losses leading to fragment 171.9715 are indic-

ative of a long-chain structure. According to this structure, the β -keto moiety might be formed via tautomerism. A level 3 confidence is therefore proposed (tentative structure).

Table C.9: Fragmentation spectrum of TP285

Mass/Charge	Intensity
171.9676	26%
197.9856	19%
225.982	25%
239.9951	58%
242.0145	100%

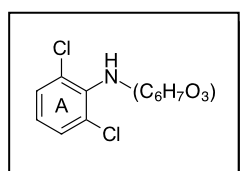
Figure C.8: Characterisation of MS² fragment ions of TP285

C.1.9 TP287

TP287 has a mass difference of only +2H compared to TP285 and also shows fragment 171.9715, the presence of which indicated that ring A is not hydroxylated. Structural characterisation of TP287 was not possible due to many possible structures on the right side of the molecule. The structure of ring A and the elemental composition of the rest of the molecule could be determined (level 4 confidence).

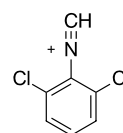
Table C.10: Fragmentation spectrum of TP287

Mass/Charge	Intensity
132.9596	17%
159.9697	98%
164.0264	21%
171.9707	59%
187.9648	21%
200.0054	14%
227.9990	100%



Monoisotopic Mass = 288.0189 u

Molecular Formula = C₁₂H₁₂Cl₂NO₃⁺



Monoisotopic Mass = 171.9715 u

Molecular Formula = C₇H₄Cl₂N⁺

Figure C.9: Characterisation of MS² fragment ions of TP287

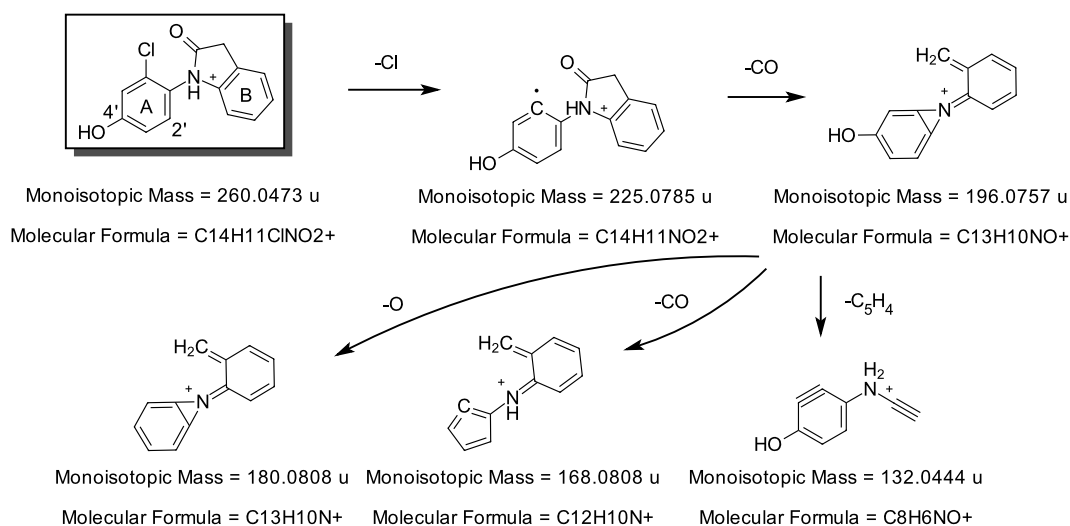
C.1.10 TP259

The mass of TP259 and the isotopic pattern indicate it has one chloride and two oxygen atoms. Since it is formed from DCF via 4HD, it is assumed that the 4'-position (ring A) is hydroxylated. The fragmentation pattern is very similar to DCF-lactam showing consecutive -CO and -Cl losses, it is therefore postulated that TP259 has a lactam structure, which also accounts for the second oxygen. To account for the extra hy-

drogen a reductive dechlorination at the 2'-position is postulated (level 3).

Table C.11: Fragmentation spectrum of TP259

Mass/Charge	Intensity
132.0451	12%
168.0807	30%
180.0799	15%
196.0747	100%
225.0781	21%

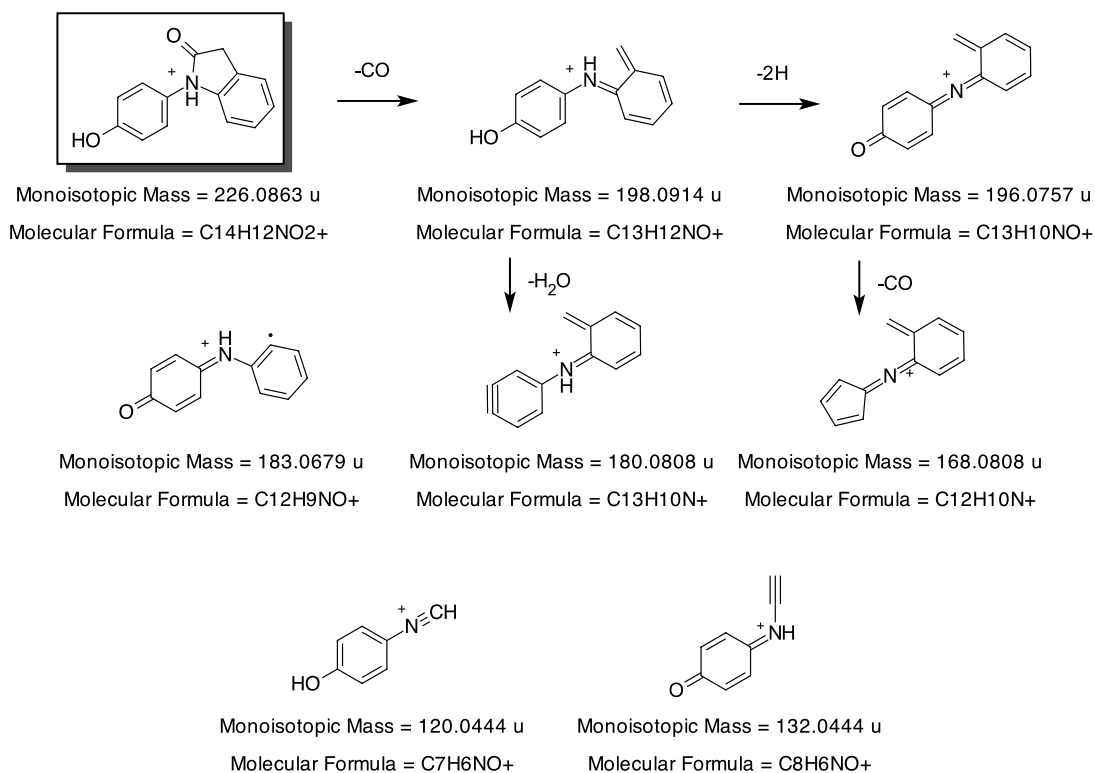
Figure C.10: Characterisation of MS² fragment ions of TP259

C.1.11 TP225

The mass and isotopic pattern of TP225 indicate that no Cl atom is present in the molecule. The similar fragmentation pattern to TP259 suggest this compound is the result of a second reductive dechlorination, which also accounts for the extra hydrogen. Therefore, a level 3 confidence is given for the structure.

Table C.12: Fragmentation spectrum of TP225

Mass/Charge	Intensity
120.0453	59%
132.0440	69%
180.0801	86%
183.0634	43%
196.0745	100%
198.0912	53%

Figure C.11: Characterisation of MS² fragment ions of TP225

C.1.12 TP293a

This TP was formed from both DCF-lactam and 5HD. Due to the parent TPs and the fragmentation pattern, the structure can be given at level 2 confidence. Several isomers of this TP were detected, with similar retention times and MS² spectra. It is postulated that these are formed by hydroxylation of

ring B at different positions.

Table C.13: Fragmentation spectrum of TP293a

Mass/Charge	Intensity
266.0128	40%
238.0187	40%
202.0415	60%
168.0817	100%

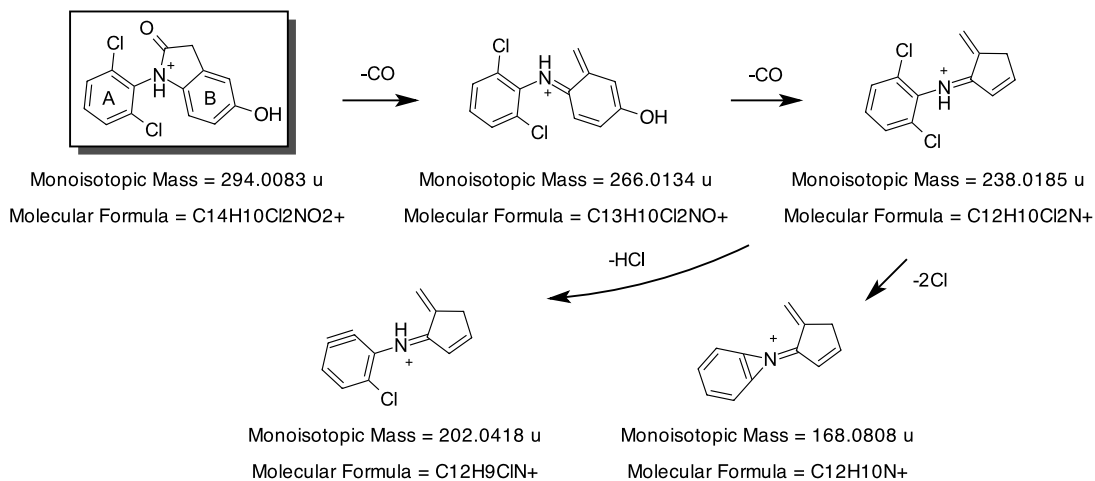


Figure C.12: Characterisation of MS² fragment ions of TP293a

C.1.13 TP293b

This TP is an isomer of TP293a but is formed from 4HD or DCF-lactam and not formed from 5HD and was previously detected in WWTP effluents, where it was identified as a human metabolite of DCF (Stülten et al., 2008). It has a different MS² spectrum since ring A is hydroxylated. A level 2 confidence is

given for this structure.

Table C.14: Fragmentation spectrum of TP293b

Mass/Charge	Intensity
230.0366	100%
224.0696	50%
132.0437	45%

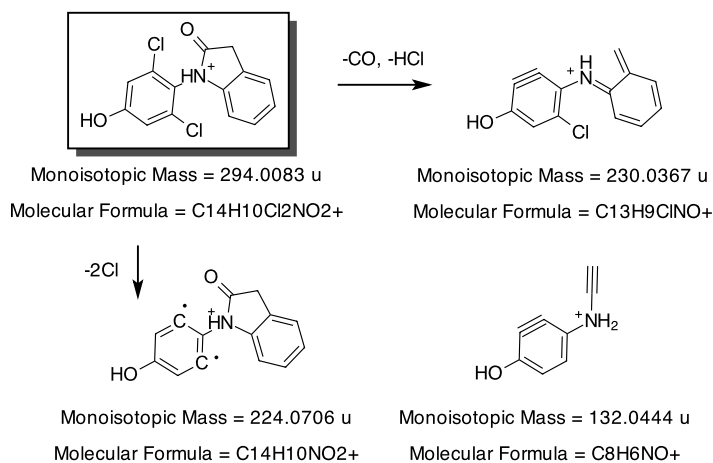


Figure C.13: Characterisation of MS² fragment ions of TP293b.

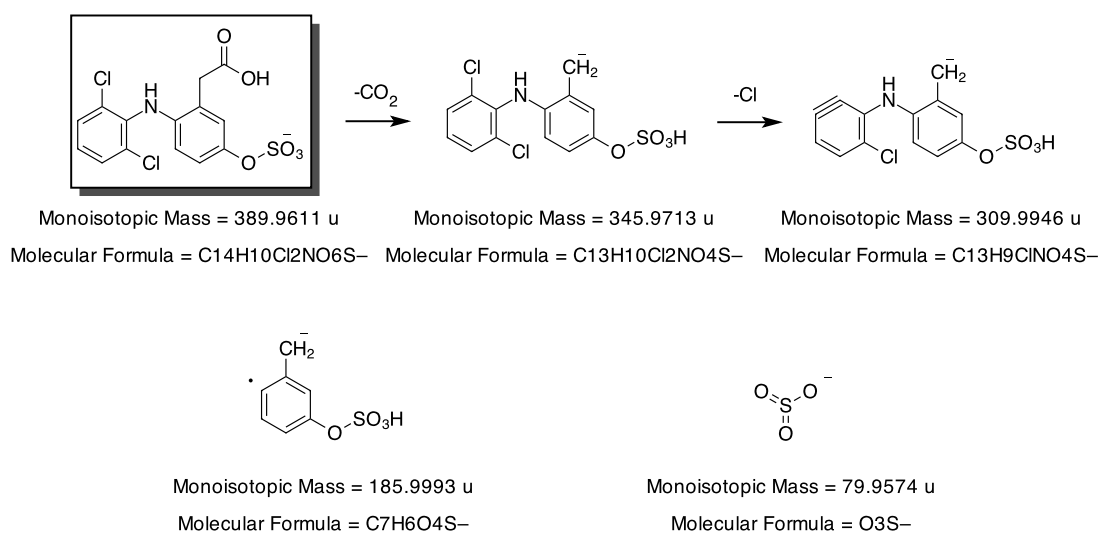
C.1.14 TP391a

This DCF-TP is formed via 5HD. The molecular formula and characteristic -SO₃ loss indicate that this TP is the result of sulfate conjugation of 5HD. Due to the observed fragments, and in comparison to similar sulfate conjugation reactions observed at aromatic hydroxy groups in activated sludge (Jewell et al., 2014), it is postulated the conjugation occurs at the hydroxylated 5-

position (ring B). Thus, level 2 confidence is given for the structure.

Table C.15: Fragmentation spectrum of TP391a

Mass/Charge	Intensity
79.9572	100%
185.9972	29%
309.9933	42%
345.9676	78%

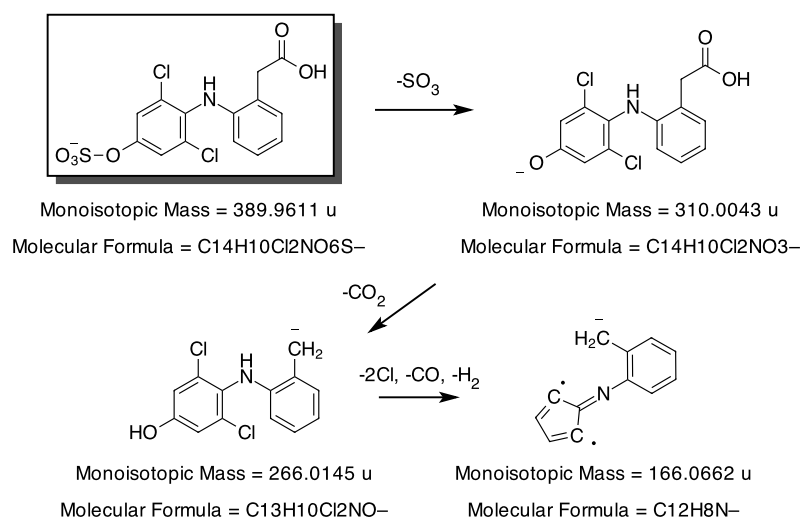
Figure C.14: Characterisation of MS² fragment ions of TP391a.

C.1.15 TP391b

This TP is formed from 4HD similarly to TP391a. It is postulated the conjugation occurs at the 4'-position (ring A). Level 2 confidence is given for the structure.

Table C.16: Fragmentation spectrum of TP391b

Mass/Charge	Intensity
310.0047	30%
266.0127	100%
166.0639	30%

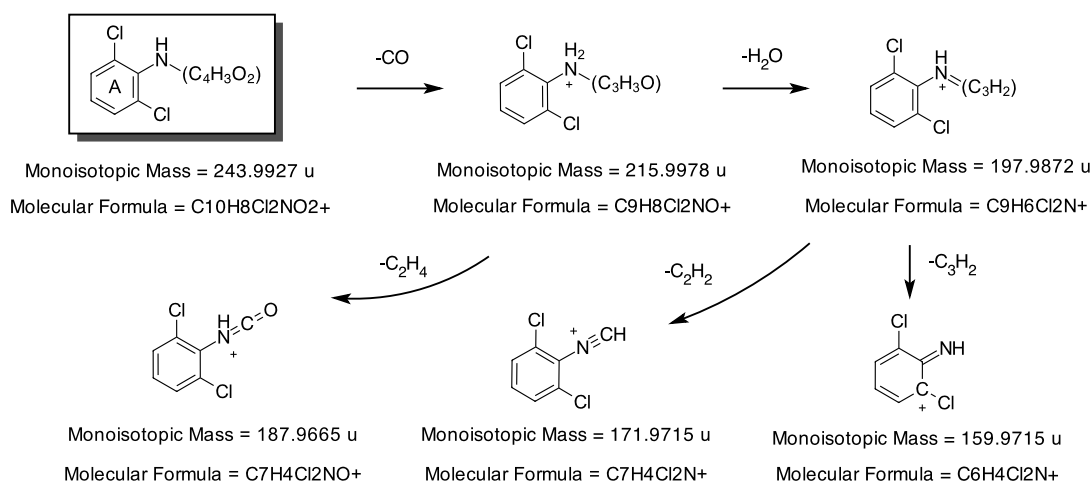
Figure C.15: Characterisation of MS² fragment ions of TP391b.

C.1.16 TP243

This DCF-TP is formed via 5HD and has a similar fragmentation pattern to TP285 and TP287, sharing, for example, the fragment 171.9713. This fragment is again an indication that ring A is not hydroxylated. The two oxygen atoms from the formula are thus likely to be on the right side of the molecule. Due to the ambiguous fragmentation pattern, a tentative structure cannot be suggested (level 4). However, the low number of carbons on the right side of the molecule

Table C.17: Fragmentation spectrum of TP243

Mass/Charge	Intensity
216.0006	25%
197.9881	25%
187.9664	25%
171.9713	5%
159.9712	100%
132.9608	25%

Figure C.16: Characterisation of MS² fragment ions of TP243

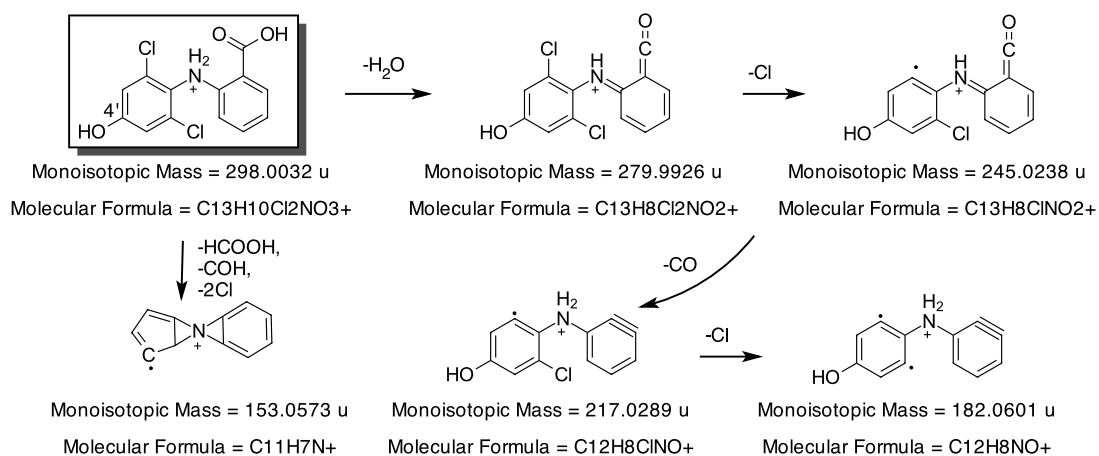
C.1.17 TP297

This TP was formed from both 4HD and DCF-BA and to a minor extent 5HD. The molecular formula indicates it is formed as a result of the combination of reactions which lead to the parent TPs, i.e., a hydroxylation and a decarboxylation followed by oxidation to carboxylic acid. Two isomers of this compound are formed with retention times 10.68 min and 11.08 min, but both with identical fragmentation patterns. It is expected that these are the result of the hydroxylations at different ring positions, i.e., 4'-, or 5-position. The isomer at

10.68 is only formed via 5HD, whereas the isomer at 11.08 is only formed via 4HD and both isomers are formed via DCF-BA. Level 2 confidence is given for this structure.

Table C.18: Fragmentation spectrum of TP297

Mass/Charge	Intensity
153.0562	8%
182.0601	13%
217.0291	17%
245.0236	100%
279.9942	19%

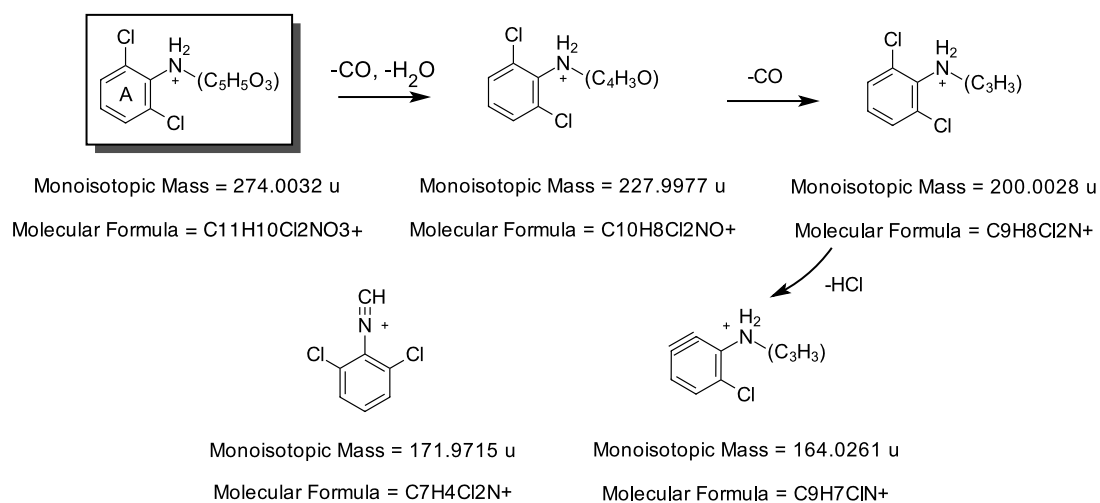
Figure C.17: Characterisation of MS² fragment ions of TP297

C.1.18 TP273

This DCF-TP is formed via 5HD and, (level 4 confidence), as with TP243, TP285 and TP287 has a fragmentation pattern indicating ring A is not hydroxylated (fragment with mass 171.9718). The fragmentation pattern indicates several -CO losses however a unambiguous structure cannot be postulated for the right side of the molecule

Table C.19: Fragmentation spectrum of TP273

Mass/Charge	Intensity
164.0262	55%
171.9718	100%
200.0017	35%
227.9985	75%

Figure C.18: Characterisation of MS² fragment ions of TP273

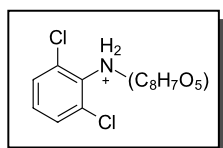
C.1.19 TP343a

This TP of DCF and 5HD has a formula with +2O in comparison to 5HD, suggesting that oxidative reactions took place. A characteristic fragment at 159.9731 indicates that ring A is likely not hydroxylated. The remaining fragments show multiple $-H_2O$ and $-CO$ losses (parent mass \rightarrow 326.0028 \rightarrow 298.0026 \rightarrow 270.0039 \rightarrow 251.9964 \rightarrow 224.0014) indicating a structure with multiple hydroxy carboxyl groups. However an clear structure can not be postu-

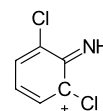
lated from the fragments (level 4).

Table C.20: Fragmentation spectrum of TP343b

Mass/Charge	Intensity
159.9731	20%
217.0294	30%
224.0014	15%
251.9964	100%
270.0039	25%
298.0026	60%
326.0028	15%



Monoisotopic Mass = 344.0092 u
Molecular Formula = C₁₄H₁₂Cl₂NO₅⁺



Monoisotopic Mass = 159.9715 u
Molecular Formula = C₆H₄Cl₂N⁺

Figure C.19: Characterisation of MS² fragment ion of TP343a

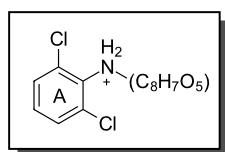
C.1.20 TP343b

This DCF-TP is formed via 5HD and has a formula with +2O in comparison to 5HD, suggesting that oxidative reactions took place. Although the characteristic fragment at mass 171.9715 was not observed, a similar mass at 173.9834 is again an indication that ring A is not hydroxylated. The other fragments do not allow a full characterisation of the right side of the molecule (level 4). However, multiple -CO₂ losses, e.g., from parent mass → 298.0063 → 254.0122, suggest the presence of carboxylic acid groups. This compound has a similar retention time (δ 0.5 min) to the struc-

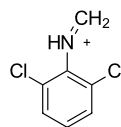
tural isomer TP343a, however these TPs do not have similar fragmentation patterns.

Table C.21: Fragmentation spectrum of TP343b

Mass/Charge	Intensity
173.9834	10%
177.0338	35%
190.0415	35%
204.0208	15%
218.0365	55%
237.9802	20%
254.0122	60%
283.9882	100%
298.0063	10%



Monoisotopic Mass = 344.0092 u

Molecular Formula = C₁₄H₁₂Cl₂NO₅⁺

Monoisotopic Mass = 173.9872 u

Molecular Formula = C₇H₆Cl₂N⁺Figure C.20: Characterisation of MS² fragment ions of TP343b

C.1.21 TP275

TP275 was formed via 4HD. The molecular formula indicated a loss of Cl and one H. The fragmentation spectrum was similar to 4HD and 4HDQI showing CO, H₂O, Cl and HCl losses. Since other reductive dechlorinations were observed, forming TPs 259 and 225, it was postulated that this TP was also formed through reductive dechlorination. To account for the loss of H an oxidation via dehydrogenation was proposed, similar to the reactions forming 4HDQI and 5HDQI. It was unclear if TP275

was formed directly from 4HD or via TP259. In the later case the reaction would be equivalent to the formation of 4HDQI from DCF-lactam (confidence level 3).

Table C.22: Fragmentation spectrum of TP275

Mass/Charge	Intensity
140.0524	15%
167.0717	100%
194.0606	15%
202.0426	20%
230.0372	30%

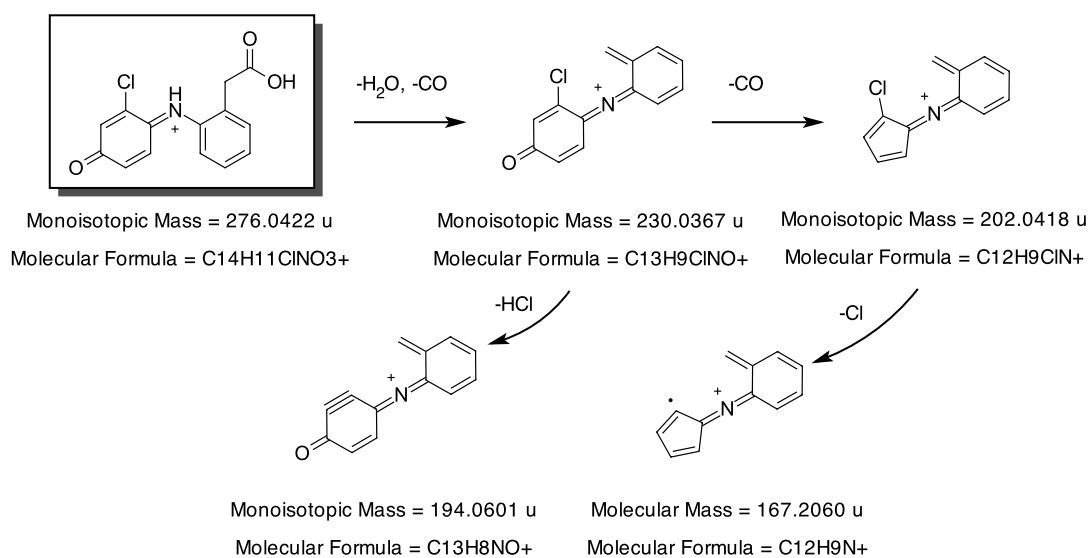


Figure C.21: Characterisation of MS² fragment ion of TP275

C.2 Additional figures and tables

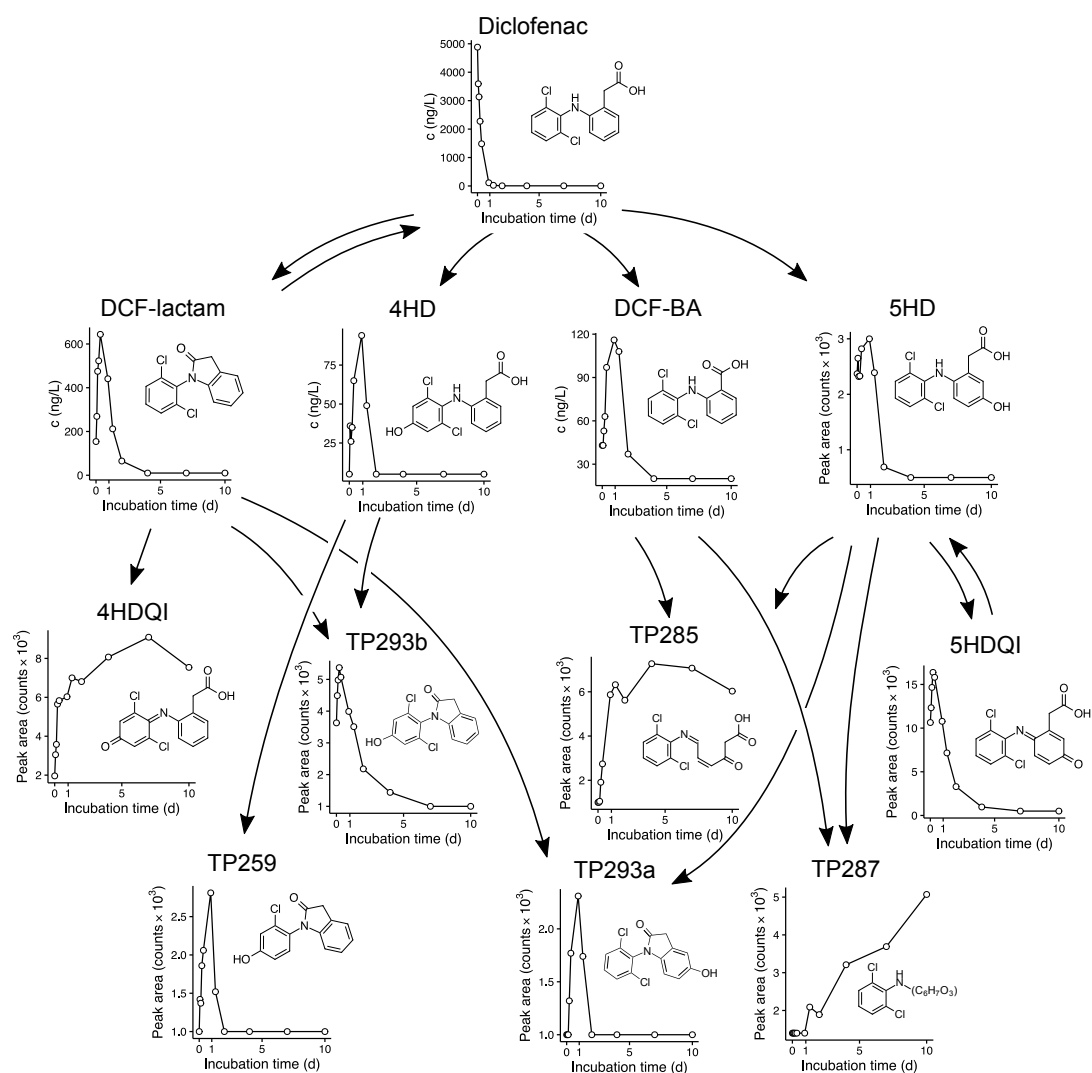


Figure C.22: Transformation reactions of DCF (spike concentration 5 µg/L) in incubation experiments inoculated with carriers from WWTP Bad Ragaz.

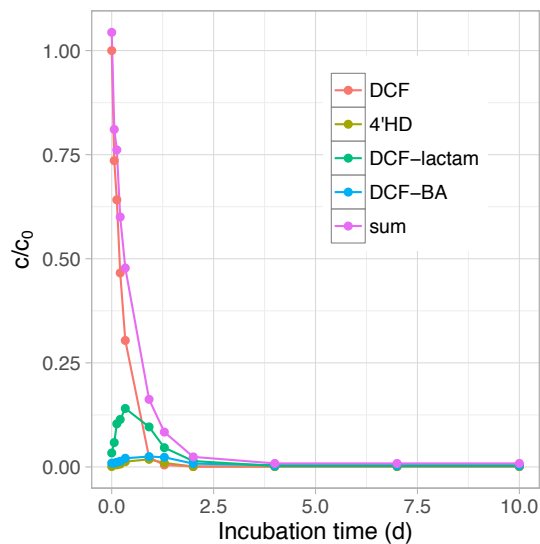


Figure C.23: DCF transformation showing sum of TPs and DCF concentration at each time point (spike concentration 5 $\mu\text{g/L}$) in incubation experiments inoculated with carriers from WWTP-BR (Bad Ragaz, hybrid-MBBR).

Table C.23: TPs formed from primary DCF TPs

Parent	TPs					
DCF-Lactam	DCF-BA	4HDQI	TP293b	TP285		
4HD	TP293b	TP259	TP225	TP275	TP391b	TP297
5HD	5HDQI	TP287	TP285	TP343a	TP343b	TP391a
	TP273a	TP243	TP293a			
DCF-BA	TP297	TP285	TP287			

Table C.24: DCF-TPs detected during lab-scale experiments with carriers from WWTP Klippan

	DCF-lactam	DCF-BA	TP285
Retention time (min)	12.42	12.88	8.44
Retention time of standard (min)	12.39	12.89	8.62 ^a
[M + H] ⁺ mass (u)	278.0131	282.0072	286.0027
Calculated mass (u)	278.0134	282.0083	286.0032
		166.0649	
MS ² Spectrum	214.0445	201.0349	242.0151
		229.0297	

^aStandard not available, retention time was compared to a previous lab-scale incubation experiment using carriers from WWTP Bad Ragaz.

Bibliography

- Al-Obaidi, U., Moodie, R., 1985. The nitrous acid-catalysed nitration of phenol, *Journal of the Chemical Society, Perkin Transactions 2*, vol. -, no. 3, pp. 467–472, doi:[10.1039/P29850000467](https://doi.org/10.1039/P29850000467).
- Alexander, M., 1981. Biodegradation of chemicals of environmental concern, *Science*, vol. 211, no. 4478, pp. 132–138, doi:[10.1126/science.7444456](https://doi.org/10.1126/science.7444456).
- Alexander, J., Knopp, G., Dötsch, A., Wieland, A., Schwartz, T., 2016. Ozone treatment of conditioned wastewater selects antibiotic resistance genes, opportunistic bacteria, and induce strong population shifts, *Science of The Total Environment*, vol. 559, pp. 103–112, doi:[10.1016/j.scitotenv.2016.03.154](https://doi.org/10.1016/j.scitotenv.2016.03.154).
- Atkins, P., de Paula, J., 2002. *Atkins' Physical Chemistry*, Oxford Univeristy Press, Oxford, 7 edn.
- Babu, S., Pathak, C., Uppu, S., Jones, C., Fronczek, F.R., Uppu, R.M., 2011. 3,3'-dinitrophenol A, *Acta Crystallographica Section E Structure Reports Online*, vol. 67, pp. o2556–o2557, doi:[10.1107/S1600536811035458](https://doi.org/10.1107/S1600536811035458).
- Batt, A.L., Kim, S., Aga, D.S., 2006. Enhanced biodegradation of iopromide and trimethoprim in nitrifying activated sludge., *Environmental Science & Technology*, vol. 40, pp. 7367–73, doi:[10.1021/es060835v](https://doi.org/10.1021/es060835v).
- Beake, B.D., Constantine, J., Moodie, R.B., 1994. Nitration and oxidation of 4-methoxyphenol by nitrous acid in aqueous acid solution, *Journal of the Chemical Society, Perkin Transactions 2*, vol. 17, p. 335, doi:[10.1002/ibd.21577](https://doi.org/10.1002/ibd.21577).
- Beel, R., Lütke Eversloh, C., Ternes, T.A., 2013. Biotransformation of the UV-filter sulisobenzone: challenges for the identification of transformation

- products, *Environmental Science & Technology*, vol. 47, no. 13, pp. 6819–6828, doi:[10.1021/es400451w](https://doi.org/10.1021/es400451w).
- Beeman, R.E., Bleckmann, C.A., 2002. Sequential anaerobic-aerobic treatment of an aquifer contaminated by halogenated organics: field results, *Journal of Contaminant Hydrology*, vol. 57, pp. 147–159, doi:[10.1016/S0169-7722\(02\)00008-6](https://doi.org/10.1016/S0169-7722(02)00008-6).
- Benner, J., Helbling, D.E., Kohler, H.P.E., Wittebol, J., Kaiser, E., Prasse, C., Ternes, T.A., Albers, C.N., Aamand, J., Horemans, B., et al., 2013. Is biological treatment a viable alternative for micropollutant removal in drinking water treatment processes?, *Water Research*, vol. 47, no. 16, pp. 5955–5976, doi:[10.1016/j.watres.2013.07.015](https://doi.org/10.1016/j.watres.2013.07.015).
- Beretsou, V.G., Psoma, A.K., Gago-Ferrero, P., Aalizadeh, R., Fenner, K., Thomaidis, N.S., 2016. Identification of biotransformation products of citalopram formed in activated sludge, *Water Research*, vol. 103, pp. 205–214, doi:[10.1016/j.watres.2016.07.029](https://doi.org/10.1016/j.watres.2016.07.029).
- Boix, C., Ibáñez, M., Sancho, J.V., Parsons, J.R., de Voogt, P., Hernández, F., 2016. Biotransformation of pharmaceuticals in surface water and during waste water treatment: Identification and occurrence of transformation products, *Journal of Hazardous Materials*, vol. 302, pp. 175–187, doi:[10.1016/j.jhazmat.2015.09.053](https://doi.org/10.1016/j.jhazmat.2015.09.053).
- Bouju, H., Nastold, P., Beck, B., Hollender, J., Corvini, P.F.X., Wintgens, T., 2016. Elucidation of biotransformation of diclofenac and 4'-hydroxydiclofenac during biological wastewater treatment, *Journal of Hazardous Materials*, vol. 301, pp. 443–452, doi:[10.1016/j.jhazmat.2015.08.054](https://doi.org/10.1016/j.jhazmat.2015.08.054).
- Brenner, C.G.B., Mallmann, C.A., Arsand, D.R., Mayer, F.M., Martins, A.F., 2011. Determination of sulfamethoxazole and trimethoprim and their metabolites in hospital effluent, *CLEAN – Soil, Air, Water*, vol. 39, no. 1, pp. 28–34, doi:[10.1002/clean.201000162](https://doi.org/10.1002/clean.201000162).
- Brezina, E., Prasse, C., Wagner, M., Ternes, T.A., 2015. Why small differences matter: Elucidation of the mechanisms underlying the transformation of 2OH- and 3OH-carbamazepine in contact with sand filter mater-

- ial, *Environmental Science & Technology*, vol. 49, no. 17, pp. 10 449–10 456, doi:[10.1021/acs.est.5b02737](https://doi.org/10.1021/acs.est.5b02737).
- Brogden, R.N., Carmine, A.A., Heel, R.C., Speight, T.M., Avery, G.S., 1982. Trimethoprim: a review of its antibacterial activity, pharmacokinetics and therapeutic use in urinary tract infections, *Drugs*, vol. 23, no. 6, pp. 405–430, doi:[10.2165/00003495-198223060-00001](https://doi.org/10.2165/00003495-198223060-00001).
- Burke, V., Richter, D., Hass, U., Duennbier, U., Greskowiak, J., Massmann, G., 2014. Redox-dependent removal of 27 organic trace pollutants: compilation of results from tank aeration experiments, *Environmental Earth Sciences*, vol. 71, no. 8, pp. 3685–3695, doi:[10.1007/s12665-013-2762-8](https://doi.org/10.1007/s12665-013-2762-8).
- Chen, X., Casas, M.E., Nielsen, J.L., Wimmer, R., Bester, K., 2015. Identification of triclosan-*O*-sulfate and other transformation products of triclosan formed by activated sludge, *Science of The Total Environment*, vol. 505, pp. 39 – 46, doi:[10.1016/j.scitotenv.2014.09.077](https://doi.org/10.1016/j.scitotenv.2014.09.077).
- Chen, X., Nielsen, J.L., Furgal, K., Liu, Y., Lolas, I.B., Bester, K., 2011. Biodegradation of triclosan and formation of methyl-triclosan in activated sludge under aerobic conditions., *Chemosphere*, vol. 84, pp. 452–6, doi:[10.1016/j.chemosphere.2011.03.042](https://doi.org/10.1016/j.chemosphere.2011.03.042).
- Chen, W.W., Niepel, M., Sorger, P.K., 2010. Classic and contemporary approaches to modeling biochemical reactions, *Genes and Development*, vol. 24, no. 17, pp. 1861–1875, doi:[10.1101/gad.1945410](https://doi.org/10.1101/gad.1945410).
- Cheng, H.m., Eto, M., Kuwatsuka, S., Oshima, Y., 1968. Studies on the phenylphenol derivatives with biological activity part I. herbicidal activity of nitro-substituted phenylphenols, *Agricultural and Biological Chemistry*, vol. 32, pp. 345–352, doi:[10.1080/00021369.1968.10859062](https://doi.org/10.1080/00021369.1968.10859062).
- Chiron, S., Gomez, E., Fenet, H., 2010. Nitration processes of acetaminophen in nitrifying activated sludge., *Environmental Science & Technology*, vol. 44, pp. 284–289, doi:[10.1021/es902129c](https://doi.org/10.1021/es902129c).
- Collado, N., Buttiglieri, G., Ferrando-Climent, L., Rodriguez-Mozaz, S., Barceló, D., Comas, J., Rodriguez-Roda, I., 2012. Removal of ibuprofen and its trans-

- formation products: experimental and simulation studies, *Science of The Total Environment*, vol. 433, pp. 296–301, doi:[10.1016/j.scitotenv.2012.06.060](https://doi.org/10.1016/j.scitotenv.2012.06.060).
- Coutu, S., Rossi, L., Barry, D.A., Rudaz, S., Vernaz, N., 2013. Temporal variability of antibiotics fluxes in wastewater and contribution from hospitals, *Plos One*, vol. 8, no. 1, p. e53592, doi:[10.1371/journal.pone.0053592](https://doi.org/10.1371/journal.pone.0053592).
- Daughton, C.G., Ruhoy, I.S., 2009. Environmental footprint of pharmaceuticals: the significance of factors beyond direct excretion to sewers, *Environmental Toxicology and Chemistry*, vol. 28, no. 12, pp. 2495–2521, doi:[10.1897/08-382.1](https://doi.org/10.1897/08-382.1).
- Daughton, C., Ternes, T., 1999. Pharmaceuticals and personal care products in the environment: agents of subtle change?, *Environmental Health Perspectives*, vol. 107, no. Suppl. 6, pp. 907–938.
- de Beer, D., Schramm, A., Santegoeds, C.M., Köhl, M., 1997. A nitrite microsensor for profiling environmental biofilms., *Applied and Environmental Microbiology*, vol. 63, p. 973.
- Dodgen, L.K., Li, J., Wu, X., Lu, Z., Gan, J.J., 2014. Transformation and removal pathways of four common PPCP/EDCs in soil, *Environmental Pollution*, vol. 193, pp. 29–36, doi:[10.1016/j.envpol.2014.06.002](https://doi.org/10.1016/j.envpol.2014.06.002).
- Eggen, R.I.L., Hollender, J., Joss, A., Schärer, M., Stamm, C., 2014. Reducing the discharge of micropollutants in the aquatic environment: The benefits of upgrading wastewater treatment plants, *Environmental Science & Technology*, vol. 48, no. 14, pp. 7683–7689, doi:[10.1021/es500907n](https://doi.org/10.1021/es500907n).
- Eichhorn, P., Ferguson, P.L., Pérez, S., Aga, D.S., 2005. Application of ion trap-MS with H/D exchange and QqTOF-MS in the identification of microbial degradates of trimethoprim in nitrifying activated sludge, *Analytical Chemistry*, vol. 77, pp. 4176–4184, doi:[10.1021/ac050141p](https://doi.org/10.1021/ac050141p).
- Escher, B.I., Fenner, K., 2011. Recent advances in environmental risk assessment of transformation products., *Environmental Science & Technology*, vol. 45, pp. 3835–47, doi:[10.1021/es1030799](https://doi.org/10.1021/es1030799).
- Escolà Casas, M., Chhetri, R.K., Ooi, G., Hansen, K.M.S., Litty, K., Christensson, M., Kragelund, C., Andersen, H.R., Bester, K., 2015. Biodegradation of pharma-

- ceuticals in hospital wastewater by staged moving bed biofilm reactors (MBBR), *Water Research*, vol. 83, pp. 293–302, doi:[10.1016/j.watres.2015.06.042](https://doi.org/10.1016/j.watres.2015.06.042).
- European Parliament and Council of the European Union, 2000. Directive 2000/60/EC of the European parliament and of the Council establishing a framework for community action in the field of water policy, Official Journal of the European Communities L 327/1.
- European Parliament and Council of the European Union, 2013. Council Directive 2013/39/EU amending directives 2000/60/EC and 2008/105/EC as regards priority substances in the field of water policy, Official Journal of the European Union L 226.
- Exner, M., Färber, H., 2006. Perfluorinated surfactants in surface and drinking waters, *Environmental Science and Pollution Research*, vol. 13, no. 5, pp. 299–307, doi:[10.1065/espr2006.07.326](https://doi.org/10.1065/espr2006.07.326).
- Falås, P., Longrée, P., la Cour Jansen, J., Siegrist, H., Hollender, J., Joss, A., 2013. Micropollutant removal by attached and suspended growth in a hybrid biofilm-activated sludge process, *Water Research*, vol. 47, no. 13, pp. 4498–4506, doi:[10.1016/j.watres.2013.05.010](https://doi.org/10.1016/j.watres.2013.05.010).
- Falås, P., Wick, A., Castronovo, S., Habermacher, J., Ternes, T.A., Joss, A., 2016. Tracing the limits of organic micropollutant removal in biological wastewater treatment, *Water Research*, vol. 95, pp. 240–249, doi:[10.1016/j.watres.2016.03.009](https://doi.org/10.1016/j.watres.2016.03.009).
- Fent, K., Weston, A.A., Caminada, D., 2006. Ecotoxicology of human pharmaceuticals, *Aquatic Toxicology*, vol. 76, no. 2, pp. 122–159, doi:[10.1016/j.aquatox.2005.09.009](https://doi.org/10.1016/j.aquatox.2005.09.009).
- Fernandez-Fontaina, E., Carballa, M., Omil, F., Lema, J.M., 2014. Modelling cometabolic biotransformation of organic micropollutants in nitrifying reactors, *Water Research*, vol. 65, pp. 371–383, doi:[10.1016/j.watres.2014.07.048](https://doi.org/10.1016/j.watres.2014.07.048).
- Ferrer-Sueta, G., Radi, R., 2009. Chemical biology of peroxyxynitrite: kinetics, diffusion, and radicals., *ACS Chemical Biology*, vol. 4, pp. 161–77, doi:[10.1021/cb800279q](https://doi.org/10.1021/cb800279q).

- Fetzner, S., 1998. Bacterial dehalogenation, *Applied Microbiology and Biotechnology*, vol. 50, pp. 633–657, doi:[10.1007/s002530051346](https://doi.org/10.1007/s002530051346).
- Fischer, K., Majewsky, M., 2014. Cometabolic degradation of organic wastewater micropollutants by activated sludge and sludge-inherent microorganisms, *Applied Microbiology and Biotechnology*, vol. 98, no. 15, pp. 6583–6597, doi:[10.1007/s00253-014-5826-0](https://doi.org/10.1007/s00253-014-5826-0).
- Garg, R., Kurup, A., Hansch, C., 2001. Comparative QSAR: on the toxicology of the phenolic OH moiety., *Critical Reviews in Toxicology*, vol. 31, pp. 223–45, doi:[10.1080/20014091111686](https://doi.org/10.1080/20014091111686).
- Gasser, G., Pankratov, I., Elhanany, S., Werner, P., Gun, J., Gelman, F., Lev, O., 2012. Field and laboratory studies of the fate and enantiomeric enrichment of venlafaxine and *O*-desmethylvenlafaxine under aerobic and anaerobic conditions., *Chemosphere*, vol. 88, pp. 98–105, doi:[10.1016/j.chemosphere.2012.02.074](https://doi.org/10.1016/j.chemosphere.2012.02.074).
- Gaulke, L.S., Strand, S.E., Kalhorn, T.F., Stensel, H.D., 2009. Estrogen nitration kinetics and implications for wastewater treatment, *Water Environment Research*, vol. 81, pp. 772–778, doi:[10.2175/106143009X407285](https://doi.org/10.2175/106143009X407285).
- Göbel, A., McArdell, C.S., Joss, A., Siegrist, H., Giger, W., 2007. Fate of sulfonamides, macrolides, and trimethoprim in different wastewater treatment technologies, *Science of The Total Environment*, vol. 372, no. 2–3, pp. 361–371, doi:[10.1016/j.scitotenv.2006.07.039](https://doi.org/10.1016/j.scitotenv.2006.07.039).
- Göbel, A., Thomsen, A., McArdell, C.S., Joss, A., Giger, W., 2005. Occurrence and sorption behavior of sulfonamides, macrolides, and trimethoprim in activated sludge treatment, *Environmental Science & Technology*, vol. 39, no. 11, pp. 3981–3989, doi:[10.1021/es048550a](https://doi.org/10.1021/es048550a).
- Goldstein, S., Russo, A., Samuni, A., 2003. Reactions of PTIO and carboxy-PTIO with $\cdot\text{NO}$, $\cdot\text{NO}_2$, and $\text{O}_2^{\cdot-}$., *The Journal of Biological Chemistry*, vol. 278, pp. 50 949–50 955, doi:[10.1074/jbc.M308317200](https://doi.org/10.1074/jbc.M308317200).
- Goyal, S., Hafez, A., 1995. Phosphate-catalyzed decomposition of nitrite to nitrate during freezing and thawing of solutions, *Journal of Agricultural and Food Chemistry*, vol. 43, pp. 2641–2645, doi:[10.1021/jf00058a016](https://doi.org/10.1021/jf00058a016).

- Gröning, J., Held, C., Garten, C., Claussnitzer, U., Kaschabek, S.R., Schlömann, M., 2007. Transformation of diclofenac by the indigenous microflora of river sediments and identification of a major intermediate., *Chemosphere*, vol. 69, pp. 509–516, doi:[10.1016/j.chemosphere.2007.03.037](https://doi.org/10.1016/j.chemosphere.2007.03.037).
- Grossi, L., Montevecchi, P.C., 2002. *S*-nitrosocysteine and cystine from reaction of cysteine with nitrous acid. a kinetic investigation., *The Journal of Organic Chemistry*, vol. 67, pp. 8625–8630, doi:[10.1021/jo026154+](https://doi.org/10.1021/jo026154+).
- Gulde, R., Meier, U., Schymanski, E.L., Kohler, H.P.E., Helbling, D.E., Derrer, S., Rentsch, D., Fenner, K., 2016. Systematic exploration of biotransformation reactions of amine-containing micropollutants in activated sludge, *Environmental Science & Technology*, vol. 50, no. 6, pp. 2908–2920, doi:[10.1021/acs.est.5b05186](https://doi.org/10.1021/acs.est.5b05186).
- Halling-Sørensen, B., Lützhøft, H.C.H., Andersen, H.R., Ingerslev, F., 2000. Environmental risk assessment of antibiotics: comparison of mecillinam, trimethoprim and ciprofloxacin, *Journal of Antimicrobial Chemotherapy*, vol. 46, pp. 53–58, doi:[10.1093/jac/46.suppl_1.53](https://doi.org/10.1093/jac/46.suppl_1.53).
- Hapeshi, E., Lambrianides, A., Koutsoftas, P., 2013. Investigating the fate of iodinated X-ray contrast media iohexol and diatrizoate during microbial degradation in an MBBR system treating urban wastewater, *Environmental Science and Pollution Research*, vol. 20, pp. 3592–3606, doi:[10.1007/s11356-013-1605-1](https://doi.org/10.1007/s11356-013-1605-1).
- Hebig, K.H., Nödler, K., Licha, T., Scheytt, T.J., 2014. Impact of materials used in lab and field experiments on the recovery of organic micropollutants, *Science of The Total Environment*, vol. 473–474, pp. 125–131, doi:[10.1016/j.scitotenv.2013.12.004](https://doi.org/10.1016/j.scitotenv.2013.12.004).
- Helbling, D.E., Hollender, J., Kohler, H.P.E., Singer, H., Fenner, K., 2010. High-throughput identification of microbial transformation products of organic micropollutants, *Environmental Science & Technology*, vol. 44, no. 17, pp. 6621–6627, doi:[10.1021/es100970m](https://doi.org/10.1021/es100970m).
- Helbling, D.E., Johnson, D.R., Honti, M., Fenner, K., 2012. Micropollutant biotransformation kinetics associate with wwtp process parameters and microbial community characteristics, *Environmental Science & Technology*, vol. 46, pp. 10 579–10 588, doi:[10.1021/es3019012](https://doi.org/10.1021/es3019012).

- Henneberg, A., Bender, K., Blaha, L., Giebner, S., Kuch, B., Köhler, H.R., Maier, D., Oehlmann, J., Richter, D., Scheurer, M., 2014. Are in vitro methods for the detection of endocrine potentials in the aquatic environment predictive for in vivo effects? Outcomes of the projects SchussenAktiv and SchussenAktiv plus in the Lake Constance area, Germany, *PloS one*, vol. 9, no. 6, p. e98307, doi:[10.1371/journal.pone.0098307](https://doi.org/10.1371/journal.pone.0098307).
- Hillenbrand, T., Tettenborn, F., Menger-Krug, E., Marscheider-Weidemann, F., Fuchs, S., Toshovski, S., Kittlaus, S., Metzger, S., Tjoeng, I., Wermter, P., Kersting, M., Abegglen, C., 2015. Measures to minimise the input of micropollutants in surface waters (in German), German Environment Agency (UBA), Dessau, Germany.
- Hirte, K., Seiwert, B., Schüürmann, G., Reemtsma, T., 2016. New hydrolysis products of the beta-lactam antibiotic amoxicillin, their pH-dependent formation and search in municipal wastewater, *Water Research*, vol. 88, pp. 880–888, doi:[10.1016/j.watres.2015.11.028](https://doi.org/10.1016/j.watres.2015.11.028).
- Hollender, J., Zimmermann, S.G., Koepke, S., Krauss, M., Mc Ardell, C.S., Ort, C., Singer, H., von Gunten, U., Siegrist, H., 2009. Elimination of organic micropollutants in a municipal wastewater treatment plant upgraded with a full-scale post-ozonation followed by sand filtration, *Environmental Science & Technology*, vol. 43, no. 20, pp. 7862–7869, doi:[10.1021/es9014629](https://doi.org/10.1021/es9014629).
- Houston, P.L., 2006. *Chemical kinetics and reaction dynamics*, Dover, Mineola, New York.
- Ike, M., Jin, C.S., Fujita, M., 2000. Biodegradation of bisphenol A in the aquatic environment, *Water Science and Technology*, vol. 42, no. 7–8, pp. 31–38.
- Jakoby, W.B., Ziegler, D.M., 1990. The enzymes of detoxication, *Journal of Biological Chemistry*, vol. 265, no. 34, pp. 20715–20718.
- Jewell, K.S., Castronovo, S., Wick, A., Falås, P., Joss, A., Ternes, T.A., 2016a. New insights into the transformation of trimethoprim during biological wastewater treatment, *Water Research*, vol. 88, pp. 550–557, doi:[10.1016/j.watres.2015.10.026](https://doi.org/10.1016/j.watres.2015.10.026).
- Jewell, K.S., Falås, P., Wick, A., Joss, A., Ternes, T.A., 2016b. Transformation

- of diclofenac in hybrid biofilm-activated sludge processes, *Water Research*, vol. 105, pp. 559–567, doi:[10.1016/j.watres.2016.08.002](https://doi.org/10.1016/j.watres.2016.08.002).
- Jewell, K.S., Wick, A., Ternes, T.A., 2014. Comparisons between abiotic nitration and biotransformation reactions of phenolic micropollutants in activated sludge, *Water Research*, vol. 48, pp. 478–489, doi:[10.1016/j.watres.2013.10.010](https://doi.org/10.1016/j.watres.2013.10.010).
- Johnson, D.R., Helbling, D.E., Lee, T.K., Park, J., Fenner, K., Kohler, H.P.E., Ackermann, M., 2015. Association of biodiversity with the rates of micropollutant biotransformations among full-scale wastewater treatment plant communities, *Applied and Environmental Microbiology*, vol. 81, no. 2, pp. 666–675, doi:[10.1128/aem.03286-14](https://doi.org/10.1128/aem.03286-14).
- Joss, A., Keller, E., Alder, A.C., Göbel, A., McArdell, C.S., Ternes, T., Siegrist, H., 2005. Removal of pharmaceuticals and fragrances in biological wastewater treatment., *Water Research*, vol. 39, pp. 3139–52, doi:[10.1016/j.watres.2005.05.031](https://doi.org/10.1016/j.watres.2005.05.031).
- Joss, A., Zabczynski, S., Göbel, A., Hoffmann, B., Löffler, D., McArdell, C.S., Ternes, T.A., Thomsen, A., Siegrist, H., 2006. Biological degradation of pharmaceuticals in municipal wastewater treatment: Proposing a classification scheme, *Water Research*, vol. 40, no. 8, pp. 1686–1696, doi:[10.1016/j.watres.2006.02.014](https://doi.org/10.1016/j.watres.2006.02.014).
- Kaiser, E., Prasse, C., Wagner, M., Bröder, K., Ternes, T.A., 2014. Transformation of oxcarbazepine and human metabolites of carbamazepine and oxcarbazepine in wastewater treatment and sand filters, *Environmental Science & Technology*, vol. 48, no. 17, pp. 10 208–10 216, doi:[10.1021/es5024493](https://doi.org/10.1021/es5024493).
- Kassotaki, E., Buttiglieri, G., Ferrando-Climent, L., Rodriguez-Roda, I., Pijuan, M., 2016. Enhanced sulfamethoxazole degradation through ammonia oxidizing bacteria co-metabolism and fate of transformation products, *Water Research*, vol. 94, pp. 111–119, doi:[10.1016/j.watres.2016.02.022](https://doi.org/10.1016/j.watres.2016.02.022).
- Kern, S., Fenner, K., Singer, H.P., Schwarzenbach, R.P., Hollender, J., 2009. Identification of transformation products of organic contaminants in natural waters by computer-aided prediction and high-resolution mass spectrometry, *Environmental Science & Technology*, vol. 43, no. 18, pp. 7039–7046, doi:[10.1021/es901979h](https://doi.org/10.1021/es901979h).
- Khalafi, L., Rafiee, M., 2010. Kinetic study of the oxidation and nitration of cat-

- echols in the presence of nitrous acid ionization equilibria, *Journal of Hazardous Materials*, vol. 174, pp. 801–806, doi:[10.1016/j.jhazmat.2009.09.123](https://doi.org/10.1016/j.jhazmat.2009.09.123).
- Khan, S.J., Wang, L., Hashim, N.H., McDonald, J.A., 2014. Distinct enantiomeric signals of ibuprofen and naproxen in treated wastewater and sewer overflow, *Chirality*, vol. 26, no. 11, pp. 739–746, doi:[10.1002/chir.22258](https://doi.org/10.1002/chir.22258).
- Khunjar, W.O., Love, N.G., 2011. Sorption of carbamazepine, 17 alpha-ethinylestradiol, iopromide and trimethoprim to biomass involves interactions with exocellular polymeric substances, *Chemosphere*, vol. 82, no. 6, pp. 917–922, doi:[10.1016/j.chemosphere.2010.10.046](https://doi.org/10.1016/j.chemosphere.2010.10.046).
- Khunjar, W.O., Mackintosh, S.a., Skotnicka-Pitak, J., Baik, S., Aga, D.S., Love, N.G., 2011. Elucidating the relative roles of ammonia oxidizing and heterotrophic bacteria during the biotransformation of 17 α -ethinylestradiol and trimethoprim, *Environmental Science & Technology*, vol. 45, pp. 3605–12, doi:[10.1021/es1037035](https://doi.org/10.1021/es1037035).
- Kleeschulte, P., Schafer, O., Klung, M., Puttmann, A., 2007. Erfahrungen eines Gesundheitsamtes bei der Belastung von Trinkwasser durch perfluorierte Tenside (PFT), *Umweltmedizin in Forschung und Praxis*, vol. 12, no. 2, p. 73.
- Kohler, H.P.E., Kohler-Staub, D., Focht, D.D., 1988. Degradation of 2-hydroxybiphenyl and 2,2'-dihydroxybiphenyl by *Pseudomonas* sp. strain HBP1, *Applied and Environmental Microbiology*, vol. 54, no. 11, pp. 2683–2688.
- König, A., Weidauer, C., Seiwert, B., Reemtsma, T., Unger, T., Jekel, M., 2016. Reductive transformation of carbamazepine by abiotic and biotic processes, *Water Research*, vol. 101, pp. 272–280, doi:[10.1016/j.watres.2016.05.084](https://doi.org/10.1016/j.watres.2016.05.084).
- Kormos, J.L., Schulz, M., Ternes, T.a., 2011. Occurrence of iodinated X-ray contrast media and their biotransformation products in the urban water cycle., *Environmental Science & Technology*, vol. 45, no. 20, pp. 8723–8732, doi:[10.1021/es2018187](https://doi.org/10.1021/es2018187).
- Kortenkamp, A., 2007. Ten years of mixing cocktails: A review of combination effects of endocrine-disrupting chemicals, *Environmental Health Perspectives*, vol. 115, no. Suppl 1, pp. 98–105, doi:[10.1289/ehp.9357](https://doi.org/10.1289/ehp.9357).
- Kosjek, T., Heath, E., Pérez, S., Petrović, M., Barceló, D., 2009. Metabolism

- studies of diclofenac and clofibrac acid in activated sludge bioreactors using liquid chromatography with quadrupole – time-of-flight mass spectrometry, *Journal of Hydrology*, vol. 372, no. 1–4, pp. 109–117, doi:[10.1016/j.jhydrol.2009.04.006](https://doi.org/10.1016/j.jhydrol.2009.04.006).
- Kosjek, T., Negreira, N., de Alda, M.L., Barceló, D., 2015. Aerobic activated sludge transformation of methotrexate: Identification of biotransformation products, *Chemosphere*, vol. 119 Suppl., pp. S42–S50, doi:[10.1016/j.chemosphere.2014.04.081](https://doi.org/10.1016/j.chemosphere.2014.04.081).
- Kovalova, L., Siegrist, H., Singer, H., Wittmer, A., McArdell, C.S., 2012. Hospital wastewater treatment by membrane bioreactor: Performance and efficiency for organic micropollutant elimination, *Environmental Science & Technology*, vol. 46, no. 3, pp. 1536–1545, doi:[10.1021/es203495d](https://doi.org/10.1021/es203495d).
- Kumar, V., Johnson, A.C., Nakada, N., Yamashita, N., Tanaka, H., 2012. Deconjugation behavior of conjugated estrogens in the raw sewage, activated sludge and river water, *Journal of hazardous materials*, vol. 227–228, pp. 49–54, doi:[10.1016/j.jhazmat.2012.04.078](https://doi.org/10.1016/j.jhazmat.2012.04.078).
- Lambropoulou, D.A., Nollet, L.M. (eds.), 2014. *Transformation products of emerging contaminants in the environment: Analysis, processes, occurrence, effects and risks*, John Wiley & Sons, Chichester, UK.
- Le-Minh, N., Khan, S.J., Drewes, J.E., Stuetz, R.M., 2010. Fate of antibiotics during municipal water recycling treatment processes, *Water Research*, vol. 44, no. 15, pp. 4295–4323, doi:[10.1016/j.watres.2010.06.020](https://doi.org/10.1016/j.watres.2010.06.020).
- Lee, H.J., Lee, E., Yoon, S.H., Chang, H.R., Kim, K., Kwon, J.H., 2012. Enzymatic and microbial transformation assays for the evaluation of the environmental fate of diclofenac and its metabolites, *Chemosphere*, vol. 87, no. 8, pp. 969–974, doi:[10.1016/j.chemosphere.2012.02.018](https://doi.org/10.1016/j.chemosphere.2012.02.018).
- Lindberg, R.H., Olofsson, U., Rendahl, P., Johansson, M.I., Tysklind, M., Andersson, B.A.V., 2006. Behavior of fluoroquinolones and trimethoprim during mechanical, chemical, and active sludge treatment of sewage water and digestion of sludge, *Environmental Science & Technology*, vol. 40, no. 3, pp. 1042–1048, doi:[10.1021/es0516211](https://doi.org/10.1021/es0516211).
- Lindsay, R., Priest, F., 1975. Decarboxylation of substituted cinnamic acids by

- enterobacteria: the influence on beer flavour, *Journal of Applied Bacteriology*, vol. 39, no. 2, pp. 181–187.
- Luo, Y., Guo, W., Ngo, H.H., Nghiem, L.D., Hai, F.I., Zhang, J., Liang, S., Wang, X.C., 2014. A review on the occurrence of micropollutants in the aquatic environment and their fate and removal during wastewater treatment, *Science of The Total Environment*, vol. 473–474, pp. 619–641, doi:[10.1016/j.scitotenv.2013.12.065](https://doi.org/10.1016/j.scitotenv.2013.12.065).
- Machatha, S.G., Yalkowsky, S.H., 2005. Comparison of the octanol/water partition coefficients calculated by ClogP, ACDlogP and KowWin to experimentally determined values, *International Journal of Pharmaceutics*, vol. 294, no. 1–2, pp. 185 – 192, doi:<http://dx.doi.org/10.1016/j.ijpharm.2005.01.023>.
- Magdeburg, A., Stalter, D., Schlüsener, M., Ternes, T., Oehlmann, J., 2014. Evaluating the efficiency of advanced wastewater treatment: Target analysis of organic contaminants and (geno-) toxicity assessment tell a different story, *Water Research*, vol. 50, pp. 35–47, doi:[10.1016/j.watres.2013.11.041](https://doi.org/10.1016/j.watres.2013.11.041).
- Malaj, E., von der Ohe, P.C., Grote, M., Kühne, R., Mondy, C.P., Usseglio-Polatera, P., Brack, W., Schäfer, R.B., 2014. Organic chemicals jeopardize the health of freshwater ecosystems on the continental scale, *Proceedings of the National Academy of Sciences*, vol. 111, no. 26, pp. 9549–9554, doi:[10.1073/pnas.1321082111](https://doi.org/10.1073/pnas.1321082111).
- Malojčić, G., Glockshuber, R., 2010. The paps-independent aryl sulfotransferase and the alternative disulfide bond formation system in pathogenic bacteria, *Antioxidants and Redox Signaling*, vol. 13, pp. 1247–59, doi:[10.1089/ars.2010.3119](https://doi.org/10.1089/ars.2010.3119).
- Margot, J., Rossi, L., Barry, D.A., Holliger, C., 2015. A review of the fate of micropollutants in wastewater treatment plants, *Wiley Interdisciplinary Reviews: Water*, vol. 2, no. 5, pp. 457–487, doi:[10.1002/wat2.1090](https://doi.org/10.1002/wat2.1090).
- Marti, E., Variatza, E., Luis Balcazar, J., 2014. The role of aquatic ecosystems as reservoirs of antibiotic resistance, *Trends in Microbiology*, vol. 22, no. 1, pp. 36–41, doi:[10.1016/j.tim.2013.11.001](https://doi.org/10.1016/j.tim.2013.11.001).
- Matsuno, T., Matsukawa, T., Yoshirharu, S., Kunieda, T., 1989. A new nitration

- product, 3-nitro-4-acetamidophenol, obtained from acetaminophen with nitrous acid, *Chemical and Pharmaceutical Bulletin*, vol. 37, pp. 1422–1423.
- Mazioti, A.A., Stasinakis, A.S., Psoma, A.K., Thomaidis, N.S., Andersen, H.R., 2016. Hybrid moving bed biofilm reactor for the biodegradation of benzotriazoles and hydroxy-benzothiazole in wastewater, *Journal of Hazardous Materials*, p. in press, doi:[10.1016/j.jhazmat.2016.06.035](https://doi.org/10.1016/j.jhazmat.2016.06.035).
- McPherson, M.B., Schneider, W.J., 1974. Problems in modeling urban watersheds, *Water Resources Research*, vol. 10, no. 3, pp. 434–440, doi:[10.1029/WR010i003p00434](https://doi.org/10.1029/WR010i003p00434).
- Meckenstock, R.U., Safinowski, M., Griebler, C., 2004. Anaerobic degradation of polycyclic aromatic hydrocarbons, *FEMS Microbiology Ecology*, vol. 49, no. 1, pp. 27–36, doi:[10.1016/j.femsec.2004.02.019](https://doi.org/10.1016/j.femsec.2004.02.019).
- Melvin, S.D., Leusch, F.D., 2016. Removal of trace organic contaminants from domestic wastewater: A meta-analysis comparison of sewage treatment technologies, *Environment International*, vol. 92, pp. 183–188, doi:[10.1016/j.envint.2016.03.031](https://doi.org/10.1016/j.envint.2016.03.031).
- Metcalf, C.D., Chu, S., Judt, C., Li, H., Oakes, K.D., Servos, M.R., Andrews, D.M., 2010. Antidepressants and their metabolites in municipal wastewater, and downstream exposure in an urban watershed., *Environmental Toxicology and Chemistry*, vol. 29, pp. 79–89, doi:[10.1002/etc.27](https://doi.org/10.1002/etc.27).
- Michael, I., Hapeshi, E., Osorio, V., Perez, S., Petrovic, M., Zapata, A., Malato, S., Barceló, D., Fatta-Kassinos, D., 2012. Solar photocatalytic treatment of trimethoprim in four environmental matrices at a pilot scale: Transformation products and ecotoxicity evaluation, *Science of The Total Environment*, vol. 430, pp. 167–173, doi:[10.1016/j.scitotenv.2012.05.003](https://doi.org/10.1016/j.scitotenv.2012.05.003).
- Miller, T.R., Heidler, J., Chillrud, S.N., DeLaquil, A., Ritchie, J.C., Mihalic, J.N., Bopp, R., Halden, R.U., 2008. Fate of triclosan and evidence for reductive dechlorination of triclocarban in estuarine sediments, *Environmental Science & Technology*, vol. 42, no. 12, pp. 4570–4576, doi:[10.1021/es702882g](https://doi.org/10.1021/es702882g).
- Ministry for Climate Protection, 2014. *Programm Reine Ruhr zur Strategie einer nachhaltigen Verbesserung der Gewässer- und Trinkwasserqualität in Nordrhein-*

- Westfalen*, Ministry for Climate Protection, Environment, Agriculture, Conservation and Consumer Protection of North Rhein-Westfalia, Düsseldorf.
- Murata, A., Takada, H., Mutoh, K., Hosoda, H., Harada, A., Nakada, N., 2011. Nationwide monitoring of selected antibiotics: Distribution and sources of sulfonamides, trimethoprim, and macrolides in Japanese rivers, *Science of The Total Environment*, vol. 409, no. 24, pp. 5305–5312, doi:[10.1016/j.scitotenv.2011.09.014](https://doi.org/10.1016/j.scitotenv.2011.09.014).
- Neilson, A.H., Allard, A.S., 2007. *Degradation and transformation of organic chemicals*, CRC Press, Boca Raton, Florida.
- Nguyen, L.A., He, H., Pham-Huy, C., 2006. Chiral drugs: An overview, *International Journal of Biomedical Science*, vol. 2, no. 2, pp. 85–100.
- Noble, D.R., Williams, D.L.H., 2002. Nitrosation products from *S*-nitrosothiols via preliminary nitric oxide formation, *Journal of the Chemical Society, Perkin Transactions 2*, vol. -, no. 11, pp. 1834–1838, doi:[10.1039/b206854k](https://doi.org/10.1039/b206854k).
- Nödler, K., Licha, T., Barbieri, M., Pérez, S., 2012. Evidence for the microbially mediated abiotic formation of reversible and non-reversible sulfamethoxazole transformation products during denitrification., *Water Research*, vol. 46, pp. 2131–2139, doi:[10.1016/j.watres.2012.01.028](https://doi.org/10.1016/j.watres.2012.01.028).
- Nödler, K., Licha, T., Bester, K., Sauter, M., 2010. Development of a multi-residue analytical method, based on liquid chromatography-tandem mass spectrometry, for the simultaneous determination of 46 micro-contaminants in aqueous samples., *Journal of Chromatography A*, vol. 1217, pp. 6511–6521, doi:[10.1016/j.chroma.2010.08.048](https://doi.org/10.1016/j.chroma.2010.08.048).
- Noguera-Oviedo, K., Aga, D.S., 2016. Lessons learned from more than two decades of research on emerging contaminants in the environment, *Journal of Hazardous Materials*, vol. 316, pp. 242–251, doi:[10.1016/j.jhazmat.2016.04.058](https://doi.org/10.1016/j.jhazmat.2016.04.058).
- Nürenberg, G., Schulz, M., Kunkel, U., Ternes, T.A., 2015. Development and validation of a generic nontarget method based on liquid chromatography – high resolution mass spectrometry analysis for the evaluation of different wastewater treatment options, *Journal of Chromatography A*, vol. 1426, pp. 77–90, doi:[10.1016/j.chroma.2015.11.014](https://doi.org/10.1016/j.chroma.2015.11.014).

- Oaks, J.L., Gilbert, M., Virani, M.Z., Watson, R.T., Meteyer, C.U., Rideout, B.A., Shivaprasad, H.L., Ahmed, S., Iqbal Chaudhry, M.J., Arshad, M., Mahmood, S., Ali, A., Ahmed Khan, A., 2004. Diclofenac residues as the cause of vulture population decline in Pakistan, *Nature*, vol. 427, no. 6975, pp. 630–633, doi:[10.1038/nature02317](https://doi.org/10.1038/nature02317).
- Oehlmann, J., Schulte-Oehlmann, U., Bachmann, J., Oetken, M., Lutz, I., Kloas, W., Ternes, T.A., 2006. Bisphenol A induces superfeminization in the ramshorn snail (gastropoda: Prosobranchia) at environmentally relevant concentrations, *Environmental Health Perspectives*, vol. 114, pp. 127–133, doi:[10.1289/ehp.8065](https://doi.org/10.1289/ehp.8065).
- Park, J., Lee, Y.N., 1988. Solubility and decomposition kinetics of nitrous acid in aqueous solution, *The Journal of Physical Chemistry*, vol. 92, pp. 6294–6302, doi:[10.1021/j100333a025](https://doi.org/10.1021/j100333a025).
- Patiny, L., Borel, A., 2013. Chemcalc: A building block for tomorrow's chemical infrastructure, *Journal of Chemical Information and Modeling*, vol. 53, no. 5, pp. 1223–1228, doi:[10.1021/ci300563h](https://doi.org/10.1021/ci300563h).
- Patrolecco, L., Capri, S., Ademollo, N., 2015. Occurrence of selected pharmaceuticals in the principal sewage treatment plants in rome (Italy) and in the receiving surface waters, *Environmental Science and Pollution Research*, vol. 22, no. 8, pp. 5864–5876, doi:[10.1007/s11356-014-3765-z](https://doi.org/10.1007/s11356-014-3765-z).
- Pence, H.E., Williams, A., 2010. Chemspider: An online chemical information resource, *Journal of Chemical Education*, vol. 87, no. 11, pp. 1123–1124, doi:[10.1021/ed100697w](https://doi.org/10.1021/ed100697w).
- Pérez, S., Barceló, D., 2008. First evidence for occurrence of hydroxylated human metabolites of diclofenac and aceclofenac in wastewater using QqLIT-MS and QqTOF-MS, *Analytical Chemistry*, vol. 80, no. 21, pp. 8135–45, doi:[10.1021/ac801167w](https://doi.org/10.1021/ac801167w).
- Petrie, B., Barden, R., Kasprzyk-Hordern, B., 2015. A review on emerging contaminants in wastewaters and the environment: Current knowledge, understudied areas and recommendations for future monitoring, *Water Research*, vol. 72, pp. 3–27, doi:[10.1016/j.watres.2014.08.053](https://doi.org/10.1016/j.watres.2014.08.053).
- Poirier-Larabie, S., Segura, P., Gagnon, C., 2016. Degradation of the pharmaceut-

- icals diclofenac and sulfamethoxazole and their transformation products under controlled environmental conditions, *Science of The Total Environment*, vol. 557–558, pp. 257–267, doi:[10.1016/j.scitotenv.2016.03.057](https://doi.org/10.1016/j.scitotenv.2016.03.057).
- Poon, G.K., Chen, Q., Teffera, Y., Ngui, J.S., Griffin, P.R., Braun, M.P., Doss, G.A., Freeden, C., Stearns, R.A., Evans, D.C., Baillie, T.A., Tang, W., 2001. Bioactivation of diclofenac via benzoquinone imine intermediates-identification of urinary mercapturic acid derivatives in rats and humans, *Drug Metabolism and Disposition*, vol. 29, no. 12, pp. 1608–1613.
- Prasse, C., Wagner, M., Schulz, R., Ternes, T.A., 2011. Biotransformation of the antiviral drugs acyclovir and penciclovir in activated sludge treatment, *Environmental Science & Technology*, vol. 45, pp. 2761–2769, doi:[10.1021/es103732y](https://doi.org/10.1021/es103732y).
- Quintana, J.B., Weiss, S., Reemtsma, T., 2005. Pathways and metabolites of microbial degradation of selected acidic pharmaceutical and their occurrence in municipal wastewater treated by a membrane bioreactor, *Water Research*, vol. 39, no. 12, pp. 2654–2664, doi:[10.1016/j.watres.2005.04.068](https://doi.org/10.1016/j.watres.2005.04.068).
- R Core Team, 2015. *R: A Language and Environment for Statistical Computing*, R Foundation for Statistical Computing, Vienna, Austria.
- Radjenović, J., Petrović, M., Barceló, D., 2009. Fate and distribution of pharmaceuticals in wastewater and sewage sludge of the conventional activated sludge (cas) and advanced membrane bioreactor (mbr) treatment., *Water Research*, vol. 43, pp. 831–841, doi:[10.1016/j.watres.2008.11.043](https://doi.org/10.1016/j.watres.2008.11.043).
- Randall, C.W., Buth, D., 1984. Nitrite build-up in activated sludge resulting from temperature effects, *Journal (Water Pollution Control Federation)*, vol. 56, pp. 1039–1044.
- Reemtsma, T., Jekel, M., 1997. Dissolved organics in tannery wastewaters and aerobic treatment, *Water Research*, vol. 31, no. 5, pp. 1035–1046, doi:[10.1016/S0043-1354\(96\)00382-X](https://doi.org/10.1016/S0043-1354(96)00382-X).
- Reineke, W., 2001. Aerobic and anaerobic biodegradation potentials of microorganisms, in: B. Beek (ed.), *Biodegradation and Persistence*, vol. 2/2K of *The Handbook of Environmental Chemistry*, pp. 1–160, Springer Verlag, Berlin, Heidelberg, doi:[10.1007/10508767_1](https://doi.org/10.1007/10508767_1).

- Ridd, J., 1991. The range of radical processes in nitration by nitric acid, *Chemical Society Reviews*, vol. 20, pp. 149–165, doi:[10.1039/CS9912000149](https://doi.org/10.1039/CS9912000149).
- Roberts, P.H., Thomas, K.V., 2006. The occurrence of selected pharmaceuticals in wastewater effluent and surface waters of the lower tyne catchment, *Science of The Total Environment*, vol. 356, no. 1–3, pp. 143–153, doi:[10.1016/j.scitotenv.2005.04.031](https://doi.org/10.1016/j.scitotenv.2005.04.031).
- Rubirola, A., Llorca, M., Rodriguez-Mozaz, S., Casas, N., Rodriguez-Roda, I., Barceló, D., Buttiglieri, G., 2014. Characterization of metoprolol biodegradation and its transformation products generated in activated sludge batch experiments and in full scale WWTPs, *Water Research*, vol. 63, pp. 21–32, doi:[10.1016/j.watres.2014.05.031](https://doi.org/10.1016/j.watres.2014.05.031).
- Rudel, R.A., Melly, S.J., Geno, P.W., Sun, G., Brody, J.G., 1998. Identification of alkylphenols and other estrogenic phenolic compounds in wastewater, septage, and groundwater on Cape Cod, Massachusetts, *Environmental Science & Technology*, vol. 32, no. 7, pp. 861–869, doi:[10.1021/es970723r](https://doi.org/10.1021/es970723r).
- Sangster, J., 1997. *Octanol-water partition coefficients : fundamentals and physical chemistry*, John Wiley & Sons, Chichester, UK.
- Sarda, S., Page, C., Pickup, K., Schulz-Utermoehl, T., Wilson, I., 2012. Diclofenac metabolism in the mouse: Novel in vivo metabolites identified by high performance liquid chromatography coupled to linear ion trap mass spectrometry, *Xenobiotica*, vol. 42, no. 2, pp. 179–194, doi:[10.3109/00498254.2011.607865](https://doi.org/10.3109/00498254.2011.607865).
- Schlüsener, M.P., Kunkel, U., Ternes, T.A., 2015. Quaternary triphenylphosphonium compounds: A new class of environmental pollutants, *Environmental Science & Technology*, vol. 49, no. 24, pp. 14282–14291, doi:[10.1021/acs.est.5b03926](https://doi.org/10.1021/acs.est.5b03926).
- Schmidt, S., Wittich, R.M., Fortnagel, P., Erdmann, D., Francke, W., 1992. Metabolism of 3-methyldiphenyl ether by *Sphingomonas* sp. SS31, *FEMS Microbiology Letters*, vol. 96, no. 2-3, pp. 253–258, doi:[10.1111/j.1574-6968.1992.tb05426.x](https://doi.org/10.1111/j.1574-6968.1992.tb05426.x).
- Schwarzenbach, R.P., Gschwend, P.M., Imboden, D.M., 2005. *Environmental*

- Organic Chemistry*, John Wiley & Sons, Inc., Hoboken, New Jersey, doi:[10.1002/0471649643.ch17](https://doi.org/10.1002/0471649643.ch17).
- Schymanski, E.L., Jeon, J., Gulde, R., Fenner, K., Ruff, M., Singer, H.P., Hollender, J., 2014. Identifying small molecules via high resolution mass spectrometry: Communicating confidence, *Environmental Science & Technology*, vol. 48, no. 4, pp. 2097–2098, doi:[10.1021/es5002105](https://doi.org/10.1021/es5002105).
- Seitz, S., Boelsterli, U.A., 1998. Diclofenac acyl glucuronide, a major biliary metabolite, is directly involved in small intestinal injury in rats, *Gastroenterology*, vol. 115, no. 6, pp. 1476–1482, doi:[10.1016/S0016-5085\(98\)70026-5](https://doi.org/10.1016/S0016-5085(98)70026-5).
- Sengupta, A., Lyons, J.M., Smith, D.J., Drewes, J.E., Snyder, S.A., Heil, A., Maruya, K.A., 2014. The occurrence and fate of chemicals of emerging concern in coastal urban rivers receiving discharge of treated municipal wastewater effluent, *Environmental Toxicology and Chemistry*, vol. 33, no. 2, pp. 350–358, doi:[10.1002/etc.2457](https://doi.org/10.1002/etc.2457).
- Sigel, C.W., Kunin, C.M., Grace, M.E., Nichol, C.A., 1973. Metabolism of trimethoprim in man and measurement of a new metabolite: a new fluorescence assay, *Journal of Infectious Diseases*, vol. 128, no. 3 Suppl., pp. S580–S583, doi:[10.1093/infdis/128.Supplement_3.S580](https://doi.org/10.1093/infdis/128.Supplement_3.S580).
- Singhal, N., Perez-Garcia, O., 2016. Degrading organic micropollutants: The next challenge in the evolution of biological wastewater treatment processes, *Frontiers in Environmental Science*, vol. 4, p. 36.
- Skotnicka-Pitak, J., Garcia, E., Pitak, M., Aga, D., 2008. Identification of the transformation products of 17α -ethinylestradiol and 17β -estradiol by mass spectrometry and other instrumental techniques, *TrAC Trends in Analytical Chemistry*, vol. 27, pp. 1036–1052, doi:[10.1016/j.trac.2008.10.003](https://doi.org/10.1016/j.trac.2008.10.003).
- Skutlarek, D., Exner, M., Färber, H., 2006. Perfluorierte Tenside (PFT) in der aquatischen Umwelt und im Trinkwasser, *Umweltwissenschaften und Schadstoff-Forschung*, vol. 18, no. 3, pp. 151–154, doi:[10.1065/uwsf2006.07.128](https://doi.org/10.1065/uwsf2006.07.128).
- Souchier, M., Benali-Raclot, D., Casellas, C., Ingrand, V., Chiron, S., 2016a. Enantiomeric fractionation as a tool for quantitative assessment of biode-

- gradation: The case of metoprolol, *Water Research*, vol. 95, pp. 19–26, doi:[10.1016/j.watres.2016.03.010](https://doi.org/10.1016/j.watres.2016.03.010).
- Souchier, M., Casellas, C., Ingrand, V., Chiron, S., 2016b. Insights into reductive dechlorination of triclocarban in river sediments: Field measurements and in vitro mechanism investigations, *Chemosphere*, vol. 144, pp. 425–432, doi:[10.1016/j.chemosphere.2015.08.083](https://doi.org/10.1016/j.chemosphere.2015.08.083).
- Stevens-Garmon, J., Drewes, J.E., Khan, S.J., McDonald, J.A., Dickenson, E.R.V., 2011. Sorption of emerging trace organic compounds onto wastewater sludge solids, *Water Research*, vol. 45, no. 11, pp. 3417–3426, doi:[10.1016/j.watres.2011.03.056](https://doi.org/10.1016/j.watres.2011.03.056).
- Stierlin, H., Faigle, J.W., Sallmann, A., Küng, W., Richter, W.J., Kriemler, H.P., Alt, K.O., Winkler, T., 1979. Biotransformation of diclofenac sodium (Voltaren) in animals and in man. I. isolation and identification of principal metabolites, *Xenobiotica*, vol. 9, no. 10, pp. 601–610, doi:[10.3109/00498257909042327](https://doi.org/10.3109/00498257909042327).
- Stülten, D., Zühlke, S., Lamshöft, M., Spiteller, M., 2008. Occurrence of diclofenac and selected metabolites in sewage effluents, *Science of The Total Environment*, vol. 405, pp. 310–316, doi:[10.1016/j.scitotenv.2008.05.036](https://doi.org/10.1016/j.scitotenv.2008.05.036).
- Su, L., Aga, D., Chandran, K., Khunjar, W.O., 2015. Factors impacting biotransformation kinetics of trace organic compounds in lab-scale activated sludge systems performing nitrification and denitrification, *Journal of Hazardous Materials*, vol. 282, pp. 116–124, doi:[10.1016/j.jhazmat.2014.08.007](https://doi.org/10.1016/j.jhazmat.2014.08.007).
- Sun, Q., Li, Y., Chou, P.H., Peng, P.Y., Yu, C.P., 2012. Transformation of bisphenol a and alkylphenols by ammonia-oxidizing bacteria through nitration., *Environmental Science & Technology*, vol. 46, pp. 4442–4448, doi:[10.1021/es204424t](https://doi.org/10.1021/es204424t).
- Sundaramurthi, P., Shalaev, E., Suryanarayanan, R., 2010. "pH swing" in frozen solutions—consequence of sequential crystallization of buffer components, *The Journal of Physical Chemistry Letters*, vol. 1, no. 1, pp. 265–268, doi:[10.1021/jz900164q](https://doi.org/10.1021/jz900164q).
- Suzuki, J., Sato, T., Ito, a., Suzuki, S., 1990. Mutagen formation and nitration by exposure of phenylphenols to sunlight in water containing nitrate or nitrite ion.,

- Bulletin of Environmental Contamination and Toxicology*, vol. 45, pp. 516–522, doi:[10.1007/BF01700623](https://doi.org/10.1007/BF01700623).
- Svan, A., Hedeland, M., Arvidsson, T., Jasper, J.T., Sedlak, D.L., Pettersson, C.E., 2016. Identification of transformation products from β -blocking agents formed in wetland microcosms using LC-Q-ToF, *Journal of Mass Spectrometry*, vol. 51, no. 3, pp. 207–218, doi:[10.1002/jms.3737](https://doi.org/10.1002/jms.3737).
- Swain, M., 2012. chemicalize.org, *Journal of Chemical Information and Modeling*, vol. 52, no. 2, pp. 613–615, doi:[10.1021/ci300046g](https://doi.org/10.1021/ci300046g).
- Ternes, T.A., Joss, A. (eds.), 2006. *Human pharmaceuticals, hormones and fragrances a challenge for urban water management*, IWA Publishing, London.
- The European Commission, 2012. Proposal for a directive of the European Parliament and of the Council amending directives 2000/60/EC and 2008/105/EC as regards priority substances in the field of water policy.
- Thurman, E.M., Ferrer, I., 2012. Liquid chromatography/quadrupole-time-of-flight mass spectrometry with metabolic profiling of human urine as a tool for environmental analysis of dextromethorphan., *Journal of Chromatography. A*, vol. 1259, pp. 158–566, doi:[10.1016/j.chroma.2012.03.008](https://doi.org/10.1016/j.chroma.2012.03.008).
- Tomei, M.C., Annesini, M.C., Luberti, R., Cento, G., Senia, A., 2003. Kinetics of 4-nitrophenol biodegradation in a sequencing batch reactor., *Water Research*, vol. 37, pp. 3803–3814, doi:[10.1016/S0043-1354\(03\)00297-5](https://doi.org/10.1016/S0043-1354(03)00297-5).
- Topp, E., Hendel, J.G., Lapen, D.R., Chapman, R., 2008. Fate of the nonsteroidal anti-inflammatory drug naproxen in agricultural soil receiving liquid municipal biosolids, *Environmental Toxicology and Chemistry*, vol. 27, no. 10, pp. 2005–2010, doi:[10.1897/07-644.1](https://doi.org/10.1897/07-644.1).
- Toyoizumi, T., Deguchi, Y., Masuda, S., Kinae, N., 2008. Genotoxicity and estrogenic activity of 3,3'-dinitrobisphenol A in goldfish, *Bioscience, Biotechnology, and Biochemistry*, vol. 72, pp. 2118–2123, doi:[10.1271/bbb.80193](https://doi.org/10.1271/bbb.80193).
- Tran, N.H., Urase, T., Kusakabe, O., 2009. The characteristics of enriched nitrifier culture in the degradation of selected pharmaceutically active compounds, *Journal of Hazardous Materials*, vol. 171, no. 1–3, pp. 1051–1057, doi:[10.1016/j.jhazmat.2009.06.114](https://doi.org/10.1016/j.jhazmat.2009.06.114).

- Triebskorn, R., Casper, H., Heyd, A., Eikemper, R., Köhler, H.R., Schwaiger, J., 2004. Toxic effects of the non-steroidal anti-inflammatory drug diclofenac: Part II. Cytological effects in liver, kidney, gills and intestine of rainbow trout (*Oncorhynchus mykiss*), *Aquatic Toxicology*, vol. 68, no. 2, pp. 151 – 166, doi:[10.1016/j.aquatox.2004.03.015](https://doi.org/10.1016/j.aquatox.2004.03.015).
- Udert, K.M., Larsen, T.a., Gujer, W., 2005. Chemical nitrite oxidation in acid solutions as a consequence of microbial ammonium oxidation., *Environmental Science & Technology*, vol. 39, pp. 4066–4075.
- UN General Assembly, 2015. *Transforming our world: the 2030 Agenda for Sustainable Development. Resolution adopted by the General Assembly on 25 September 2015*, no. A/RES/70/1, United Nations, New York.
- Urase, T., Kikuta, T., 2005. Separate estimation of adsorption and degradation of pharmaceutical substances and estrogens in the activated sludge process, *Water Research*, vol. 39, no. 7, pp. 1289–1300, doi:[10.1016/j.watres.2005.01.015](https://doi.org/10.1016/j.watres.2005.01.015).
- van Beek, S., Priest, F.G., 2000. Decarboxylation of substituted cinnamic acids by lactic acid bacteria isolated during malt whisky fermentation, *Applied and Environmental Microbiology*, vol. 66, no. 12, pp. 5322–5328.
- van Dongen, U., Jetten, M.S.M., van Loosdrecht, M.C.M., 2001. The Sharon–Anammox process for treatment of ammonium rich wastewater, *Water Science and Technology*, vol. 44, pp. 153–160.
- Verlicchi, P., Zambello, E., Al Aukidy, M., 2012. Occurrence of pharmaceutical compounds in urban wastewater: removal, mass load and environmental risk after a secondary treatment—a review., *Science of the Total Environment*, vol. 429, pp. 123–155, doi:[10.1016/j.scitotenv.2012.04.028](https://doi.org/10.1016/j.scitotenv.2012.04.028).
- Vieno, N., Sillanpää, M., 2014. Fate of diclofenac in municipal wastewater treatment plant - a review, *Environment International*, vol. 69, pp. 28–39, doi:[10.1016/j.envint.2014.03.021](https://doi.org/10.1016/j.envint.2014.03.021).
- Vione, D., Belmondo, S., Carnino, L., 2004a. A kinetic study of phenol nitration and nitrosation with nitrous acid in the dark, *Environmental Chemistry Letters*, vol. 2, no. 3, pp. 135–139, doi:[10.1007/s10311-004-0088-1](https://doi.org/10.1007/s10311-004-0088-1).
- Vione, D., Maurino, V., Minero, C., Lucchiari, M., Pelizzetti, E.,

- 2004b. Nitration and hydroxylation of benzene in the presence of nitrite/nitrous acid in aqueous solution., *Chemosphere*, vol. 56, pp. 1049–1059, doi:[10.1016/j.chemosphere.2004.05.027](https://doi.org/10.1016/j.chemosphere.2004.05.027).
- Viswanadhan, V.N., Ghose, A.K., Revankar, G.R., Robins, R.K., 1989. Atomic physicochemical parameters for three dimensional structure directed quantitative structure-activity relationships. 4. additional parameters for hydrophobic and dispersive interactions and their application for an automated superposition of certain naturally occurring nucleoside antibiotics, *Journal of Chemical Information and Computer Sciences*, vol. 29, no. 3, pp. 163–172, doi:[10.1021/ci00063a006](https://doi.org/10.1021/ci00063a006).
- Voordeckers, J.W., Fennell, D.E., Jones, K., Häggblom, M.M., 2002. Anaerobic biotransformation of tetrabromobisphenol a, tetrachlorobisphenol a, and bisphenol a in estuarine sediments, *Environmental Science & Technology*, vol. 36, no. 4, pp. 696–701, doi:[10.1021/es011081h](https://doi.org/10.1021/es011081h).
- Wang, J., Wang, S., 2016. Removal of pharmaceuticals and personal care products (PPCPs) from wastewater: A review, *Journal of Environmental Management*, vol. 182, pp. 620–640, doi:[10.1016/j.jenvman.2016.07.049](https://doi.org/10.1016/j.jenvman.2016.07.049).
- White, G.F., Russell, N.J., Tidswell, E.C., 1996. Bacterial scission of ether bonds., *Microbiological Reviews*, vol. 60, pp. 216–232.
- Wick, A., Fink, G., Joss, A., Siegrist, H., Ternes, T.A., 2009. Fate of beta blockers and psycho-active drugs in conventional wastewater treatment, *Water Research*, vol. 43, pp. 1060–1074, doi:[10.1016/j.watres.2008.11.031](https://doi.org/10.1016/j.watres.2008.11.031).
- Wick, A., Marincas, O., Moldovan, Z., Ternes, T.a., 2011a. Sorption of biocides, triazine and phenylurea herbicides, and uv-filters onto secondary sludge., *Water Research*, vol. 45, pp. 3638–3652, doi:[10.1016/j.watres.2011.04.014](https://doi.org/10.1016/j.watres.2011.04.014).
- Wick, A., Wagner, M., Ternes, T.A., 2011b. Elucidation of the transformation pathway of the opium alkaloid codeine in biological wastewater treatment., *Environmental Science & Technology*, vol. 45, pp. 3374–3385, doi:[10.1021/es103489x](https://doi.org/10.1021/es103489x).
- Wickham, H., 2009. *ggplot2: elegant graphics for data analysis*, Springer New York.

- World Health Organisation, 2002. *The World Health Report 2002: Reducing risks, promoting healthy life*, Geneva, Switzerland.
- Xu, Y., Yuan, Z., Ni, B.J., 2016. Biotransformation of pharmaceuticals by ammonia oxidizing bacteria in wastewater treatment processes, *Science of The Total Environment*, vol. 566–567, pp. 796–805, doi:[10.1016/j.scitotenv.2016.05.118](https://doi.org/10.1016/j.scitotenv.2016.05.118).
- Yi, T., Barr, W., Harper, W.F., 2012. Electron density-based transformation of trimethoprim during biological wastewater treatment, *Water Science and Technology*, vol. 65, no. 4, pp. 689–696, doi:[10.2166/wst.2012.917](https://doi.org/10.2166/wst.2012.917).
- Zhang, C., Bennett, G.N., 2005. Biodegradation of xenobiotics by anaerobic bacteria, *Applied Microbiology and Biotechnology*, vol. 67, pp. 600–618.
- Zhang, Y., Geißen, S.U., Gal, C., 2008. Carbamazepine and diclofenac: Removal in wastewater treatment plants and occurrence in water bodies, *Chemosphere*, vol. 73, no. 8, pp. 1151–1161, doi:[10.1016/j.chemosphere.2008.07.086](https://doi.org/10.1016/j.chemosphere.2008.07.086).
- Zhao, J., Li, Y., Zhang, C., Zeng, Q., Zhou, Q., 2008. Sorption and degradation of bisphenol A by aerobic activated sludge, *Journal of Hazardous Materials*, vol. 155, pp. 305–311, doi:[10.1016/j.jhazmat.2007.11.075](https://doi.org/10.1016/j.jhazmat.2007.11.075).
- Zheng, C., Focks, A., Ellebrake, K., Eggers, T., Fries, E., 2011. Sorption of ortho-phenylphenol to soils, *CLEAN Soil Air Water*, vol. 39, pp. 116–120, doi:[10.1002/clen.201000269](https://doi.org/10.1002/clen.201000269).
- Zipper, C., Bolliger, C., Fleischmann, T., Suter, M.J., Angst, W., Müller, M.D., Kohler, H.P., 1999. Fate of the herbicides mecoprop, dichlorprop, and 2,4-D in aerobic and anaerobic sewage sludge as determined by laboratory batch studies and enantiomer-specific analysis, *Biodegradation*, vol. 10, pp. 271–278, doi:[10.1023/A:1008396022622](https://doi.org/10.1023/A:1008396022622).
- Zipper, C., Suter, M.J.F., Haderlein, S.B., Gruhl, M., Kohler, H.P.E., 1998. Changes in the enantiomeric ratio of (*R*)- to (*S*)-mecoprop indicate in situ biodegradation of this chiral herbicide in a polluted aquifer, *Environmental Science & Technology*, vol. 32, no. 14, pp. 2070–2076, doi:[10.1021/es970880q](https://doi.org/10.1021/es970880q).
- Zupanc, M., Kosjek, T., Petkovšek, M., Dular, M., Kompare, B., Širok, B., Blažeka, Ž., Heath, E., 2013. Removal of pharmaceuticals from wastewater by

biological processes, hydrodynamic cavitation and UV treatment, *Ultrasonics Sonochemistry*, vol. 20, no. 4, pp. 1104–1112, doi:[10.1016/j.ultsonch.2012.12.003](https://doi.org/10.1016/j.ultsonch.2012.12.003).

Curriculum Vitae

Name **Jewell, Kevin Sean**
Address Johannesstraße 37, 56112 Lahnstein, Germany
Email jewell@bafg.de
Nationality Italy and USA
Date of birth 21/05/1984 in Frankfurt am Main

Education

Secondary education King George 5th School, Hong Kong, 1995 – 2000
GCSE level

Frankfurt International School, Oberursel, Germany, 2001 – 2003
Secondary school level (International Baccalaureate Diploma)

University studies University of British Columbia, Vancouver, Canada, 2003 – 2008
B.Sc. Chemistry, Bachelor thesis supervised by Prof. D. P. Gates titled *Towards the cationic addition polymerization of phosphalkenes: Preparation of a novel terphenyl stabilized phosphalkene as a potential monomer.*

Justus Liebig University, Gießen, Germany, 2008 – 2011
M.Sc. Chemistry, Master thesis supervised by Prof. P. R. Schreiner titled *Investigations into the Suzuki-Miyaura cross-coupling of 2,6-substituted aryl iodides and arylboronic acids: optimization of reaction conditions and studies into the tolerance for para-substituents.*

Federal Institute of Hydrology (BfG), Koblenz, Germany, 2011 – 2017
PhD Chemistry, Doctoral thesis supervised by Prof. T. A. Ternes titled *Investigations of chemically and biologically induced transformation reactions of micropollutants during biological wastewater treatment processes.*

Work experience

Place and Date Federal Institute of Hydrology (BfG), Koblenz, Germany, 2011 – present
Position Research assistant in the Department of Water Chemistry (G2)